



Universitat d'Alacant  
Universidad de Alicante

Sustainable catalytic systems  
based on imidazole derivatives

Mario Martos González



Tesis **Doctorales**

UNIVERSIDAD de ALICANTE

Unitat de Digitalització UA  
Unidad de Digitalización UA



Universitat d'Alacant  
Universidad de Alicante



**Institute of Organic Synthesis**

Faculty of Sciences

## **Sustainable catalytic systems based on imidazole derivatives**

Manuscript thesis submitted to apply for the Degree of Philosophiæ Doctor with  
International Mention at the University of Alicante  
by:

**MARIO MARTOS GONZÁLEZ**

Alicante, March 2023

Doctoral Program: Organic Synthesis

Scientific advisor: Prof. Isidro M. Pastor Beviá



---

## **Preface**





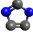
---

Universitat d'Alacant  
Universidad de Alicante



The research developed in this thesis has been carried out at the Institute of Organic Synthesis (ISO) of the University of Alicante under the supervision of Prof. Isidro M. Pastor Beviá. The findings detailed in this manuscript are related to the study of functionalized imidazolium salts as components of catalytic systems for sustainable organic transformations and novel materials. The core aim of this work is highlighting the versatility of the imidazolium scaffold and the exploitation of such flexibility for the development of alternative synthetic methodologies to obtain highly valuable compounds with reduced environmental impact.

The results described in this thesis have been published in the following international journals:

-  "Imidazolium-urea low transition temperature mixtures for the UHP-promoted oxidation of boron compounds" Martos, M.; Pastor, I. M. *J. Mol. Liq.* **2022**, 347, 118349.
-  "Iron-based imidazolium salt as dual Lewis acid and redox catalyst for the aerobic synthesis of quinazolines" Martos, M.; Pastor, I. M. *Eur. J. Org. Chem.* **2022**, e202200839.
-  "1,3-Bis(3-carboxypropyl)-1*H*-imidazole" Martos, M.; Albert-Soriano, M.; Pastor, I. M. *Molbank*, **2022**, 2022, M1480.
-  "DES-type interactions to promote solvent-free and metal-free reactions between nitrogen-containing heterocycles and allylic alcohols" Martos, M.; Pérez-Almarcha, Y.; Pastor, I. M. *Eur. J. Org. Chem.* **2022**, e202201221.
-  "Sulfoimidazolium salts. Second-generation IOS for heterogeneous-phase metal-free Brønsted-acidic catalysis" Martos, M.; Guapacha, A. M.; Pastor, I. M. **2023**, *Manuscript in preparation*.

This work has been possible thanks to funding from the Spanish Ministerio de Ciencia, Innovación y Universidades (PGC2018-096616-B-I00), the Spanish Ministerio de Ciencia e Innovación (PID2021-127332NB-I00), the Generalitat Valenciana (AICO/2021/013 and IDIFEDER/2021/013) and the University of Alicante (VIGROB-316, UADIF20-106, UAUSTI21-15). The author wishes to express his gratitude to the Institute of Organic Synthesis, for a research contract (I-PI/57-20), the Institute of Electrochemistry (I-PI 55/19) and to the University of Alicante-Banco Santander consortium for a grant to carry out a three-month research stay at Gothenburg University, Sweden.





---

## Summary

---

Universitat d'Alacant  
Universidad de Alicante





This doctoral thesis describes the development of several catalytic systems containing imidazolium salts. It has been divided into four chapters:

Chapter 1 describes a novel low transition temperature mixture (LTTM) based on 1-(methoxycarbonylmethyl)-3-methylimidazolium chloride and urea. The LTTM was characterized and then applied to the oxidation of boron compounds (i.e., boronic acids, boronic esters and trifluoroborates) to the corresponding alcohols, obtaining excellent results in short reaction times. The system, which acts as a co-solvent as well as source of oxidizer, achieved three synthetic cycles with a single imidazolium loading, greatly reducing the environmental impact of the protocol.

Chapter 2 compiles our findings about the use of a LTTM based on iron(III) and 1-butyl-3-(methoxycarbonylmethyl)imidazolium chloride as a catalyst for the synthesis of quinazolines. The mixture, named IBIS, presents a bifunctional character as both Lewis acid and redox catalyst, affording the desired products in moderate to excellent yields using air as the terminal oxidant in the absence of solvent. In addition, a methodology for the direct synthesis of 2-arylquinazolines from 2-nitrobenzaldehydes is presented and discussed.

Chapter 3 details the study of ionic organic solids (IOS) as metal-free heterogeneous catalysts. The IOS 1,3-bis(carboxymethyl)imidazolium chloride effectively catalyzed the C-3 allylation of indoles, providing a single regioisomer in up to quantitative yields and often, pure after simply filtering off the catalyst. The reaction could be performed in gram scale and the catalyst could be reused up to 5 consecutive times without loss of activity. The protocol was then extended to other  $\pi$ -excessive heterocycles, which experienced selective N-allylation. Overall, this methodology proved to be significantly superior in terms of sustainability than those reported in the literature. This chapter also presents the first synthesis of 1,3-bis(sulfomethyl)imidazole and a comparative study of its catalytic activity against carboxy-based IOS in the synthesis of quinolines as well as the allylation reaction discussed above.

Chapter 4 describes the synthesis and characterization of a series of metal-organic frameworks based on 1,3-bis(carboxymethyl)imidazole and zirconium salts using a water-based methodology, as well as the preparation and study of a series of metal-organic gels based on the same components. The project is still ongoing, so only preliminary results are discussed.

Sustainability metrics were calculated in all the above-mentioned projects, in order to unbiasedly assess the environmental impact of our synthetic protocols, as well as to compare with previously reported methodologies.





---

# Resumen

---

Universitat d'Alacant  
Universidad de Alicante



La presente tesis doctoral describe el desarrollo de diversos sistemas catalíticos basados en derivados del imidazol y ha sido dividida en cuatro capítulos.

El capítulo 1 describe una novedosa mezcla de bajo punto de transición (LTTM, del inglés *Low Transition Temperature Mixture*) compuesta por cloruro de 1-metil-3-(metoxicarbonilmetil)imidazolio (**mcmimCl**) y urea. Desde su descubrimiento a principios de la década de los 2000, los LTTMs han sido estudiados como una alternativa sostenible y altamente modulable a los disolventes convencionales (conocidos comúnmente como VOCs, del inglés *Volatile Organic Compounds*), cuyo uso presenta problemas entre los que se incluyen polución atmosférica, toxicidad hacia el medio ambiente y baja biodegradabilidad. En términos generales, los LTTMs consisten en mezclas de dos o más componentes cuya interacción ocasiona una depresión en el punto de fusión del sistema. La definición es lo suficientemente amplia como para aunar diversos sistemas, entre los que se encuentran los DES (del inglés *Deep Eutectic Solvents*) y las mezclas ideales con bajo punto de transición. El modo de interacción varía según el tipo de mezcla, pero el más conocido es la interacción entre un aceptor de enlaces de hidrógeno (HBA, del inglés *Hydrogen Bond Acceptor*, comúnmente un haluro metálico o una sal orgánica) y un donador de enlaces de hidrógeno (HBD, del inglés *Hydrogen Bond Donor*, alcoholes, agua, aminas, etc.). Miles de componentes son compatibles con la formación de LTTMs, lo que les proporciona una modularidad incomparable. Además, muchos de ellos (urea, glicerol, glúcidos, etc.) proceden de fuentes renovables, por lo que el impacto medioambiental de su uso es reducido en comparación con disolventes convencionales.

Los LTTM comparten cierta similitud con los líquidos iónicos (ILs, del inglés *Ionic Liquids*), por definición, sales orgánicas con puntos de fusión menores a 100 °C. Estas sustancias presentan una serie de ventajas análogas a los LTTMs, entre las que se encuentran nula volatilidad y alta modularidad. Entre las estructuras más utilizadas para la producción de ILs se encuentran las sales de imidazolio, cuya gran estabilidad, bajo punto de fusión y síntesis generalmente sencilla las hace ideales para este rol. Además, presentan una acidez de Lewis significativa al igual que la posibilidad de formar carbenos N-heterocíclicos (NHCs, del inglés *N-Heterocyclic Carbenes*), por lo que resultan idóneas como disolventes catalíticamente activos para llevar a cabo ciertos procesos. En su momento, los ILs fueron considerados como una gran alternativa a los VOCs. Sin embargo, el coste de producción de ILs es elevado, son persistentes en el medio ambiente y su toxicidad puede ser importante, por lo que, a lo largo de la segunda mitad de la década de los 2000, fueron relegadas a usos específicos.

Las sales de imidazolio son compatibles con la formación de LTTMs (normalmente como HBA), aunque tan sólo existen algunos precedentes en la bibliografía, principalmente debido a la asociación de éstas con los ILs. Sin embargo, esta aplicación ofrece un gran potencial, ya que el hipotético LTTM debería mantener la mayoría de las propiedades relevantes de las sales de imidazolio (i.e., acidez de

Lewis, formación de NHCs, etc.), estando compuesto en su mayoría por una sustancia biodegradable y de bajo coste.

Con esta premisa en mente, cuatro sales derivadas de aminoácidos de conocida actividad catalítica, 1,3-bis(carboximetil)imidazol (**bcmim**), su clorhidrato (**bcmimCl**), cloruro de 1-(carboximetil)-3-metilimidazolio (**cmimCl**) y **mcmimCl** fueron combinadas como HBA con urea o cloruro de guanidinio (como HBD) en proporción molar 1:1 y analizadas por calorimetría diferencial de barrido (DSC, del inglés *Differential Scanning Calorimetry*) a fin de determinar la formación de LTTMs por análisis de los eventos térmicos presentes. Utilizando urea como HBD, se apreció una depresión en el punto de fusión en todas las mezclas, con **cmimCl** y **mcmimCl** formando LTTMs a temperatura cercana a ambiente. El uso de cloruro de guanidinio no fue tan exitoso, ya que tan sólo se observó formación de mezclas con éstos últimos. Ya que el **cmimCl** deriva del **mcmimCl** y no dio tan buenos resultados, el sistema compuesto por **mcmimCl** y urea fue seleccionado para estudios posteriores. De este modo, una serie de mezclas cubriendo el rango completo de composiciones fueron preparadas y analizadas por DSC, obteniendo los correspondientes diagramas de composición-punto de fusión y entalpía de formación-punto de fusión. La temperatura más baja registrada fue de 35.2 °C para la mezcla con  $\chi_{\text{mcmimCl}} = 0.66$ , aunque los puntos de fusión de las mezclas se mantienen en torno a ambiente para un rango relativamente amplio de composiciones e inferiores a 100 °C en todos los casos.

Tras estudiar el comportamiento térmico del sistema, se decidió aplicar el LTTM a la oxidación de compuestos de boro a alcoholes. Esta reacción se suele llevar a cabo con catalizadores metálicos y/o utilizando gran exceso de peróxido de hidrógeno concentrado, cuyo uso requiere precauciones para evitar accidentes, debido a su gran reactividad. En este sentido, el uso de reactivos más seguros, como el aducto de urea y peróxido de hidrógeno (UHP, del inglés *Urea-Hydrogen Peroxide adduct*) es deseable aunque, hasta el momento, tan sólo un trabajo describe el uso de este oxidante para la transformación de interés. En general, la UHP es estable, liberando el oxidante a temperaturas superiores a 70 °C o mediante catálisis. De acuerdo al mecanismo de formación del LTTM (que implica la formación de enlaces de hidrógeno entre la urea y el anión de la sal de imidazolio), la interacción entre los componentes debería ser capaz de forzar la liberación de peróxido de hidrógeno de la UHP. Ya que esto ocurre lentamente a temperatura ambiente, el sistema **mcmimCl**:UHP liberaría peróxido de hidrógeno al medio de forma continuada, incrementando la eficiencia. Para el primer experimento, la formación de 4-fenilfenol a partir del ácido borónico correspondiente fue seleccionada como modelo. Sin embargo, la elevada oxofilia del boro implica un mecanismo altamente exotérmico, que acelera la formación del LTTM y la liberación de más oxidante en el medio, causando el descontrol térmico del proceso. A modo de solución, el ácido borónico se añadió suspendido en acetato de etilo (un disolvente sostenible, que sería necesario añadir de cualquier modo para extraer el producto). El acetato de etilo es inmiscible con el LTTM y la solubilidad de los compuestos de boro de interés es

baja en él, mientras que la de los alcoholes resultantes de la reacción es muy alta. De esta forma, cumple el triple rol de disminuir la velocidad de reacción, extraer el producto y proporcionar masa térmica para el proceso. Con este procedimiento, la transformación del ácido bifenilborónico en el producto correspondiente se produjo con rendimiento cuantitativo y obteniendo el producto puro tras simple decantación y filtrado de la fase orgánica. A continuación, se estudió el alcance de la reacción, obteniendo un total de 18 alcoholes aromáticos a partir de los correspondientes ácidos borónicos con rendimientos buenos a cuantitativos y en escalas preparativas de hasta 5 milimoles. No se observó influencia alguna de la naturaleza electrónica de los sustituyentes en el resultado del proceso, aunque sí se detectó un efecto estérico notable para sustratos impedidos. En ningún caso fue necesario purificar los productos obtenidos. El uso de ésteres borónicos y trifluoroboratos de potasio resultó ser compatible con el proceso, obteniendo 5 productos más, entre los que se incluyen alcoholes alifáticos, con rendimientos de buenos a cuantitativos sin purificación adicional.

A fin de explorar la reusabilidad del sistema, se diseñó un proceso de síntesis secuencial, en la que el LTTM se recargó con reactivo y un equivalente de UHP tras el primer ciclo de reacción. De esta forma, la reacción se llevó a cabo tres veces consecutivas sin pérdida de actividad catalítica.

Finalmente, el impacto medioambiental del proceso se determinó de manera objetiva mediante el uso de métricas de sostenibilidad, obteniendo un E-factor de 9.4 (cercano al rango de producción en masa de productos químicos), un VMR (calculado a partir del rendimiento de la reacción, economía atómica del proceso, factor estequiométrico, factor de recuperación y eficiencia másica de reacción) de 0.611 (de un máximo de 1) y una puntuación EcoScale de 81 (excelente). En comparación con otros métodos descritos, con puntuaciones inferiores en general, el uso del LTTM formado por **mcmimCl** y UHP ofrece una significativa mejora en términos de sostenibilidad y seguridad.

El capítulo 2 recoge los resultados obtenidos en el estudio de un LTTM basado en hierro(III) y cloruro de 1-butil-3-(metoxicarbonilmetil)imidazolium (**IBIS**, del inglés *Iron-Based Imidazolium Salt*) como catalizador para la síntesis de quinazolinas. El desarrollo de nuevas metodologías sintéticas para esta familia de compuestos es de elevado interés por su presencia en gran variedad de moléculas con actividad biológica, incluyendo alcaloides naturales y fármacos. En particular, las quinazolinas 2,4-disustituidas han demostrado actividad antibacteriana, antineoplásica y antifúngica. La mayoría de métodos descritos para su preparación parten de derivados del ácido antranílico (2-aminobenzoico) en combinación con sintones de uno o dos átomos. Entre estos procedimientos, la condensación-ciclación de 2-aminobenzofenonas o 2-aminobenzaldehídos con bencilaminas es uno de los más populares, por su aparente sencillez y posibilidad de control absoluto de los patrones de sustitución de los compuestos resultantes. Sin embargo, este proceso requiere altas temperaturas para completar el paso de ciclación de la imina resultante de la condensación del carbonilo y la bencilamina a la correspondiente tetrahydroquinazolina, así como la presencia de especies oxidantes en el medio para la aromatización de esta a la quinazolina final. De este modo, la mayor parte de las metodologías



descritas en la bibliografía utilizan disolventes de alto punto de ebullición (xileno, tolueno, etc.) y oxidantes para llevar a cabo el proceso. Entre estos, el más común es el hidroperóxido de *tert*-butilo (TBHP, del inglés *tert-Butyl Hydroperoxide*), un peróxido orgánico fuertemente oxidante. Desde un punto de vista sostenible y práctico, el uso de disolventes y reactivos peligrosos es indeseable. El **IBIS** es un catalizador multipropósito con carácter ácido de Lewis y redox, capaz de llevar a cabo procesos de oxidación utilizando el oxígeno del aire como oxidante terminal. Asimismo, tratándose de un LTTM, favorece la integración de los componentes de la reacción, incluso en proporción catalítica, eliminando la necesidad de utilizar disolvente adicional. De este modo, la reacción entre la 2-aminobenzofenona y la bencilamina en presencia de 10% (en mol) de **IBIS** fue seleccionada como modelo para llevar a cabo estudios de optimización.

En la primera reacción a 110 °C durante 16 h, la formación de 2,4-difenilquinazolina fue de tan sólo un 12%, aunque la conversión total del producto de partida a la 2,4-difeniltetrahydroquinazolina fue de más de un 70%. Dado el uso de tubos estrechos de vidrio y la ausencia de disolvente, se teorizó acerca de la posibilidad de que se estuviese formando una atmósfera pobre en oxígeno dentro del recipiente por mala convección. De este modo, insertando una corriente de aire dentro de la reacción, la conversión a producto aumentó a un 41%. Finalmente, incrementando la temperatura a 130 °C y el tiempo de reacción a 24 h, se obtuvo una conversión a 2,4-difenilquinazolina de un 97%. Con las condiciones de reacción optimizadas, se procedió al estudio del alcance de la reacción. Una serie de 2-aminobenzofenonas fueron combinadas con bencilamina en presencia de **IBIS**, obteniendo las correspondientes 2,4-difenilquinazolininas con buenos rendimientos. La metodología fue asimismo aplicada a sustratos alquílicos y 2-aminobenzaldehídos, obteniendo rendimientos moderados a buenos. En este caso, el uso de sustratos pobres en densidad electrónica resultó en tiempos de reacción más prolongados y rendimientos generalmente más bajos que sus homólogos ricos en electrones. Un total de 9 sustratos fueron obtenidos. De la misma forma, se exploraron diferentes derivados de la bencilamina, incluyendo sistemas aromáticos extendidos y heterocíclicos, en combinación con 2-aminobenzofenona, obteniendo un total de 10 quinazolininas en rendimientos de buenos a excelentes. No se observó ninguna tendencia clara de reactividad en este caso.

Nuevamente, el impacto medioambiental de la reacción fue estudiado y comparado con otros métodos descritos en la bibliografía mediante métricas de sostenibilidad. En términos generales, el proceso demostró ser comparable con metodologías descritas con catalizadores no metálicos en ausencia de disolvente, y muy superior a procedimientos empleando disolventes y oxidantes. Respecto a los primeros, la metodología catalizada por **IBIS** ofrece una ventaja significativa por el uso de aire como oxidante terminal, en lugar de oxígeno puro.

Explotando el potencial como catalizador redox del **IBIS** y el elevado potencial de oxidación de la bencilamina, se diseñó un proceso para la preparación de quinazolininas libres en la posición 4, partiendo directamente de 2-nitrobenzaldehído, precursor de los inestables 2-aminobenzaldehídos

comúnmente utilizados. Así, la oxidación de la bencilamina (añadida en exceso) mediada por **IBIS** utilizaría como contraparte la reducción del 2-nitrobenzaldehído, generando el sustrato *in situ*. De este modo, varios 2-nitrobenzaldehídos fueron ensayados en esta transformación, aunque en ningún caso se obtuvieron rendimientos superiores al 25%, pese a observar conversiones cuantitativas. Tras una serie de ensayos, se llegó a la conclusión de que reacciones secundarias de polimerización eran las responsables del completo consumo del 2-aminobenzaldehído generado, por lo que, por razones de tiempo y escasez de recursos humanos, no se continuó con este estudio.

El capítulo 3 contiene un estudio sobre el uso de sólidos iónicos orgánicos (IOS, del inglés *Ionic Organic Solids*) como catalizadores heterogéneos para la alilación de indoles mediante sustitución nucleófila con alcoholes alílicos. Tradicionalmente, este proceso se ha llevado a cabo empleando sustratos sustituidos en posición alílica con buenos grupos salientes, como haluros, acetatos, tosilatos, etc. El uso de alcoholes alílicos es deseable desde un punto de vista sostenible, ya que los pseudohaluros mencionados anteriormente derivan de éstos, por lo que su uso directo evita un paso de reacción adicional e incrementa la economía atómica del proceso. Sin embargo, los alcoholes son mucho menos reactivos, por lo que requieren la presencia de catalizadores altamente eficientes. En general, las metodologías descritas se dividen en dos categorías en función del modo de activación del sustrato. Por una parte, se encuentran los procesos catalizados por metales preciosos, en los que la reacción ocurre a través de un intermedio  $\pi$ -alílico catiónico. Entre estos procedimientos, la reacción de Tsuji-Trost, catalizada por paladio es el más representativo. Por otra parte, se encuentran las metodologías en las que el alcohol es activado mediante catálisis ácida (de Lewis o Brønsted) utilizando metales de transición o ácidos orgánicos. El uso de metales preciosos, escasos y de alto precio, es indeseable para este tipo de transformaciones. Por otra parte, los ácidos empleados suelen ser especies altamente corrosivas e incompatibles con la humedad (triflatos metálicos o ácidos sulfónicos), con los problemas de manipulación asociados a ello.

En este sentido, el uso de IOS ofrece una serie de ventajas, entre las que se encuentran total compatibilidad con el aire y la humedad, facilidad de manipulación, robustez, bajo coste y ausencia total de metales. Además, los IOS basados en sales de imidazolio son capaces de establecer interacciones tipo LTTM con los componentes, proporcionando sustratos altamente activados, así como un medio de dispersión en el que llevar a cabo la reacción. De esta forma, la alilación de indol con (*E*)-1,3-difenilprop-2-en-1-ol en ausencia de disolvente utilizando **bcmim** y sus cloruro, bromuro y yoduro correspondientes como catalizadores fue seleccionada como reacción modelo. En las condiciones iniciales, los haluros de **bcmim** proporcionaron selectivamente el producto de alilación en la posición C-3 del indol en rendimientos cuantitativos. Sin embargo, el **bcmim** no resultó ser catalíticamente activo en esta transformación, probablemente debido a las fuertes interacciones entre moléculas presentes en su estructura sólida. Debido a su mayor robustez y menor coste, el **bcmimCl** fue seleccionado para explorar el alcance de la reacción. Empleando las condiciones estándar, 11

indoles con diferentes sustituyentes (atendiendo a factores electrónicos y estéricos) fueron alilados regioselectivamente en la posición C-3 con rendimientos de buenos a cuantitativos, varios de ellos sin necesidad de purificación posterior. No se observó ninguna influencia electrónica o estérica de los sustituyentes en los anillos de los indoles, salvo en las posiciones 2 (debido a impedimentos estéricos en la interacción tipo LTTM entre los componentes) y 1 (por la formación de un intermedio de reacción formalmente catiónico), en las que se obtuvieron rendimientos ligeramente inferiores. Las condiciones modelo fueron aplicadas también a diferentes alcoholes alílicos simétrica y asimétricamente sustituidos, en combinación con indol. Nuevamente, los productos fueron obtenidos en rendimientos de buenos a cuantitativos como mezclas inseparables de regioisómeros en proporción 1:1 para los alcoholes no simétricos. Aunque esto sugiere la formación de un intermedio carbocatiónico, no se dispone de suficiente información para confirmarlo.

Posteriormente, el procedimiento se extendió a la alilación de otros *N*-heterociclos con alta densidad electrónica. De este modo, pirazoles, triazoles, tetrazoles, carbazoles, indazoles y benzotriazoles demostraron compatibilidad con la metodología diseñada, con los correspondientes alilheterociclos obtenidos en rendimientos de buenos a cuantitativos, nuevamente sin necesidad de purificación adicional para varios productos. En este caso, la alilación se produjo de forma selectiva en los átomos de nitrógeno de los anillos, con sustratos no simétricos resultando en mezclas de regioisómeros de acuerdo con las tendencias esperables.

Para demostrar la aplicabilidad de la metodología, la alilación del indol se escaló a 5 milimoles, obteniendo el producto deseado con un rendimiento cuantitativo y puro tras filtrar el catalizador. Asimismo, se llevaron a cabo pruebas de reusabilidad del IOS, disolviendo el producto en acetato de etilo tras la reacción y separando el catalizador sólido por decantación, para después añadir una nueva ronda de reactivos. De este modo, el **bcmimCl** pudo ser reutilizado hasta 5 veces sin sufrir ninguna clase de reducción en su actividad catalítica, demostrando la gran robustez del IOS.

Como en los dos capítulos anteriores, la metodología diseñada se comparó con otros procedimientos descritos en la bibliografía mediante métricas de sostenibilidad. En este caso, el proceso catalizado por **bcmimCl** demostró ser ampliamente superior a todas las metodologías estudiadas, obteniendo un E-factor de 1.9, un VMR de 0.790 y una puntuación EcoScale de 89. Estos valores indican un procedimiento limpio, seguro y muy eficiente en su diseño.

Tras completar este estudio, se diseñó un procedimiento sintético para la preparación de IOS de segunda generación basados en sales de sulfoimidazolio. Los ácidos sulfónicos tienen una acidez de Brønsted varios órdenes de magnitud superiores a sus homólogos basados en carbono. De esta forma, el 1,3-bis(sulfometil)imidazol (**bsmim**) fue seleccionado como estructura base para el diseño y preparación de IOS de segunda generación. La síntesis del **bsmim** no tiene precedente en la bibliografía, por lo que se diseñó un procedimiento análogo a la preparación del **bcmim** mediante

reacción de Arduengo con glioxal, formaldehído y ácido aminometanosulfónico. Sin embargo, en las condiciones estándar (2 horas a 95 °C), la mezcla de reacción se transformó en una pasta negra con un fuerte olor a caramelo de la que no se pudo aislar el producto. Inicialmente, esto se atribuyó a la baja solubilidad del ácido aminometanosulfónico en agua resultando en la polimerización y descomposición del glioxal por tiempo de residencia excesivo en el medio de reacción. Añadiendo 2 mL adicionales de agua, se obtuvo **bsmim** con un rendimiento de un 41%, aunque con una pureza de tan sólo un 76%. El análisis por resonancia magnética nuclear (RMN) del producto reveló, además de las señales correspondientes al **bsmim**, la presencia de ácido aminometanosulfónico sin reaccionar y una sal de imidazolio desconocida. De las señales observadas, se identificó el producto como el 1-metil-3-(sulfometil)imidazol (**msmim**), generado mediante descomposición térmica *via* extrusión de trióxido de azufre del **bsmim**. De este modo, la siguiente serie de experimentos tuvieron como objetivo el total consumo del reactivo de partida evitando a la vez la formación de **msmim**. Tras varias pruebas, ambos problemas fueron solucionados mediante la adición de ácido sulfúrico en cantidad catalítica, obteniendo **bsmim** puro con un rendimiento del 49%. Pese a que las métricas de sostenibilidad del proceso se ven seriamente afectadas por la baja cantidad obtenida, los valores obtenidos son aceptables (E-factor de 18.5, VMR de 0.623 y EcoScale de 64).

En cuanto a la actividad catalítica del **bsmim**, se decidió compararla con los IOS de primera generación en la síntesis de Friedländer de quinolinas, descrita en la bibliografía. En las mismas condiciones, el proceso catalizado por **bsmim** obtuvo rendimientos superiores en la preparación de una variedad de quinolinas a aquellos descritos utilizando **bcmimCl**. Cabe destacar que la comparación real entre generaciones implica al **bcmim**, que sólo es capaz de generar el producto con un 9% de conversión. Continuando con el estudio de la actividad catalítica del **bsmim**, la alilación de heterociclos diseñada en la primera parte del capítulo fue la siguiente reacción escogida. Nuevamente, el **bsmim** demostró una actividad similar a la del **bcmimCl** en la alilación de varios sustratos, observándose también la misma regioselectividad. El **bcmim**, sin embargo, no fue capaz de promover la reacción en absoluto, lo que nuevamente demuestra la gran diferencia entre las generaciones de IOS.

El capítulo 4 describe la síntesis y caracterización de una serie de estructuras metal-orgánicas (MOFs, del inglés *Metal-Organic Frameworks*) basadas en derivados del **bcmim** y sales de zirconio, así como la preparación y estudio de hidrogeles metal-orgánicos (MOGs, del inglés *Metal-Organic Gels*) obtenidos con los mismos componentes bajo condiciones sintéticas distintas. Los MOFs son una familia de materiales porosos basados en redes bi o tridimensionales formadas por centros metálicos unidos entre sí mediante moléculas orgánicas (conocidas como *linkers*). Los centros metálicos pueden ser cationes aislados, con modos de coordinación sencillos, o estructuras inorgánicas polidimensionales conocidas como SBUs (del inglés *Secondary Building Units*), con hasta

66 posiciones de coordinación. En lo que respecta a los *linkers*, son ligandos orgánicos rígidos con múltiples grupos funcionales con capacidad quelante.

La presencia de porosidad permanente es precisamente la propiedad más importante de los MOFs, cuyo origen se encuentra en la rigidez de la estructura reticular. En comparación con otros materiales porosos de origen inorgánico, los MOFs presentan porosidades muy superiores (rondando los 2000 m<sup>2</sup>/g, con algunas estructuras llegando hasta más de 7000 m<sup>2</sup>/g), así como una mayor capacidad de modulación. Además del enorme número de componentes disponibles, el concepto de síntesis isorecticular abre la posibilidad de sintetizar un gran número de MOFs partiendo de una misma estructura base. Generalmente, los centros metálicos dictan la geometría de la estructura, mientras que los *linkers* determinan la distancia entre centros, así como los tamaños de las aperturas presentes en el material. De este modo, es posible utilizar *linkers* elongados (con unidades rígidas como anillos aromáticos o dobles enlaces) para fabricar MOFs isorectulares con tamaños de poro y superficies diferentes.

Un factor importante a la hora de sintetizar MOFs es la compatibilidad entre el centro metálico y el *linker*, que responde a la teoría ácido-base duro-blando de Pearson (HSAB, del inglés *Hard-Soft Acid-Base*). En términos generales, metales de transición con altos estados de oxidación (duros, de acuerdo con la definición HSAB) forman complejos estables con aniones poco polarizables, como carboxilatos. De la misma forma, metales con bajos estados de oxidación (cobre, zinc, etc.) prefieren ligandos polarizables (como azoles). Mediante la adecuada selección de componentes, es posible construir estructuras con alta estabilidad térmica, mecánica y química.

La preparación de MOFs se suele llevar a cabo mediante procesos solvotermales a alta temperatura, en los que la estructura precipita inmediatamente como un polvo escasamente cristalino, con el tratamiento posterior permitiendo la reorganización de la estructura en un material de alta cristalinidad. Una forma de mejorar el proceso es mediante el uso de moduladores, especies monodentadas con la misma funcionalidad que el *linker* que se añaden en exceso a la mezcla de reacción. De este modo, las moléculas de modulador saturan el centro metálico, por lo que para formar la estructura, el *linker* debe desplazar progresivamente al modulador. Aunque el proceso está fuertemente favorecido por la precipitación del material, es suficiente para ralentizar de forma significativa la formación del MOF, lo que resulta en una estructura altamente cristalina.

El uso de **bcmim** como *linker* en la preparación de MOFs se encuentra limitado mayormente a la preparación de estructuras con metales alcalinos, de transición blandos y de transición interna. A pesar de tener grupos quelantes teóricamente duros, la naturaleza zwitteriónica del **bcmim** le confiere la capacidad de establecer enlaces con los centros metálicos con una amplia variedad de geometrías y modos de coordinación. Unido a la flexibilidad que le confieren los grupos metileno que separan los carboxilatos del anillo central cargado, hacen del **bcmim** un ligando idóneo para metales del bloque

f, cuyo gran radio, baja densidad electrónica y gran cantidad de vacantes de coordinación dificulta la formación de MOFs estables, al igual que para metales alcalinos, que experimentan problemas similares debido a su pequeño tamaño.

No existe precedente en la bibliografía describiendo la preparación de MOFs basados en metales de transición duros (titanio, zirconio, hafnio, etc.) con **bcmim** como *linker*. La preparación de estas estructuras es de interés, especialmente con zirconio, ya que los MOFs basadas en ligandos carboxilato con este metal (entre las que destaca la familia UiO-6x, utilizando derivados del ácido tereftálico como *linkers*) tienden a ser altamente estables, lo que facilita su estudio, modificación y aplicación.

De este modo, se resolvió desarrollar una metodología para la preparación del MOF **bcmimZr** basada en un protocolo en agua descrito recientemente para el UiO-66. Comúnmente, la preparación de MOFs se lleva a cabo mediante procesos solvotermales a alta temperatura (entre 80 y 120 °C) durante periodos de tiempo prolongados (de 24 a 72 horas) en disolventes de alto punto de ebullición (como la *N,N*-dimetilformamida o DMF). Esto tiene un impacto medioambiental significativo, y, aunque la preparación de MOFs es intrínsecamente ineficiente en términos materiales, el uso de disolventes más benignos y un menor gasto energético siempre es deseable. Así, **bcmim** fue combinado con cloruro de zirconilo (previamente tratado con ácido acético como modulador) a temperatura ambiente durante 24 h, tras las cuales se forzó la precipitación del MOF utilizando metanol, dejando reposar la mezcla en condiciones estáticas durante 24 h adicionales para garantizar la completa formación del producto. Por otra parte, otra prueba fue preparada en ausencia de modulador, con el fin de evaluar la influencia de éste en la cristalinidad y morfología de la estructura obtenida. Los resultados obtenidos fueron dispares; por una parte, de la reacción modulada se obtuvo un material pulverulento incoloro, mientras que la reacción sin modulador resultó en la formación de un gel blanco opaco. Con el fin de estudiar la estructura de ambos materiales, se eliminó el disolvente de ambos y se analizaron por difracción de rayos X en polvo (PXRD, del inglés *Powder X-ray Diffraction*). De acuerdo con los difractogramas obtenidos, ambas sustancias son diferentes al **bcmim** y entre sí. El polvo blanco, identificado como **bcmimZr**, presenta un patrón de difracción similar al del UiO-66, lo que sugiere la formación de una estructura isoreticular a este MOF. Por otra parte, el difractograma del xerogel presenta bandas anchas y poco definidas, que, junto a la formación del gel observada durante la síntesis, sugieren la presencia de un material nanocristalino, con un tamaño de partícula aproximado de 1 nm.

La preparación de MOGs ha sido descrita para varios sistemas conocidos, entre los que se encuentran los UiO, MIL y HKUST, y se propone como una alternativa viable para la fabricación de MOFs monolíticos con formas determinadas. En términos más generales, el desarrollo de hidrogeles es de interés por sus potenciales aplicaciones en biomedicina, ciencia de materiales y electrónica. Por ello, se decidió continuar el estudio sobre la formación de MOGs basados en **bcmim** y zirconio. Con

el fin de determinar la dependencia de la formación del gel con diversos parámetros, se llevaron a cabo una serie de experimentos. De estos, se constató la formación de hidrogeles con **bcmim**, así como su sal sódica (**bcmimNa**) y clorhidrato (**bcmimCl**, aunque posterior análisis de los xerogeles formados con este último reveló la presencia de una estructura diferente a la obtenida con el zwitterión). De la misma forma, tanto el cloruro de zirconilo como el cloruro de zirconio son compatibles como fuente de metal. El sistema tolera concentraciones mínimas de zirconio de 0.25% en masa, así como temperaturas de formación de hasta 120 °C, así como la inclusión de metanol como co-disolvente en el proceso de gelación.

Con el fin de determinar la temperatura de transición sol-gel de los MOGs de **bcmimZr** y su posible dependencia con la concentración de zirconio, tres muestras con concentraciones entre 1 y 0.5 % fueron preparadas y analizadas por DSC desde temperatura ambiente hasta 150 °C. En ningún caso se observaron eventos térmicos compatibles con transiciones sol-gel, aunque las trazas de los MOGs con 1 y 0.75% de zirconio presentan pequeñas bandas de emisión de calor en torno a 100 °C, que podrían ser consistentes con una reorganización de la estructura a una de mayor orden. En cualquier caso, de las pruebas anteriores a los análisis por DSC, se estableció que los hidrogeles de **bcmimZr** son estables al menos hasta 120 °C durante 24 h, lo que les da una ventaja significativa sobre otros sistemas, cuya tolerancia a la temperatura es significativamente menor (algunos empiezan a descomponerse a tan solo 80 °C).

Dada la alta estabilidad térmica de los MOGs, a la naturaleza iónica del **bcmim** y la presencia de importantes cantidades de iones cloruro, se consideró la posibilidad de diseñar electrolitos sólidos para baterías basados en hidrogeles de **bcmimZr**. De este modo, se midió la conductividad eléctrica de los MOGs analizados anteriormente y se comparó con la de un hidrogel basado en zinc descrito en la bibliografía, registrando un valor máximo de 44 mS/cm, significativamente superior al valor obtenido por el material de referencia (32 mS/cm).

A fin de estudiar los enlaces presentes en el MOG y el rol del **bcmim** en la formación del hidrogel, se preparó una muestra al 1% de zirconio en óxido de deuterio y se analizó por RMN. De acuerdo con los resultados obtenidos, la agregación de las partículas para la formación del MOG no parece estar asociada a entrecruzamiento mediante enlaces de hidrógeno con el anillo de imidazolio. Sin embargo, por razones temporales, no fue posible incluir más resultados sobre la caracterización de los MOFs y MOGs de **bcmimZr** en este manuscrito.

Finalmente, se determinó la puntuación EcoScale para la preparación del MOF de **bcmimZr** y se comparó con una metodología solvotermal representativa para la síntesis del UiO-66. El procedimiento aquí descrito obtuvo una puntuación de 62, frente a los 55 puntos del proceso en DMF, con la diferencia atribuible a la mayor cantidad de disolvente requerido (por la menor solubilidad de los productos en DMF) y la toxicidad de éste.

---

# Contents

---



Universitat d'Alacant  
Universidad de Alicante





|  |    |
|--|----|
| Preface.....   | 3  |
| Summary.....   | 7  |
| Resumen.....   | 11 |
| Contents.....  | 23 |
| General Introduction.....  | 29 |
| Gl.1. Imidazole .....  | 31 |
| Gl.1.1. Name, structure and properties.....  | 31 |
| Gl.1.2. Synthesis.....   | 32 |
| Gl.1.3. Natural occurrence and pharmaceutical relevance of imidazoles .....                            | 38 |
| Gl.2. Imidazolium salts .....  | 41 |
| Gl.2.1. Synthesis.....   | 41 |
| Gl.2.2. Catalytic systems based on imidazolium salts .....   | 43 |
| Gl.3. Sustainable chemistry.....   | 51 |
| Gl.3.1. Challenges in the design of sustainable chemical processes .....                               | 51 |
| Gl.3.2. Sustainability metrics .....   | 53 |
| General Objectives.....  | 59 |
| Chapter 1. Imidazolium-UHP Low Transition Temperature Mixtures. Development and application.....       | 63 |
| C1.1. Antecedents.....   | 65 |
| C1.1.1. Alternative solvent systems.....   | 65 |
| C1.1.2. Low transition temperature mixtures .....  | 69 |
| C1.2. Objectives .....   | 73 |
| C1.3. Results and discussion .....   | 75 |
| C1.4. Conclusions .....  | 89 |
| Chapter 2. Iron-Based Imidazolium Salts as multirole catalysts for the synthesis of quinazolines ..... | 91 |
| C2.1. Antecedents.....   | 93 |

|   |     |
|---|-----|
| C2.1.1. Quinazolines. Structure and significance .....  | 93  |
| C2.1.2. Synthesis of quinazolines.....  | 96  |
| C2.2. Objectives .....  | 101 |
| C2.3. Results and discussion .....  | 103 |
| C2.4. Conclusions .....   | 113 |
| Chapter 3. Brønsted-acidic Ionic Organic Solids based on carboxy- and sulfoimidazolium salts<br>..... | 115 |
| C3.1. Antecedents.....  | 117 |
| C3.1.1. Ionic organic solids.....   | 117 |
| C3.1.2. Imidazolium IOS as components of catalytic systems .....                                      | 121 |
| C3.2. Objectives .....  | 123 |
| C3.3. Results and discussion .....  | 125 |
| C3.4. Conclusions .....   | 143 |
| Chapter 4. Novel zirconium Metal-Organic Frameworks derived from carboxy-imidazolium salts<br>.....   | 145 |
| C4.1. Antecedents.....  | 147 |
| C4.1.1. Metal-Organic Frameworks. General considerations .....  | 147 |
| C4.1.2. Metal-Organic Frameworks based on 1,3-bis(carboxymethyl)imidazole.....                        | 154 |
| C4.2. Objectives .....  | 157 |
| C4.3. Results and discussion.....   | 159 |
| C4.4. Conclusions .....   | 167 |
| General conclusions .....   | 169 |
| Experimental section.....   | 173 |
| E.1. General remarks .....  | 175 |
| E.1.1. Materials and methods.....   | 175 |
| E.1.2. Sustainability metrics.....  | 176 |
| E.2. Detailed experimental protocols.....   | 177 |
| E.2.1. Chapter 1.....   | 177 |

---

|  |     |
|--|-----|
| E.2.2. Chapter 2.....                    | 178 |
| E.2.3. Chapter 3.....                    | 180 |
| E.2.4. Chapter 4.....                    | 181 |
| E.3. Spectral data of all compounds..... | 183 |
| E.3.1. Chapter 1.....                    | 183 |
| E.3.2. Chapter 2.....                    | 186 |
| E.3.3. Chapter 3.....                    | 193 |
| Abbreviations, units and symbols.....    | 207 |
| Acknowledgements.....                    | 217 |



Universitat d'Alacant  
Universidad de Alicante





---

# **General Introduction**

---

Universitat d'Alacant  
Universidad de Alicante



## GI.1. Imidazole

### GI.1.1. Name, structure and properties

Coined by Arthur R. Hantzsch in 1887, the term “imidazole” refers to five-membered aromatic heterocycles containing two nitrogen atoms in positions 1 and 3.<sup>1</sup> Imidazole itself, 1,3-diazole, is a white, crystalline solid, which produces a mildly alkaline solution when dissolved in water. Structurally, it is a planar, almost regularly pentagon-shaped molecule.<sup>2</sup>

Imidazole is highly stable, decomposing at temperatures exceeding 500 °C, and exhibits a series of interesting properties.<sup>3</sup> It is a highly polar compound (3.67 D in gas phase),<sup>4</sup> with most of its electron density localized at the nitrogen atoms (**Figure 1**).<sup>2</sup> It also exhibits a marked amphoteric character. The conjugate acid of the pyridinic nitrogen of imidazole has a  $pK_a$  of 7.0, more basic than that of pyridine itself, whereas the pyrrolic nitrogen has a  $pK_a$  of 14.5, slightly more acidic than pyrrole. Both prospective ions, imidazolium and imidazolate, are symmetric owing to charge delocalization between the nitrogen atoms.<sup>3</sup>

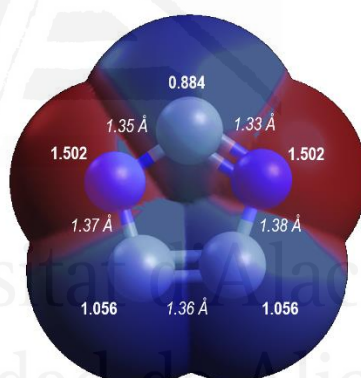


**Figure 1.** Imidazole ring charge density map (average  $\pi$ -electron density values in bold, bond length for the represented tautomer in italics).

This amphoteric character has several implications; it means imidazole is able to form extensive hydrogen bonding networks, which is the reason behind its high solubility in water and relatively high melting and boiling points when compared to its isomeric form, pyrazole (90 and 256 °C for imidazole

<sup>1</sup> Hantzsch, A.; Weber, J. H. *Ber. Dtsch. Chem. Ges.* **1887**, *20*, 3118–3132.

<sup>2</sup> Ji Ram, V.; Sethi, A.; Nath, M.; Pratap, R. *The Chemistry of Heterocycles*, 5<sup>th</sup> ed; Elsevier, 2019.

<sup>3</sup> Eicher, T.; Hauptmann, S. *The Chemistry of Heterocycles* 2<sup>nd</sup> ed.; Wiley-VCH, 2003.

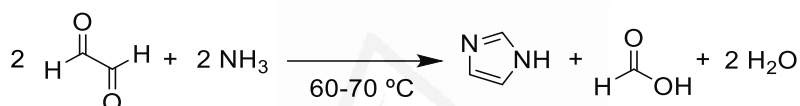
<sup>4</sup> Christen, D.; Griffiths, J. H.; Sheridan, J. Z. *Naturforsch.* **1981**, *36*, 1378–1385.



to 70 and 187 °C for pyrazole).<sup>3</sup> Another important consequence is annular tautomerism for 1,3-unsubstituted imidazoles, which results in 4-substituted imidazoles converting to the 5-substituted isomer and *vice-versa* via proton transfer between the nitrogen atoms. This process is highly dependent on the electronic nature of the substituents, which dictate which tautomeric form is favored.<sup>3,5</sup>

### GI.1.2. Synthesis

While imidazole derivatives had been discovered as early as 1841,<sup>6</sup> the first synthesis of imidazole was not reported until 1858, by the German chemist Heinrich Debus.<sup>7</sup> In his work, Debus synthesized imidazole by heating a mixture of glyoxal and ammonia, observing the formation of imidazole, then called glyoxaline, in low yield, along with formic acid and water (**Scheme 1**).



**Scheme 1.** Debus' synthesis of imidazole.

In 1882, the Polish chemist Bronisław L. Radziszewski theorized about the mechanism of the reaction, proposing that formaldehyde could be forming by cleavage of glyoxal under the influence of ammonia.<sup>8</sup> Over the next few years Radziszewski, along with the British chemist Francis R. Japp, devoted significant effort to the structural elucidation of several imidazole derivatives, as well as to develop the multicomponent version of Debus' protocol.<sup>9-17</sup> This methodology, involving a dicarbonyl compound, an aldehyde and ammonia to afford 2,4,5-substituted imidazoles would be eventually known as the Debus-Radziszewski-Japp reaction (**Scheme 2**).

<sup>5</sup>Joule, J. A.; Mills, K. *Heterocyclic Chemistry*, 4<sup>th</sup> ed.; Blackwell Science, 2000.

<sup>6</sup>Japp, F. R.; Robinson, H. H. L. *J. Chem. Soc. Trans.* **1882**, 41, 323–329.

<sup>7</sup>Debus, H. *Liebigs Ann.* **1858**, 107, 199–208.

<sup>8</sup>Radziszewski, B. *Ber. Dtsch. Chem. Ges.* **1882**, 15, 2706–2708.

<sup>9</sup>Radziszewski, B. *Ber. Dtsch. Chem. Ges.* **1882**, 15, 1493–1496.

<sup>10</sup>Radziszewski, Br. *Ber. Dtsch. Chem. Ges.* **1883**, 16, 487–494.

<sup>11</sup>Radziszewski, Br. *Ber. Dtsch. Chem. Ges.* **1883**, 16, 747–749.

<sup>12</sup>Japp, F. R.; Streatfeild, F. W. *J. Chem. Soc. Trans.* **1882**, 41, 146–156.

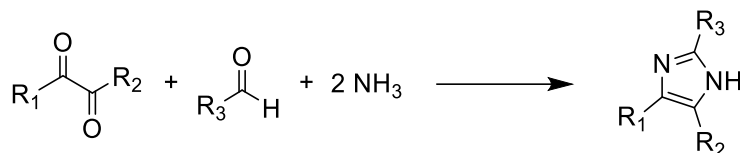
<sup>13</sup>Japp, F. R. *J. Chem. Soc. Trans.* **1883**, 43, 9–18.

<sup>14</sup>Japp, F. R. *J. Chem. Soc. Trans.* **1883**, 43, 197–200.

<sup>15</sup>Japp, F. R.; Hooker, S. C. *J. Chem. Soc. Trans.* **1884**, 45, 672–685.

<sup>16</sup>Japp, F. R.; Wynne, W. P. *J. Chem. Soc. Trans.* **1886**, 49, 462–472.

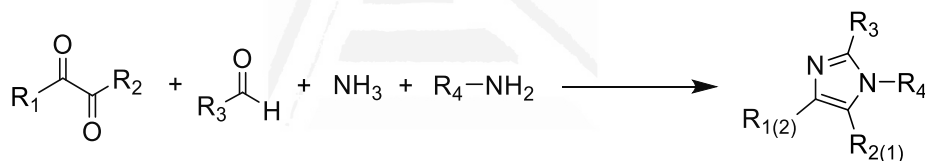
<sup>17</sup>Japp, F. R. L. *J. Chem. Soc. Trans.* **1887**, 51, 557–564.



**Scheme 2.** Debus-Radziszewski-Japp reaction.

Over the years, several approaches have been explored for the synthesis of imidazole derivatives, resulting in hundreds of methodologies reported in literature.<sup>18,19</sup> Overall, they can fit into three distinct categories: ring formation, ring transformation and substitution reactions.

Ring formation reactions are by far the most common and are usually classified according to the number of bonds formed, subdivided by the identity of those involved. The Debus-Radziszewski-Japp reaction, which is still a relevant methodology today, is a prime example of a four-bond forming reaction. An interesting take on this reaction was reported in 1960 by Günther Drefahl and Heinz Herma, in whose paper they describe the synthesis of 1,2,4,5-tetrasubstituted imidazoles by replacing one equivalent of ammonia with a primary amine (**Scheme 3**).<sup>20</sup>



**Scheme 3.** Drefahl-Herma modification of the Debus-Radziszewski-Japp reaction.

Further refinement of this protocol found that ammonium acetate could be used to replace the unwieldy ammonia solutions. Reactions could also be ran using acetic acid as both solvent and promoter.<sup>18</sup> A similar synthetic methodology is the copper(I)-catalyzed Weidenhagen-Herrmann reaction, in which the dicarbonyl compound is replaced by an  $\alpha$ -hydroxyketone.<sup>21</sup>

The Maquenne reaction is another representative example, which involves the use of 2,3-dinitrosuccinic acid and an aldehyde in the presence of ammonia. This protocol was originally designed for the synthesis of 4,5-dicarboxyimidazoles, although it has been phased out in favor of other methodologies (**Scheme 4**).<sup>22</sup>

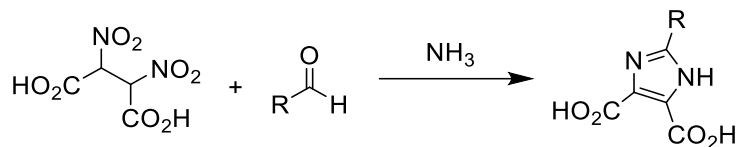
<sup>18</sup>Rossi, R.; Angelici, G.; Casotti, G.; Manzini, C.; Lessi, M. *Adv. Synth. Catal.* **2019**, *361*, 2737–2803.

<sup>19</sup>Shabalin, D. A.; Camp, J. E. *Org. Biomol. Chem.* **2020**, *18*, 3950–3964.

<sup>20</sup>Drefahl, G.; Herma, H. *Chem. Ber.* **1960**, *93*, 486–492.

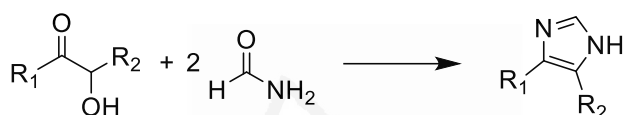
<sup>21</sup>Weidenhagen, R.; Herrmann, R. *Ber. Dtsch. Chem. Ges.* **1935**, *68*, 1953–1961.

<sup>22</sup>Maquenne, H. *Ann. Chim. Phys.* **1891**, *24*, 525.



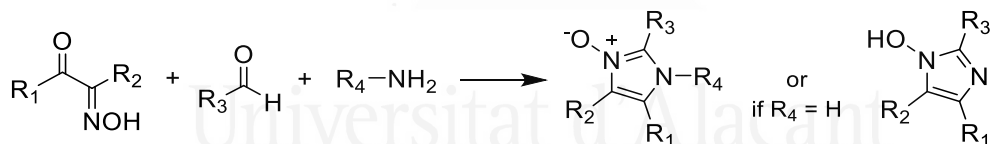
**Scheme 4.** Maquenne synthesis of imidazoles.

Regarding protocols involving the formation of three bonds, one of the most well-known is the Bredereck imidazole synthesis, whereby a formamide reacts with an  $\alpha$ -hydroxyketone to yield 4,5-disubstituted imidazoles (**Scheme 5**). Modifications of this protocol include the use of  $\alpha$ -halo-,  $\alpha$ -acetoxy- and  $\alpha$ -aminoketones as precursors.<sup>23</sup>



**Scheme 5.** Bredereck imidazole synthesis.

Another common methodology, first reported by Ronald Breslow, involves the use of  $\alpha$ -hydroximinoketones in combination with ammonia and an aldehyde, widely employed for the synthesis of 1-hydroxyimidazoles or, if ammonia is replaced by an amine, imidazole *N*-oxides (**Scheme 6**).<sup>23,24</sup>



**Scheme 6.** Synthesis of 1-hydroxyimidazoles and imidazole *N*-oxides.

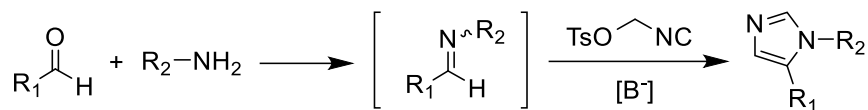
Among the existing protocols for imidazole synthesis by two-bond formation reactions, the Van Leusen reaction stands out. First reported in 1977, this approach involves the use of tosylmethyl isocyanide (TosMIC) in combination with an aldimine in basic conditions.<sup>25</sup> Later on, the protocol was developed further by forming the aldimine *in-situ*, converting it into a two-step process (**Scheme 7**).<sup>26</sup>

<sup>23</sup>Grimmett, M. R. *Science of Synthesis* vol. 12; Thieme Chemistry, 2002.

<sup>24</sup>Breslow, R.; Chung, S. *Tetrahedron Lett.* **1989**, 30, 4353–4356.

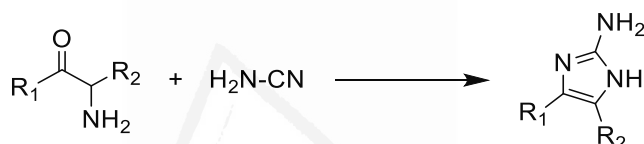
<sup>25</sup>Van Leusen, A. M.; Wildeman, J.; Oldenziel, O. H. *J. Org. Chem.* **1977**, 42, 1153–1159.

<sup>26</sup>Sisko, J.; Kassick, A. J.; Mellinger, M.; Filan, J. J.; Allen, A.; Olsen, M. A. *J. Org. Chem.* **2000**, 65, 1516–1524.



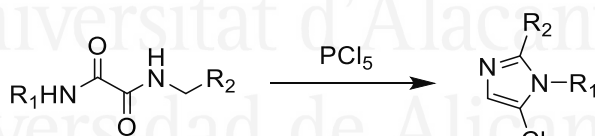
**Scheme 7.** Van Leusen synthesis of imidazoles.

Amidines, guanidines, nitriles and ureas are interesting substrates, offering obvious pathways for imidazole synthesis *via* formation of two C-N bonds. Indeed, numerous methodologies have been described in which they have been combined with a variety of substrates, including diketones,  $\alpha$ -functionalized ketones, isocyanates and activated alkenes, amongst others.<sup>18,19,23</sup> In this regard, the most relevant protocol is the Marckwald reaction, whereby an  $\alpha$ -aminoketone reacts with cyanamide to afford 2-aminoimidazoles (**Scheme 8**).<sup>3</sup>



**Scheme 8.** Marckwald 2-aminoimidazole synthesis.

Protocols involving the formation of a single bond take place through cyclization of a suitable linear substrate. The earliest reported example is the Wallach reaction, in which a *N,N*-disubstituted oxamide undergoes cyclization upon treatment with phosphorus pentachloride, affording 5-chloroimidazole derivatives (**Scheme 9**).<sup>27</sup>



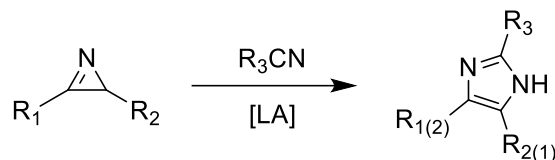
**Scheme 9.** Wallach synthesis of 5-chloroimidazoles.

The formation of imidazoles *via* ring transformation can be approached from several fronts. Ring-size modifications, isomerizations, rearrangements or complete transformations have all been reported as suitable methodologies. For instance, 2*H*-azirines in combination with nitriles readily undergo ring expansion to the corresponding imidazoles in the presence of Lewis acids (**Scheme 10**).<sup>28</sup> Photochemical versions of such approach have also been developed.<sup>29</sup>

<sup>27</sup>Wallach, O. *Liebigs Ann.* **1877**, *184*, 1–127.

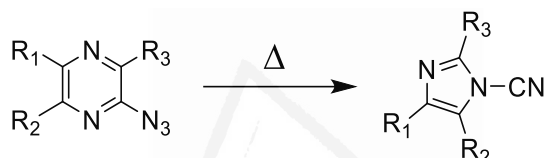
<sup>28</sup>Bader, H.; Hansen, H.-J. *Helv. Chim. Acta* **1978**, *61*, 286–304.

<sup>29</sup>McConaghy, J. S.; Lwowski, W. *J. Am. Chem. Soc.* **1967**, *89*, 4450–4456.



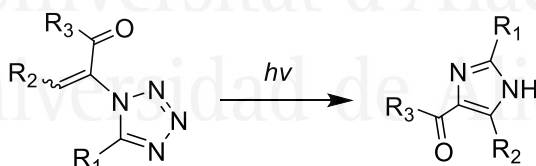
**Scheme 10.** Bader synthesis of imidazoles by ring expansion of 2*H*-azirines.

Similarly, ring contraction reactions of six- or seven-membered heterocycles affording imidazoles have also been described, commonly under harsh thermal, acid-base or redox conditions.<sup>23</sup> One example is the pyrolysis of 2-azidopyrazines, which yields imidazole-1-carbonitriles (**Scheme 11**).<sup>30</sup>



**Scheme 11.** Synthesis of imidazole-1-carbonitriles by pyrolytic ring contraction of pyrazines.

Five-membered heterocyclic compounds can also be transformed into imidazoles. An interesting procedure involves the photochemical isomerization of 1-vinyltetrazoles, which can be used to prepare synthetically challenging 4-acylimidazoles (**Scheme 12**).<sup>31</sup> Other rearrangements affording imidazoles include the Dimroth rearrangement of 5-aminothiazoles<sup>32</sup> and the photoinduced isomerization of pyrazoles.<sup>33</sup>



**Scheme 12.** Synthesis of 4-acylimidazoles by photoinduced rearrangement of 1-vinyltetrazoles.

Relatively labile mononitrogenated heterocycles can be transformed into imidazoles by heating them in the presence of a nitrogen source, such as formamide or ammonia. Oxazoles are a well-known

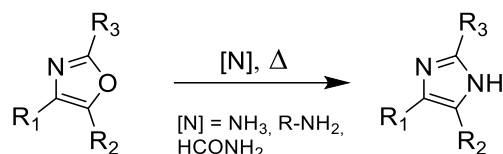
<sup>30</sup>Ohta, A.; Watanabe, T.; Nishiyama, J.; Uehara, K.; Hirate, R. *Heterocycles* **1980**, *14*, 1963–1966.

<sup>31</sup>Casey, M.; Moody, C. J.; Flees, C. W.; Young, R. G. *J. Chem. Soc. Perkin Trans. 1* **1985**, 741–745.

<sup>32</sup>L'Abbé, G.; Meutermans, W.; Bruynseels, M. *Bull. Soc. Chim. Belg.* **1986**, *95*, 1129–1130.

<sup>33</sup>Connors, R. E.; Burns, D. S.; Kurzweil, E. M.; Pavlik, J. W. *J. Org. Chem.* **1992**, *57*, 1937–1940.

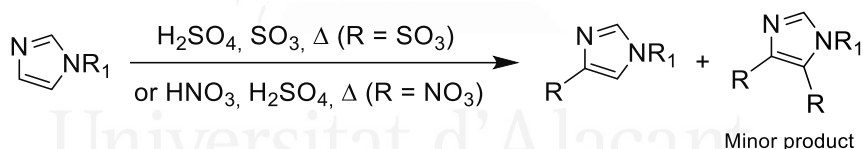
example, readily transforming into imidazoles under such conditions, often assisted by an acidic catalyst (**Scheme 13**).<sup>34–36</sup>



**Scheme 13.** Synthesis of imidazoles from oxazoles.

The last group of synthetic protocols involve the modification of the imidazole core by substitution reactions. The reactivity pattern can be rationalized based on the electron density distribution of the ring and its resonance contributors.

Imidazole is a  $\pi$ -excessive ring, so it readily undergoes aromatic electrophilic substitution reactions. While the most nucleophilic position is the pyridinic nitrogen, actual reactivity depends on the conditions in which the reaction is carried out. For instance, nitration and sulfonation, involving strong mineral acids, happen at positions 4 and 5 (with a marked preference for the former), as the protonation of the nitrogen atom under the reaction conditions inhibits the reaction at both nitrogen-3 itself and carbon-2 (**Scheme 14**).<sup>2</sup>



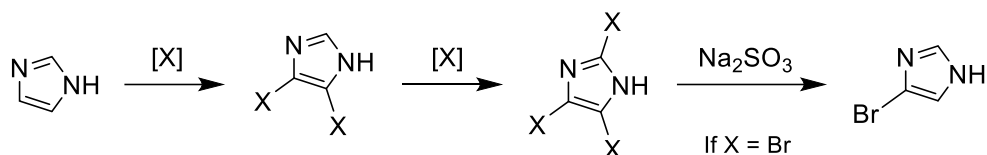
**Scheme 14.** Sulfonation and nitration of imidazole.

The halogenation of imidazole rings is also well-known and takes place under mild conditions. Generally, halogenation occurs at the 4 and 5 positions first, with further treatment resulting in substitution at the 2-position. In the case of bromination, 4-bromoimidazole can be selectively obtained by either treating the corresponding 2,4,5-tribromoimidazole with refluxing aqueous sodium sulfite or by using *N*-bromosuccinimide (NBS) as source of bromine (**Scheme 15**).<sup>2</sup>

<sup>34</sup>Bredereck, H.; Gompper, R.; Wild, H. *Chem. Ber.* **1955**, *88*, 1351–1352.

<sup>35</sup>Bredereck, H.; Gompper, R.; Reich, F. *Chem. Ber.* **1960**, *93*, 723–736.

<sup>36</sup>Sasaki, H.; Kitagawa, T. *Chem. Pharm. Bull.* **1988**, *36*, 3646–3649.



**Scheme 15.** Halogenation of imidazole.

Nucleophilicity at carbon-2 can be greatly enhanced by deprotonation with strong bases, such as *n*-butyllithium, enabling pathways to different substitution patterns.<sup>2,5</sup>

On the other hand, imidazole is not particularly inclined towards aromatic nucleophilic substitution, with C-2 as the most reactive position. Still, 2-haloimidazoles react sluggishly with nucleophiles, often requiring electron withdrawing substituents in the ring to achieve decent conversions.<sup>2</sup>

### GI.1.3. Natural occurrence and pharmaceutical relevance of imidazoles

The imidazole core is ubiquitous in nature and thus, present in a wide variety of biologically relevant compounds. The most important of those is the proteinogenic amino-acid histidine, in which the amphoteric character of the imidazole core is put to good use in enzymatic acid-base catalysis, acting as a proton shuttle.<sup>3</sup> Histidine is also important as a metal-binding cofactor for some metalloproteins, such as hemoglobin. This behavior is exploited as a means to purify proteins by tagging them with multiple histidine residues, then passing them through columns containing metallic cations.<sup>37</sup> Histamine, a vasodilator responsible for allergic reactions, derives from histidine *via* enzymatic decarboxylation (**Figure 2**).<sup>3</sup>

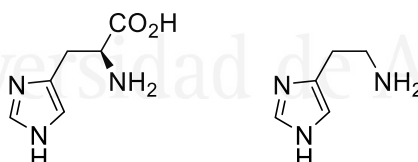


**Figure 2.** L-Histidine (left) and histamine (right).

Multiple commercially available drugs contain imidazole rings. Antifungals, such as Clotrimazole and Eberconazole particularly rely on the imidazole core,<sup>38</sup> although it is also used in the

<sup>37</sup>Bornhorst, J. A.; Falke, J. J. Purification of Proteins Using Polyhistidine Affinity Tags. In *Methods in Enzymology*; Academic Press, 2000, pp 245–254.

<sup>38</sup>Del Palacio, A.; Ortiz, F. J.; Pérez, A.; Pazos, C.; Garau, M.; Font, E. *Mycoses* **2001**, *44*, 173–180.

antibiotic Metronidazole,<sup>3</sup> antineoplastics such as Dacarbazine<sup>2</sup> and the antihypertensive Eprosartan,<sup>3</sup> amongst others (Figure 3).

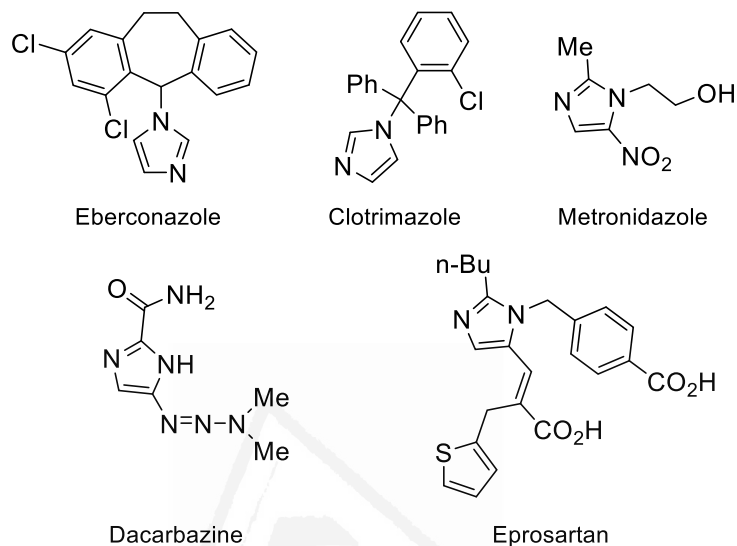


Figure 3. Representative examples of commercialized drugs containing imidazole.



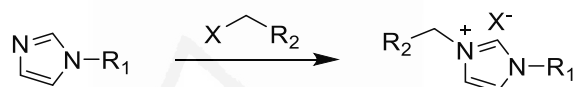


## GI.2. Imidazolium salts

### GI.2.1. Synthesis

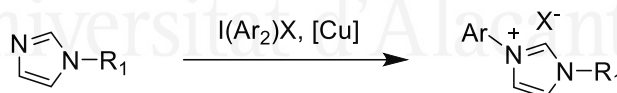
Imidazolium salts consist of cationic 1,3-disubstituted imidazole cores and suitable counter-anions, which can be discrete atom/molecules (halide, tosylate, acetate) or be self-contained within the molecule (e.g., carboxylates) leading to zwitterionic structures.<sup>39</sup>

The most immediately obvious approach for the synthesis of imidazolium salts is by nucleophilic substitution of 1-substituted imidazoles with suitable electrophilic reagents. This methodology is straightforward and simple, allowing to introduce a wide range of functionalized alkyl chains, with the leaving group remaining as counter-anion (**Scheme 16**).<sup>40</sup>



**Scheme 16.** Synthesis of imidazolium salts by nucleophilic substitution.

However, this protocol is mostly limited to alkyl derivatives, owing to the generally low reactivity of their aryl counterparts towards  $S_N2$  processes. Indeed, only strongly electron-deficient aromatic systems react smoothly, with other substrates requiring extremely long reaction times or very harsh conditions.<sup>41,42</sup> More recently, the use of hypervalent iodine species under copper catalysis has been reported for the arylation of *N*-substituted imidazoles, circumventing this issue (**Scheme 17**).<sup>43</sup>



**Scheme 17.** Copper-catalyzed arylation of *N*-substituted imidazoles with hypervalent iodine reagents.

Besides further functionalization of *N*-substituted imidazoles, imidazolium salts can also be directly synthesized, forming the heterocyclic core from scratch. This possibility first became apparent in 1988 after Velišek and coworkers reported the discovery of the zwitterionic 1,3-bis(carboxymethyl)imidazole in a mixture of glyoxal and glycine,<sup>44</sup> in conditions alike to Debus' first

<sup>39</sup>Kratochvíl, B.; Ondráček, J.; Velišek, J.; Hašek, J. *Acta Crystallogr. C* **1988**, *44*, 1579–1582.

<sup>40</sup>Allegue, A.; Albert-Soriano, M.; Pastor, I. M. *Appl. Organomet. Chem.* **2015**, *29*, 624–632.

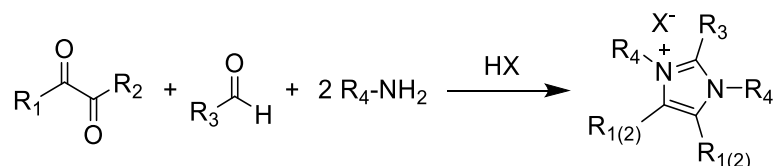
<sup>41</sup>Zhu, Z.-Q.; Xiang, S.; Chen, Q.-Y.; Chen, C.; Zeng, Z.; Cui, Y.-P.; Xiao, J.-C. *Chem. Commun.* **2008**, 5016–5018.

<sup>42</sup>Truscott, B. J.; Klein, R.; Kaye, P. T. *Tetrahedron Lett.* **2010**, *51*, 5041–5043.

<sup>43</sup>Lv, T.; Wang, Z.; You, J.; Lan, J.; Gao, G. *J. Org. Chem.* **2013**, *78*, 5723–5730.

<sup>44</sup>Velišek, J.; Davídek, T.; Davíek, J.; Trška, P.; Kvasnička, F.; Velcová, K. *J. Food Sci.* **1989**, *54*, 1544–1546.

report of imidazole.<sup>39</sup> Following up on this, the US chemist Anthony J. Arduengo III patented in 1991 his synthesis of imidazolium salts as an evolution of the Drefahl-Herma modification of the Debus-Radziszewski-Japp reaction, in which both equivalents of ammonia were replaced by a primary amine and a hydrohalic acid was used both as a catalyst and as a source of counter-anion (**Scheme 18**).<sup>45</sup>



**Scheme 18.** Arduengo synthesis of imidazolium salts.

Arduengo's synthesis is one of the most widely used protocols for the synthesis of symmetrically substituted imidazolium salts.<sup>46</sup> Its main drawbacks are the lack of selectivity when using two different primary amines, as well as its general incompatibility with arylamines, which require a two-step approach—forming the diimine first, then reacting with an aldehyde or orthoformate—to form the ring effectively.<sup>47</sup>

Imidazolium salts can also be obtained from the corresponding oxazolium salts and a primary amine, as described in section **GI.1.2** of this manuscript (**Scheme 13**). It is worth noting that this methodology is compatible with aliphatic and aromatic substrates alike.<sup>48</sup>

The modification of imidazolium salts is mostly analogous to that of imidazole itself, although its cationic nature results in markedly different reactivity. The most important type of transformation for these systems, however, does not involve the imidazolium ring, but the counter-anion. Anion-exchange reactions are ubiquitous in imidazolium salt chemistry, as the counter-anion has a massive influence on the physical-chemical properties of the system. As direct reaction with the alkyl/aryl/acid derivatives is not always possible, exchange becomes the only way to introduce exotic anions, such as  $\text{PF}_6^-$ ,  $\text{BF}_4^-$  or  $\text{SbF}_6^-$ . Commonly, the protocol involves the treatment of the precursor imidazolium salt with excess salt containing the desired anion.<sup>48</sup>

<sup>45</sup>Arduengo, A. J. Preparation of 1,3-Disubstituted Imidazolium Salts. US5182405A, 1991.

<sup>46</sup>Martos, M.; Albert-Soriano, M.; Pastor, I. M. *Molbank* **2022**, M1480.

<sup>47</sup>Pesch, J.; Harms, K.; Bach, T. *Eur. J. Org. Chem.* **2004**, 2025–2035.

<sup>48</sup>Topchiy, M. A.; Zotova, M. A.; Masoud, S. M.; Mailyan, A. K.; Ananyev, I. V.; Nefedov, S. E.; Asachenko, A. F.; Osipov, S. N. *Chem. Eur. J.* **2017**, *23*, 6663–6674.

## GI.2.2. Catalytic systems based on imidazolium salts

In lieu of their ease of obtention and modification, their high stability and some unique intrinsic properties, imidazolium salts are present in a broad range of catalytic systems. In this section, the role of imidazolium salts in *N*-heterocyclic carbene chemistry and ionic liquids will be presented. Low transition temperature mixtures, ionic organic solids and metal-organic frameworks based on imidazolium salts will be described in detail in their corresponding chapters (Chapters 1, 3 and 4, respectively).

### *N*-Heterocyclic carbenes

One of the main features of imidazolium salts is the possibility of forming the corresponding *N*-heterocyclic carbenes (NHCs) by deprotonation at the C-2 position. The resulting carbenes, formally neutral divalent carbon atoms, are stabilized by charge delocalization from the  $\pi$ -orbitals of neighboring nitrogen atoms to the empty  $p_{\pi}$  orbital of the carbene. This effectively forms a four-electron, three-center system, which helps mitigate the electron deficiency of the carbene, thus making it abnormally stable (Figure 4).<sup>49</sup>

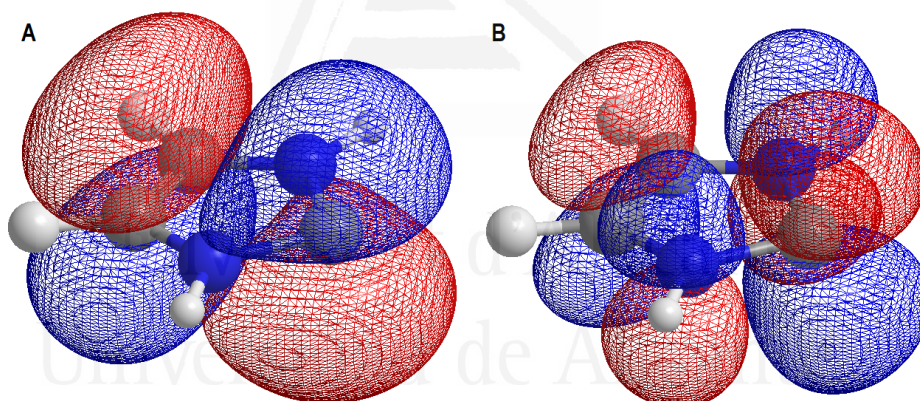


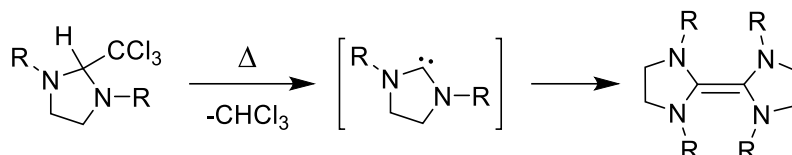
**Figure 4.** (A)  $\pi$ -Orbitals (HOMO-1) and (B) empty  $p_{\pi}$  orbitals (LUMO) (B) of a model NHC.

NHCs had been known since as early as 1957, when Ronald Breslow published a report about the base-promoted hydrogen-deuterium exchange at the C-2 position of thiazoles.<sup>50</sup> Interest in the field quickly arose and in 1960, Hans-Werner Wanzlick and coworkers reported the first evidence of imidazole-based NHCs. They had envisioned the formation of the carbene by vacuum pyrolysis of 2-trichloromethylidihydroimidazoles and, although the resulting carbene was too unstable to be isolated,

<sup>49</sup>Diez-Gonzalez, S. *N-Heterocyclic Carbenes*; The Royal Society of Chemistry, 2011

<sup>50</sup>Breslow, R. *J. Am. Chem. Soc.* **1957**, *79*, 1762–1763.

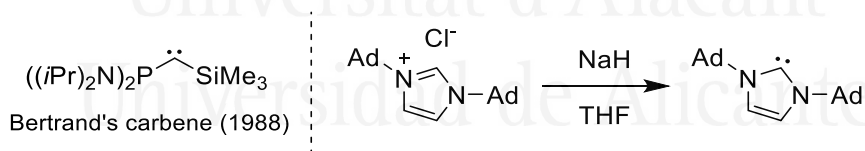
the obtention of the dihydroimidazol-2-ylidene dimer suggested the presence of an imidazolium-NHC intermediate (**Scheme 19**).<sup>51,52</sup>



**Scheme 19.** First evidence of an imidazole-NHC formation by Wanzlick.

Although these results were compelling evidence that carbenic species were actually forming (the formation of the dimer from the free carbene would be eventually known as Wanzlick's equilibrium),<sup>53</sup> NHCs themselves remained elusive throughout the 1960s. In 1968, Wanzlick proposed a C-2 deprotonation approach for the obtention of NHCs starting from imidazolium salts, and managed to trap the carbene intermediate with water and mercury salts, the latter of which became the first report of a transition metal NHC complex.<sup>54</sup> Later that year, Öfele and coworkers also reported the formation of chromium imidazolium-NHCs.<sup>55</sup> Still, attempts at obtaining free carbenes were unsuccessful all the way to the 1990s.

It was not until 1991 when Arduengo's group, inspired by Bertrand's 1988 report of a stable phosphinocarbene, created the first isolable imidazolium NHC, following the deprotonation pathway originally postulated by Wanzlick.<sup>49</sup> The key element in their approach was the use of bulky adamantyl groups as *N*-substituents, which provided shielding and electron density (via  $\sigma$ -back donation) to the carbenic center, preventing dimerization (**Scheme 20**).<sup>56</sup>



**Scheme 20.** Arduengo's synthesis of isolable carbenes. Note the similarities in the steric environment of Arduengo's and Bertrand's carbenes.

<sup>51</sup>Wanzlick, H.-W.; Schikora, E. *Angew. Chem.* **1960**, *72*, 494.

<sup>52</sup>Wanzlick, H.-W.; Schikora, E. *Chem. Ber.* **1961**, *94*, 2389–2393.

<sup>53</sup>Nicholls, T. P.; Williams, J. R.; Willans, C. E. Reactivities of N-Heterocyclic Carbenes at Metal Centers. In *Advances in Organometallic Chemistry*; Pérez, P. J., Ed.; Academic Press, 2021, pp 245–329.

<sup>54</sup>Wanzlick, H.-W.; Schönherr, H.-J. *Angew. Chem. Int. Ed.* **1968**, *7*, 141–142.

<sup>55</sup>Öfele, K. *J. Organomet. Chem.* **1968**, *12*, 42–43.

<sup>56</sup>Arduengo, A. J.; Harlow, R. L.; Kline, M. A. *J. Am. Chem. Soc.* **1991**, *113*, 361–363.

Arduengo's report reignited the interest of the scientific community in NHCs, and their potential as components of catalytic systems did not go unnoticed.<sup>57</sup> From there, two distinct fields of research in NHC catalysis emerged, their use as ligands for transition metal complexes and as standalone organocatalysts.

Imidazolium NHCs are  $\sigma$ -basic ligands for metals, with an electronic behavior akin to that of phosphines.<sup>57</sup> The first report of a reaction employing a transition metal NHC complex was the palladium-catalyzed Heck olefination of aryl halides, published by Herrmann and coworkers in 1995, in which the remarkable stability and high turnover of the NHC catalyst was highlighted.<sup>58</sup> NHCs proved to be particularly good ligands for palladium, as their strong  $\sigma$ -donating character enables the use of challenging substrates, e.g., aryl chlorides or unactivated C-H bonds for cross-coupling reactions. Over the next decade, the research groups of Herrmann, Nolan, Beller and Caddick each developed their own NHC ligands for palladium.<sup>59</sup>

In 2006, Organ and coworkers presented the PEPPSI (standing for Pyridine-Enhanced Precatalyst Preparation, Stabilization, Initiation) family of palladium-NHC complexes (**Figure 5**). These were simple and very effective catalytic systems, prepared in up to kilogram scale from readily available components, thus representing a major improvement over previously reported systems and a breakthrough in the industrialization of NHC catalysts.<sup>57,60</sup> PEPPSI complexes have been used to promote a broad range of cross-coupling transformations, including Suzuki-Miyaura, Negishi, Buchwald-Hartwig and Kumada-Tadao reactions.<sup>57,59</sup>

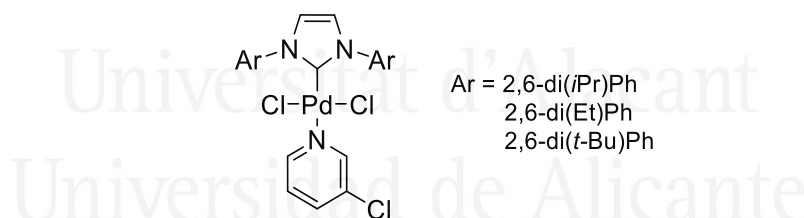


**Figure 5.** Representative PEPPSI complexes.

<sup>57</sup>Cazin, C. S. J. *N-Heterocyclic Carbenes in Transition Metal Catalysis and Organocatalysis*; Springer International Publishing, 2011.

<sup>58</sup>Herrmann, W. A.; Elison, M.; Fischer, J.; Köcher, C.; Artus, G. R. J. *Angew. Chem. Int. Ed.* **1995**, *34*, 2371–2374.

<sup>59</sup>Organ, M. G.; Chass, G. A.; Fang, D.-C.; Hopkinson, A. C.; Valente, C. *Synthesis* **2008**, 2776–2797.

<sup>60</sup>O'Brien, C. J.; Kantchev, E. A. B.; Valente, C.; Hadei, N.; Chass, G. A.; Lough, A.; Hopkinson, A. C.; Organ, M. G. *Chem. Eur. J.* **2006**, *12*, 4743–4748.

Besides palladium chemistry, NHCs are very present in ruthenium-catalyzed processes, most notably as ligands from the second generation onwards of Grubbs olefin metathesis catalysts, including the Hoveyda-Grubbs and Zhan catalysts (**Figure 6**).<sup>61,62</sup>

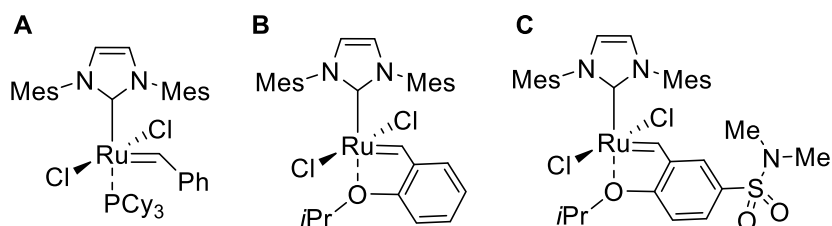


**Figure 6.** Second-generation Grubbs (A), Hoveyda-Grubbs (B) and Zhan (C) catalysts.

The field of NHC-metal catalysis is in constant expansion, and although palladium still holds a dominant position in NHC chemistry, complexes of other metals, such as nickel, iridium, rhodium or cobalt have been applied to a broad range of reactions, including carbonylations, hydroformylations and oxidations.<sup>57</sup>

Regarding the use of standalone NHCs as organocatalysts, the field has experienced massive growth over the last few decades.<sup>63</sup> The first investigations in the matter arose from Breslow's groundbreaking 1958 report on the mechanism of action of vitamin B1, thiamine, which contains a thiazolium core (**Figure 7**).<sup>64</sup>

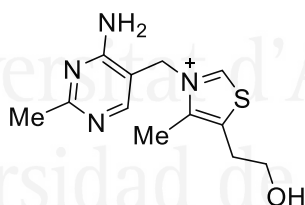


**Figure 7.** Thiamine (vitamin B1).

Ugai and coworkers had previously demonstrated that thiazolium salts could be used to catalyze the self-condensation of benzaldehyde to generate benzoin, although there was not a consensus about the actual mechanism of the reaction.<sup>63,65</sup> Inspired by Lapworth's 1903 mechanistic proposal on the cyanide-catalyzed benzoin condensation and his recent discovery of the H/D exchange

<sup>61</sup>Ogba, O. M.; Warner, N. C.; O'Leary, D. J.; Grubbs, R. H. *Chem. Soc. Rev.* **2018**, *47*, 4510–4544.

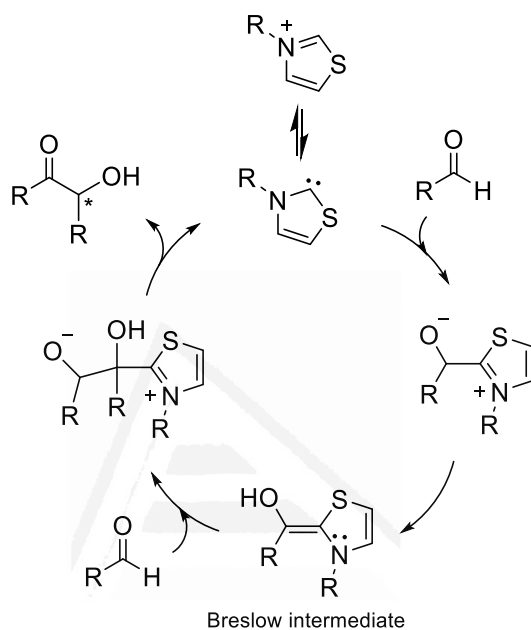
<sup>62</sup>Zhan, Z.-Y. *Recyclable Ruthenium Catalysts for Methatesis Reactions*. US20070043180A1, 2006.

<sup>63</sup>Enders, D.; Niemeier, O.; Henseler, A. *Chem. Rev.* **2007**, *107*, 5606–5655.

<sup>64</sup>Breslow, R. *J. Am. Chem. Soc.* **1958**, *80*, 3719–3726.

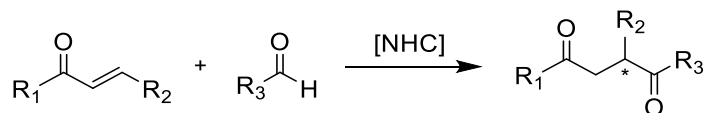
<sup>65</sup>Marion, N.; Díez-González, S.; Nolan, S. P. *Angew. Chem. Int. Ed.* **2007**, *46*, 2988–3000.

in thiazoles, Breslow proposed a reaction mechanism *via* enaminol intermediate (**Scheme 21**).<sup>64</sup> After some discussion in the scientific community, including the proposal of dimeric carbene species being the actual catalysts, Breslow's theory was accepted, with the key intermediate of the reaction bearing his name.<sup>63</sup>



**Scheme 21.** NHC-catalyzed benzoin condensation mechanism proposed by Breslow. Note the formation of a stereocenter in the product.

In consequence, NHC organocatalysis is mostly centered around carbonyl compounds, where the nucleophilic character of the Breslow intermediate is exploited to great effect for umpolung carbonyl reactions.<sup>57,63,65</sup> Among these, the benzoin condensation has long been the benchmark for the development of novel NHC catalysts. A notable variant of this transformation is the Stetter reaction, in which a Michael acceptor is used as a partner for the acyl anion surrogate (**Scheme 22**).<sup>66,67</sup>



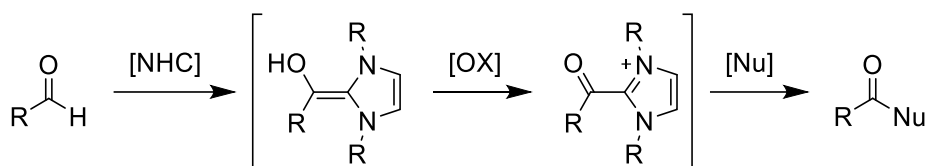
**Scheme 22.** General scheme of the Stetter reaction.

<sup>66</sup>Stetter, H.; Schreckenberger, M. *Angew. Chem. Int. Ed.* **1973**, *12*, 81.

<sup>67</sup>Stetter, H.; Rämisch, R. Y.; Kuhlmann, H. *Synthesis* **1976**, 733–735.



Benzoin and Stetter reactions have been extensively studied, with intramolecular cyclizations, multicomponent and tandem processes as well as asymmetric variants being reported over the years.<sup>57,63,65</sup> A relatively recent development in NHC organocatalyzed reactions is the oxidation of the Breslow intermediate to the corresponding acyl azolium.<sup>57,68</sup> This highly activated intermediate allows the direct introduction of nucleophiles in aldehydes, thus being a powerful synthetic tool (**Scheme 23**).



**Scheme 23.** Oxidative NHC catalysis.

### Ionic liquids (ILs)

Ionic liquids (ILs) are liquid substances composed entirely by ionic species. Although by definition any molten salt could qualify as an IL, the general consensus is to narrow down the definition of IL as any fully ionic substance with a melting point under 100 °C.<sup>69</sup> Most ILs consist of organic cations (alkyl/arylammonium, pyridinium, imidazolium, phosphonium, sulfonium, etc.) and a variety of weakly coordinating counter-anions (**Figure 8**).<sup>69-71</sup>

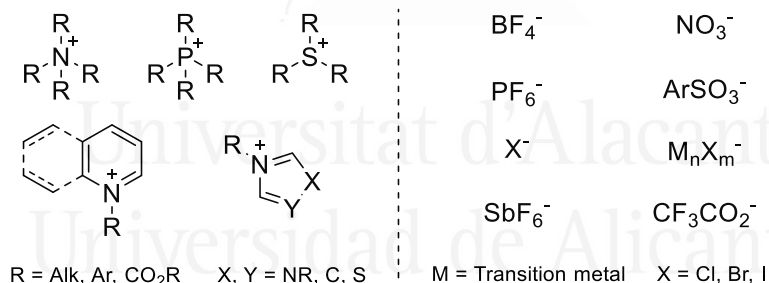


**Figure 8.** Representative components of ILs.

ILs are not a recent discovery. With a melting point of 55 °C, ethanolanmonium nitrate, reported by Gabriel and Weiner in 1888, was by definition the first IL ever described.<sup>72</sup> Ethylanmonium nitrate

<sup>68</sup>Bacaicoa, S.; Goossens, E.; Sundén, H. *Org. Lett.* **2022**, *24*, 9146–9150.

<sup>69</sup>Crosthwaite, J. M.; Muldoon, M. J.; Dixon, J. K.; Anderson, J. L.; Brennecke, J. F. *J. Chem. Thermodyn.* **2005**, *37*, 559–568.

<sup>70</sup>Plechova, N. V.; Seddon, K. R. *Chem. Soc. Rev.* **2008**, *37*, 123–150.

<sup>71</sup>Sheldon, R. *Chem. Commun.* **2001**, 2399–2407.

<sup>72</sup>Gabriel, S.; Weiner, J. *Ber. Dtsch. Chem. Ges.* **1888**, *21*, 2669–2679.

(m.p. 12 °C), discovered by Paul Walden in 1914, is widely considered to be the first room-temperature IL (RTIL).<sup>73</sup> Relegated to obscurity for a long time, with some brief appearances from the 1930s to 50s,<sup>70,71,74</sup> ILs started to gain traction after a 1975 report by Osteryoung and coworkers, in which they studied the electrochemical behavior of iron complexes in an ethylpyridinium chloroaluminate RTIL.<sup>75</sup> Further research in the field resulted in the first imidazolium RTILs, reported by Wilkes and coworkers in 1982,<sup>76</sup> which were later shown to be able to promote Friedel-Crafts alkylations.<sup>77</sup>

While RTILs with chloroaluminate counter-anions were indeed effective for acidic catalysis (for instance, emimAlCl<sub>4</sub> has a Hammett acidity of -18) and showed interesting electrochemical properties<sup>71,75,76</sup> their sensitivity to air and moisture severely limited their applicability, and thus, interest in them remained moderate.<sup>71</sup> In 1992, the group of Wilkes made a major breakthrough with their report of stable RTILs based on dialkylimidazolium cations and tetrafluoroborate anions,<sup>78</sup> with the corresponding hexafluorophosphate following suit two years later.<sup>79</sup> The advent of stable RTILs resulted in a massive expansion of the field, with many research groups devoting their efforts to study these new systems.<sup>70</sup> The implementation of RTILs as prospective replacement for common organic solvents was a field of particular interest, in which these systems offered interesting advantages.

First, due to the high number of interactions present within ILs, arising from their purely ionic nature, their volatility is almost non-existent, thus avoiding solvent-borne atmospheric pollution. Depending on the components, they also offer broad thermal stability ranges, with some imidazolium ILs only decomposing at temperatures exceeding 400 °C, and are generally non-flammable as well.<sup>70,71</sup>

Secondly, the synthetic protocols to obtain ILs are relatively simple, and the combination of cations and anions is virtually limitless. Therefore, parameters such as polarity, lipophilicity/hydrophilicity, melting point or viscosity can be easily tailored to suit any prospective application.<sup>70</sup> Additionally, the intrinsic ionic nature of ILs means they can effectively dissolve a broad range of different substrates, from inorganic compounds to gasses.<sup>71</sup> It is important to note that adequately functionalized ILs, as the original chloroaluminate liquids, can act as non-innocent solvents, providing both dispersion media and catalyst for the reaction in a single component.<sup>77</sup>

Over the following two decades, RTILs were applied as solvents and catalysts to numerous reactions, with imidazolium-based systems having a dominant role, as they offered superior stability,

<sup>73</sup>Walden, P. *Bull. Acad. Imper. Sci.* **1914**, 1800.

<sup>74</sup>Hurley, F. H.; Wier, T. P. *J. Electrochem. Soc.* **1951**, 98, 207.

<sup>75</sup>Chum, H. L.; Koch, V. R.; Miller, L. L.; Osteryoung, R. A. *J. Am. Chem. Soc.* **1975**, 97, 3264–3265.

<sup>76</sup>Wilkes, J. S.; Levisky, J. A.; Wilson, R. A.; Hussey, C. L. *Inorg. Chem.* **1982**, 21, 1263–1264.

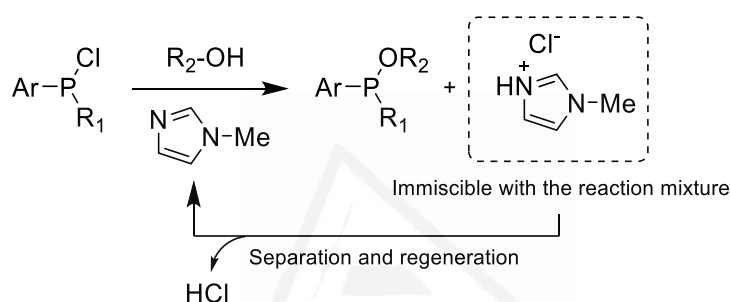
<sup>77</sup>Boon, J. A.; Levisky, J. A.; Pflug, J. L.; Wilkes, J. S. *J. Org. Chem.* **1986**, 51, 480–483.

<sup>78</sup>Wilkes, J. S.; Zaworotko, M. J. *J. Chem. Soc. Chem. Commun.* **1992**, 965–967.

<sup>79</sup>Fuller, J.; Carlin, R. T.; De Long, H. C.; Haworth, D. *J. Chem. Soc. Chem. Commun.* **1994**, 299–300.

modularity, greater liquid ranges and chemical characteristics (such as the possibility of forming NHCs *in-situ*)<sup>80,81</sup> than their pyridinium, ammonium or phosphonium counterparts while having a generally lower cost.<sup>82</sup>

ILs were not limited to lab-scale research, with some innovations reaching the industry. The Eastman Chemical Company had been utilizing ILs at industrial scale since 1996, whereas the German multinational BASF implemented several synthetic protocols relying on imidazolium ILs in the early 2000s, including the award-winning BASIL (from Biphasic Acid Scavenging utilizing Ionic Liquids) process in 2002 (**Scheme 24**).<sup>70</sup>



**Scheme 24.** BASIL process developed by BASF.

Although initially promising, ILs suffered from a series of severe drawbacks. Due to the impossibility of cost-effective purification (as distillation of ILs is limited to a few select examples under ultrahigh vacuum),<sup>83</sup> synthetic protocols need to be very clean, which is not always possible. Concerns were raised about the toxicity and low biodegradability of the components, as well as the steep cost of operation, as ILs are in excess of a hundred times more expensive per mole than common organic solvents.<sup>70,84</sup> These issues would eventually result in ILs being phased out in favor of emerging alternative solvent systems,<sup>84</sup> although they still are present in catalysis,<sup>81</sup> as well as in some specialized applications.<sup>70</sup>

<sup>80</sup>Wellens, S.; Brooks, N. R.; Thijs, B.; Meervelt, L. V.; Binnemans, K. *Dalton Trans.* **2014**, 43, 3443–3452.

<sup>81</sup>Axelsson, A.; Ta, L.; Sundén, H. *Catalysts* **2015**, 5, 2052–2067.

<sup>82</sup>Subasree, N.; Selvi, J. A. *Heliyon* **2020**, 6, e03498.

<sup>83</sup>Armstrong, J. P.; Hurst, C.; Jones, R. G.; Licence, P.; Lovelock, K. R. J.; Satterley, C. J.; Villar-Garcia, I. J. *Phys. Chem. Chem. Phys.* **2007**, 9, 982–990.

<sup>84</sup>Alonso, D. A.; Baeza, A.; Chinchilla, R.; Guillena, G.; Pastor, I. M.; Ramón, D. J. *Eur. J. Org. Chem.* **2016**, 612–632.

## GI.3. Sustainable chemistry

### GI.3.1. Challenges in the design of sustainable chemical processes

Throughout the last few decades, the general public has been experiencing a steady increase in environmental awareness, as the consequences of uncontrolled human activity have become increasingly noticeable. Pollution in all its variants as well as the eventual depletion of non-renewable resources are the main concerns voiced.<sup>84</sup> To ensure humankind's expansion and ever-increasing development do not become its undoing, science has stepped up to the challenge of sustainability, approaching the issue from several fronts.

In the field of chemistry, many—at times overlooked—advances have been made throughout the years. One of such examples is the development of high-octane unleaded gasoline. The anti-knock properties of tetraethyllead (TEL) were discovered by Midgey and coworkers at the General Motors research laboratory in 1921 and resulted in its rapid and widespread implementation as a petrol additive during the 1920s. This resulted in internal combustion engines (ICEs) being able to run at higher compression ratios, increasing thermal efficiency and power output while decreasing fuel consumption. However, the ill-effects of lead in the environment were well-known and during the 1970s, governments started banning leaded gasoline. Thus, high-octane rating unleaded gasolines were developed using methyl *tert*-butyl ether (MTBE) as well as aromatic hydrocarbons as anti-knock additives.<sup>85</sup> This went in hand with the development and implementation of the three-way catalytic converter, one of the most widespread and important inventions for pollution control, which drastically reduces NO<sub>x</sub>, CO and particle emissions of ICEs.<sup>86,87</sup>

These developments are examples of how research on sustainable chemistry focuses on the development of new protocols with reduced environmental impact, be it completely novel processes or refinements of established methodologies.

When considering a model reaction, there are several ways in which its environmental impact can be reduced.<sup>88</sup> First and foremost, proper design and refinement of the synthetic protocol is of the utmost importance to ensure maximum efficiency, minimize byproduct formation and guarantee safe operation.<sup>89</sup> Often, equivalents of reagents, solvent volume and reaction temperature can all be reduced without significantly impacting yields and reaction times. A difference of 10 °C, 0.1 equivalents

<sup>85</sup>Thomas, V. M. *Annu. Rev. Energy. Environ.* **1995**, *20*, 301–324.

<sup>86</sup>Kašpar, J.; Fornasiero, P.; Hickey, N. *Catal. Today* **2003**, *77*, 419–449.

<sup>87</sup>Bell, A. T. The Impact of Nanoscience on Heterogeneous Catalysis. *Science* **2003**, *299*, 1688–1691.

<sup>88</sup>Clark, J. H.; Macquarrie, D. J. *Handbook of Green Chemistry and Technology*; Blackwell Science, 2002.

<sup>89</sup>Tang, S. L. Y.; Smith, R. L.; Poliakov, M. *Green Chem.* **2005**, *7*, 761–762.

of reagent, or 5% more byproduct may be insignificant at lab scale, but quickly add up at industrial level.

Catalysis is the main tool in the arsenal of the modern chemist. Catalysts reduce the energetic requirements of reactions, usually resulting in increased yields, lower reaction times, higher selectivity (i.e., less byproducts) and at times, catalysis becomes the only way to carry out certain types of reactions. It is clear then, why it is such an invaluable asset for sustainable chemistry.<sup>90,91</sup>

Another way of approaching sustainable transformations is to replace reaction components for less harmful equivalents.<sup>92</sup> When dealing with reactants, more often than not, this goes in hand with catalysis. For instance, from an environmental and economic standpoint, alcohols are preferable to halides for substitution reactions, but they are way less reactive, thus requiring more effective catalysts.<sup>93</sup> The purest form of this approach is the use of alternative solvents, which rose to prominence in the early 1990s, after the massive environmental impact of the then ubiquitous halogenated solvents was finally realized.<sup>84</sup> Less dangerous substances also result in lower costs, which carry over to any derived products.

Chemistry still relies heavily on non-renewable assets. Precious metals or fossil fuel derivatives (reactants and solvents) are limited resources, the depletion of which is inevitable given enough time. Thus, when possible, feedstocks should be obtained from renewable sources, to ensure sustainable chemical processes.<sup>94</sup> An excellent way of addressing this issue is to use byproducts from a given process as feedstock for another, the so-called circular economy, which has the added benefit of massively reducing the overall waste generation.<sup>95</sup>

These principles are very clear and offer guidance for the design of minimally harmful processes. However, the actual implementation is not as straightforward as it looks, as some of these interfere with each other. Often, the perfect synthesis in economic terms may be horrible in terms of sustainability, both immediate and long term, and *vice-versa* and thus, compromises must be made.

One of the most obvious examples are iridium complexes. They are top-of-the-line catalysts for a wide array of transformations and can very effectively promote reactions at trace concentrations (as low as 0.1 mol%). However, iridium is very scarce and thus, hardly sustainable, besides being extremely expensive. Still, one could argue that it is active in so little amount, it is actually better to just

---

<sup>90</sup>Clark, J. H. *Pure Appl. Chem.* **2001**, *73*, 103–111.

<sup>91</sup>Kaneda, K.; Mizugaki, T.; Mitsudome, T. *Encyclopedia of Catalysis*, 2010.

<sup>92</sup>Sheldon, R. A. *Chem. Soc. Rev.* **2012**, *41*, 1437–1451.

<sup>93</sup>Martos, M.; Pérez-Almarcha, Y.; Pastor, I. M. *Eur. J. Org. Chem.* **2022**, e202201221.

<sup>94</sup>Zakzeski, J.; Bruijninx, P. C. A.; Jongerius, A. L.; Weckhuysen, B. M. *Chem. Rev.* **2010**, *110*, 3552–3599.

<sup>95</sup>Keijer, T.; Bakker, V.; Slootweg, J. C. *Nat. Chem.* **2019**, *11*, 190–195.

stick to iridium rather than using 100 times more amount (which would be just 10 mol%) of an abundant but less effective catalyst. Reagents are not exempt of such controversy. Is it worse to use moderately harmful reagents (acyl chlorides, for instance) rather than using 10 times the amount of a more benign but also less active compound, generating much more waste?

These are only two examples of the issues which may arise when designing any given chemical process. It is clear then, that sustainability cannot be easily determined at first glance, and quantitative means of comparison are needed. To this end, sustainability metrics have been developed over the years, providing means to unbiasedly assess and compare the environmental impact of chemical protocols.

### GI.3.2. Sustainability metrics

Generally, sustainability metrics fall into two main categories depending on their focus. Mass efficiency metrics quantitatively analyze the use of mass in the reaction and quantify waste generation. Impact metrics, on the other hand, are semiquantitative methods which take into account the actual environmental footprint of the materials and protocols involved.<sup>88,96,97</sup>

For mass efficiency analysis, the most representative metrics are reaction yield, atom economy, E-factor, reaction mass efficiency, stoichiometric factor and materials recovery parameter.

#### Reaction yield (Y)

Calculating reaction yields has traditionally been the first way of comparing the overall performance of a given synthetic protocol with previously established methodologies. It is obtained as the actual mass of product obtained over the theoretical value and expressed as a percentage (Equation 1).<sup>97</sup>

$$Y = \frac{\text{Mass of product obtained}}{\text{Theoretical mass of product}} \cdot 100 \quad (1)$$

#### Atom economy (AE)

The very first proper sustainability metric was atom economy, introduced by Barry Trost in 1991.<sup>98</sup> AE is a measure of how many atoms of the reactants end up in the product, providing an overview on how well-designed a reaction is. Thus, AE is calculated as the molecular weight of the product ( $MW_P$ ) over the sum of the adjusted molecular weight of the reactants ( $MW_R$  times  $S_R$ , where

<sup>96</sup>Curzons, A. D.; Constable, D. J. C.; Mortimer, D. N.; Cunningham, V. L. *Green Chem.* **2001**, 3, 1–6.

<sup>97</sup>Andraos, J. *Reaction Green Metrics. Problems, Exercises and Solutions*; CRC Press, 2019.

<sup>98</sup>Trost, B. *Science* **1991**, 254, 1471–1477.

the latter is the stoichiometric coefficient of the reactant) and expressed as a percentage (**Equation 2**). Only stoichiometric reactants are considered and 100% yield is assumed, so AE is a purely theoretical metric.<sup>97</sup>

$$AE = \frac{MW_P}{\sum (S_R \cdot MW_R)} \cdot 100 \quad (2)$$

### E-factor

The E-factor was proposed by Roger Sheldon in 1992,<sup>99</sup> as means of quantifying the overall waste production relative to product output. It provides the mass of waste generated per unit mass of product, calculated as mass of all components used generated minus mass of product over mass of product (**Equation 3**). The obtained value is the raw E-factor, which may be adjusted accounting for the recovery of components. The individual contributions for reagents, solvents, catalysts and purification to the overall E-factor can be calculated using the same equation and provide a more detailed insight on the process.<sup>97</sup>

$$E\text{-factor} = \frac{\sum \text{Mass of components} - \text{Mass of product}}{\text{Mass of product}} \quad (3)$$

The E factor is one of the most widespread green metrics. Target E-factor intervals have been defined for several industrial sectors, allowing for quick assessment of any given process (**Table 1**). In general terms, the tolerance for E-factors depends on the added value of the product.<sup>100</sup>

**Table 1.** Target E-factor intervals for the chemical industry.

| Industry level  | Desirable E-Factor range |
|-----------------|--------------------------|
| Oil refining    | < 0.1                    |
| Bulk chemicals  | 1 to 5                   |
| Fine chemicals  | 5 to 50                  |
| Pharmaceuticals | 25 to 100                |

### Reaction Mass Efficiency (RME) and Process Mass Intensity (PMI)

The concept of RME was first introduced by Alan Curzons and coworkers in 2001, as an evolution of AE.<sup>96</sup> It represents the amount of reagent mass that ends up in the product, expressed as a percentage. Thus, it is obtained by dividing the isolated mass of product by the total mass of reagents.

<sup>99</sup>Sheldon, R. A. *Chem. Ind.* **1992**, 903–906.

<sup>100</sup>Sheldon, R. A. *Green Chem.* **2007**, 9, 1273–1283.

The inverse of  $RME_{Curzons}$  is known as PMI and is used to the same effect (**Equation 4**).<sup>97</sup> These metrics provide a better picture of the process than AE, as yields and the actual quantities of reactants are taken into account, although solvents and catalysts are excluded.

$$RME_{Curzons} = \frac{\text{Mass of product}}{\sum \text{Mass of reagents}} \cdot 100 = \frac{1}{PMI} \quad (4)$$

A few years later, John Andraos proposed an updated definition of RME, taking into account all components, including catalysts and solvents and adjusting for recovery (**Equation 5**).<sup>97,101</sup>

$$RME_{Andraos} = \frac{\text{Mass of product}}{\sum \text{Mass of components} - \sum \text{Mass recovered}} \cdot 100 \quad (5)$$

### Stoichiometric factor (SF)

SF is a straightforward metric defined by Andraos in 2005, as part of his extensive work in the mathematics of sustainability metrics.<sup>101</sup> It is defined as the quotient between the actual mass of reagents used and the stoichiometric amount required (**Equation 6**). A value above 1 indicates excess reagents are being used.<sup>97,102</sup>

$$SF = \frac{\text{Mass of product}}{\text{Mass of stoichiometric reagents}} \cdot 100 \quad (6)$$

### Materials Recovery Parameter (MRP)

The MRP was introduced by Andraos in 2019 to quantify the recovery of the auxiliary materials used throughout the synthetic process, particularly targeting solvents and catalysts. The mathematical expression for MRP involves Curzons' definition of RME and the recovery-adjusted E-factor of the auxiliary materials, as described in **Equation 7**.<sup>97</sup>

$$MRP = \frac{1}{(1 + RME_{Curzons} \cdot E_{Aux})} \cdot 100 \quad (7)$$

For easier interpretation, all metrics with values ranging from 0 to 1 (yield, AE, RME, inverse of SF and MRP) can be combined into a vector magnitude ratio (VMR), which describes the overall material efficiency of the reaction (**Equation 8**).<sup>97</sup>

<sup>101</sup>Andraos, J. *Org. Process Res. Dev.* **2005**, 9, 149–163.

<sup>102</sup>Andraos, J. *ACS Sustain. Chem. Eng.* **2018**, 6, 3206–3214.



$$\text{VMR} = \frac{1}{\sqrt{5}} \sqrt{(Y)^2 + (\text{AE})^2 + (\text{RME})^2 + \left(\frac{1}{\text{SF}}\right)^2 + (\text{MRP})^2} \quad (8)$$

Regarding impact metrics, their semiquantitative nature makes them difficult to implement, as there is no consensus on what should be considered to be hazardous and what should not. However, there are notable metrics which are accepted and used in the literature, namely the environmental quotient, effective mass yield and the EcoScale.

### Environmental Quotient (EQ)

The concept of EQ was introduced by Sheldon in 1994.<sup>103</sup> In his paper, he proposed to multiply the E-factor by an environmental unfriendliness quotient (Q), which would have a value starting from 1 for innocuous compounds and higher for more hazardous substances. Hungerbühler and coworkers refined EQ in 1998, developing a methodology to obtain Q based on a series of parameters, including materials sourcing as well as water, land and air pollution.<sup>104</sup>

### Effective mass yield (EMY)

The EMY was proposed by Hudlicky and collaborators in 1999. It is obtained in the same way as the E-factor any environmentally friendly substances are excluded. This provides a measure of the amount of hazardous waste generated per unit mass of product.<sup>105</sup>

### EcoScale

The EcoScale is one of the most advanced and novel metrics, developed by Van Aken, Streckowski and Patiny in 2006.<sup>106</sup> It involves a penalty-based scoring system, in which a synthetic protocol is penalized based on yields, cost and toxicity of materials, safety, technical setup, reaction conditions and work-up, then ranked on a scale from 0 to 100 (**Table 2**). The EcoScale provides a quick and comprehensive assessment of the sustainability of a process, although it is important to mention that it is specifically designed for lab-scale operation.

---

<sup>103</sup>Sheldon, R. A. *Chemtech* **1994**, 38–47.

<sup>104</sup>Heinzle, E.; Weirich, D.; Brogli, F.; Hoffmann, V. H.; Koller, G.; Verduyn, M. A.; Hungerbühler, K. *Ind. Eng. Chem. Res.* **1998**, 37, 3395–3407.

<sup>105</sup>Hudlicky, T.; A. Frey, D.; Koroniak, L.; D. Claeboe, C.; E. Brammer, L. *Green Chem.* **1999**, 1, 57–59.

<sup>106</sup>Van Aken, K.; Streckowski, L.; Patiny, L. *Beilstein J. Org. Chem.* **2006**, 2, 3.

**Table 2.** EcoScale scoring system.

| Score    | Classification |
|----------|----------------|
| > 75     | Excellent      |
| 75 to 50 | Acceptable     |
| < 50     | Inadequate     |

Besides these sustainability metrics, industries often use more complex metrics for energetic and economic analysis, often with their own proprietary calculations and carry out life cycle assessments (LCA) for their products, which involve standardized methodologies (the ISO 14000 family of standards)<sup>107</sup> to determine the environmental impact of all stages of the product's life, from synthesis to disposal or recycling.<sup>88,96</sup>



Universitat d'Alacant  
Universidad de Alicante

<sup>107</sup>Corbett, C. J.; Kirsch, D. A. *Prod. Oper. Manag.* **2001**, *10*, 327–342.



---

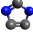
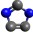
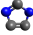
# **General Objectives**

---

Universitat d'Alacant  
Universidad de Alicante



Based on the described antecedents, the following general objectives were established for this doctoral thesis:

-  To develop novel catalytic systems based on imidazole derivatives, focusing on the versatility of the imidazole scaffold.
-  To design sustainable synthetic protocols using the catalytic systems prepared.
-  To assess the environmental impact of the protocols developed using a variety of mass efficiency and impact metric and compare them with established methodologies.



Universitat d'Alacant  
Universidad de Alicante



---

# **Chapter 1.**

**Imidazolium-UHP Low Transition Temperature  
Mixtures. Development and application.**

---

Universitat d'Alacant  
Universidad de Alicante





## C1.1. Antecedents

### C1.1.1. Alternative solvent systems

As mentioned before, one way of achieving more sustainable synthetic processes is to replace reaction components for less hazardous and renewable equivalents. Solvents are major contributors to waste generation, as they constitute by far the main components of reaction mixtures by weight,<sup>108</sup> and their reuse, if possible at all, often involves distillation, which consumes huge amounts of energy.<sup>109</sup> Most commonly used solvents are volatile (the so-called volatile organic compounds, VOCs), thus being contributors to atmospheric pollution, and are flammable and toxic.<sup>84</sup> While the best alternative would be to run reactions in total absence of solvent (the so-called neat conditions), this is not always possible due to solid reactants, mass transport and heat dissipation issues.<sup>84,110</sup> Thus, from the 1990s, the design of alternative solvents has been a very active field of study.<sup>108</sup>

#### Water

One can think of water as nature's solvent of choice. Indeed, life, understood as a complex array of reactions and processes leading to an enormously broad range of compounds is based entirely in water. Thus, when concerned about replacing VOCs with environmentally friendly systems, water becomes an obvious choice.<sup>111,112</sup>

For many years, scientists have been attracted to the idea of using water for their reactions, as it is inherently safe, non-flammable, has a significant liquid range, is abundant and cheap. Its highly polar character has also been demonstrated to be rate-enhancing for several types of transformations, and its high heat capacity ensures safer operation when dealing with exothermic reactions.<sup>112</sup> However, due to its intrinsic nature, the use of water as a replacement for VOCs presents some challenges. The most serious is the almost complete insolubility of most organic compounds in water, hampering or totally inhibiting reactivity. Several workarounds have been proposed, including the use of organic co-solvents, phase-transfer catalysis or surfactants.<sup>112-114</sup> Notably, high rates have been observed for certain reactions even without significant solubilization of the components, giving rise to the so-called synthesis "on water".<sup>111</sup>

---

<sup>108</sup>Jessop, P. G. *Green Chem.* **2011**, *13*, 1391–1398.

<sup>109</sup>Constable, D. J. C.; Jimenez-Gonzalez, C.; Henderson, R. K. *Org. Process Res. Dev.* **2007**, *11*, 133–137.

<sup>110</sup>Gu, Y.; Jérôme, F. *Chem. Soc. Rev.* **2013**, *42*, 9550–9570.

<sup>111</sup>Narayan, S.; Muldoon, J.; Finn, M. G.; Fokin, V. V.; Kolb, H. C.; Sharpless, K. B. *Angew. Chem. Int. Ed.* **2005**, *44*, 3275–3279.

<sup>112</sup>Chanda, A.; Fokin, V. V. *Chem. Rev.* **2009**, *109*, 725–748.

<sup>113</sup>Cicco, S. R.; Farinola, G. M.; Martinelli, C.; Naso, F.; Tiecco, M. *Eur. J. Org. Chem.* **2010**, 2275–2279.

<sup>114</sup>Simon, M.-O.; Li, C.-J. *Chem. Soc. Rev.* **2012**, *41*, 1415–1427.

Still, running a reaction in water is not necessarily convenient or sustainable when considering everything involved in the process. Water is not an innocent solvent and can interfere with some reactions and most organometallic and alkylating reagents are incompatible with it, which forces time and resource-consuming workarounds. Also, water's high heat capacity results in increased energy requirements to achieve a certain reaction temperature, or to remove it by distillation. This means decontaminating water for safe disposal requires significant amounts of energy. Besides, although in reduced quantities, organic solvents may still be needed for work-up and purification.<sup>114</sup> This combination of factors can quickly offset any sustainability gains, and thus, water has not been able to displace VOCs in organic synthesis.

### Supercritical fluids

Outside stars or extreme conditions, pure substances exist as solids, liquids or gasses. While different for each substance, every state has a well-delimited range of pressures and temperatures in which it can exist, which are separated by boundaries where two or more phases may co-exist. The critical point is the endpoint of the liquid-gas phase, defined by a critical temperature ( $T_c$ ) and critical pressure ( $P_c$ ). Over this point, gas (defined as gaseous phase above  $T_c$ , as opposed to vapor, gaseous phase under  $T_c$ ) can no longer be liquefied by pressure alone. If below the minimum pressure required to condense into a solid (which tends to be several orders of magnitude above  $P_c$ ),<sup>115</sup> the resulting phase is known as a supercritical fluid (**Figure 9**).<sup>116,117</sup>

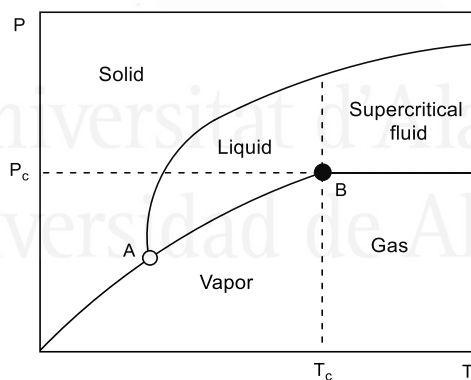


**Figure 9.** Pressure-temperature (PT) diagram of a model system. A: Triple point, B: Critical point. Axis not linearly scaled.

<sup>115</sup>Oakes, R. S.; Clifford, A. A.; Rayner, C. M. *J. Chem. Soc. Perkin Trans. 1* **2001**, 917–941

<sup>116</sup>Jessop, P. G.; Leitner, W. *Chemical Synthesis Using Supercritical Fluids*; Wiley-VCH, 1999.

<sup>117</sup>Prajapati, D.; Gohain, M. *Tetrahedron* **2004**, 60, 815–833.

Substances in supercritical phase are often regarded as being in a state between a liquid and a gas. Although physically resembling liquids, SCFs effuse through porous materials like a gas, and have very high mass transfer parameters. Density, viscosity and dielectric constant experience significant changes with relatively subtle variations of temperature and pressure. Additionally, they have substantially different properties than when in non-critical phases.<sup>115,116</sup> For instance, supercritical water is miscible with organic solvents such as cyclohexane.<sup>118</sup>

The use of SCFs as solvents for reactions was pioneered by the Russian chemist Vladimir Ipatiev in the early 1900s, as part of his groundbreaking work on heterogeneous catalysis, although interest in the field remained low for several decades.<sup>116</sup> During the early 1990s researchers studied SCFs as prospective replacements for VOCs, citing several advantages.<sup>115,119</sup> The most common substances used as SCFs (water, CO<sub>2</sub>, methanol) have significantly lower toxicities than most VOCs, and their environmental impact is very reduced or plain negligible. In terms of performance, they offer unparalleled diffusion rates, low viscosities and completely tunable solvent power, dielectric constant and density, as well as very high gas solubility.<sup>116</sup> However, the use of SCFs in synthesis never really took off and was phased out in the late 2000s due to the specialized equipment required to deal with the high pressures and the inherent danger and energetic cost associated to those (the critical point of CO<sub>2</sub> is 31 °C and 73 bar, while water achieves supercriticality above 375 °C and 220 bar).<sup>116</sup>

Nowadays, SCFs are used in applications involving mass transfer or extraction. Supercritical CO<sub>2</sub> is the most common SCF and has been used since the 1970s to decaffeinate coffee and as mobile phase in high-performance liquid chromatography (HPLC) systems, among other applications.<sup>116</sup>

### Perfluorinated compounds

As their name implies, perfluorinated compounds (PFCs) are organic molecules in which each carbon atom is fully substituted by fluorine. They are characterized by high densities (around 1.8 g/cm<sup>3</sup>) and have unusual properties derived from the strength of the C-F bond.<sup>120</sup>

PFCs are very stable and almost fully chemically inert, and the low polarizability of the bond results in these compounds being among the least polar liquids known (e.g., perfluorooctane has a  $\pi$  polarizability of -0.41, against 1.09 for water and 0 for cyclohexane),<sup>121</sup> meaning PFCs are often immiscible with common non-polar organic solvents, such as hexane.<sup>120</sup> In addition, they are only

---

<sup>118</sup>Bröll, D.; Kaul, C.; Krämer, A.; Krammer, P.; Richter, T.; Jung, M.; Vogel, H.; Zehner, P. *Angew. Chem. Int. Ed.* **1999**, *38*, 2998–3014.

<sup>119</sup>Noyori, R. *Chem. Rev.* **1999**, *99*, 353–354.

<sup>120</sup>Betzemeier, B.; Knocher, P. Perfluorinated Solvents - a Novel Reaction Medium in Organic Chemistry. In *Modern Solvents in Organic Synthesis*; Knocher, P. Ed.; Springer-Verlag, 1999.

<sup>121</sup>Boswell, P. G.; Lugert, E. C.; Rábai, J.; Amin, E. A.; Bühlmann, P. *J. Am. Chem. Soc.* **2005**, *127*, 16976–16984.

capable of weak Van der Waals interactions, so their solvent power is insignificant and their boiling points tend to be lower than their non-fluorinated counterparts.<sup>120,122</sup>

The use of PFCs in organic synthesis was pioneered by Zhu in 1993 as part of the 1990s search for alternative solvents, citing advantages such as high stability, inertness, and ease of separation.<sup>123</sup> Although many reactions were developed over the next few years (of particular interest was the application of PFCs to organic biphasic catalysis),<sup>120</sup> the drawbacks of PFCs soon became apparent. They are significantly more expensive than regular solvents, their extreme non-polarity and poor solvent power makes their usefulness situational, and their high volatility and stability makes them persistent pollutants.<sup>84,120</sup> In addition, some perfluoroalkenes, which can generate upon pyrolysis of PFCs, are extremely toxic.<sup>124</sup> These issues prevented the widespread implementation of PFCs in organic synthesis, although they are very present in electrochemistry.<sup>121</sup>

### Biomass-derived solvents

Biomass-derived solvents have been steadily rising to prominence over the last few years, and today, they present themselves as solid alternatives to VOCs. They are obtained from renewable sources, often as byproducts of the industry, and they are intrinsically biodegradable. This offers advantages in terms of resource preservation, waste prevention, economic cost and environmental impact.<sup>110,125</sup>

Pretty much any liquid or low-melting biomass-derived substance can be used as solvent. Polyols, lactic acid derivatives,  $\gamma$ -valerolactone, guaiacol, syringol or terpenes are some representative examples of current efforts,<sup>110,126–128</sup> with two particular systems standing out.

Glycerol is the main byproduct of the vegetable oil and biodiesel industries, and is obtained in large scale at a very reduced cost (around 0.73 €/kg as of February 2023).<sup>129</sup> It is immiscible with most organic solvents but less polar than water, not flammable nor volatile and its toxicity is negligible.<sup>125</sup>

---

<sup>122</sup>McBee, E. T. *Ind. Eng. Chem.* **1947**, 39, 236–237.

<sup>123</sup>Zhu, D.-W. *Synthesis* **1993**, 953–954.

<sup>124</sup>Timperley, C. M. Highly-Toxic Fluorine Compounds. In *Fluorine Chemistry at the Millennium*; Banks, R. E., Ed.; Elsevier Science, 2000; pp 499–538.

<sup>125</sup>Santoro, S.; Ferlin, F.; Luciani, L.; Ackermann, L.; Vaccaro, L. *Green Chem.* **2017**, 19, 1601–1612.

<sup>126</sup>Gevorgyan, A.; Hopmann, K. H.; Bayer, A. *ChemSusChem* **2020**, 13, 2080–2088.

<sup>127</sup>Gandeepan, P.; Kaplaneris, N.; Santoro, S.; Vaccaro, L.; Ackermann, L. *ACS Sustain. Chem. Eng.* **2019**, 7, 8023–8040.

<sup>128</sup>Lomba, L.; Zuriaga, E.; Giner, B. *Curr. Op. Green Sustain. Chem.* **2019**, 18, 51–56.

<sup>129</sup>*Glycerol US Prices*. <https://www.selinawamucii.com/insights/prices/united-states-of-america/glycerol> (accessed 13-02-2023).

Its potential as a green solvent was first explored by Wolfson in 2006,<sup>130</sup> and since, glycerol and its derivatives have been applied to a broad range of transformations.<sup>110,125</sup>

Another prime example is 2-methyltetrahydrofuran (2-MeTHF), derived from furfural and levulinic acid obtained from lignocellulosic mass.<sup>110</sup> Due to its structure, 2-MeTHF is effectively a “traditional” organic solvent of renewable origin, with properties arguably better than those of THF. It is immiscible with water, so is more stable to acids and bases, and has better stabilizing effects on organometallic reagents.<sup>110,131</sup> However, it is relatively expensive and volatile, thus contributing to airborne pollution, although it degrades abiotically relatively quickly.<sup>127</sup>

The general drawbacks of most biomass-derived solvents are their lack of tunability and relatively narrow spectrum of properties, as well as the potential for biodiversity loss due to high space requirements for crops (one of the main problems of the biodiesel industry.<sup>132</sup> Specific issues for some systems are high costs of production/purification and contribution to pollution.<sup>110</sup>

### C1.1.2. Low transition temperature mixtures

The downfall of ionic liquids left a void difficult to fill in the field of alternative solvents. While they were dubious in terms of economic viability and environmental impact, their properties were undoubtedly good, and their tunability was simply unparalleled. Thus, finding a comparable alternative was of great interest.<sup>133</sup>

Eutectic systems, defined as homogeneous mixtures of substances with lower melting points than those of the original components, have been known for a long time and are commonplace in metallurgy and protocols involving molten salts.<sup>134</sup> With this idea in mind, Andrew Abbott and coworkers introduced the possibility of using room-temperature melts of choline chloride and urea as sustainable alternatives to ILs, and coined the term “deep eutectic solvents” (DES) to refer to them.<sup>135</sup> Their 2003 report represented a major breakthrough in the field of alternative solvents, and one of the most important developments in sustainable chemistry in the last two decades.<sup>84</sup>

Initially, DES were described as mixtures of compounds with hydrogen bonding donor (HBD) and acceptor (HBA) capabilities, with the melting point depression arising from disruptions in the crystal lattice caused by hydrogen bonding between the components.<sup>135,136</sup> The definition was later expanded

---

<sup>130</sup>Wolfson, A.; Dlugy, C.; Tavor, D.; Blumenfeld, J.; Shotland, Y. *Tetrahedron Asymmetry* **2006**, *17*, 2043–2045.

<sup>131</sup>Aycock, D. F. *Org. Process Res. Dev.* **2007**, *11*, 156–159.

<sup>132</sup>Tudge, S. J.; Purvis, A.; De Palma, A. *Biodivers. Conserv.* **2021**, *30*, 2863–2883.

<sup>133</sup>Ruß, C.; König, B. *Green Chem.* **2012**, *14*, 2969–2982.

<sup>134</sup>Smith, W. F.; Hashemi, J. *Foundation of Materials Science and Engineering*, 4th ed.; McGraw-Hill, 2006.

<sup>135</sup>Abbott, A. P.; Capper, G.; Davies, D. L.; Rasheed, R. K.; Tambyrajah, V. *Chem. Commun.* **2003**, 70–71.

<sup>136</sup>Ge, X.; Gu, C.; Wang, X.; Tu, J. *J. Mater. Chem. A* **2017**, *5*, 8209–8229.

to accommodate other types of components as well as interaction modes. HBAs were almost invariably ammonium or phosphonium salts, while the nature of the second component would determine which type of DES the mixture was.<sup>137</sup> Type I and II DES had metal halides (anhydrous or hydrated, respectively) as the second component and the depression in melting point was induced by the bulk of the resulting anion.<sup>136</sup> Type III, the most interesting of the lot, used HBAs capable of establishing hydrogen bonds with the HBA, e.g., ureas, carboxylic acids or polyols (**Figure 10**).<sup>133,137,138</sup>

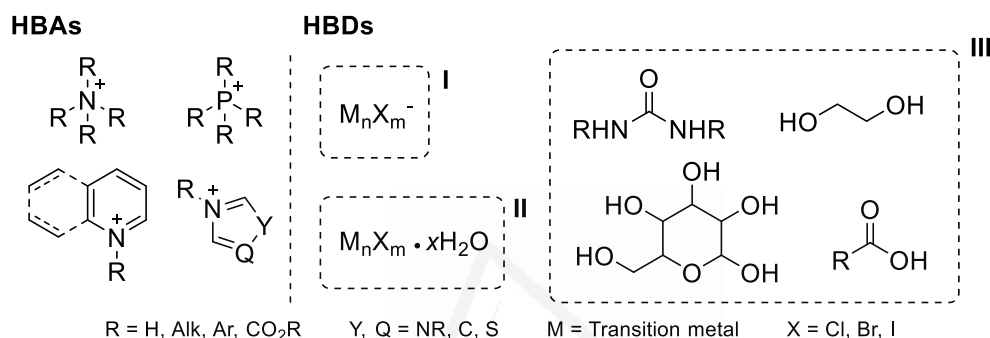


**Figure 10.** General structures of type I, II and III DES components.

However, as more and more compound combinations have been explored and new types of interactions have been discovered, the original definition of DES has become somewhat insufficient. Non-ionic mixtures (based on aminoacids and hydroxyacids,<sup>139</sup> for instance) are an example of low-melting systems which do not adjust to the original criteria.<sup>140</sup> More recently, a revised definition of DES has been proposed, whereby the main requirement is the non-ideality of the mixture, i.e., the melting point is significantly lower than what would be expected according to the predicted ideal behavior. This applies to a range of compositions, rather than a fixed stoichiometry (**Figure 11**).<sup>141</sup>

<sup>137</sup>Abbott, A. P.; Barron, J. C.; Ryder, K. S.; Wilson, D. *Chem. Eur. J.* **2007**, *13*, 6495–6501.

<sup>138</sup>García, G.; Aparicio, S.; Ullah, R.; Atilhan, M. *Energy Fuels* **2015**, *29*, 2616–2644.

<sup>139</sup>Kottaras, P.; Koulianos, M.; Makris, D. P. *Recycling* **2017**, *2*, 3.

<sup>140</sup>Francisco, M.; van den Bruinhorst, A.; Kroon, M. C. *Angew. Chem. Int. Ed.* **2013**, *52*, 3074–3085.

<sup>141</sup>Martins, M. A. R.; Pinho, S. P.; Coutinho, J. A. P. *J. Solution Chem.* **2019**, *48*, 962–982.

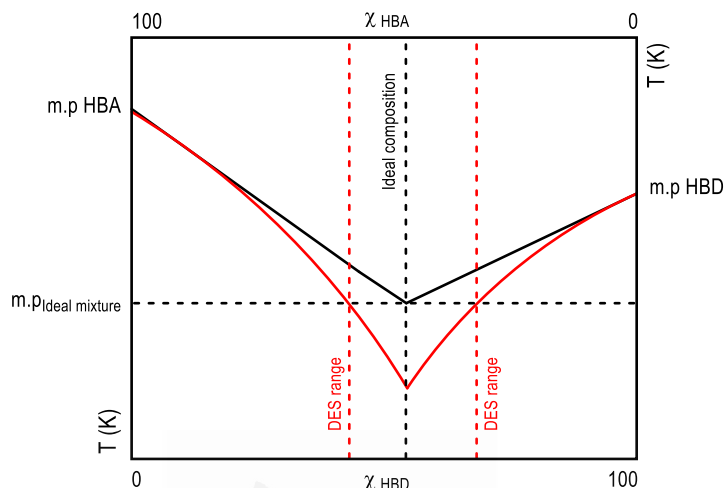


**Figure 11.** Solid-liquid equilibrium (SLE) diagram for an ideal mixture (black) and a DES (red).

Although this means the definition of DES is no longer bound by the identity of the components, but rather the actual behavior of the mixture, many useful systems still fall outside its scope. Therefore, the term Low Transition Temperature Mixtures (LTTMs) was proposed to encompass every type of low-melting mixtures, including DES.<sup>138,140,142</sup>

LTTMs are elegant systems which offer significant advantages over other alternative solvents.<sup>140</sup> A massive number of compounds can form LTTMs, so their prospective tunability is even higher than that of ILs, while being also significantly simpler.<sup>140</sup> The formation of LTTMs is a process with 100% atom economy and only requires combining the components under gentle heating.<sup>84</sup> Along with the many naturally occurring or biomass-derived compounds able to form LTTMs (natural DES or NADES are prime examples),<sup>143</sup> they offer all of the advantages of ILs (modularity, non-flammability, catalytic activity) while mitigating most of their drawbacks (cost, feedstock sustainability and environmental impact).<sup>84,133,136,139</sup> Nowadays, the scope of application of LTTMs goes past synthetic chemistry, finding use in materials science,<sup>136</sup> electrochemistry<sup>144</sup> and extraction protocols.<sup>139,145</sup>

<sup>142</sup>Costamagna, M.; Micheli, E.; Canale, V.; Ciulla, M.; Siani, G.; di Profio, P.; Tiecco, M.; Ciancaleoni, G. *J. Mol. Liq.* **2021**, *340*, 117180.

<sup>143</sup>Tiecco, M.; Cappellini, F.; Nicoletti, F.; Del Giacco, T.; Germani, R.; Di Profio, P. *J. Mol. Liq.* **2019**, *281*, 423–430.

<sup>144</sup>Suzuki, K.; Yamaguchi, M.; Kumagai, M.; Tanabe, N.; Yanagida, S. *C. R. Chim.* **2006**, *9*, 611–616.




<sup>145</sup>Idenoue, S.; Yamamoto, K.; Kadokawa, J. *ChemEngineering* **2019**, *3*, 90.





## C1.2. Objectives

The preparation of imidazolium LTTMs is interesting, as they should exhibit most of the desirable catalytic properties of imidazolium salts with a significant part of them being a renewable chemical, resulting in a drastic reduction of their environmental impact. However, only a few examples of such LTTMs are present in recent literature,<sup>145–147</sup> probably due to imidazolium salts still being associated with ionic liquids. Thus, based on the described antecedents, the following objectives were established:

-  To test the formation of LTTMs with a series of environmentally friendly imidazolium salts in combination with urea and guanidinium chloride as sustainable HBDs.
-  To characterize the resulting LTTMs by differential scanning calorimetry and obtain the corresponding composition-melting point and energy diagrams.
-  To study the activation of the urea-hydrogen peroxide adduct with imidazolium salts and the application of the resulting LTTM to oxidation reactions.

Universitat d'Alacant  
Universidad de Alicante

---

<sup>146</sup>Ji, Y.; Hou, Y.; Ren, S.; Yao, C.; Wu, W. *Energy Fuels* **2017**, *31*, 10274–10282.

<sup>147</sup>Akhmetshina, A. I.; Petukhov, A. N.; Mechergui, A.; Vorotyntsev, A. V.; Nyuchev, A. V.; Moskvichev, A. A.; Vorotyntsev, I. V. *J. Chem. Eng. Data* **2018**, *63*, 1896–1904.



### C1.3. Results and discussion

The selection of the imidazolium salts as HBA for this study was done considering several factors, i.e., environmental impact, convenience, economic viability and potential for catalytic use. Thus, four imidazolium salts meeting these criteria were selected. They would be combined with urea and guanidinium chloride, two widely available, inexpensive and renewable chemicals (**Figure 12**).

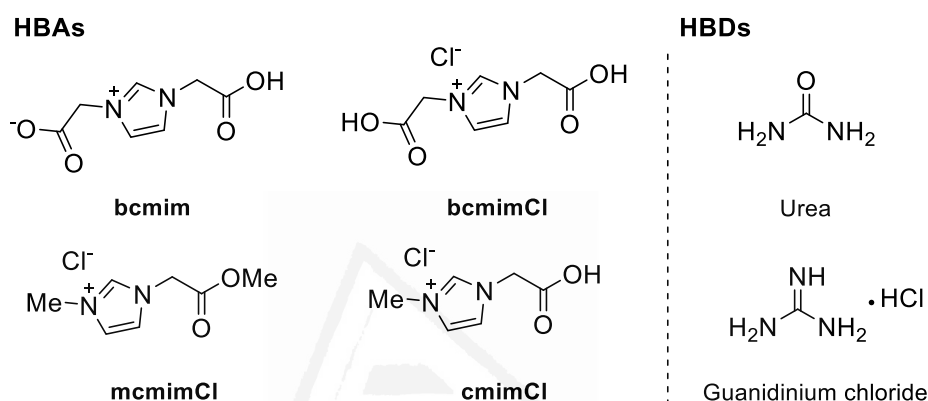


**Figure 12.** Selected components for LTTM formation assays.

The zwitterionic 1,3-bis(carboxymethyl)imidazole (**bcmim**) was first identified as a byproduct of the Maillard reaction of saccharides,<sup>148</sup> and is obtained *via* single-step, high yielding multicomponent reaction. **Bcmim** derivatives have demonstrated good catalytic performance in several types of transformations, including quinoline synthesis and allylation reactions.<sup>148,149</sup>

1-(Methoxycarbonylmethyl)-3-methylimidazolium chloride (**mcmimCl**) is synthesized from readily available methylimidazolium and methyl chloroacetate in a single, 100% atom-economic step under solventless conditions.<sup>150</sup> It is non-inhibitory for several ATCC strains of yeasts and fungi, and its biodegradability is higher than purely alkylic imidazolium salts.<sup>151,152</sup> Besides, **mcmimCl** and **cmimCl** have been studied as NHC ligands for palladium-catalyzed Matsuda-Heck cross-coupling reactions and are significantly Lewis acidic.<sup>150,153</sup>

<sup>148</sup>Gisbert, P.; Albert-Soriano, M.; Pastor, I. M. *Eur. J. Org. Chem.* **2019**, 4928–4940.

<sup>149</sup>Albert-Soriano, M.; Pastor, I. M. *Adv. Synth. Catal.* **2020**, 362, 2494–2502.

<sup>150</sup>Gisbert, P.; Trillo, P.; Pastor, I. M. *ChemistrySelect* **2018**, 3, 887–893.

<sup>151</sup>Gathergood, N.; Garcia, M. T.; Scammells, P. J. *Green Chem.* **2004**, 6, 166–175.

<sup>152</sup>Gore, R. G.; Myles, L.; Spulak, M.; Beadham, I.; Garcia, T. M.; Connon, S. J.; Gathergood, N. *Green Chem.* **2013**, 15, 2747–2760.

<sup>153</sup>Fei, Z.; Zhao, D.; Geldbach, T. J.; Scopelliti, R.; Dyson, P. J. *Chem. Eur. J.* **2004**, 10, 4886–4893.

For the initial screening, mixtures of the imidazolium salts with both HBDs in 1:1 mole ratio were subjected to heating in oil baths. The temperature was only roughly monitored for this preliminary study, as the thermocouples of the heating plates have high latency and would provide inaccurate readings.

**Table 3.** Preliminary LTTM formation studies.

| Entry | HBA            | HBD                  | Result                |
|-------|----------------|----------------------|-----------------------|
| 1     | <b>bcmim</b>   | Urea                 | LTTM formation        |
| 2     |                | Guanidinium chloride | Thermal decomposition |
| 3     | <b>bcmimCl</b> | Urea                 | LTTM formation        |
| 4     |                | Guanidinium chloride | Thermal decomposition |
| 5     | <b>cmimCl</b>  | Urea                 | LTTM formation        |
| 6     |                | Guanidinium chloride | LTTM formation        |
| 7     | <b>mcmimCl</b> | Urea                 | LTTM formation        |
| 8     |                | Guanidinium chloride | LTTM formation        |

In general terms, urea resulted to be a more convenient HBD, as it formed LTTMs in all cases (**Table 3**, all entries), whereas only monocarboximidazolium salts were able to form LTTMs with guanidinium chloride below its thermal decomposition point (**Table 3**, entries 5 to 8). Based on these results, guanidinium chloride was discarded as HBD.

As it had already been established that urea formed LTTMs with all imidazolium salts, the next step was to accurately determine the melting point<sup>†</sup> of the mixtures. To this end, samples of the imidazolium salts with urea in 1:1 ratio were prepared by grinding both components using a mortar and pestle to ensure maximum homogeneity and analyzed by differential scanning calorimetry (DSC) (**Table 4**).

**Table 4.** DSC analyses of imidazolium salt-urea mixtures. Pure compounds for reference.

| Entry | HBA            | LTTM m.p. (°C) | Pure HBA m.p. (°C) <sup>†</sup> |
|-------|----------------|----------------|---------------------------------|
| 1     | <b>bcmim</b>   | 122.6          | 305                             |
| 2     | <b>bcmimCl</b> | 116.5          | 223                             |
| 3     | <b>cmimCl</b>  | N/D            | 220                             |
| 4     | <b>mcmimCl</b> | N/D            | 205                             |

<sup>†</sup>Determined by conventional heating with a Reichert-Thermovar heating plate microscope.

<sup>†</sup>The term "melting point" will be used indistinctly to refer to actual melting points and transition temperatures.

As expected, all mixtures experienced some degree of melting point depression. This was particularly noticeable on the monocarboximidazolium salts (**Table 4**, entries 3 and 4), which experienced partial (**cmimCl**) or total melting (**mcmimCl**) upon mixing, as evidenced by their DSC traces (see section **SI.2.1** for all DSC traces).

The general trend in melting point can be rationalized according to the structural features of the imidazolium salts. Biscarboximidazolium LTTMs have the highest transition points, due to the increased number of hydrogen-bonding interactions present in the pure compounds. This is particularly relevant for **bcmim**, as its zwitterionic nature results in the formation of linear chains of molecules bonded together *via* O-H-O hydrogen bonds (**Figure 13**).<sup>39</sup>

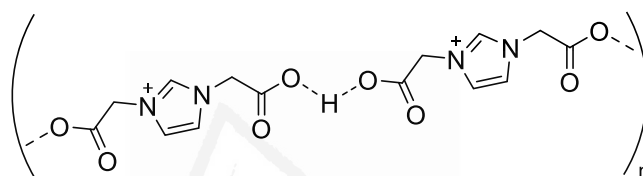


**Figure 13.** Intermolecular interactions in **bcmim** crystals.

**McmimCl** exhibits the highest LTTM-forming potential of the four, as it is the one with the least possibility of intermolecular interactions, resulting in lower energy requirements for LTTM formation and broader liquid ranges. Thus, **mcmimCl** was selected as HBA for further experiments. To study the behavior of the system, several mixtures ranging from 100% imidazolium salt to 100% urea were prepared and subjected to a cycle and a half of DSC (from -90 to 150 °C, cooling down to -90 °C and back again to 150 °C). To avoid premature melting while ensuring maximum homogeneity, samples were carefully grinded on a cooled mortar under a flow of argon to prevent moisture buildup. The results are compiled in **Table 5** and **Figure 14**.

**Table 5.** Melting point, glass transitions ( $T_g$ ) and enthalpy of formation of the **mcmimCl**:urea LTTMs.

| Entry | <b>mcmimCl</b> :urea (mol/mol) | $\chi_{\text{mcmimCl}}$ | LTTM m.p. (°C)     | $T_g$ (°C) | Enthalpy of melting (kJ/mol) |
|-------|--------------------------------|-------------------------|--------------------|------------|------------------------------|
| 1     | Pure urea                      | 0                       | 135.7 <sup>†</sup> | -          | 10.20                        |
| 2     | 1:3                            | 0.25                    | 79.2               | N/D        | 6.95                         |
| 3     | 1:2                            | 0.33                    | 45.5               | -28.57     | 7.47                         |
| 4     | 1:1                            | 0.5                     | 40.4               | -33.98     | 9.15                         |
| 5     | 2:1                            | 0.66                    | 35.2               | -26.79     | 9.05                         |
| 6     | 3:1                            | 0.75                    | 51.8               | -30.75     | 8.27                         |
| 7     | Pure <b>mcmimCl</b>            | 1                       | 201.4 <sup>†</sup> | -          | 26.73                        |

<sup>†</sup>Determined by conventional heating with a Reicher-Thermovar heating plate microscope.

The lowest melting point (35.2 °C) was registered with a 2:1 mixture of **mcmimCl** and urea ( $\chi_{\text{mcmimCl}} = 0.66$ , **Table 5**, entry 5), albeit transition temperatures do remain within a reasonably narrow margin throughout a wide composition range, and well under 100 °C in all cases. The formation enthalpies are lower than the enthalpies of melting for the pure components, which suggests favorable interactions between them.

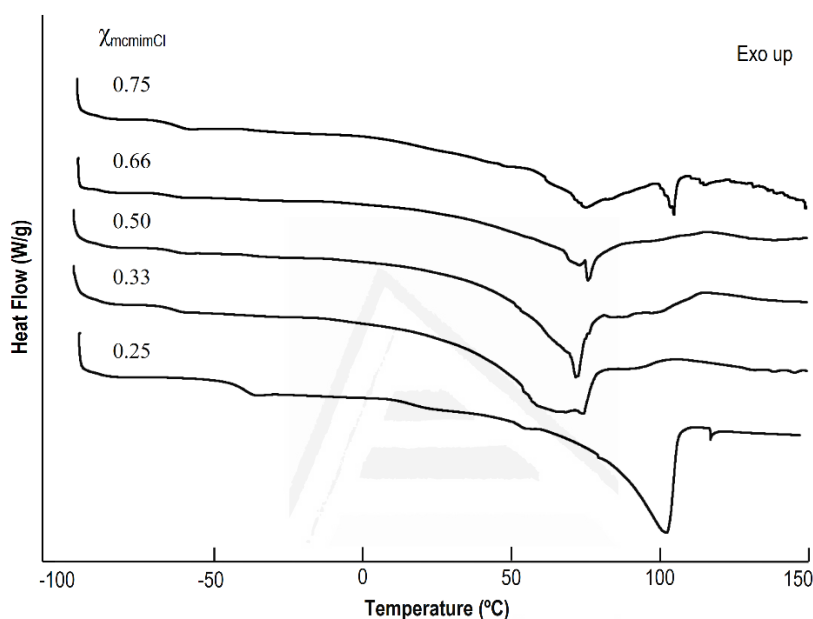


**Figure 14.** DSC traces (heating ramp) of the **mcmimCl**:urea LTTMs (Heat Flow axis not to scale).

The heating-ramp DSC traces present a single endothermic thermal event corresponding to the formation of the LTTM, which becomes increasingly broad and jagged as the molar fraction of **mcmimCl** goes up (**Figure 14**). This is related to **mcmimCl** having a molecular weight three times as high as that of urea while being less dense, with the sheer difference in bulk hindering the initial interaction between the components. This results in slow and non-uniform mixing, hence the broad and uneven DSC traces.

Notably, the trace for the 3:1 **mcmimCl**:urea LTTM ( $\chi_{\text{mcmimCl}} = 0.75$ ) exhibits a small secondary peak after the main thermal event (**Figure 14**, top). While this could be explained by slow LTTM formation kinetics, it could also be caused by having reached an upper limit in composition for the single-phase system, with the secondary peak corresponding to the heat of solubilization of excess **mcmimCl** in the LTTM.

The full cycle DSC of the mixtures (see section **SI.2.1**) reveals some interesting behavior. The formation of the 1:3 **mcmimCl:urea** LTTM ( $\chi_{\text{mcmimCl}} = 0.25$ ) seems fully reversible, as demonstrated by an exothermic event at 47.5 °C on the cooling cycle equal on energy to the melting event (**Figure S2.C1.6**), followed by formation of the LTTM once more in the second heating ramp. This is in stark contrast to the rest of the LTTMs ( $\chi_{\text{mcmimCl}} = 0.33$  to 0.75), which show no events save from glass transitions during cooling.

Regarding the second heating cycle, no events besides glass transitions are apparent for any of the LTTMs except the 1:3 (discussed above) and 1:1 mixtures. Indeed, the DSC trace of the latter ( $\chi_{\text{mcmimCl}} = 0.5$ ) presents an exothermic band which immediately leads to an endothermic event of the same energy, with the crossover point being the exact melting point determined in the first cycle (**Figure 15**).

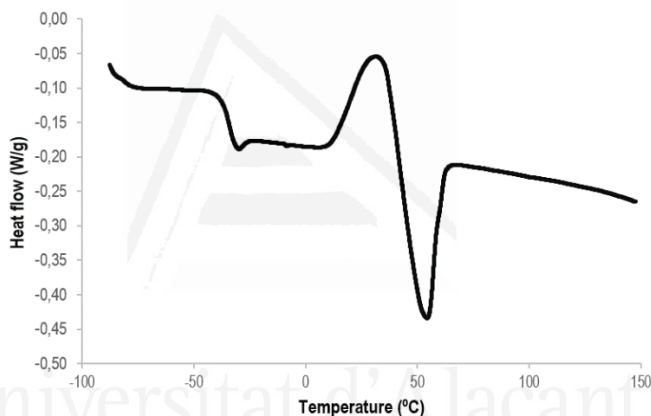


**Figure 15.** DSC trace of second heating ramp of the 1:1 **mcmimCl:urea** LTTM.

This behavior could be attributed to the LTTM becoming subcooled, in which case the molten phase becomes metastable upon cooling, with slow phase-change kinetics.<sup>154</sup> This theory is supported by our naked eye observations of the LTTMs, with the 1:1 mixture taking up to two years at room temperature for distinct phases to be visible (as homogeneous opaque dots within the transparent main phase, see **Figure S5.C1.1**), while no change whatsoever was observed for the rest of the LTTMs.

Using the DSC data gathered, the corresponding transition temperature-composition and enthalpy-composition diagrams were elaborated (**Figure 16**).

<sup>154</sup>Hall, C. L.; Potticary, J.; Hamilton, V.; Gaisford, S.; Buanz, A.; Hall, S. R. *Chem. Commun.* **2020**, 56, 10726–10729.



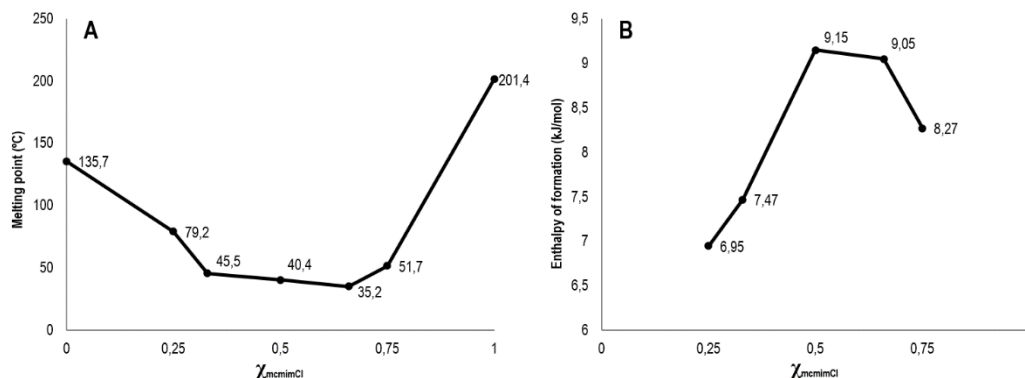


Figure 16. Melting point (A) and LTTM formation enthalpy (B) composition diagrams.

Having studied the composition range and thermal behavior of the **mcmimCl**:urea mixtures, the next step was their application to sustainable organic synthesis.

The oxidation of boron compounds to the corresponding alcohols is a well-known reaction, famously applied to the anti-Markovnikov hydration of double bonds *via* hydroboration.<sup>155</sup> Quite recently, He and coworkers reported the oxidation of boronic acids using substoichiometric amounts of choline chloride-based LTTMs as promoters and 30% aqueous  $\text{H}_2\text{O}_2$  as oxidizer.<sup>156,157</sup> This methodology is a step-up on other described procedures, which rely on transition metal catalysis,<sup>158</sup> costly<sup>159</sup> or unwieldy<sup>158,160</sup> systems, very high excess of oxidants<sup>158,161</sup> and (super)stoichiometric amounts of additives.<sup>162–166</sup>

However, the use of the term LTTM in He's work is quite liberal, as the volume of water used almost guarantees no LTTM is actually present in the reaction mixture (the mole ratio of water to choline chloride is reported as 1250:1), as the LTTM components would be completely solvated by the

<sup>155</sup>Brown, H. C.; Zweifel, G. *J. Am. Chem. Soc.* **1959**, *81*, 247–247.

<sup>156</sup>Wang, L.; Dai, D.-Y.; Chen, Q.; He, M.-Y. *Asian J. Org. Chem.* **2013**, *2*, 1040–1043.

<sup>157</sup>Wang, L.; Dai, D.; Chen, Q.; He, M. *J. Fluor. Chem.* **2014**, *158*, 44–47.

<sup>158</sup>Hao, L.; Ding, G.; Deming, D. A.; Zhang, Q. *Eur. J. Org. Chem.* **2019**, 7307–7321.

<sup>159</sup>Chen, D.-S.; Huang, J.-M. *Synlett* **2013**, *24*, 499–501.

<sup>160</sup>Bommegowda, Y. K.; Mallesha, N.; Vinayaka, A. C.; Sadashiva, M. P. *Chem. Lett.* **2016**, *45*, 268–270.

<sup>161</sup>Gogoi, A.; Bora, U. *Synlett* **2012**, *23*, 1079–1081.

<sup>162</sup>Cheng, G.; Zheng, X.; Cui, X. *Synthesis* **2014**, *46*, 295–300.

<sup>163</sup>Guo, S.; Lu, L.; Cai, H. *Synlett* **2013**, *24*, 1712–1714.

<sup>164</sup>Yang, H.; Li, Y.; Jiang, M.; Wang, J.; Fu, H. *Chem. Eur. J.* **2011**, *17*, 5652–5660.

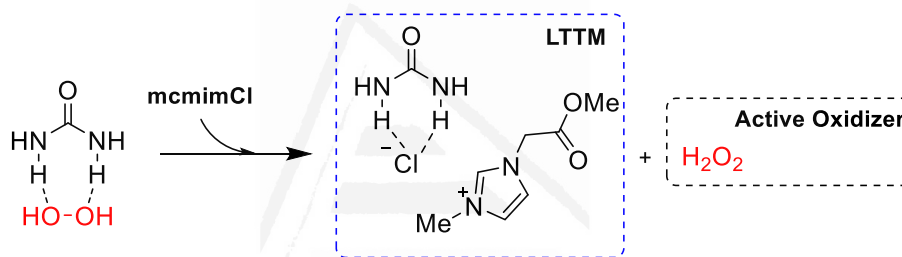
<sup>165</sup>Webb, K. S.; Levy, D. A. *Tetrahedron Lett.* **1995**, *36*, 5117–5118.

<sup>166</sup>Yin, W.; Pan, X.; Leng, W.; Chen, J.; He, H. *Green Chem.* **2019**, *21*, 4614–4618.

solvent. Albeit not as much as other methodologies, He's protocol uses a significant excess of  $\text{H}_2\text{O}_2$ , which is highly reactive and prone to dangerous thermal runaway events.

As mentioned before, the use of safer reagents is desirable when designing sustainable synthetic methodologies. Over the last few years, UHP, famously used for teeth whitening applications,<sup>167</sup> has been explored as an inexpensive, stable and safe to handle oxidizing agent in organic synthesis. However, for the oxidation of boron compounds, only two reports entertain the possibility of using UHP as oxidizer, and only one carries out a detailed study.<sup>168</sup>

Under regular circumstances, UHP thermally releases  $\text{H}_2\text{O}_2$  above  $75\text{ }^\circ\text{C}$ ,<sup>169</sup> requiring acidic or metal catalysis at lower temperatures.<sup>170</sup> In lieu of the observations made throughout this study, the possibility of using the **mcmimCl**:urea LTTM-forming interaction to trigger the release of  $\text{H}_2\text{O}_2$  from the adduct at room temperature was considered (**Scheme 25**).



**Scheme 25.**  $\text{H}_2\text{O}_2$  release mechanism by LTTM formation with UHP.

Besides being an inherently safer process, the use of **mcmimCl**:UHP LTTMs for this reaction would offer a key benefit. For systems with  $\chi_{\text{mcmimCl}} \approx 0.5$ , the formation of the LTTM slowly takes place at room temperature, providing a steady supply of oxidizer. This results in lower residency times (i.e., less degradation) and higher efficiency.

For this study, the oxidation of 4-phenylbenzeneboronic acid was selected as model reaction. It has been reported that the oxidation of phenols and naphthols to the corresponding hydroquinones starts to take place with as little as three equivalents of UHP.<sup>171</sup> Considering the prospectively higher efficiency of the LTTM, two equivalents of UHP and one equivalent of **mcmimCl** were deemed enough

<sup>167</sup>Mokhlis, G. R.; Matis, B. A.; Cochran, M. A.; Eckert, G. J. *J. Am. Dent. Assoc.* **2000**, *131*, 1269–1277.

<sup>168</sup>Gupta, S.; Chaudhary, P.; Srivastava, V.; Kandasamy, J. A. *Tetrahedron Lett.* **2016**, *57*, 2506–2510.

<sup>169</sup>Matyáš, R.; Selesovsky, J.; Pelikán, V.; Szala, M.; Cudzilo, S.; Trzciński, W. A.; Gozin, M. *Propellants Explos. Pyrotech.* **2017**, *42*, 198–203.

<sup>170</sup>Llopis, N.; Gisbert, P.; Baeza, A. *J. Org. Chem.* **2020**, *85*, 11072–11079.

<sup>171</sup>Llopis, N.; Baeza, A. *J. Org. Chem.* **2020**, *85*, 6159–6164.

to provide appropriate dispersion volume while avoiding overoxidation. No external heating was applied.

However, under these conditions the reaction carbonized after a brief induction period. The high oxophilicity of boron causes the oxidation process to be vigorously exothermic, with the heat released from the reaction accelerating the formation of the LTTM, thus increasing the rate at which  $\text{H}_2\text{O}_2$  is released to the medium. This positive feedback loop results in the heat output of the reaction spiraling out of control.

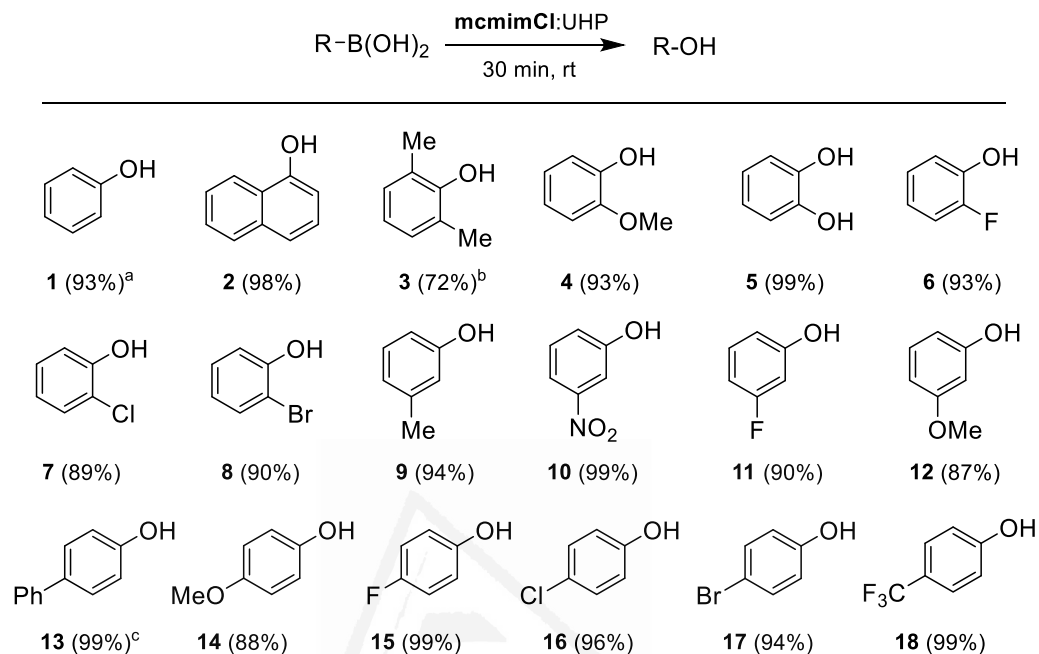
As solvent is required to extract the product from the LTTM at the end of the reaction, the possibility of adding the boron compound to the mixture as a suspension was considered to address the issue. The resulting biphasic system would have a slower reaction rate, as well as more thermal mass to help to maintain temperatures under control. At the end of the reaction, the product would be extracted by simply taking the upper organic phase. Ethyl acetate was selected for this endeavor, as it is completely immiscible with the **mcmimCl**:UHP LTTMs. It is also considered a “green solvent”, meaning its environmental impact is quite low all while being very affordable and widely available.<sup>108</sup>

Crucially, the solubility of most boronic acids and potassium trifluoroborates in ethyl acetate is quite low, while the solubility of alcohols is high, ensuring the reaction does take place within the LTTM, with the solvent relegated to delivering the starting material and extracting the product. This also provides a visual cue of the reaction progress. As the ethyl acetate-insoluble boron reagent is consumed in the LTTM, the organic phase should slowly become clear.

Thus, the same model reaction was set up, adding the 4-phenylbenzeneboronic acid as a 1 mol/mL suspension in ethyl acetate. In this case, the reaction proceeded as expected, with the top organic phase becoming completely clear after 5 minutes and the reaction vessel being only slightly warm to the touch. After 30 minutes, 4-phenylphenol was obtained in 97% yield as a pure white solid by simply taking the upper organic phase and filtering it through a thin plug of silica and magnesium sulfate.

Control experiments involved running the reaction in the absence of **mcmimCl**, resulting in wildly inconsistent results, with isolated yields ranging from 20 to 80% (probably promoted by the boronic acid itself) over five runs with no apparent reactivity pattern, and replacing it for **cmimCl**, with only 61% of product isolated after 1 hour of reaction, thus confirming the crucial role of **mcmimCl** in the process.

To prove the applicability of the method, several boronic acids were subjected to the model reaction conditions, obtaining the scope compiled in **Figure 17**.



Isolated yields. <sup>a</sup>From triphenylboroxin. <sup>b</sup>90 min of reaction time. <sup>c</sup>5 mmol scale reaction.

**Figure 17.** Scope of the reaction. Boronic acids.

In general terms, the reactions proceeded smoothly, obtaining the products in good to quantitative yields across the board. Judging by these results, the electronic nature of the substituents on the phenylboronic acids does not seem to significantly affect the outcome of the reaction. Likewise, the differences between substitution patterns are negligible. The protocol tolerates different aromatic systems, as evidenced by compound **2**, and is compatible with boronic acid anhydrides, with the oxidation of triphenylboroxin affording **1** in 93% yield. In no case was it necessary to purify the resulting compounds.

Notably, there seems to be a significant steric effect, evidenced by the results obtained in the oxidation of 2,6-dimethylbenzeneboronic acid (**Figure 17**, compound **3**). Under the standard conditions, the product could only be isolated in 51% yield, requiring an extended reaction time of 90 minutes to achieve good conversion. No extra UHP was needed, however, so this also had the effect of proving that the **mcmimCl:UHP** LTTM is able to release active oxidizer for extended periods of time.

Steric effects had not been described in previous reports<sup>157</sup>, and that might have to do with the fact that these earlier works use small molecules, such as HFIP, as catalysts for the activation of H<sub>2</sub>O<sub>2</sub>. In this case, said catalyst is the bulky imidazolium salt, which might have problems approaching hindered centers. Still, the excellent results obtained for *ortho* monosubstituted arylboronic acids

demonstrate that this is only true for severely congested centers, so this behavior could be exploited for the selective oxidation of non-hindered boron moieties.

Quite notably, the products were obtained pure after simple filtration through a thin plug of silica and magnesium sulfate. This is due to the high solubility of the boronic acids and waste products (i.e., boric acid itself) in the LTTM. Purification steps generate the most waste by far in any synthetic process, so this feature represents a major advantage in terms of sustainability.

Having obtained excellent results with boronic acids, the focus was shifted to boronic acid surrogates i.e., trifluoroborate salts and boronic esters. While the oxidation of the pinacol ester of phenylboronic acid afforded **1** in 79% NMR yield, this process releases ethyl acetate-soluble pinacol, thus requiring a final purification step. For this reason, only potassium trifluoroborates were explored as substrates, as summarized in **Figure 18**. The same conditions were applied, although reaction time was extended to 90 minutes, as these boron compounds are generally less reactive.

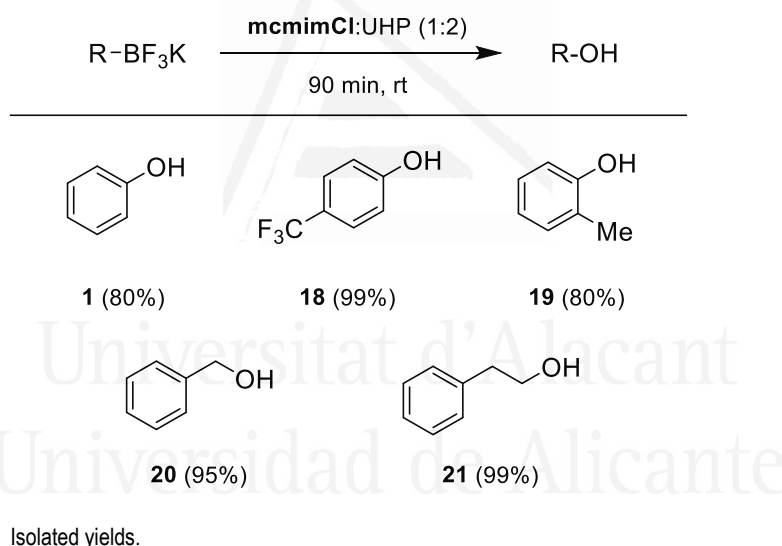


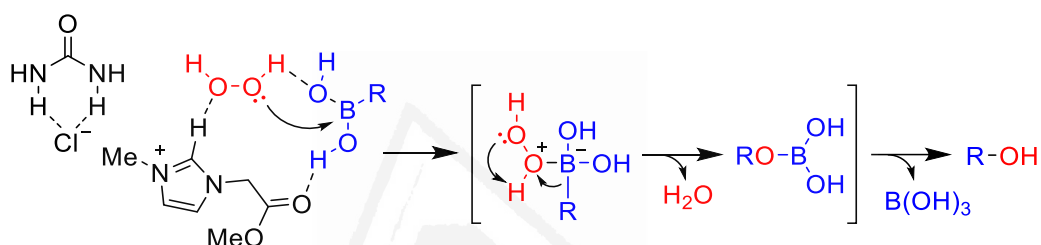
**Figure 18.** Scope of the reaction. Potassium trifluoroborates.

Once again, good to quantitative yields were obtained in this reaction. A slight preference for *para* substituted substrates was observed in this case, as phenols **1** and **19** were obtained in 80% yield whereas **18** was quantitatively isolated from its reaction. Remarkably, the methodology seems to perfectly tolerate aliphatic substrates, as both **20** and **21** were obtained in excellent and quantitative yields, respectively. Once more, no purification was required.

To assess the robustness of the **mcmimCl:UHP** LTTM system, the model reaction was performed at preparative scale. Thus, 0.99 g (5 mmol) of 4-phenylbenzeneboronic acid were used as

substrate, affording pure phenol **13** in 99% yield after 30 minutes. Most notably, the reaction vessel remained only slightly hot to the touch, not requiring slow addition of the reagent or ice baths to keep temperatures under control.

Regarding the mechanism of the reaction, after the formation of the LTTM, the just-released  $\text{H}_2\text{O}_2$  is trapped *via* hydrogen bonding with the Lewis-acidic C-2 hydrogen of **mcmimCl**. The carbonyl group present in **mcmimCl** also has the possibility of establishing hydrogen-bonding (or electrostatic) interactions with the boron compound, pulling the reagents together. Then,  $\text{H}_2\text{O}_2$  adds to the boron center, after which a rearrangement takes place, leaving a boronate which is promptly hydrolyzed under the reaction conditions, affording the product (**Scheme 26**).



**Scheme 26.** Proposed mechanism of the transformation.

Although the **mcmimCl**:UHP LTTM has been proven to be an excellent alternative for the oxidation of boron compounds, it may raise a few eyebrows in terms of sustainability. Reusability is one of the advantages LTTM (and all heterogeneous catalysts for this matter) offer, but in this particular case, it is not possible to recover the pristine LTTM. Besides, UHP has a limited amount of  $\text{H}_2\text{O}_2$  adsorbed, which cannot be reloaded, and there is not a cost-effective and environmentally friendly way of separating the **mcmimCl** from the LTTM. Although the E-factor of this protocol (7.1) comfortably sits at the lower limits of the range for Fine Chemical production (5 to 50), it is desirable to minimize the generation of waste as much as possible.

As demonstrated before, the usable composition range of the **mcmimCl**:urea LTTM is quite broad, ranging from  $\chi_{\text{mcmimCl}} = 0.75$  to 0.25. Thus, a simple way of maximizing the return on the imidazolium salt is to simply reload the LTTM with starting material and more UHP and run the reaction several times consecutively. To test this possibility, the model reaction was set up again. After each iteration, the organic phase was removed and additional UHP and fresh product suspension were added. As the volume of the dispersion media was no longer a constricting factor, only 1.1 equivalents of UHP were used from the second reaction on. This way, the reaction was successfully performed 3 consecutive times without any loss of performance, isolating compound **13** in a total cumulative yield of 98% without the need of any purification process. To quantify the decrease in environmental impact

of the sequential reaction compared to the single-run process, sustainability metrics were calculated (Table 6).

**Table 6.** Comparison between the single-run and sequential protocols for the synthesis of **13**.

| Metric                     | Single-run reaction | Sequential reaction |
|----------------------------|---------------------|---------------------|
| Yield (%)                  | 99                  | 98                  |
| AE (%)                     | 58.3                | 58.3                |
| SF                         | 1.321               | 1.128               |
| RME <sub>Andraos</sub> (%) | 12.4                | 14.5                |
| MRP                        | 0.284               | 0.287               |
| E-factor                   | 7.1                 | 5.9                 |
| EcoScale                   | 81                  | 81                  |

As expected, the metrics calculated suggest a marked decrease on the environmental impact of the synthetic protocol when using the sequential approach. The variation in RME<sub>Andraos</sub> indicates running the reaction sequentially results in ca. 15% higher material efficiency, whereas waste generation is around 20% lower for the latter process, with the E-factor nearly in the range for Bulk Chemical production (< 5). Both methodologies can be considered to perform well however, with low E-factors and excellent EcoScale scores. The AE remains unchanged between the two, as it is a theoretical measure of the atomic efficiency of the adjusted reaction. The MRP is not meaningful for this comparison either, as ethyl acetate is the only material recovered in both protocols. These results also highlight the importance of multi-metric approaches for the analysis of synthetic methodologies.

Next, metrics were calculated for the single-run synthesis of 1-naphthol (**2**) and compared with several representative protocols using a variety of oxidizers, solvents and catalysts. For easier comparison, yields, AE, SF, MRP and RME<sub>Andraos</sub> were combined into VMRs (see section **GI.3.2.** of this manuscript). As the objective is to compare the intrinsic sustainability of the reactions in lieu of their design, chromatographic purification steps were not considered (except for the EcoScale), as they would render any VMR and E-factor comparison meaningless against purification-free methods. The results are summarized in **Table 7**. More details are provided in section **S1.4.1**.

**Table 7.** Comparison between **mcmimCl**:UHP LTTM and reported protocols for the synthesis of **2**.

**2**

| Entry <sup>Ref.</sup>   | [Solv.]                       | [Cat.]                            | [OX]                              | VMR <sup>†</sup>   | E-factor           | EcoScale |
|-------------------------|-------------------------------|-----------------------------------|-----------------------------------|--------------------|--------------------|----------|
| <b>1</b>                | <b>mcmimCl</b> :UHP<br>/AcOEt | <b>mcmimCl</b>                    | UHP                               | 0.611              | 9.4                | 86       |
| <b>2</b> <sup>156</sup> | Water                         | ChCl:urea 1:2                     | aq. H <sub>2</sub> O <sub>2</sub> | 0.581 <sup>‡</sup> | 44.7 <sup>‡</sup>  | 76       |
| <b>3</b> <sup>168</sup> | Methanol                      | None                              | UHP                               | 0.664 <sup>‡</sup> | 437.7 <sup>‡</sup> | 67       |
| <b>4</b> <sup>164</sup> | Water                         | Cu <sub>2</sub> O/NH <sub>3</sub> | Air                               | 0.524              | 52.7               | 66       |
| <b>5</b> <sup>172</sup> | Water                         | Amberlite IR120                   | aq. H <sub>2</sub> O <sub>2</sub> | 0.515              | 94.3               | 79       |

<sup>†</sup>Calculated from yield, AE, SF, MRP and RME<sub>Andraos</sub>. <sup>‡</sup>Purification by column chromatography omitted.

In general terms, the methodology developed with the **mcmimCl**:UHP LTTM (**Table 7**, entry 1) proved to be markedly superior overall to the rest of the established protocols. Regarding waste generation per unit mass of product, the E-factor of the LTTM-promoted reaction is more than five times lower than its nearest purification-free competitor (**Table 7**, entries 1 and 4). This is mostly down to the **mcmimCl**:UHP protocol not requiring full-size liquid-liquid extraction or large excess of reagents.

In terms of material efficiency, measured by the VMR, this methodology sits second best, behind the procedure using UHP in methanol (**Table 7**, entry 3). However, this result is misleading, as the massive E-factor (not accounting for chromatographic purification) suggests. Upon closer analysis of the VMR calculation, the RME and MRP are a full order of magnitude lower with respect to the LTTM protocol. As these values tend to be very low, the effect on the VMR is not as significant, and in this case, is completely offset by the perfect SF (see **Figure S4.C1.9**).

The prospective environmental impact was evaluated using the EcoScale. Only the methodologies involving LTTMs (**Table 7**, entries 1 and 2) and the Amberlite-catalyzed process (**Table 7**, entry 5) managed to reach a score of “excellent” (> 75 points), with the rest of the procedures hampered by full-size extractive work-ups, excess reagents, hazardous components and purification steps. In this sense, the **mcmimCl**:UHP system is comfortably ahead, due to its operational simplicity, non-existent work-up, non-hazardous oxidant and lack of purification.





<sup>172</sup>Mulakayala, N.; Ismail; Kumar, K. M.; Rapolu, R. K.; Kandagatla, B.; Rao, P.; Oruganti, S.; Pal, M. *Tetrahedron Lett.* **2012**, 53, 6004–6007.





## C1.4. Conclusions

The following conclusions have been drawn from this chapter:

-  A variety of carboxy-functionalized imidazolium salts have been studied for the formation of LTTMs in combination with urea and guanidinium chloride. All assayed imidazolium salts experienced some degree of melting point depression when combined with urea, with **mcmimCl** giving the best results.
-  The LTTM formed by **mcmimCl** and urea has been studied in detail by DSC, obtaining the corresponding transition temperature and energy-composition diagrams. This mixture presents a broad usable composition range (1:3 to 3:1), with transition temperatures well under 100 °C in all cases.
-  The **mcmimCl**:UHP LTTM has been applied to the oxidation of boron compounds to alcohols, achieving excellent results. A sequential version of the methodology has been developed, resulting in a significant decrease in the environmental impact of the protocol.
-  The sustainability metrics associated with the process have been calculated and used to unbiasedly compare with previously reported methods. The obtained results, including an E-factor in the lower range of bulk chemical production and EcoScale score of excellent, suggest this synthetic protocol is superior to previously reported methodologies in terms of sustainability.

Universitat d'Alacant  
Universidad de Alicante



---

## **Chapter 2.**

**Iron-Based Imidazolium Salts as multirole catalysts for the synthesis of quinazolines.**

---

Universitat d'Alacant  
Universidad de Alicante



## C2.1. Antecedents

### C2.1.1. Quinazolines. Structure and significance

Quinazolines, as named by Widdege in 1887,<sup>173</sup> are heteroaromatic compounds formed by fused benzene and pyrimidine rings (**Figure 19**). The resulting bicycle is a planar, polar molecule (2.2 D),<sup>174</sup> with most of its electron density situated at the nitrogen atoms.<sup>175</sup> Physically, quinazoline is a slightly yellow, low-melting point (48 °C) solid which produces a mildly alkaline solution in water.<sup>3</sup>

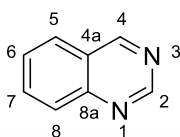


**Figure 19.** Quinazoline structure and numbering.<sup>176</sup>

The structure of quinazolines results in some interesting properties, a particularly famous example of which is their strange acid-base behavior in water. While benzocondensed diazines have properties similar to their non-fused analogues, quinazolines are much more basic than pyrimidines (pKa = 3.3 and 1.1 in water, respectively).<sup>3</sup> Related to this, quinazolines substituted at the 4 position are significantly less basic than the parent compound, regardless of the electronic nature of the substituent.<sup>175</sup>

This counterintuitive behavior was first observed by Albert, who noticed that 4-methylquinazoline was a significantly weaker base than unsubstituted quinazoline, whereas 2-methylquinazoline, followed the expected trend, being about ten times stronger than the parent compound.<sup>177</sup> Eventually, they determined that this abnormal behavior was due to hydration of the protonated quinazoline, resulting on a highly stable hydroquinazolinium cation (**Scheme 27**), for which they coined the name “amidinium”.<sup>175,177</sup>

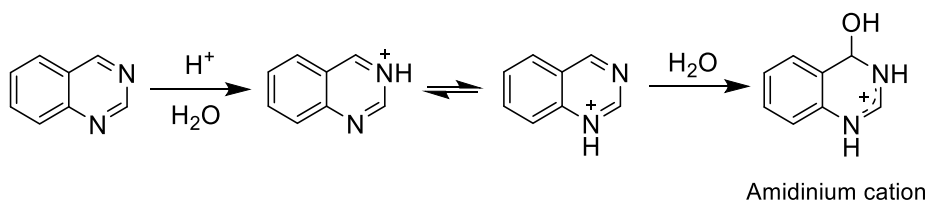
<sup>173</sup>Widdege, A. *J. Prakt. Chem.* **1887**, 36, 141.

<sup>174</sup>Büchel, K. H. *Methods of Organic Chemistry: Additional and Supplementary Volumes to the 4<sup>th</sup> Edition*; Thieme, 2001.

<sup>175</sup>Armarego, W. L. F. Quinazolines. In *Advances in Heterocyclic Chemistry*; Katritzky, A. R., Ed.; Academic Press, 1963, pp 253–309.

<sup>176</sup>Paal, C.; Busch, M. *Ber. Dtsch. Chem. Ges.* **1889**, 22, 2683.

<sup>177</sup>Albert, A. *J. Chem. Soc.* **1960**, 1790–1793.



**Scheme 27.** Formation of the amidinium cation.

The significance of quinazoline arises from its widespread presence in nature. Indeed, more than 150 alkaloids containing the quinazoline scaffold have been identified so far, with many of those exhibiting remarkable bioactivity.<sup>178</sup> The most representative example is vasicine, isolated from the leaves of *Justicia adhatoda*,<sup>179</sup> which has a potent antitussive and bronchodilator effect.<sup>178</sup> Other significant alkaloids include luotonin A, which has antineoplastic activity, asperlicin, a strong cholecystokinin antagonist, or febrifugine, a well-known antimalarial (**Figure 20**).<sup>180,181</sup>

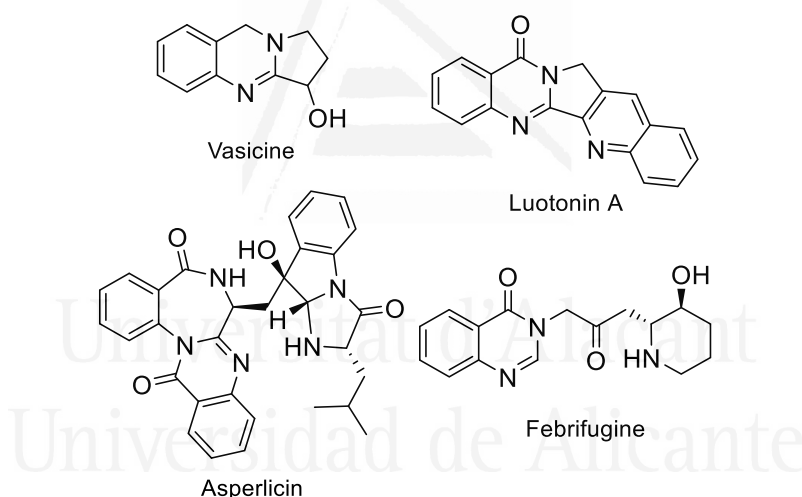


**Figure 20.** Representative examples of bioactive quinazoline alkaloids.

The ubiquitous presence of quinazoline skeleton in bioactive alkaloids led to its designation as a privileged scaffold for drug design.<sup>182</sup> However, by the late 1960s, only two compounds containing the quinazoline core were in use. Interest quickly picked up, however, and by 1980, more than 50

<sup>178</sup>Nepali, K.; Sharma, S.; Ojha, R.; Dhar, K. L. *Med. Chem. Res.* **2013**, *22*, 1–15.

<sup>179</sup>Hooper, I. D. *J. Pharm.* **1888**, *18*, 841–842.

<sup>180</sup>Witt, A.; Bergman, J. *Curr. Org. Chem.* **2003**, *7*, 659–677.

<sup>181</sup>Selvam, T. P.; Kumar, P. V. *Res. Pharm.* **2011**, *1*, 1–21.

<sup>182</sup>Welsch, M. E.; Snyder, S. A.; Stockwell, B. R. *Curr. Op. Chem. Biol.* **2010**, *14*, 347–361.

quinazoline-based drugs had been commercialized.<sup>181</sup> As of today, quinazoline-containing commercial drug formulations are used to treat a broad scope of ailments, including antihypertensives (Prazosin), diuretics (Fenquizone), antineoplastics (Gefitinib, Erlotinib), anticonvulsants (Methaqualone), antidiabetics (Linagliptin), anti-inflammatories (Proquazone), cardiotonics (Quazinone), antifungals (Albaconazole) or antivirals (Benzouracil) (**Figure 21**).<sup>181,183</sup>

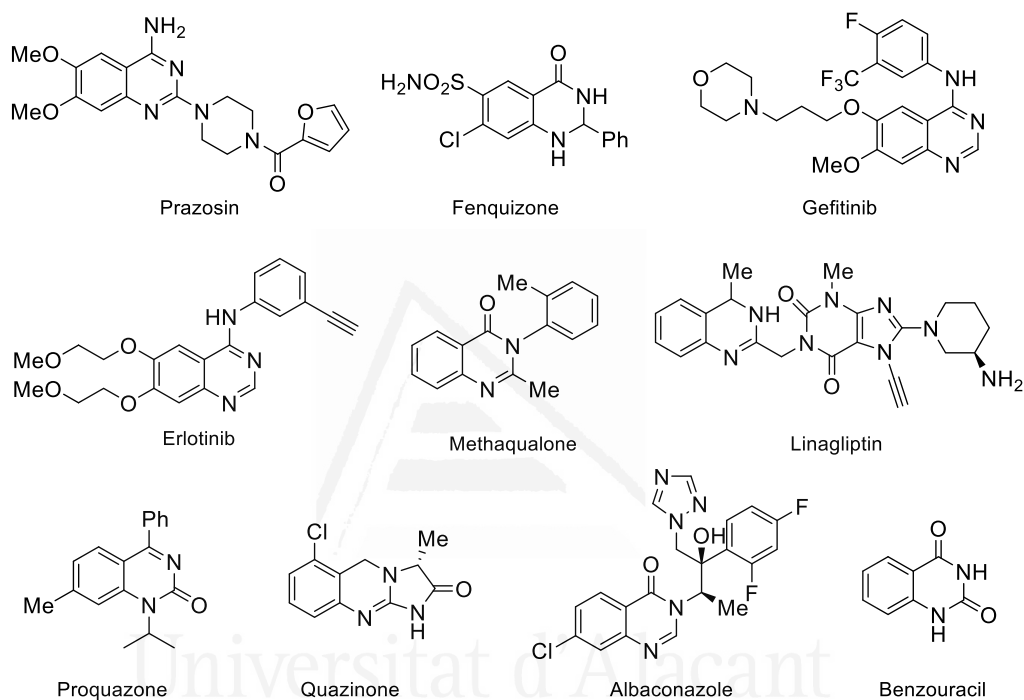


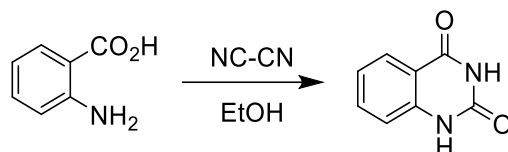
**Figure 21.** Representative examples of marketed drugs containing the quinazoline scaffold.

<sup>183</sup>Ugale, V. G.; Bari, S. B. *Eur. J. Med. Chem.* **2014**, *80*, 447–501.



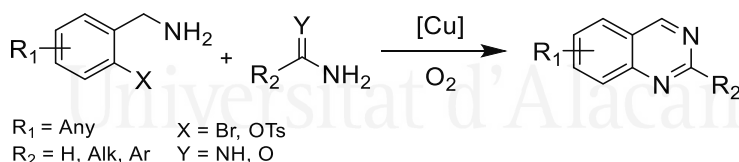
### C2.1.2. Synthesis of quinazolines

The first reported synthesis of a quinazoline derivative was described by Peter Griess in 1869, who obtained quinazoline-2,4-dione by treating anthranilic acid (2-aminobenzoic acid) with cyanogen (**Scheme 28**).<sup>184</sup>



**Scheme 28.** Griess synthesis of quinazoline-2,4-dione.

Although many years have passed since Griess's report, the basic approach for the synthesis of quinazolines has not changed significantly, with most protocols aiming for the construction of the pyrimidine ring from suitable *o*-disubstituted benzene rings *via* multicomponent reaction, although more sophisticated protocols relying on C-H activation are becoming increasingly common.<sup>185–188</sup> Nowadays, multicomponent methodologies can be roughly classified depending on whether they use 2-substituted benzylamines or anthranilic acid derivatives. The copper-catalyzed Ullmann coupling of 2-(pseudo)halobenzylamines with amides or amidines is a good example of the former (**Scheme 29**).<sup>189–191</sup> A similar approach has also been developed with 2-halonitriles.<sup>192</sup>



**Scheme 29.** Synthesis of quinazolines by Ullmann coupling.

<sup>184</sup>Griess, P. *Ber. Dtsch. Chem. Ges.* **1869**, *2*, 415–418.

<sup>185</sup>Connolly, D. J.; Cusack, D.; O'Sullivan, T. P.; Guiry, P. J. *Tetrahedron* **2005**, *61*, 10153–10202.

<sup>186</sup>Michael, J. P. *Nat. Prod. Rep.* **2008**, *25*, 166–187.

<sup>187</sup>Khan, I.; Ibrar, A.; Abbas, N.; Saeed, A. *Eur. J. Med. Chem.* **2014**, *76*, 193–244.

<sup>188</sup>Abdou, I. M.; Al-Neyadi, S. S. *Heterocycl. Commun.* **2015**, *21*, 115–132.

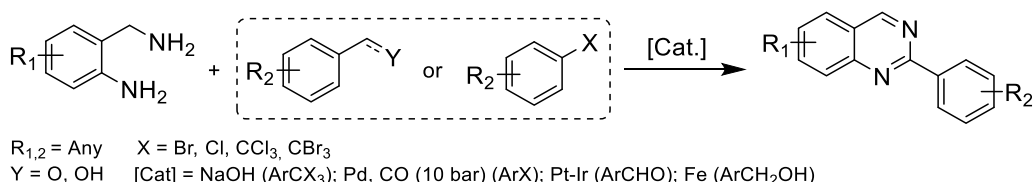
<sup>189</sup>Malakar, C. C.; Baskakova, A.; Conrad, J.; Beifuss, U. *Chem. Eur. J.* **2012**, *18*, 8882–8885.

<sup>190</sup>Liu, Q.; Zhao, Y.; Fu, H.; Cheng C. *Synlett* **2013**, *24*, 2089–2094.

<sup>191</sup>Wang, C.; Li, S.; Liu, H.; Jiang, Y.; Fu, H. *J. Org. Chem.* **2010**, *75*, 7936–7938.

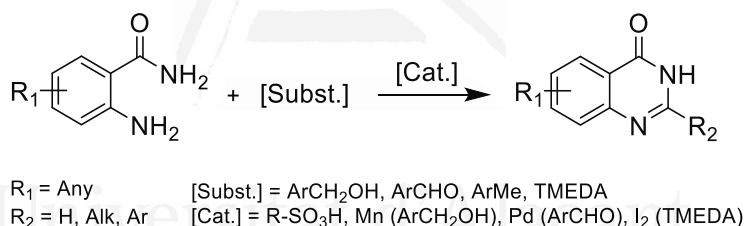
<sup>192</sup>Jia, F.-C.; Zhou, Z.-W.; Xu, C.; Cai, Q.; Li, D.-K.; Wu, A.-X. *Org. Lett.* **2015**, *17*, 4236–4239.

2-Aminobenzylamines are very convenient substrates, as they provide five of the atoms of the final pyrimidine ring. Thus, several methodologies employing carbon monoxide and ammonia,<sup>193</sup> aldehydes,<sup>194,195</sup> benzyl alcohols<sup>196</sup> or trihalobenzenes<sup>197</sup> as coupling partners have been developed (**Scheme 30**).



**Scheme 30.** Representative methodologies using 2-aminobenzylamines as substrates.

From Griess studies to Siegmund Gabriel's first synthesis of unsubstituted quinazoline in 1903,<sup>198</sup> anthranilic acid and its derivatives are the most widely used substrates for quinazoline synthesis by far, due to their convenience (providing at least atoms 1 and 4 of the target pyrimidine skeleton), ready availability and versatility. For instance, 2-aminobenzamides have been combined with one-carbon synthons to afford quinazolin-4-ones (**Scheme 31**).<sup>187,199–201</sup>



**Scheme 31.** Synthesis of quinazolin-4-ones from 2-aminobenzamides.

<sup>193</sup>Chen, J.; Natte, K.; Neumann, H.; Wu, X.-F. *RSC Adv.* **2014**, *4*, 56502–56505.

<sup>194</sup>Ma, Z.; Song, T.; Yuan, Y.; Yang, Y. *Chem. Sci.* **2019**, *10*, 10283–10289.

<sup>195</sup>Yuan, H.; Yoo, W.-J.; Miyamura, H.; Kobayashi, S. *Adv. Synth. Catal.* **2012**, *354*, 2899–2904.

<sup>196</sup>Parua, S.; Sikari, R.; Sinha, S.; Chakraborty, G.; Mondal, R.; Paul, N. D. *J. Org. Chem.* **2018**, *83*, 11154–11166.

<sup>197</sup>Chatterjee, T.; Kim, D. I.; Cho, E. J. *J. Org. Chem.* **2018**, *83*, 7423–7430.

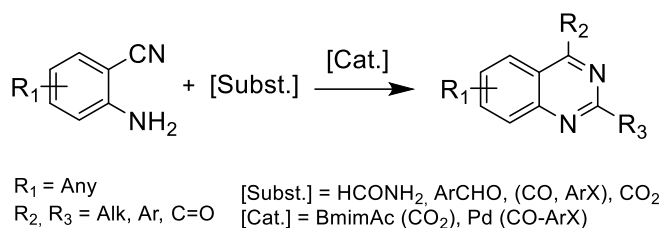
<sup>198</sup>Gabriel, S. *Ber. Dtsch. Chem. Ges.* **1903**, *36*, 800–813.

<sup>199</sup>Khan, I.; Ibrar, A.; Ahmed, W.; Saeed, A. *Eur. J. Med. Chem.* **2015**, *90*, 124–169.

<sup>200</sup>Zhang, Z.; Wang, M.; Zhang, C.; Zhang, Z.; Lu, J.; Wang, F. *Chem. Commun.* **2015**, *51*, 9205–9207.

<sup>201</sup>Yan, Y.; Xu, Y.; Niu, B.; Xie, H.; Liu, Y. *J. Org. Chem.* **2015**, *80*, 5581–5587.

Anthranilonitrile is frequently used as a precursor to 2-aminobenzophenones and 2-aminobenzimines,<sup>202</sup> although it has also been directly combined with formamide,<sup>203</sup> aldehydes, carbon monoxide and carbon dioxide (**Scheme 32**).<sup>199</sup>



**Scheme 32.** Use of anthranilonitriles as substrates for quinazoline formation.

2-Aminobenzaldehydes,<sup>204</sup> 2-nitrobenzaldehydes,<sup>205,206</sup> 2-aminobenzophenones,<sup>201,207,208</sup> and 2-aminobenzyl alcohols<sup>209–211</sup> are among the most widely used substrates for the synthesis of quinazolines in combination with a variety of one and two-carbon synthons.<sup>200,212–220</sup>

<sup>202</sup>Zhao, H.; Huang, J.; Zhang, J.; Tang, Y.; Zhang, Y. *ChemistrySelect* **2020**, *5*, 3007–3010.

<sup>203</sup>Held, F. E.; Guryev, A. A.; Fröhlich, T.; Hampel, F.; Kahnt, A.; Hutterer, C.; Steingruber, M.; Bahsi, H.; von Bojničić-Kninski, C.; Mattes, D. S.; Foertsch, T. C.; Nesterov-Mueller, A.; Marschall, M.; Tsogoeva, S. B. *Nat. Commun.* **2017**, *8*, 15071.

<sup>204</sup>Deshmukh, D. S.; Bhanage, B. M. *Synlett* **2018**, *29*, 979–985.

<sup>205</sup>Nguyen, T. B.; Le Bescont, J.; Ermolenko, L.; Al-Mourabit, A. *Org. Lett.* **2013**, *15*, 6218–6221.

<sup>206</sup>Akazome, M.; Yamamoto, J.; Kondo, T.; Watanabe, Y. *J. Organomet. Chem.* **1995**, *494*, 229–233.

<sup>207</sup>Rachakonda, S.; Pratap, P. S.; Rao, M. V. B. *Synthesis* **2012**, *44*, 2065–2069.

<sup>208</sup>Karnakar, K.; Kumar, A. V.; Murthy, S. N.; Ramesh, K.; Nageswar, Y. V. D. *Tetrahedron Lett.* **2012**, *53*, 4613–4617.

<sup>209</sup>Gopalaiah, K.; Saini, A.; Devi, A. *Org. Biomol. Chem.* **2017**, *15*, 5781–5789.

<sup>210</sup>Chen, Z.; Chen, J.; Liu, M.; Ding, J.; Gao, W.; Huang, X.; Wu, H. *J. Org. Chem.* **2013**, *78*, 11342–11348.

<sup>211</sup>Yao, S.; Zhou, K.; Wang, J.; Cao, H.; Yu, L.; Wu, J.; Qiu, P.; Xu, Q. *Green Chem.* **2017**, *19*, 2945–2951.

<sup>212</sup>Karnakar, K.; Shankar, J.; Murthy, S. N.; Ramesh, K.; Nageswar, Y. V. D. *Synlett* **2011**, 1089–1096.

<sup>213</sup>Saikia, U. P.; Borah, G.; Pahari, P. *Eur. J. Org. Chem.* **2018**, 1211–1217.

<sup>214</sup>Ferrini, S.; Ponticelli, F.; Taddei, M. *Org. Lett.* **2007**, *9*, 69–72.

<sup>215</sup>Zhao, D.; Shen, Q.; Li, J.-X. *Adv. Synth. Catal.* **2015**, *357*, 339–344.

<sup>216</sup>Zhang, J.; Zhu, D.; Yu, C.; Wan, C.; Wang, Z. *Org. Lett.* **2010**, *12*, 2841–2843.

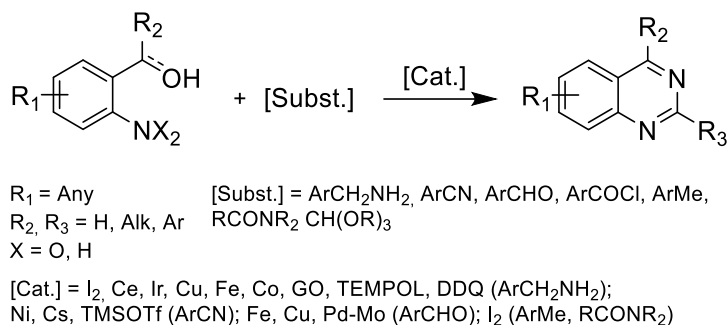
<sup>217</sup>Yan, Y.; Zhang, Y.; Feng, C.; Zha, Z.; Wang, Z. *Angew. Chem. Int. Ed.* **2012**, *51*, 8077–8081.

<sup>218</sup>Zhang, J.; Yu, C.; Wang, S.; Wan, C.; Wang, Z. *Chem. Commun.* **2010**, *46*, 5244–5246.

<sup>219</sup>Portela-Cubillo, F.; Scott, J. S.; Walton, J. C. *J. Org. Chem.* **2009**, *74*, 4934–4942.

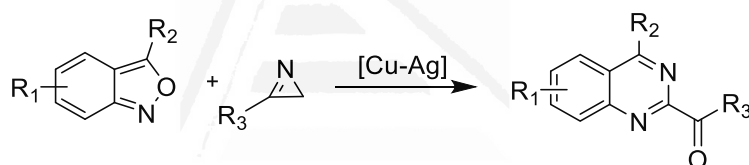
<sup>220</sup>Zhang, J.; Wang, Q.; Guo, Y.; Ding, L.; Yan, M.; Gu, Y.; Shi, J. *Eur. J. Org. Chem.* **201**, 5934–5936.

The use of transition metal catalysts is frequent, although metal-free<sup>221</sup> and catalyst-free<sup>222</sup> methods are also reported (**Scheme 33**).



**Scheme 33.** Synthesis of quinazolines with anthranilic acid derivatives.

An interesting methodology uses anthranil (2,1-benzisoxazole) in combination with azirines under copper-silver catalysis to afford synthetically challenging 2-acylquinazolines (**Scheme 34**).<sup>223</sup>



**Scheme 34.** Synthesis of 2-acylquinazolines from anthranil.

C-H activation involves the direct functionalization of unactivated carbon atoms, commonly under (pseudo)noble metal catalysis.<sup>224</sup> Often, C-H activation protocols require directing groups capable of coordinating the metal catalyst to achieve functionalization at the desired position. Thus, this approach is particularly interesting for the formation of the quinazoline ring from benzylamines or benzylimines *via* [4+2] C-H annulation, using nitriles,<sup>225</sup> azides<sup>226</sup> or dioxazolones<sup>227</sup> as coupling partners (**Scheme 35**).

<sup>221</sup>Han, B.; Wang, C.; Han, R.-F.; Yu, W.; Duan, X.-Y.; Fang, R.; Yang, X.-L. *Chem. Commun.* **2011**, 47, 7818–7820.

<sup>222</sup>Bhat, S. I.; Das, U. K.; Trivedi, D. R. *J. Heterocycl. Chem.* **2015**, 52, 1253–1259.

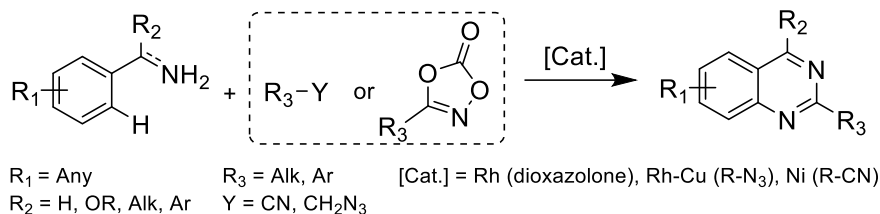
<sup>223</sup>Sun, Y.; Sun, H.; Wang, Y.; Xie, F. *Org. Lett.* **2020**, 22, 6756–6759.

<sup>224</sup>Mkhalid, I. A. I.; Barnard, J. H.; Marder, T. B.; Murphy, J. M.; Hartwig, J. F. *Chem. Rev.* **2010**, 110, 890–931.

<sup>225</sup>Sikari, R.; Chakraborty, G.; Guin, A. K.; Paul, N. D. *J. Org. Chem.* **2021**, 86, 279–290.

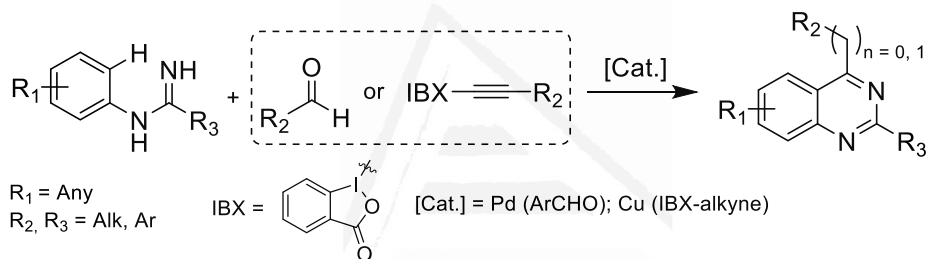
<sup>226</sup>Wang, X.; Jiao, N. *Org. Lett.* **2016**, 18, 2150–2153.

<sup>227</sup>Wang, J.; Zha, S.; Chen, K.; Zhang, F.; Song, C.; Zhu, J. *Org. Lett.* **2016**, 18, 2062–2065.



**Scheme 35.** Synthesis of quinazolines by  $\text{sp}^2$  C-H activation of benzylamine derivatives.

Arylamidines are also popular substrates for C-H activation. As they contain atoms 1 to 3 of the quinazoline ring, the protocols described involve cyclizations with one-carbon synthons such as aldehydes<sup>228</sup> or activated alkynes<sup>229</sup> (**Scheme 36**), with intramolecular versions having been developed as well.<sup>230</sup>



**Scheme 36.** Synthesis of quinazolines from arylamidines.

Universitat d'Alacant  
 Universidad de Alicante

<sup>228</sup>McGowan, M. A.; McAvoy, C. Z.; Buchwald, S. L. *Org. Lett.* **2012**, *14*, 3800–3803.

<sup>229</sup>Ohta, Y.; Tokimizu, Y.; Oishi, S.; Fujii, N.; Ohno, H. *Org. Lett.* **2010**, *12*, 3963–3965.

<sup>230</sup>Lin, J.-P.; Zhang, F.-H.; Long, Y.-Q. *Org. Lett.* **2014**, *16*, 2822–2825.

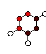
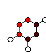
## C2.2. Objectives

Based on their antifungal, antibacterial<sup>231</sup> and anticancer properties,<sup>232</sup> 2,4 disubstituted quinazolines were selected as synthetic targets for this study. The oxidative condensation-cyclization of 2-acylanilines and benzylamines was deemed the most suitable methodology for their preparation, as it can be easily adapted to accommodate different substitution patterns over the quinazoline ring.

While this reaction had been previously studied with different catalytic systems (see section C2.1.), many of the protocols in literature present issues associated with the high temperatures required for this transformation and the surprisingly difficult final aromatization step. Toluene, xylene and acetonitrile are commonplace solvents,<sup>216,221</sup> due to their high boiling points, although solventless (neat) methodologies have also been described.<sup>218</sup>

In the majority of reports, aromatization is achieved *via* oxidation with aqueous *tert*-butyl hydroperoxide (TBHP),<sup>208,212,216,233</sup> which as an organic peroxide, is prone to dangerous reactivity, including thermal runaway and explosions in the presence of certain contaminants.<sup>234</sup> Some research groups have circumvented this issue running the reaction under pure oxygen using redox catalysts,<sup>204,221</sup> but the manipulation of gasses has its own technical problems.

Thus, based on these antecedents, the following objectives were established:

-  To develop a synthetic methodology for the preparation of potentially bioactive 2- and 2,4-substituted quinazolines from 2-carboxylanilines and benzylamines in aerobic, solventless conditions using a multirole imidazolium LTTM catalyst.
-  To assess the environmental impact of the protocol and compare it with previously reported methodologies using sustainability metrics.

<sup>231</sup>Eswararao, S. V.; Venkataramireddy, V.; Srinivasareddy, M.; Pramod, K. *Asian J. Chem.* **2017**, *29*, 1434–1440.

<sup>232</sup>Nahar, S.; Bose, D.; Kumar Panja, S.; Saha, S.; Maiti, S. *Chem. Commun.* **2014**, *50*, 4639–4642

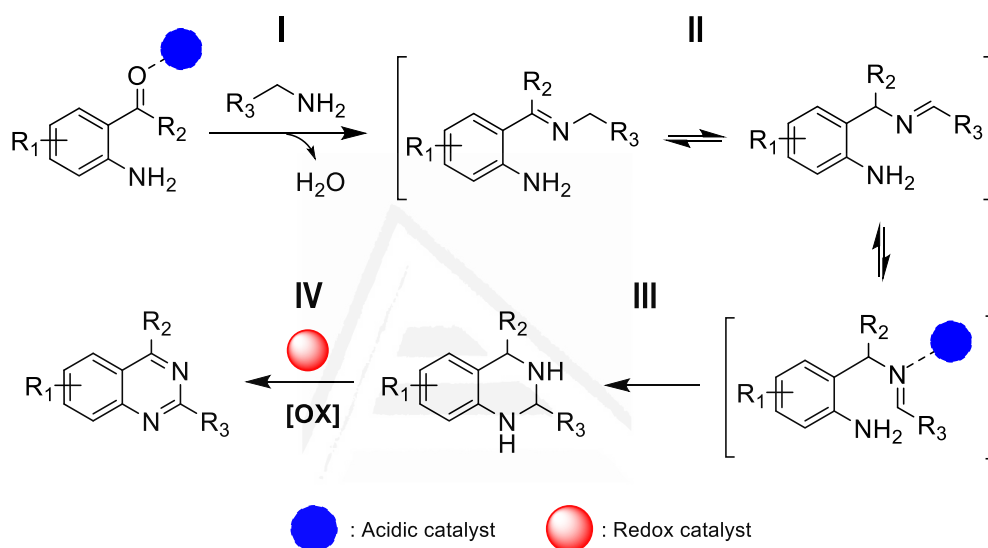
<sup>233</sup>Truong, T.; Hoang, T. M.; Nguyen, C. K.; Huynh, Q. T. N.; Phan, N. T. S. *RSC Adv.* **2015**, *5*, 24769–24776.

<sup>234</sup>Wang, Y.-W.; Duh, Y.-S.; Shu, C.-M. *J. Therm. Anal. Calorim.* **2009**, *95*, 553–557.



### C2.3. Results and discussion

The transformation in hand involves four main steps (**Scheme 37**).<sup>216</sup> First, an imine is formed by condensation of the benzylamine with the carbonyl of the aniline ring (**Scheme 37**, step I). After an intermediate tautomerization step (**Scheme 37**, step II), an intramolecular nucleophilic attack from the free nitrogen to the iminic carbon leads to the corresponding tetrahydroquinazoline (**Scheme 37**, step III), which is promptly oxidized to afford the final product (**Scheme 37**, step IV).



**Scheme 37.** Prospective mechanism of the reaction.

To achieve maximum efficiency, the catalytic system used should be able to promote the condensation and cyclization steps (**Scheme 37**, steps I and III) as well as the final aromatization step, ideally using the oxygen in air as terminal oxidant.

Based on the experience of the research group, the use of Iron-Based Imidazolium Salts (**IBIS**), LTTMs formed by combination of imidazolium salts with stoichiometric amounts of iron(III) halides,<sup>235</sup> was considered. The particular system selected for this study bears a carboxy moiety and a linear butyl chain (**Figure 22**).

<sup>235</sup>Prodius, D.; Macaev, F.; Stingaci, E.; Pogrebnoi, V.; Mereacre, V.; Novitchi, G.; Kostakis, G. E.; Anson, C. E.; Powell, A. K. *Chem. Commun.* **2013**, 49, 1915–1917.



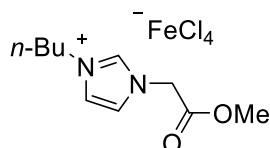
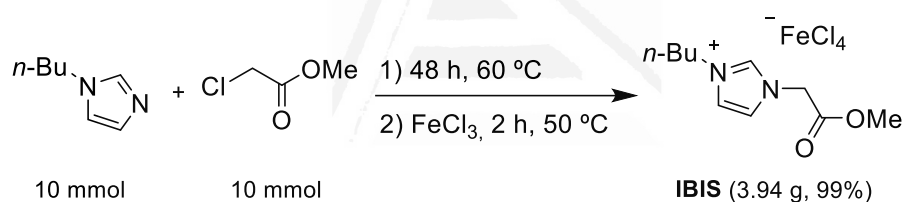


**Figure 22.** 1-Butyl-3-(methoxycarbonylmethyl)imidazolium tetrachloroferrate (**IBIS**).

Carboxy-imidazolium salts exhibit Lewis acidic behavior both by themselves<sup>153</sup> and in combination with iron,<sup>236</sup> with which they are also capable of carrying out oxidation procedures under aerobic conditions, eliminating the need for external oxidizers.<sup>235,237</sup> Therefore, these systems perfectly suit the requirements of this synthetic protocol.

**IBIS** is obtained *via* a solventless two-step, one-pot process. The first step involves the reaction of 1-butylimidazole with methyl chloroacetate at 60 °C for 48 hours, followed by addition of stoichiometric amount of iron(III) chloride to afford **IBIS** in quantitative yield after 2 hours (**Scheme 38**). The process has perfect yield, AE, SF, RME and MRP (VMR = 1) an E-factor of 0 and a EcoScale score of 76 (excellent) (see **SI.4.2** for more details).

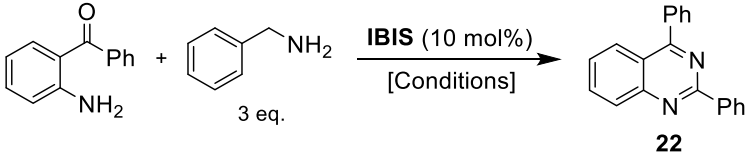


**Scheme 38.** Synthesis of **IBIS**.

The synthesis of 2,4-diphenylquinazoline (**22**) from 2-aminobenzophenone and benzylamine in the presence of catalytic amount of **IBIS** was selected as the model reaction to perform optimization studies. As the LTTM catalyst can enhance the mixing of components, the reactions were carried out in neat conditions. The results are compiled in **Table 8**.

<sup>236</sup>Trillo, P.; Pastor, I. M. *Adv. Synth. Catal.* **2016**, 358, 2929–2939.

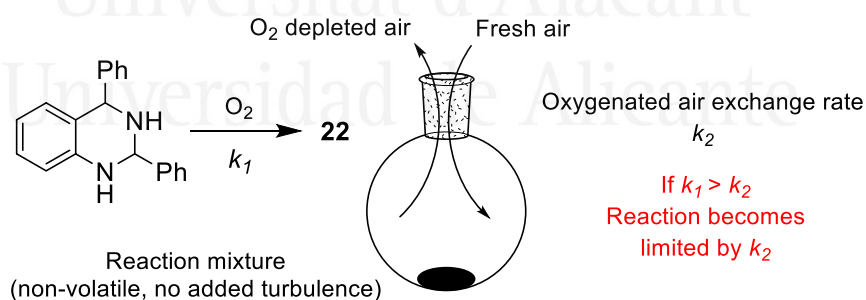
<sup>237</sup>Gisbert, P.; Pastor, I. M. *Synthesis* **2018**, 50, 3031–3040.

**Table 8.** Optimization of the reaction conditions.


| Entry | Temp. (°C) | Time (h) | Conditions            | Conv. (%) <sup>†</sup> |
|-------|------------|----------|-----------------------|------------------------|
| 1     | 110        | 16       | Open flask            | 12                     |
| 2     | 110        | 16       | Argon                 | 18                     |
| 3     | 110        | 16       | Air flow <sup>‡</sup> | 41                     |
| 4     | 110        | 24       | Air flow <sup>‡</sup> | 75                     |
| 5     | 130        | 22       | Air flow <sup>‡</sup> | 97                     |

<sup>†</sup>Determined by GC-MS using durene (1,2,4,5-tetramethylbenzene) as internal standard <sup>‡</sup>50 mL/min

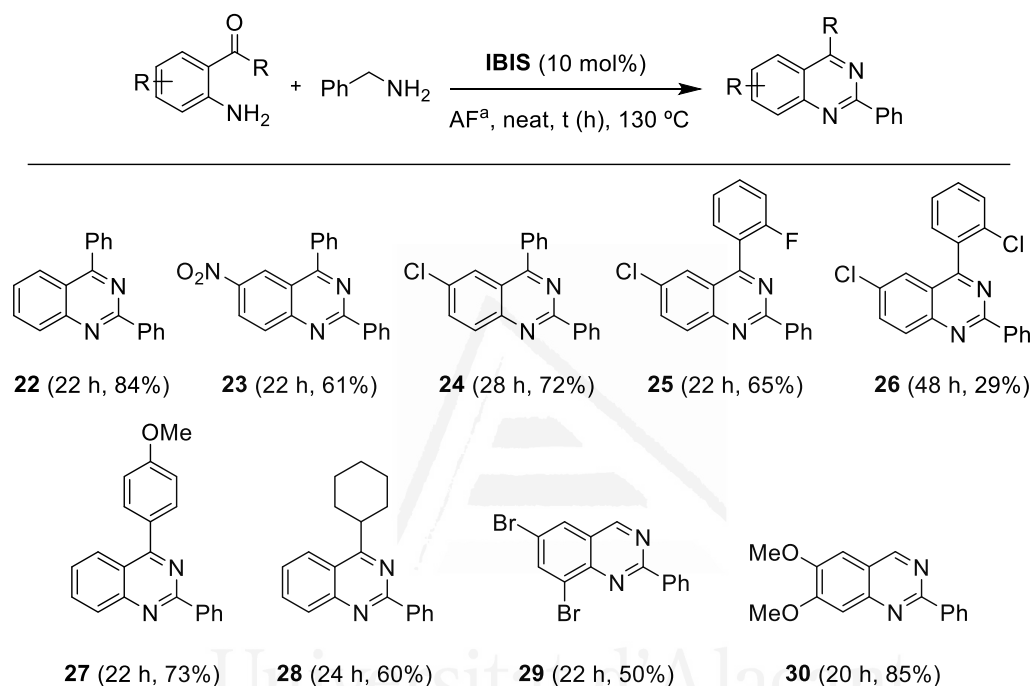
The first experiment resulted in only 12% conversion to the desired product, although overall consumption of the starting material was high, with reaction intermediates ( $m/z = 286$ ) observed in 63% conversion (**Table 8**, entry 1). Running the reaction under argon led to a very similar result (**Table 8**, entry 2), which implied that the catalyst was working as intended on its role as a Lewis acid, but it was not able to fully complete the oxidation step. After analysis of the reaction conditions, it was hypothesized that a pocket of oxygen-depleted air might be forming on top of the reactions, due to the lack of convection arising from running the reaction on non-volatile media and the neck of the vessel acting as a chokepoint (**Figure 23**). This would effectively mean that, after the first few cycles, the reaction rate becomes limited by the rate at which the inner atmosphere is re-oxygenated.

**Figure 23.** Scheme for the reaction slowdown hypothesis.

Thus, the next experiment consisted in running the reaction under a gentle stream of air to aid convection, by inserting a glass nozzle connected to a peristaltic pump into the reaction vessel. This had immediate results, with conversion to **22** jumping to 41% (**Table 8**, entry 3). Extending the reaction

time to 24 hours resulted in further increase to 75% conversion, whereas setting temperature to 130 °C resulted in almost quantitative conversion to **22** after 22 hours (Table 8, entry 4).

With the optimum reaction conditions set, the scope of the reaction was explored. First, several 2-carboxylanilines were combined with benzylamine, obtaining the results described in Figure 24.



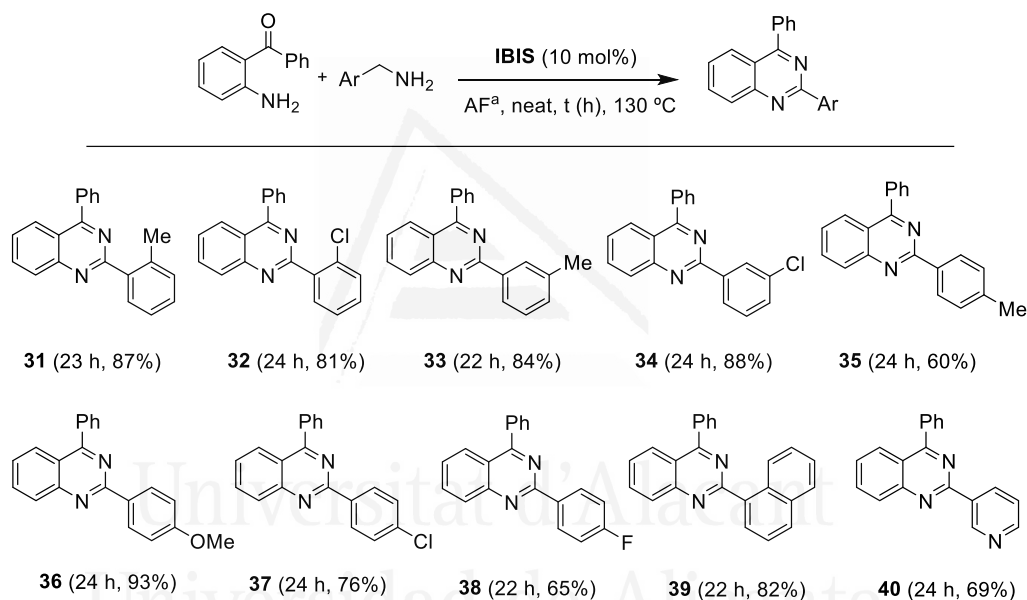
<sup>a</sup>Air flow set to 50 mL/min. Isolated yields

**Figure 24.** Scope of the reaction. 2-carboxylanilines.

Overall, the reactions proceeded smoothly, affording the desired products in moderate to good yields. 2-Carboxylanilines bearing electron withdrawing groups gave noticeably lower yields compared to the model reaction (Figure 24, compounds **23**, **24**). According to the mechanism proposed in Scheme 37, a reduction in the electron density of the substrate should facilitate the first step of the reaction (formation of the imine) while slowing down the intramolecular cyclization to the tetrahydroquinazoline. In this case, the electron-withdrawing group is in *para* position relative to the amino group and *meta* to the carbonyl, so the effect is expected to be much greater in the cyclization step, as observed. Additionally, the reaction seems to be heavily influenced by steric hindrance in the vicinity of the carbonyl. While the *o*-fluoro-substituted compound **25** was obtained in 65% yield after 22 hours, compound **26** could only be obtained in 29% yield after two days of reaction. This behavior is consistent with the findings reported in Chapter 1 of this manuscript (Figure 17, compound **3**). The

presence of electron donating groups in the secondary phenyl group result in marginally lower yields than the model reaction, due to the lower electrophilicity of the carbonyl carbon (**Figure 24**, compound **27**). Alkyl ketones were found to be compatible with this protocol, with a cyclohexyl derivative affording **28** in good yield. Lastly, 2-aminobenzaldehydes were assayed as substrates. The effect of electron density of the 2-amino component in the outcome of the reaction is particularly noticeable in this case, with the electron-poor compound **29** being isolated in just 50% yield against the 85% obtained of the electron-rich compound **30**.

Next, different benzylamine derivatives were assayed in combination with 2-aminobenzophenone, obtaining the results compiled in **Figure 25**.



<sup>a</sup>Set to 50 mL/min. Isolated yields.

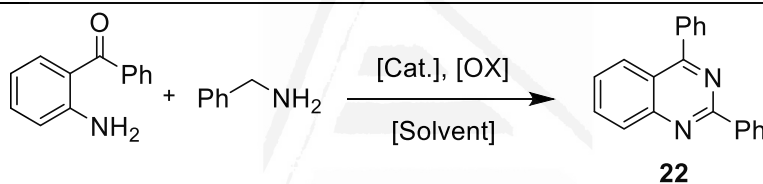
**Figure 25.** Scope of the reaction. Benzylamine derivatives.

In this case, the electronic nature of the substituents does not seem to influence the outcome of the reaction in any significant way, with isolated yields within margin of error for benzylamines substituted with both electron-donating and electron-withdrawing groups (**Figure 25**). The same applies to the relative position of the substituents in the aromatic ring, with the higher inconsistency in the yields of *para*-substituted substrates being the only noticeable difference (e.g., compounds **35** and **36**). Nevertheless, results were good, with all compounds isolated in up to excellent yield. Extended aromatic systems are well tolerated, as evidenced by the naphthyl-substituted compound **39**, isolated in 82% yield, as well as heterocycles, with 3-picolylamine affording **40** in nice yield.

To assess the robustness of the methodology, the model reaction was scaled up to 5 mmol. Under the same working conditions, 69% of product **22** was isolated. The reduction in yield is mostly attributed to oxygen-supply constraints, as the 2-aminobenzophenone was fully consumed and intermediates were detected by GC-MS in significant quantity.

Next, the designed protocol was compared with established methodologies using sustainability metrics. Thus, VMR (from reaction yield, AE,  $RME_{\text{Andraos}}$ , SF and MRP), E-factor and EcoScale were calculated for representative syntheses using metallic and non-metallic catalysts, as well as different solvents (including neat conditions) and oxidizers. As every methodology listed requires purification by column chromatography, this step was not considered for the VMR or E-factor calculations, as the contribution of purification solvents and materials would mask the differences between protocols. The synthesis of **22** was selected for this comparison, obtaining the results compiled in **Table 9** (see section **SI.4.2.** for more details).

**Table 9.** Comparison between the **IBIS** methodology and reported protocols for the synthesis of **22**.



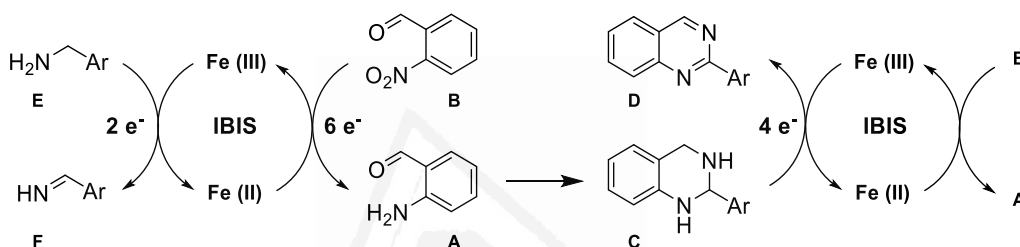
| Entry <sup>Ref.</sup>   | [Solv.]          | [Cat.]         | [OX]                    | VMR   | E-factor <sup>‡</sup> | EcoScale |
|-------------------------|------------------|----------------|-------------------------|-------|-----------------------|----------|
| <b>1</b>                | Neat             | <b>IBIS</b>    | Air                     | 0.743 | 1.6                   | 70       |
| <b>2</b> <sup>204</sup> | Neat             | I <sub>2</sub> | O <sub>2</sub> (1 atm.) | 0.761 | 1.5                   | 62       |
| <b>3</b> <sup>207</sup> | Toluene          | DDQ            | TBHP                    | 0.627 | 148.5                 | 51       |
| <b>4</b> <sup>221</sup> | <i>o</i> -Xylene | TEMPOL         | O <sub>2</sub> (1 atm.) | 0.696 | 2.3                   | 74       |
| <b>5</b> <sup>233</sup> | Toluene          | ZIF-67         | TBHP                    | 0.546 | 451.3                 | 55       |
| <b>6</b> <sup>218</sup> | Neat             | Cu NPs         | TBHP                    | 0.642 | 60.6                  | 61       |

<sup>†</sup>Calculated from yield, AE, SF, MRP and  $RME_{\text{Andraos}}$ . <sup>‡</sup>Purification by column chromatography omitted.

In general terms, the **IBIS**-catalyzed protocol is well designed, being comfortably ahead of other metal-catalyzed processes in terms of E-factor, VMR and EcoScale (**Table 9**, entry 1, 5 and 6). The material efficiency metrics are highest for methodologies using neat conditions (**Table 9**, entries 1 and 2) and oxygen as oxidant, due to the lack of work-up required before purification (**Table 9**, entries 1, 2, 4). The EcoScale scores are somewhat low in general, due to the 10-point penalty for chromatographic purification applied to every entry, although they clearly reflect the safety issues associated to the use of TBHP and toxic aromatic solvents (**Table 9**, entries 3, 5, 6).

One of the main drawbacks of this synthetic methodology is related to the availability of 2-aminobenzaldehydes. Due to their low stability, commercial sources of 2-aminobenzaldehydes are limited to compounds substituted with electron-withdrawing groups, with the associated reactivity issues. Any other substrates are usually obtained from stable 2-nitrobenzaldehydes, which can be reduced to the corresponding amino derivatives *via* Béchamp reaction with excess metallic iron in refluxing hydrochloric acid.<sup>238</sup> In terms of sustainability, this is clearly unacceptable.

Thus, the next stage of this study involved the design of a synthetic protocol for the direct formation of 2-arylquinazolines from 2-nitrobenzaldehydes and benzylamines, based on Nguyen and coworkers' synthesis of benzimidazoles from 2-nitroanilines (**Scheme 39**).<sup>205</sup>



**Scheme 39.** Iron-catalyzed direct synthesis of 2-arylquinazolines from 2-nitrobenzaldehydes.

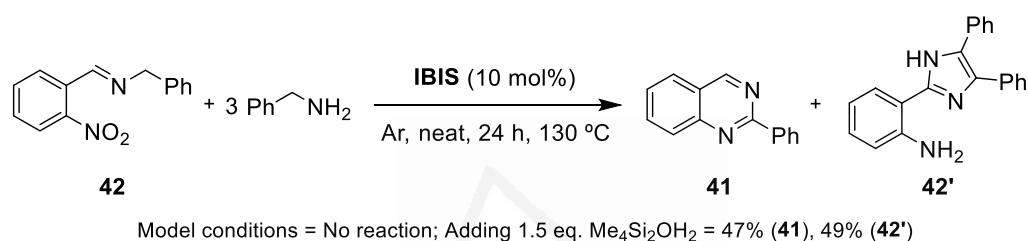
The designed protocol involves the six-electron reduction of 2-nitrobenzaldehyde to the corresponding amine derivative (**Scheme 39**, A to B) promoted by **IBIS**. Benzylamine, which has a relatively high oxidation potential ( $E_{ox} = 0.43$  V against SCE in water)<sup>239</sup> can be used as terminal reductant to regenerate the **IBIS** (**Scheme 39**, E to F). As three equivalents of benzylamine are added to the reaction, but only one is required, the excess amount is available for oxidation, being able to provide up to four electrons. On the other hand, the two-step oxidation of tetrahydroquinazoline yields an additional four electrons (**Scheme 39**, C to D), for a total of up to eight equivalents of electrons.

Based on this, the model conditions for the reaction of 2-nitrobenzaldehyde and benzylamine were set. Three equivalents of benzylamine were combined with one equivalent of 2-nitrobenzaldehyde and 10 mol% of **IBIS** at 130 °C for 24 hours under argon, to avoid the interference of air. After the reaction time had elapsed, GC-MS analysis indicated total consumption of the 2-nitrobenzaldehyde. However, 2-phenylquinazoline (**41**) could only be isolated in 21% yield (**Figure 26**). As the starting material was fully consumed, the initial hypothesis pointed to the well-known tendency of 2-aminobenzaldehydes to polymerize.

<sup>238</sup>Béchamp, M. A. *Ann. Chim. Phys.* **1854**, 42, 186–196.

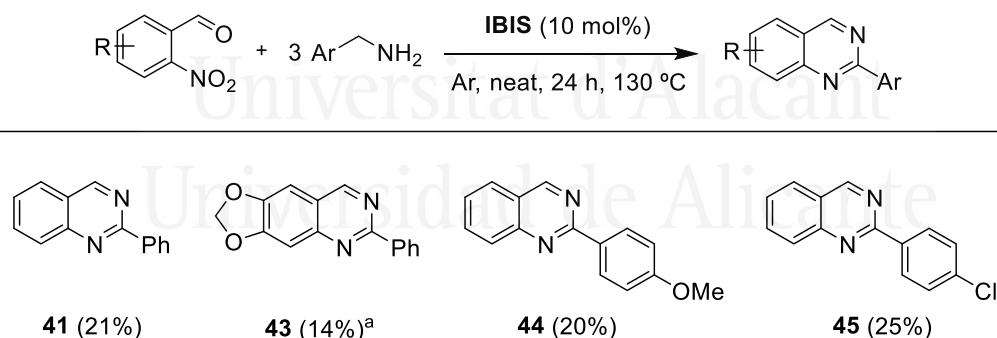
<sup>239</sup>Luczak, T. *J. Appl. Electrochem.* **2008**, 38, 43–50.

To explore this possibility, the imine of 2-nitrobenzaldehyde and benzylamine (**42**) was prepared and subjected to the same working conditions (**Scheme 40**), although no change was observed after 24 hours. Thus, stoichiometric amount of a mild reductant was added, resulting in 47% conversion after an additional 24 hours. However, a previously unknown compound of  $m/z = 311$  was also formed in 49% conversion. A tentative structure (**42'**) is proposed for the byproduct, which would be consistent with the reaction of reduced imine **42** with another equivalent of benzylamine, followed by cyclization. It must be noted that further characterization has not been attempted due to time constraints, therefore the structure proposed for **42'** is purely speculative.



**Scheme 40.** Control experiment. Synthesis of compound **41** from imine **42**.

The next series of experiments aimed at spotting patterns of reactivity based on substitution, using different 2-nitrobenzaldehydes and benzylamines under the model conditions. The results obtained are compiled in **Figure 26**.



<sup>a</sup>NMR yield using hexamethylbenzene as internal standard.

**Figure 26.** Assays for the direct synthesis of 2-arylquinazolines from 2-nitrobenzaldehydes.

From the obtained results, the only apparent pattern in reactivity seems to arise from the electron density of the components. For instance, the electron-rich 2-nitropiperonal resulted in lower yields of product than the standard 2-nitrobenzaldehyde (**Figure 26**, compounds **43** and **41**,

respectively), whereas the opposite effect is observed for benzylamines, with 4-methoxybenzylamine affording **44** in lower yield than its chloro- counterpart (**Figure 26**, compound **45**).

These results, along with the control experiment described in **Scheme 40** point to side-reactions involving the highly nucleophilic benzylamine as the most likely cause of the low yields obtained. This is consistent with the tentative structure proposed for **42'**, as well as 4-chlorobenzylamine giving better results than its 4-methoxy and unsubstituted counterparts (**Figure 26**, compounds **45**, **44** and **41**) In lieu of time and resource constraints, no further studies were carried out for this particular transformation.



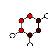
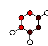
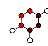
Universitat d'Alacant  
Universidad de Alicante





## C2.4. Conclusions

The following conclusions were drawn from this study:

-  The Lewis-acidic and redox-active **IBIS** has been applied as catalyst for the synthesis of quinazoline derivatives in the absence of solvent and using atmospheric oxygen as oxidant. This way, a variety of 2- and 2,4-substituted quinazolines have been obtained in moderate to excellent yields.
-  The design of the protocol has been compared to representative methodologies reported in literature using sustainability metrics. The results obtained show that the **IBIS**-catalyzed process is comparable to the best-scoring syntheses in terms of material efficiency and classifies in the higher range of acceptable EcoScale scores (> 50).
-  A methodology for the direct synthesis of 2-arylquinazolines from 2-aminobenzaldehydes has been designed, and preliminary studies have been carried out, obtaining low yields (ca. 20%) of the desired products due to side reactivity issues. Further studies were not pursued due to time and resource constraints.



---

## **Chapter 3.**

**Brønsted-acidic Ionic Organic Solids based  
on carboxy- and sulfoimidazolium salts.**

---

Universitat d'Alacant  
Universidad de Alicante



## C3.1. Antecedents

### C3.1.1. Ionic organic solids

Ionic Organic Solids (IOS) are formally ionic solid compounds formed by organic cations and a variety of counter-anions. This definition is complementary to that of ILs, therefore, any organic salt with a melting point over 100 °C satisfies the requirements to be considered an IOS.

Although the term IOS did not appear in literature until 1974,<sup>240</sup> research on these compounds has been active since the mid-20th century,<sup>241</sup> particularly in the fields of molecular electronics, optics, materials science and catalysis. Like ILs, IOS enjoy unparalleled modularity, as their conductivity, crystal structure or catalytic activity can be easily modulated *via* modification of the cation or anion.<sup>242,243</sup> Within molecular electronics, they are mostly present in the form of charge-transfer (CT) salts, prepared by combining electron-donor and electron-acceptor compounds to afford an ionic, electrically conductive (commonly semiconductive) solid.<sup>240</sup> Chloranil and tetracyanoquinodimethane (TCNQ) are the most representative electron acceptors, whereas diaminobenzenes or tetrathiafulvalene (TTF) derivatives (known as Bechgaard and Fabre salts) are popular electron donors (**Figure 27**).<sup>240,244</sup> Additionally, both components may also form CT-IOS in combination with organic cations and anions, respectively.<sup>240,244</sup> A well-known example is tetramethyltetraselenafulvalene hexafluorophosphate ((TMTSF)<sub>2</sub>PF<sub>6</sub>), which in 1980 became the first purely organic superconductor described, with a transition temperature of 0.9 K at 12 kbar of pressure.<sup>245</sup>

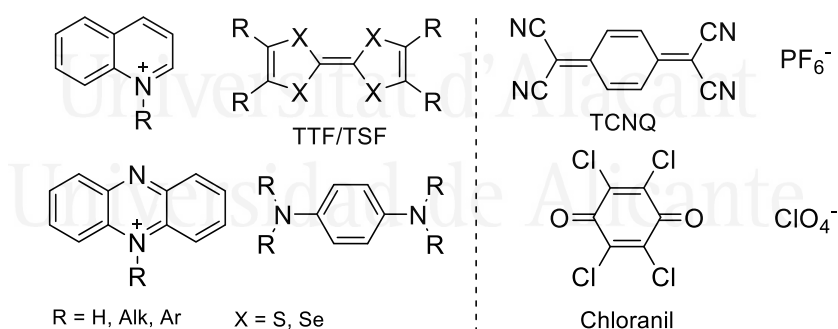


**Figure 27.** Representative examples of components of CT-IOS.

<sup>240</sup>Soos, Z. G. *Annu. Rev. Phys. Chem.* **1974**, *25*, 121–153.

<sup>241</sup>Matsunaga, Y. *J. Chem. Phys.* **1964**, *41*, 1609–1613.

<sup>242</sup>Torrance, J. B. *J. Solid State Chem.* **1992**, *96*, 59–66.

<sup>243</sup>Liu, X.; Yang, Z.; Wang, D.; Cao, H. *Crystals* **2016**, *6*, 158.

<sup>244</sup>Soos, Z. G.; Keller, H. J.; Moroni, W.; Noethe, D. *J. Am. Chem. Soc.* **1977**, *99*, 5040–5044.

<sup>245</sup>Jérome, F.; Mazaud, A.; Ribault, M.; Bechgaard, K. *J. Physique Lett.* **1980**, *41*, 95–98.

IOS are also very present in the field of non-linear optics (NLO) as components of optical frequency converters, high-speed processing and spectroscopy systems as well as terahertz (THz) wave generators and detectors.<sup>243,246,247</sup>

Organic NLO systems perform better than inorganic materials such as ZnTe or GaAs, due to faster polarizability response times and generally better optical properties, as well as much higher tunability.<sup>243,246</sup> In this field, the state-of-the-art materials consist of single-crystal IOS formed by a stilbeneazolum or stilbeneazinium cationic backbone with a sulfonate counter-anion. Popular cations include quinolinium,<sup>246</sup> benzothiazolum,<sup>247</sup> pyridinium<sup>243</sup> and indolium<sup>248</sup> while the anion is almost invariably an arylsulfonate derivative (**Figure 28**).<sup>246</sup> Besides these, zwitterionic structures based on indolium squaraine have also been studied.<sup>249</sup>

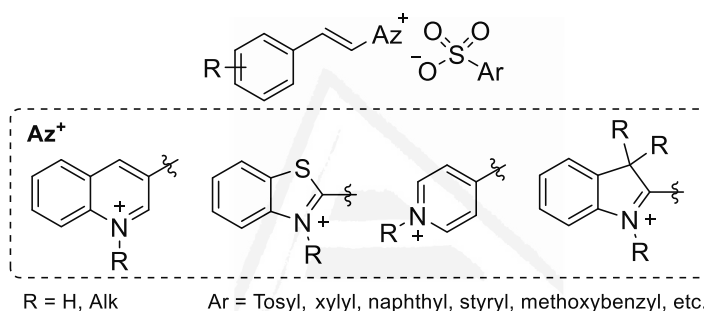


**Figure 28.** IOS based on stilbeneazolum and stilbeneazinium sulfonates for NLO applications.

Supramolecular chemistry also makes good use of IOS. For instance, treating long-chain trialkylammonium cations with an iodine source results in IOS formed by a self-assembled polyiodide linear structure encapsulated by cations.<sup>250,251</sup> Polyiodides are of great importance for dye-sensitized solar cells, superconductors and optic materials, as well as effective systems for the selective separation of diiodoperfluoroalkanes, notoriously difficult to purify but crucial intermediates in the

<sup>246</sup>Kim, P.-J.; Jeong, J.-H.; Jazbinsek, M.; Choi, S.-B.; Baek, I.-H.; Kim, J.-T.; Rotermund, F.; Yun, H.; Lee, Y. S.; Günter, P.; Kwon, O.-P. *Adv. Funct. Mater.* **2012**, *22*, 200–209.

<sup>247</sup>Lee, S.-H.; Lu, J.; Lee, S.-J.; Han, J.-H.; Jeong, C.-U.; Lee, S.-C.; Li, X.; Jazbinšek, M.; Yoon, W.; Yun, H.; Kang, B. J.; Rotermund, F.; Nelson, K. A.; Kwon, O.-P. *Adv. Mater.* **2017**, *29*, 1701748.

<sup>248</sup>Palaniyasan, E.; Radhakrishnan, A.; Maidur, S. R.; Patil, P. S.; Muppudathi, A. L.; Jeyaperumal, K. S. *J. Electron. Mater.* **2022**, *51*, 3531–3541.

<sup>249</sup>Zhou, W.; Wu, X.; Ma, P.; Zhou, F.; Li, Z.; Niu, R.; Yang, J.; Wang, Y.; Zhang, X.; Song, Y.; Liu, D. *Opt. Mater.* **2022**, *126*, 112178.

<sup>250</sup>Abate, A.; Brischetto, M.; Cavallo, G.; Lahtinen, M.; Metrangolo, P.; Pilati, T.; Radice, S.; Resnati, G.; Rissanen, K.; Terraneo, G. *Chem. Commun.* **2010**, *46*, 2724–2726.

<sup>251</sup>Lin, J.; Martí-Rujas, J.; Metrangolo, P.; Pilati, T.; Radice, S.; Resnati, G.; Terraneo, G. *Cryst. Growth Des.* **2012**, *12*, 5757–5762.

synthesis of fluorinated elastomers.<sup>252</sup> On the other hand, IOS formed by *p*-sulfo[4]calixarenes in combination with phosphonium and ammonium cations are of interest for the selective absorption of small chemical species (i.e., lithium, hydrogen) for energy storage applications (**Figure 29**).<sup>253,254</sup>

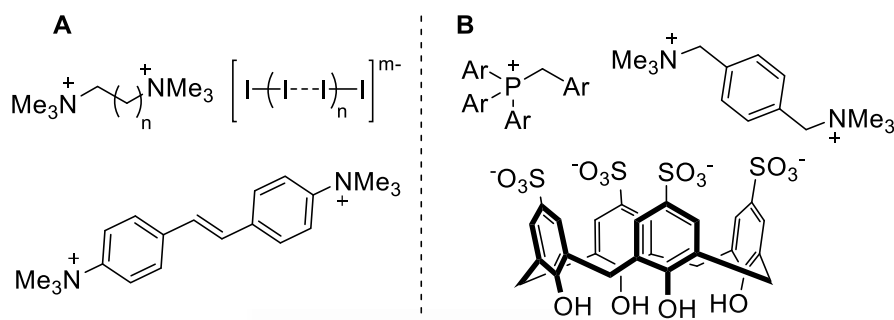


**Figure 29.** Components for IOS based on (A) polyiodides (B) *p*-sulfo[4]calixarenes.

An interesting class of IOS are organic ionic plastic crystals (OIPCs), intermediate substances whose properties lie between pure crystalline solids and ILs.<sup>255</sup> These materials consist on cationic structures analogous to those of ILs, but using a different selection of anions (**Figure 30**). OIPCs present crystalline long-range order but short-range disorder arising from molecular rotation, which results in highly malleable crystal structures. Thus, they exhibit high ionic conductivity as well as mechanical plasticity, both depending on temperature, which makes them suitable for electrochemical applications, particularly as electrolytes in solid-state batteries.<sup>255</sup>

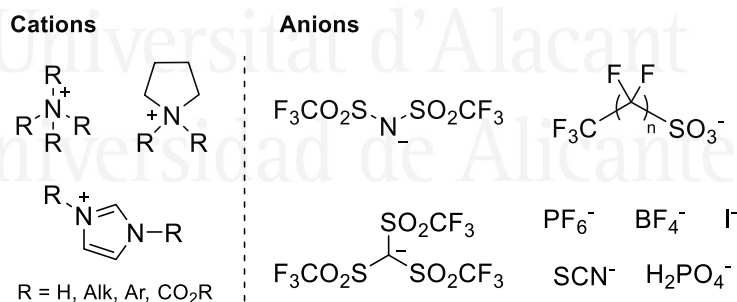


**Figure 30.** Components of OIPCs.

<sup>252</sup>Metrangolo, P.; Carcenac, Y.; Lahtinen, M.; Pilati, T.; Rissanen, K.; Vij, A.; Resnati, G. *Science* **2009**, 323, 1461–1464.

<sup>253</sup>Makha, M.; Alias, Y.; Raston, C. L.; Sobolev, A. N. *New J. Chem.* **2007**, 31, 662–668.

<sup>254</sup>Ling, I.; Sobolev, A. N.; Raston, C. L. *CrystEngComm* **2015**, 17, 1526–1530.

<sup>255</sup>Pringle, J. M.; Howlett, P. C.; MacFarlane, D. R.; Forsyth, M. *J. Mater. Chem.* **2010**, 20, 2056–2062.



Regarding catalysis, the range of application of IOS is very extensive, partly due to the broad scope of the IOS definition. Although they can be found in almost any organocatalyzed reaction, IOS are particularly important in the field of photochemistry (many solid photocatalysts contain charged heterocyclic cores, including acridinium,<sup>256</sup> pyrylium or thiazinium<sup>257,258</sup>) and in asymmetric organocatalysis, where MacMillan's imidazolidinones<sup>259</sup> or cinchonidinium salts—used as phase-transfer asymmetric catalysts<sup>260</sup> are prime examples (Figure 31).

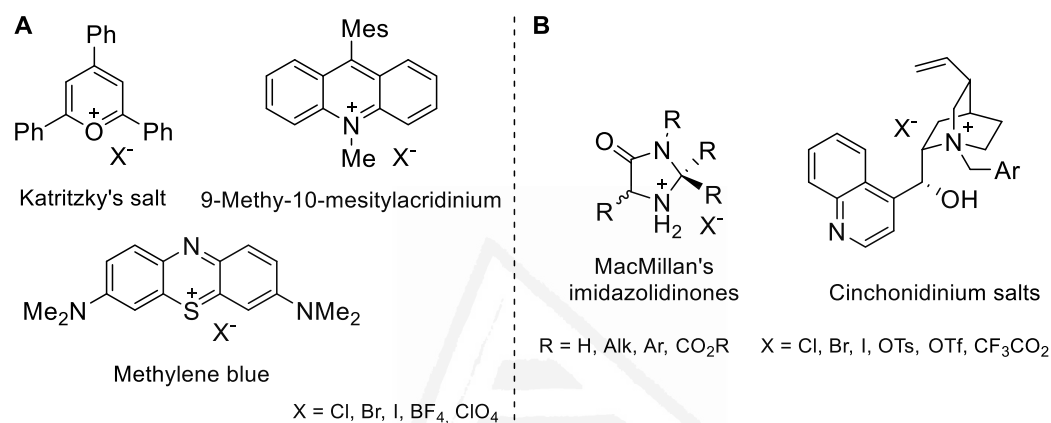


Figure 31. Representative IOS used as (A) photocatalysts (B) asymmetric organocatalysts.

Universitat d'Alacant  
Universidad de Alicante

<sup>256</sup>Laze, L.; Romero, P.; Bosque, I.; González-Gómez, J. C. *Eur. J. Org. Chem.* **2022**, e202201484.

<sup>257</sup>Torregrosa-Chinillach, A.; Chinchilla, R. *Molecules* **2021**, 26, 974.

<sup>258</sup>Torregrosa-Chinillach, A.; Chinchilla, R. *Molecules* **2022**, 27, 497.

<sup>259</sup>Jen, W. S.; Wiener, J. J. M.; MacMillan, D. W. C. *J. Am. Chem. Soc.* **2000**, 122, 9874–9875.

<sup>260</sup>Itsumo, S.; Yamamoto, S.; Takata, S. *Tetrahedron Lett.* **2014**, 55, 6117–6120.

### C3.1.2. Imidazolium IOS as components of catalytic systems

Imidazolium IOS are mostly comprised of aryl-<sup>68</sup> and acylimidazolium salts,<sup>40</sup> as well as some alkylimidazolium salts with highly branched or bulky side-chains,<sup>56</sup> as they tend to have much higher melting points than their linear alkyl counterparts.

The presence of imidazolium IOS in catalysis is mostly related to NHCs (as ligands for metals<sup>150,261</sup> or standalone organocatalysts,<sup>68</sup> see section **GI.2.2.** of this manuscript), metal-organic frameworks (MOFs, see Chapter 4)<sup>262,263</sup> and Lewis/Brønsted-acid catalysis (**Figure 32**).<sup>148,264</sup>

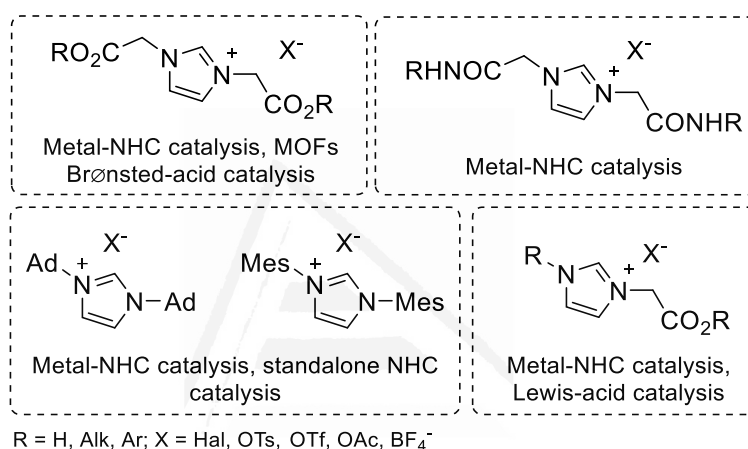


**Figure 32.** Imidazolium IOS in catalysis.

Regarding acidic catalysis with imidazolium IOS, the vast majority of reports describe the use of the amino-acid-based **bcmim** derivatives, as they constitute fantastic heterogeneous catalysts due to their substantial Brønsted acidity (**bcmimCl** has a pK<sub>a</sub> of 1.3), absolute insolubility in aprotic and certain protic organic solvents,<sup>148</sup> and high robustness.<sup>265</sup> Indeed, **bcmimCl** has been applied as a promoter to a variety of synthetic protocols, including the preparation of quinolines *via* Friedländer reaction,<sup>148</sup> the synthesis of dihydropyrimidones by multicomponent Biginelli reaction,<sup>266</sup> the obtention of 2,4-diaryltiophenes<sup>267</sup> or the allylation of anilines with allylic alcohols (**Scheme 41**).<sup>149,265</sup> The latter is

<sup>261</sup>Martínez, R.; Pastor, I. M.; Yus, M. *Synthesis* **2014**, 46, 2965–2975.

<sup>262</sup>Albert-Soriano, M.; Pastor, I. M. *Eur. J. Org. Chem.* **2016**, 5180–5188

<sup>263</sup>Albert-Soriano, M.; Trillo, P.; Soler, T.; Pastor, I. M. *Eur. J. Org. Chem.* **2017**, 6375–6381.

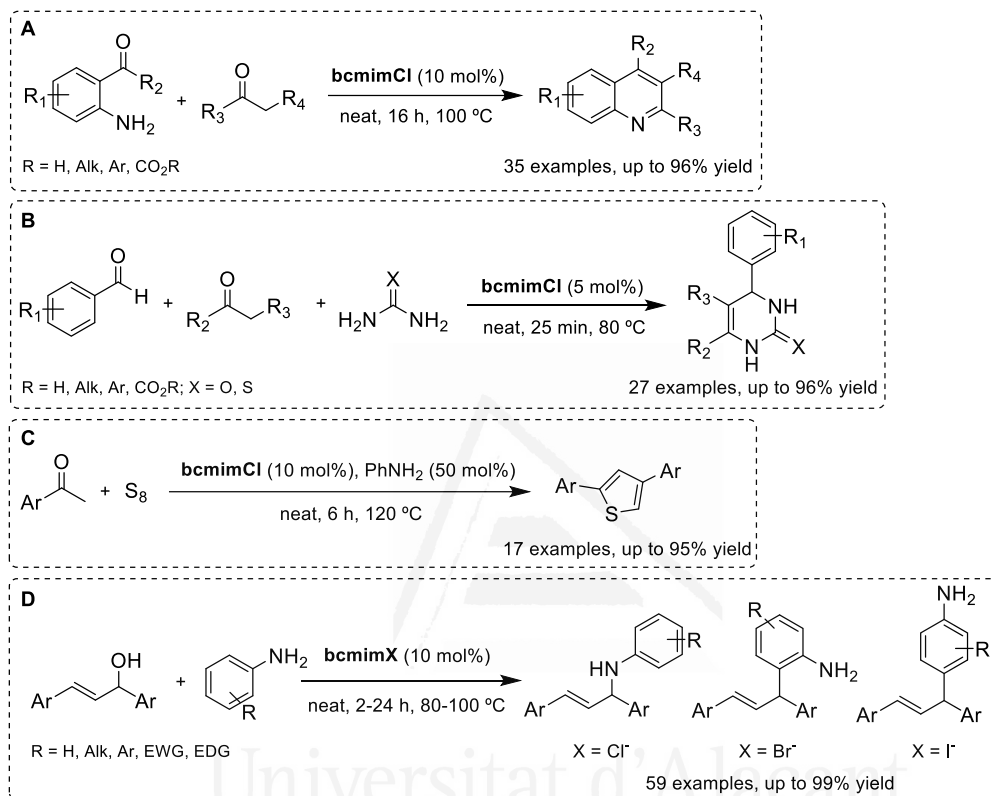
<sup>264</sup>Zhang, Y.; Hu, H.; Liu, C.-J.; Cao, D.; Wang, B.; Sun, Y.; Abdukader, A. *Asian J. Org. Chem.* **2017**, 6, 102–107.

<sup>265</sup>Albert-Soriano, M.; Hernández-Martínez, L.; Pastor, I. M. *ACS Sustain. Chem. Eng.* **2018**, 6, 14063–14070.

<sup>266</sup>Davanagere, M. P.; Maiti, B. *ACS Omega* **2021**, 6, 26035–26047.

<sup>267</sup>Gisbert, P.; Pastor, I. M. *Eur. J. Org. Chem.* **2020**, 4319–4325.

particularly interesting, as the regioselectivity of the process could be controlled by changing the counter-anion of **bcmim**.






**Scheme 41.** Protocols catalyzed by **bcmim** derivatives. (A) Synthesis of quinolines (B) synthesis of dihydropyrimidones (C) synthesis of 2,4-diaryltiophenes (D) regioselective allylation of anilines


## C3.2. Objectives

Sustainable synthetic processes can be significantly improved by using imidazolium IOS as heterogeneous catalysts. In particular, **bcmim** derivatives are of great interest in lieu of their renewable origin, high intrinsic catalytic activity and robustness, as well as their complex interaction capabilities.

The electrophilic allylation of indoles is a protocol which may greatly benefit from the LTTM-forming characteristics of **bcmimCl**. The most direct route for this transformation involves direct nucleophilic substitution of allyl halides, acetates, phosphates or carbonates with the corresponding indole.<sup>268,269</sup> More recently, methodologies focusing on the use of allyl alcohols as coupling partners have been developed.<sup>269</sup> Allylic alcohols are more desirable substrates, as they are less expensive (allylic alcohols are the actual precursors to the compounds listed above), more stable and produce water as a harmless byproduct. Thus, the following objectives for this study were established:

-  To develop a methodology for allylation of indoles with allylic alcohols promoted by **bcmimCl** in neat conditions.
-  To study the application of the designed synthetic methodology to the allylation of other  $\pi$ -excessive heterocycles.
-  To assess the environmental impact of the transformation and compare with established protocols in literature using sustainability metrics.

Regarding Brønsted-acid catalysis, the development of imidazolium IOS bearing sulfonic acids is also interesting, as sulfo-functionalized imidazolium ILs have demonstrated good catalytic activity in several transformations. Therefore, an additional objective was set:

-  To prepare the sulfo- analogue of **bcmim** and perform a comparative study between the two catalytic systems.

---

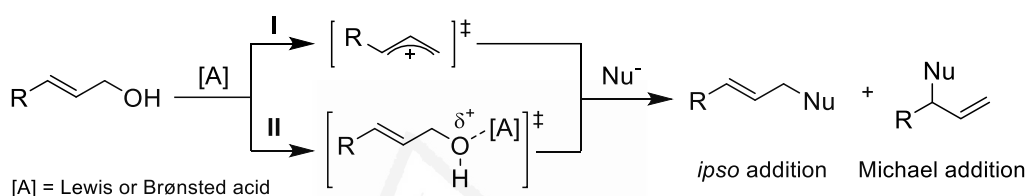
<sup>268</sup>Westermaier, M.; Mayr, H. *Org. Lett.* **2006**, *8*, 4791–4794.

<sup>269</sup>Baeza, A.; Nájera, C. *Synthesis* **2013**, *46*, 25–34.



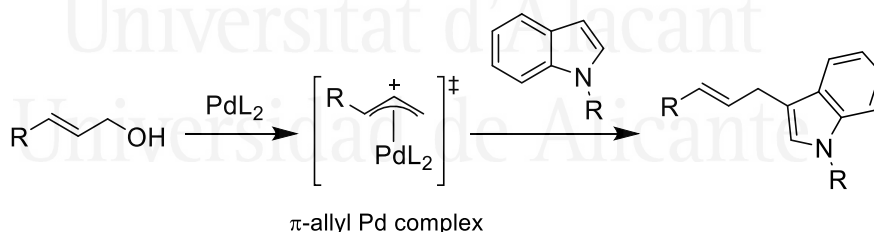
### C3.3. Results and discussion

Although more convenient in economic and sustainable terms than their (pseudo)halide derivatives, allylic alcohols are also less reactive, thus requiring more efficient activation mechanisms. In general, this reaction involves the catalytic activation of the alcohol moiety with a Lewis or Brønsted acid, followed by either elimination of the hydroxyl group, resulting in the formation of an allylic carbocation (**Scheme 42**, pathway I) or displacement of said activated moiety *via* nucleophilic attack (**Scheme 42**, pathway II). Either way, both *ipso* and Michael-type addition products may be formed, with the ratio between them depending on the stability and/or reactivity of the intermediate.<sup>269</sup>



**Scheme 42.** Scheme of the plausible reaction pathways and products.

Regarding the functionalization of indoles with allyl alcohols, most examples in literature use metallic catalysts to promote the reaction, with the palladium-catalyzed Tsuji-Trost reaction being one of the most representative examples.<sup>270–272</sup> Originally developed<sup>273</sup> by Jiro Tsuji in 1965 and modified by Barry Trost in 1973,<sup>274</sup> this transformation relies on the formation of a  $\pi$ -allyl complex with palladium for the activation of the substrate, which is then promptly attacked by the nucleophile (**Scheme 43**).



**Scheme 43.** C-3 allylation of indoles *via* Tsuji-Trost reaction.

<sup>270</sup>Akkarasamiyo, S.; Sawadjoon, S.; Orthaber, A.; Samec, J. S. M. *Chem. Eur. J.* **2018**, *24*, 3488–3498.

<sup>271</sup>Xu, C.; Murugan, V. K.; Pullarkat, S. A. *Org. Biomol. Chem.* **2012**, *10*, 3875–3881.

<sup>272</sup>Das, D.; Pratihar, S.; Roy, U. K.; Mal, D.; Roy, S. *Org. Biomol. Chem.* **2012**, *10*, 4537–4542.

<sup>273</sup>Tsuji, J.; Takahashi, H.; Morikawa, M. *Tetrahedron Lett.* **1965**, *6*, 4387–4388.

<sup>274</sup>Trost, B. M.; Fullerton, T. J. *J. Am. Chem. Soc.* **1973**, *95*, 292–294.

Although palladium catalysts are the most popular choice, salts and complexes of other noble metals are also capable of similar activation mechanisms for allylic alcohols, including gold,<sup>275–277</sup> ruthenium,<sup>278</sup> and iridium.<sup>279</sup> Besides precious metals, systems based on aluminum,<sup>280</sup> zinc,<sup>281,282</sup> iron,<sup>283–285</sup> ytterbium,<sup>286</sup> molybdenum<sup>287</sup> or indium<sup>288–290</sup> as well as supported catalysts based on copper nanoparticles<sup>291</sup> or phosphomolybdic acid.<sup>292</sup> Metal-free alternatives employ a variety of Brønsted acidic catalysts, mostly relying on sulfonic acids,<sup>283,293–298</sup> or fluorinated alcohols<sup>299</sup> although other catalytic systems based on iodine<sup>300</sup> or frustrated Lewis pairs can promote this transformation.<sup>301</sup> Catalyst-free syntheses using pressurized high-temperature water are known as well.<sup>302</sup>

---

<sup>275</sup>Rao, W.; Chan, P. W. H. *Org. Biomol. Chem.* **2008**, *6*, 2426–2433.

<sup>276</sup>Lu, Y.; Du, X.; Jia, X.; Liu, Y. *Adv. Synth. Catal.* **2009**, *351*, 1517–1522.

<sup>277</sup>Huang, K.; Wang, H.; Liu, L.; Chang, W.; Li, J. *Chem. Eur. J.* **2016**, *22*, 6458–6465.

<sup>278</sup>Gruber, S.; Zaitsev, A. B.; Wörle, M.; Pregosin, P. S.; Veiros, L. F. *Organometallics* **2008**, *27*, 3796–3805.

<sup>279</sup>Chatterjee, P. N.; Roy, S. *Tetrahedron* **2012**, *68*, 3776–3785.

<sup>280</sup>Cullen, A.; Muller, A. J.; Williams, D. B. G. *RSC Adv.* **2017**, *7*, 42168–42171.

<sup>281</sup>Bertuzzi, G.; Lenti, L.; Giorgiana Bisag, D.; Fochi, M.; Petrini, M.; Bernardi, L. *Adv. Synth. Catal.* **2018**, *360*, 1296–1302.

<sup>282</sup>Fan, G.-P.; Liu, Z.; Wang, G.-W. *Green Chem.* **2013**, *15*, 1659–1664.

<sup>283</sup>Trillo, P.; Baeza, A.; Nájera, C. *Eur. J. Org. Chem.* **2012**, 2929–2934.

<sup>284</sup>Trillo, P.; Baeza, A.; Nájera, C. *ChemCatChem* **2013**, *5*, 1538–1542.

<sup>285</sup>Jana, U.; Maiti, S.; Biswas, S. *Tetrahedron Lett.* **2007**, *48*, 7160–7163.

<sup>286</sup>Huang, W.; Shen, Q.-S.; Wang, J.-L.; Zhou, X.-G. *Chinese J. Chem.* **2008**, *26*, 729–735.

<sup>287</sup>Yang, H.; Fang, L.; Zhang, M.; Zhu, C. *Eur. J. Org. Chem.* **2009**, 666–672.

<sup>288</sup>Yasuda, M.; Somyo, T.; Baba, A. *Angew. Chem. Int. Ed.* **2006**, *45*, 793–796.

<sup>289</sup>Yadav, J. S.; Reddy, B. V. S.; Aravind, S.; Kumar, G. G. K. S. N.; Reddy, A. S. *Tetrahedron Lett.* **2007**, *48*, 6117–6120.

<sup>290</sup>Yadav, J. S.; Reddy, B. V. S.; Rao, K. V. R.; Kumar, G. G. K. S. N. *Synthesis* **2007**, 3205–3210.

<sup>291</sup>Mallick, S.; Mukhi, P.; Kumari, P.; Mahato, K. R.; Verma, S. K.; Das, D. *Catal. Lett.* **2019**, *149*, 3501–3507.

<sup>292</sup>Yadav, J. S.; Reddy, B. V. S.; Reddy, A. S. *J. Mol. Catal. A Chem.* **2008**, *280*, 219–223.

<sup>293</sup>Shirakawa, S.; Kobayashi, S. *Org. Lett.* **2007**, *9*, 311–314.

<sup>294</sup>Le Bras, J.; Muzart, J. *Tetrahedron* **2007**, *63*, 7942–7948.

<sup>295</sup>Sayin, S.; Yilmaz, M. *Tetrahedron* **2016**, *72*, 6528–6535.

<sup>296</sup>Liu, Y.-L.; Liu, L.; Wang, Y.-L.; Han, Y.-C.; Wang, D.; Chen, Y.-J. *Green Chem.* **2008**, *10*, 635–640.

<sup>297</sup>Sanz, R.; Martínez, A.; Miguel, D.; Álvarez-Gutiérrez, J. M.; Rodríguez, F. *Adv. Synth. Catal.* **2006**, *348*, 1841–1845.

<sup>298</sup>Suárez, A.; Gohain, M.; Fernández-Rodríguez, M. A.; Sanz, R. *J. Org. Chem.* **2015**, *80*, 10421–10430.

<sup>299</sup>Trillo, P.; Baeza, A.; Nájera, C. *J. Org. Chem.* **2012**, *77*, 7344–7354.

<sup>300</sup>Liu, Z.; Wang, D.; Chen, Y. *Lett. Org. Chem.* **2011**, *8*, 73–80.

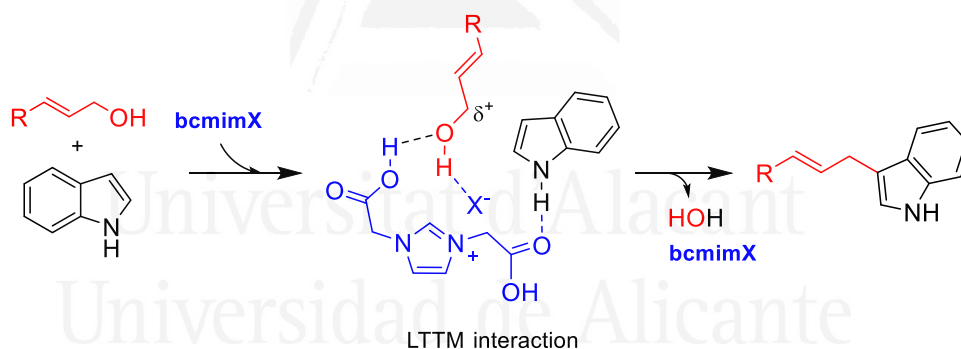
<sup>301</sup>Zhang, H.; Zhan, X.-Y.; Dong, Y.; Yang, J.; He, S.; Shi, Z.-C.; Zhang, X.-M.; Wang, J.-Y. *RSC Adv.* **2020**, *10*, 16942–16948.

<sup>302</sup>Hirashita, T.; Kuwahara, S.; Okochi, S.; Tsuji, M.; Araki, S. *Tetrahedron Lett.* **2010**, *51*, 1847–1851.

The most immediate issues associated with these methodologies are directly related to the nature of the catalysts used. The majority of metal-catalyzed protocols rely on either expensive precious metals or highly Lewis-acidic transition metal salts (moisture-sensitive and highly corrosive triflates are the usual choice) to promote the reactions. Metal-free procedures, on the other hand, lean heavily towards the use of liquid sulfonic acids and fluorinated alcohols, which are highly corrosive — on top of that, fluorinated alcohols are also volatile— and somewhat dangerous to manipulate.

The use of **bcmim** derivatives as promoters for this reaction offers an efficient and safe alternative to the reported methodologies, as they are metal-free, air- and moisture-stable and non-corrosive solids. These IOS are known to be robust catalysts, and their heterogeneous nature enables easy recovery and reuse, while being much simpler than other systems, especially those based on supported species.

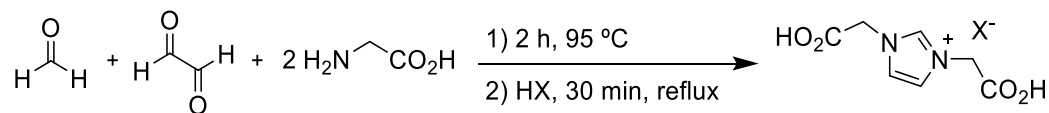
The prospective mode of activation of allyl alcohols with **bcmimX** involves the formation of a LTTM, in which the IOS acts as HBA and the allylic alcohol as HBD (**Scheme 44**). The interaction between the components has the double effect of providing a highly activated substrate for nucleophilic substitution and decreasing the melting point of the reaction mixture, potentially enabling solvent-free operation (see section **SI.2.3.** for the DSC trace of a **bcmimCl**:(*E*)-1,3-diphenylprop-2-en-1-ol mixture).



**Scheme 44.** Prospective mechanism of the reaction. Note the LTTM interaction between the highlighted components.

**BcmimX** are easily prepared from inexpensive and readily available glycine, glyoxal and formaldehyde *via* Arduengo reaction, followed by treatment with the corresponding aqueous hydrohalic acid. This protocol is straightforward, scalable and does not require any sort of purification (**Scheme 45**).<sup>148,149</sup>





**Scheme 45.** General synthetic protocol for the preparation of **bcmimX**.

For this study, the allylation of 1*H*-indole with (*E*)-1,3-diphenylprop-2-en-1-ol was selected as the model reaction. The reactions were run under aerobic solventless conditions at 80 °C for two hours using **bcmim** and its chloride, bromide and iodide derivatives as promoters, obtaining the results detailed in **Table 10**.

**Table 10.** Initial studies for the allylation of indole with allylic alcohols.

| Entry | [Cat.]         | Conv. (%) <sup>†</sup> |
|-------|----------------|------------------------|
| 1     | None           | 0                      |
| 2     | <b>Bcmim</b>   | 0                      |
| 3     | <b>BcmimCl</b> | >99 (93) <sup>‡</sup>  |
| 4     | <b>BcmimBr</b> | >99                    |
| 5     | <b>BcmimI</b>  | >99                    |

<sup>†</sup>Determined by GC-MS using durene as internal standard. <sup>‡</sup>Isolated yield after filtration.

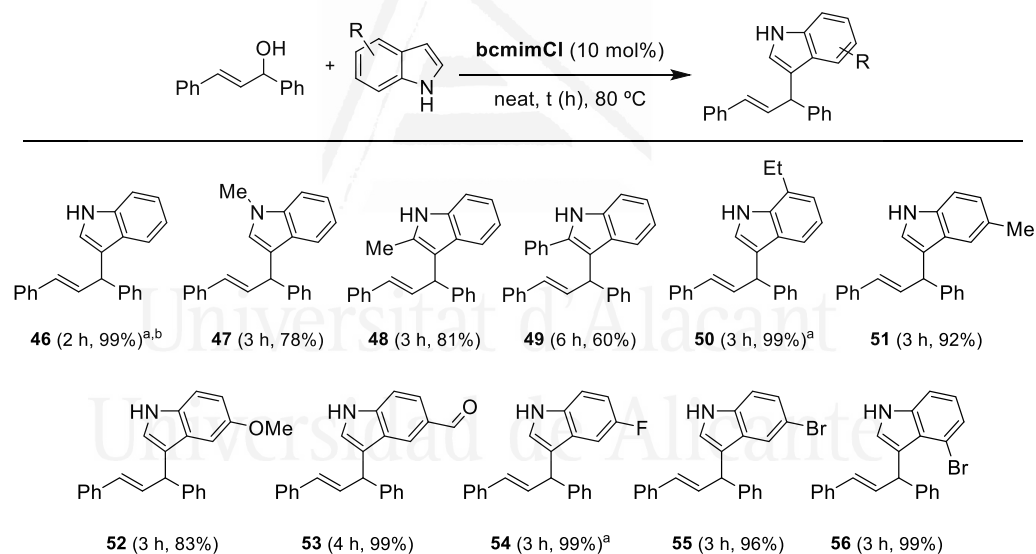
The results obtained provide an interesting insight into the particularities of the **bcmim** IOS. While every **bcmim** halide performs flawlessly in this transformation, affording **46** in quantitative conversions, their zwitterionic precursor is not capable of promoting the reaction whatsoever, not even traces of product being detected. This stark difference in performance has been noted in other transformations reported in literature,<sup>265</sup> and is probably related to the lower acidity of **bcmim** compared to its hydrohalide counterparts ( $pK_a = 2.9$  in water for **bcmim** against ca. 1.5 for **bcmimX**),<sup>153</sup> and its highly stable linear hydrogen-bonded crystal structure (see Chapter 1, **Scheme 13**), which may prevent the acidic carboxyl groups from interacting with the substrate.

Interestingly, —although expectedly, given the actual electron movement involved— total selectivity towards C-3 allylation of the *N*-unsubstituted substrate was observed regardless of the counter-anion used. As full conversion was achieved and stoichiometric amounts of reagents were

used, this meant **46** could be obtained pure in excellent yield after filtering off the catalyst, resulting in a highly environmentally friendly protocol.

In lieu of the results obtained, **bcmimCl** was selected as catalyst for the remainder of the study, as it is produced from the most readily available and least expensive acid of the three systems assayed. It has also been reported to be much more robust than its bromide and iodide counterparts, while being more acidic—as the acidity of the **bcmim** salts is directly related to that of the acid used to neutralize the zwitterion—.<sup>153</sup> For instance, in the allylation of anilines with allylic alcohols, **bcmimCl** resulted in the shortest reaction times (conversion wise) while managing fifteen catalytic cycles without loss of activity against the five of **bcmimBr** and three of **bcmimI**.<sup>149,265</sup>

With everything set in place, the scope of the transformation was explored. First, several indoles were precisely combined with stoichiometric amount of (*E*)-1,3-diphenylprop-2-en-1-ol under solventless conditions in the presence of **bcmimCl** (**Figure 33**). The progress of the transformation was monitored by GC-MS, with stationary state being considered as the end of the reaction.



Isolated yields. <sup>a</sup>Obtained pure after filtration. <sup>b</sup>5 mmol scale reaction.

**Figure 33.** Scope of the reaction. 1*H*-Indoles.

In general terms, the protocol proved to be very effective, isolating the corresponding 3-allylindoles in moderate to quantitative yields, with some examples being obtained pure after simple filtration (**Figure 33**, compounds **46**, **50** and **54**). Electronic effects do not seem to influence the outcome of the reaction, as no significant difference was observed between substrates containing electron-withdrawing or electron-donating groups, and perfectly tolerates sensitive substrates, with 5-

formylindole affording **53** in quantitative yield. There is, however, a significant steric effect for indoles substituted at the 2-position, as evidenced by compounds **48** and **49**, which could be attributed to a more difficult approximation to the activated allylic alcohol (**Figure 34**). No steric effect whatsoever was observed at any other position.

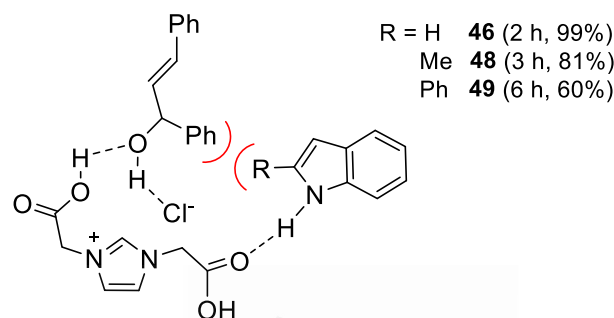
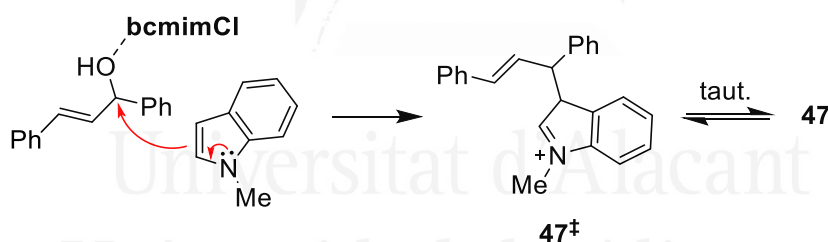


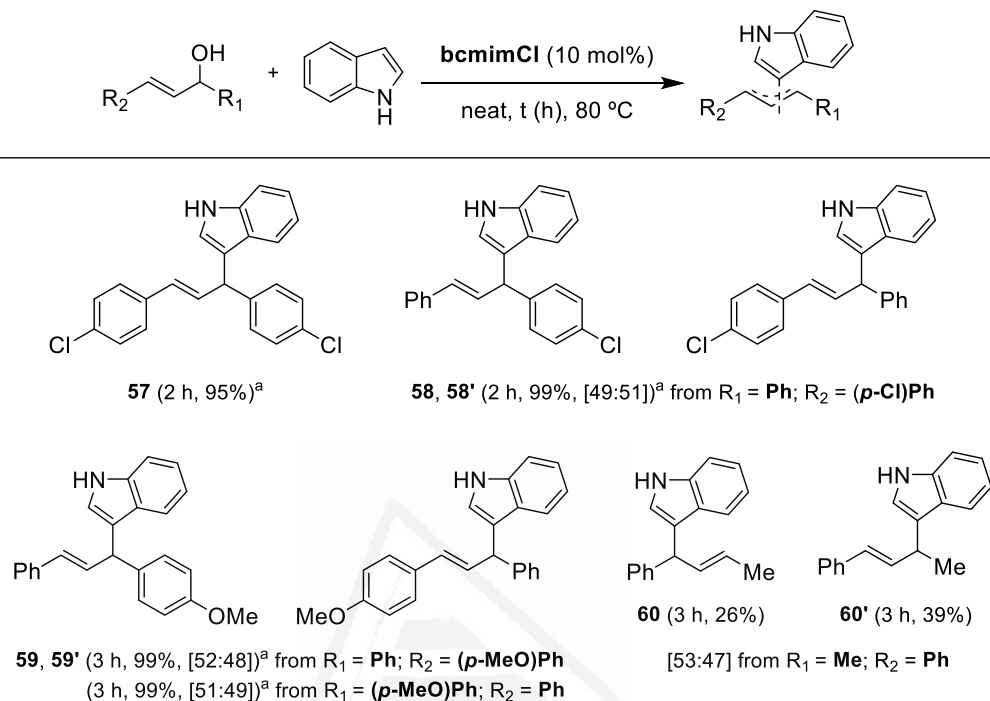
**Figure 34.** Steric effects for 2-substituted indoles.

*N*-Substituted substrates also perform slightly worse (**Figure 33**, compound **47**), due to the impossibility of interacting with **bcmimCl** as well as the higher energy requirements of the formally cationic intermediate—the corresponding *3H*-indole tautomer (**47<sup>‡</sup>**)—(**Scheme 46**).



**Scheme 46.** Simplified mechanism of the formation of compound **47**.

Next, a variety of allylic alcohols were combined with *1H*-indole under the same reaction conditions, obtaining the results detailed in **Figure 35**.



Isolated yields. In brackets, ratio between components in the crude reaction mixture determined by GC-MS or <sup>1</sup>H NMR.  
<sup>a</sup>Obtained pure (as a mixture of inseparable regioisomers for **58** and **59**) after filtration.

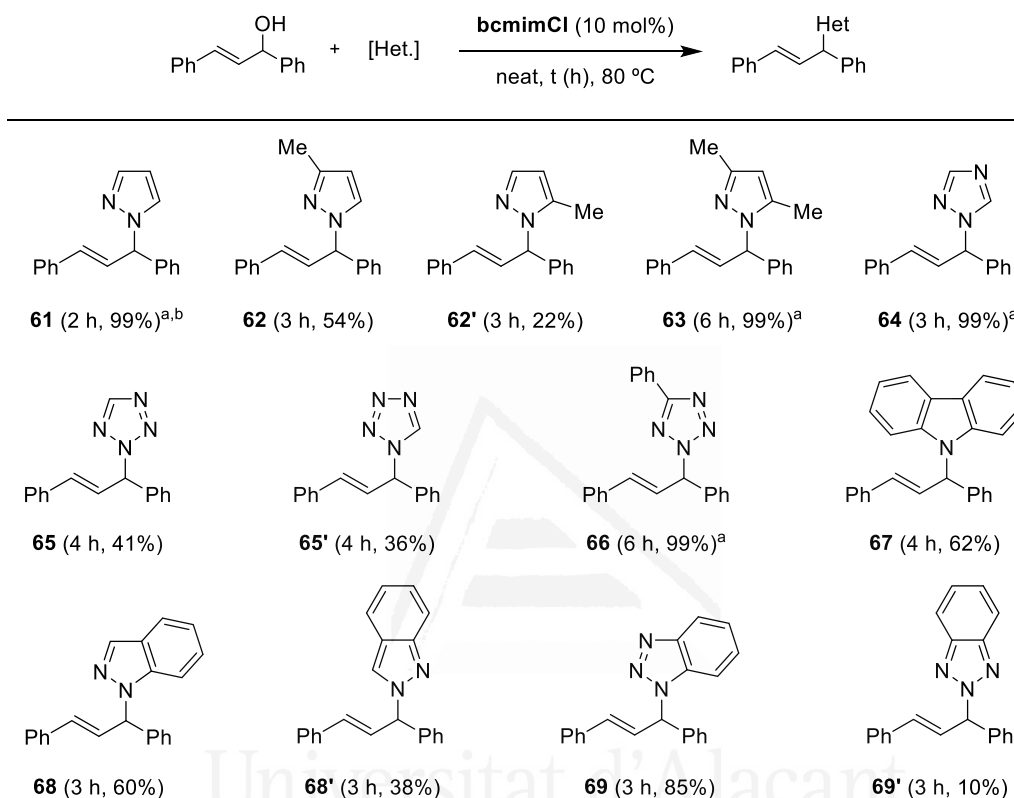
**Figure 35.** Scope of the reaction. Allylic alcohols.

Once more, the transformation proceeded smoothly, with products isolated in good to quantitative yields. Regarding the electronic nature of the substituents, no differences were observed in yields, albeit slightly longer reaction times were required for allylic alcohols bearing electron-donating groups (**Figure 35**, compounds **59**). The methodology also tolerates alkyl-derived allylic alcohols, as evidenced by compounds **60**, obtained in combined 65% yield.

The most important finding, however, is the total lack of regioselectivity observed with unsymmetrically substituted allylic alcohols as substrates, which afforded both regioisomers in ca. 1:1 ratio regardless of the nature of the side-chains (**Figure 35**, compounds **58**, **59** and **60**). From those, only **60** and **60'** could be separated *via* chromatography, the rest being obtained as mixtures of pure compounds after filtration. This effect had been previously reported in the allylation of anilines with **bcmimCl**,<sup>265</sup> although it does not provide enough information to unequivocally assign the actual mechanism of the reaction to an allylic carbocation intermediate.

After exploring the allylation of indoles, the focus was shifted to other nitrogenated heterocyclic systems. Thus, a plethora of  $\pi$ -excessive heterocycles were combined with (*E*)-1,3-diphenylprop-2-

en-1-ol in the presence of **bcmimCl** and subjected to the model conditions, obtaining the results described in **Figure 36**.



Isolated yields. <sup>a</sup>Obtained pure after filtration. <sup>b</sup>Same results using **bcmimBr** and **bcmimI**, no reaction with **bcmim**.

**Figure 36.** Scope of the reaction. *N*-Heterocycles.

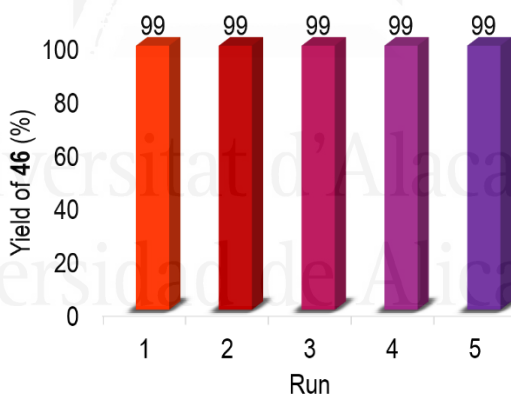
The protocol was found to be compatible with a variety of heterocycles, affording the corresponding products in good to quantitative yields. In this case, total selectivity towards *N*-substitution was observed, which, once again, was independent on the counter-anion of the **bcmim** IOS used (**Figure 36**, compound **61**).

Pyrazoles gave good results, even for the sterically congested 3,5-dimethylpyrazole, which afforded compound **63** in quantitative yield after simple filtration, although it required an additional four hours of reaction time. 1,2,4-Triazole and tetrazoles were also suitable substrates, obtaining the corresponding allyl derivatives in very good to quantitative yields (**Figure 36**, compounds **64** to **66**). Carbazole was also found to be compatible with this protocol, affording compound **67** in good yield, as were condensed cycles such as indazole and benzotriazole, which provided the desired products in

excellent yields (**Figure 36**, compounds **68** and **69**). Regioselectivity for reactions with several possible outcomes was mostly governed by steric and stability effects. For instance, 3-methylpyrazole returned two products in 70:30 ratio, with the major isomer being the less sterically congested **62**. In the case of tetrazole, the two possible isomers, sterically identical, were obtained in ca. 1:1 ratio (**Figure 36**, compounds **65**), whereas full selectivity towards a single product was observed with 5-phenyltetrazole (**Figure 36**, compound **66**). A high degree of selectivity was also observed for indazole and particularly benzotriazole, both strongly favoring the formation of the product with the least disturbance on the aromatic system of their fused benzene ring (**Figure 36**, compound **68** and **69**).

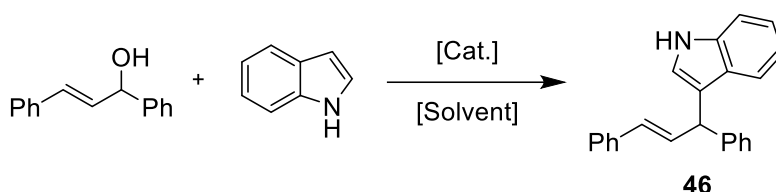
After exploring the scope of the reaction, a scale-up to 5 mmol of the model reaction was carried out, obtaining the pure product **46** in quantitative yield after filtration. No change was required in the model conditions, which proves the applicability of the methodology.

The next set of experiments were catalyst recyclability studies. To this end, the synthesis of **46** was carried out under model conditions, after which the crude product was dissolved in ethyl acetate and decanted off. The insoluble IOS was then washed with a portion of ethyl acetate, vacuum dried, and added to a tube with fresh reagents to start another reaction cycle. This way, the catalyst could be reused five times without any loss of activity, with every single cycle affording pure **46** in quantitative yield after filtration (**Figure 37**), demonstrating the robustness of the **bcmimCl** IOS.



**Figure 37.** Catalyst recyclability studies for the synthesis of **46**.

For the final part of the heterocycle allylation study, sustainability metrics were used to assess the environmental impact of the protocol and unbiasedly compare it with representative methodologies using metallic and non-metallic catalysts described in literature. For the sake of comparison, chromatographic purification was once more omitted from the VMR and E-factor calculations. The synthesis of **46** was selected for this study, obtaining the results compiled in **Table 11** (see section **SI.4.3.** for more details).

**Table 11.** Comparison between the **bcmimCl**-catalyzed synthesis and reported protocols for the preparation of **46**.

| Entry <sup>Ref.</sup>   | [Solvent]       | [Cat.]                              | VMR <sup>†</sup>   | E-factor          | EcoScale |
|-------------------------|-----------------|-------------------------------------|--------------------|-------------------|----------|
| <b>1</b>                | Neat            | <b>bcmimCl</b>                      | 0.790              | 1.9               | 89       |
| <b>2</b> <sup>284</sup> | Water           | FeCl <sub>3</sub> ·H <sub>2</sub> O | 0.668 <sup>‡</sup> | 17.6 <sup>‡</sup> | 70       |
| <b>3</b> <sup>280</sup> | Nitroethane     | Al(OTf) <sub>3</sub>                | 0.728 <sup>‡</sup> | 91.4 <sup>‡</sup> | 73       |
| <b>4</b> <sup>294</sup> | Dichloromethane | <i>p</i> -TSA                       | 0.748 <sup>‡</sup> | 94.8 <sup>‡</sup> | 79       |
| <b>5</b> <sup>299</sup> | HFIP            | HFIP                                | 0.776 <sup>‡</sup> | 1.4 <sup>‡</sup>  | 77       |

<sup>†</sup>Calculated from yield, AE, SF, MRP and RME<sub>Andraos</sub>. <sup>‡</sup>Purification by column chromatography omitted.

Judging by the results obtained, the **bcmimCl** methodology seems to be a well-rounded in terms of sustainability, with very low E-factor—well within the range for bulk chemical production—, high VMR and “excellent” EcoScale classification (**Table 11**, entry 1).

Compared to other methodologies, the use of neat conditions results in a significant decrease on the waste generated, especially in regard to protocols using solvents and/or performing full extractive work-ups, which clearly reflects on the E-factors (**Table 11**, entry 1 against entries 2 to 4). This is also true for the HFIP-promoted process, whose total lack of work-up besides recovering the solvent results in very low intrinsic waste generation, although this is totally offset by the need of posterior chromatographic purification (**Table 11**, entry 5). It is precisely this last step which separates the IOS-catalyzed process from the rest on the EcoScale scores, and represents a significant advantage in economic, operational, and sustainable terms.

Overall, the **bcmimCl**-promoted process is resolutely superior to all previously reported methods for the allylation of heterocycles studied, and ticks many of the boxes to be considered a sustainable process, i.e., low waste generation (low E-factor), operational simplicity, low cost and non-harmful reactants (high EcoScale) as well as high intrinsic material efficiency (high VMR).

In lieu of the excellent results obtained with **bcmim** derivatives, the next series of experiments were focused on the preparation of second-generation Brønsted-acidic imidazolium IOS based on the same substructure. Compared to carboxylic or hydrohalic acids, sulfonic acids are stronger by several

orders of magnitude (triflic acid has a  $pK_a$  in water of -14.7 against 0.5 for its carbon-based analogue, trifluoroacetic acid, or -5.9 for pure hydrogen chloride gas),<sup>303,304</sup> while being non-oxidizing (unlike comparably strong mineral acids such as perchloric acid) and having non-nucleophilic conjugate bases, thus avoiding side reactivity issues.

Sulfoimidazolium salts are well-known Brønsted acidic catalysts, with sulfoalkyl- or sulfoimidazolium ILs having been applied to a variety of transformations, including the synthesis of benzimidazoles *via* double condensation of benzaldehydes and 2-phenylenediamine<sup>305</sup> or the preparation of coumarins by Pechmann reaction,<sup>306</sup> as well as the depolymerization of lignocellulosic materials.<sup>307</sup> Based on these antecedents, the sulfo- analogue of **bcmim**, 1,3-bis(sulfomethyl)imidazole (**bsmim**) was selected as the parent compound for the new generation of imidazolium IOS (**Figure 38**).

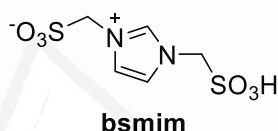


**Figure 38.** Structure of 1,3-bis(sulfomethyl)imidazole (**bsmim**).

Regarding this compound, little to no information can be found in literature, with the only report being a patent filed in 2014 by Armand and collaborators in which **bsmim**, among other sulfonates, is proposed as a component for solid electrolytes in lithium-ion batteries, but no further information regarding its synthesis or properties is provided.<sup>308</sup>

Therefore, a multicomponent synthetic methodology for the preparation of **bsmim** based on Arduengo's imidazolium synthesis was devised. Two equivalents of aminomethanesulfonic acid (**AMS**) were combined with aqueous solutions of glyoxal and formaldehyde, obtaining the results compiled in **Table 12**.

<sup>303</sup>Trummal, A.; Lipping, L.; Kaljurand, I.; Koppel, I. A.; Leito, I. *J. Phys. Chem. A* **2016**, *120*, 3663–3669.

<sup>304</sup>Zhang, S.; Baker, J.; Pulay, P. A. *J. Phys. Chem. A* **2010**, *114*, 432–442.

<sup>305</sup>Khazaei, A.; Zolfigol, M. A.; Moosavi-Zare, A. R.; Zare, A.; Ghaemi, E.; Khakyzadeh, V.; Asgari, Z.; Hasaninejad, A. *Sci. Iran* **2011**, *18*, 1365–1371.

<sup>306</sup>Khaligh, N. G.; Mihankhah, T.; Johan, M. R. *Polycycl. Aromat. Compd.* **2021**, *41*, 1712–1721.

<sup>307</sup>Sharghi, H.; Shiri, P.; Aberi, M. *Beilstein J. Org. Chem.* **2018**, *14*, 2745–2770.

<sup>308</sup>Jónsson, E.; Armand, M. B.; Johansson, J. P. Anions and Derived Salts with High Dissociation in Non-Protogenic Solvents. US9269987, 2016.

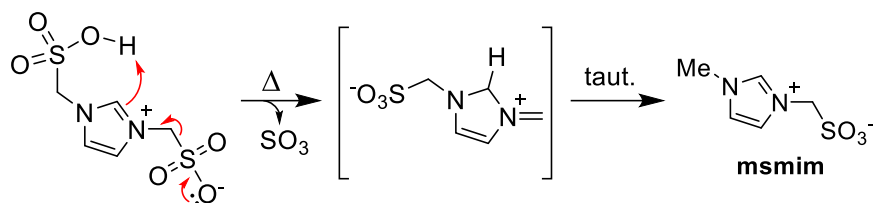


**Table 12.** Optimization studies for the synthesis of **bsmim**.

| Entry | [Cond.]  | t (min) | T (°C) | Yield (%) | bsmim (%) <sup>‡</sup> | msmim (%) <sup>‡</sup> | AMS (%) <sup>‡</sup> |
|-------|--|---------|--------|-----------|------------------------|------------------------|----------------------|
| 1     | Standard <sup>†</sup>  | 120     | 95     | 0         | -                      | -                      | -                    |
| 2     | 2 mL H <sub>2</sub> O  | 120     | 95     | 45        | 76                     | 9                      | 15                   |
| 3     | 1.5 eq. reactants  | 120     | 95     | 0         | -                      | -                      | -                    |
| 4     | 2 mL H <sub>2</sub> O  | 20      | 95     | 47        | 86                     | 9                      | 5                    |
| 5     | 2 mL H <sub>2</sub> O  | 20      | 120    | 41        | 75                     | 12                     | 13                   |
| 6     | 2 mL H <sub>2</sub> O  | 40      | 120    | 45        | 68                     | 20                     | 12                   |
| 7     | 100 μL H <sub>2</sub> SO <sub>4</sub>                        | 20      | 95     | 30        | 100                    | 0                      | 0                    |
| 8     | 2 mL H <sub>2</sub> O, 100 μL H <sub>2</sub> SO <sub>4</sub> | 20      | 95     | 49        | 100                    | 0                      | 0                    |

<sup>†</sup>5 mmol of formaldehyde and glyoxal, 10 mmol of AMS, no additional solvent. <sup>‡</sup>Determined by NMR analysis of the isolated product.

From the results obtained, it quickly became apparent why the synthesis of **bsmim** had no precedent in literature, as it presents a series of challenges, one of which is the very low solubility of **AMS** in water. Under the standard conditions—as used for the preparation of **bcmim**—, **AMS** dissolved only partially, with the unreacted formaldehyde and glyoxal forming a sticky black tar from which no product could be isolated (**Table 12**, entry 1). As an attempt to mitigate this issue, additional water was added to the reaction (2 mL per 10 mmol of **AMS**), observing full dissolution of the starting material within 20 minutes. After the reaction time had elapsed, a dark brown solid was isolated by solvent-induced precipitation in 45% yield (**Table 12**, entry 2). <sup>1</sup>H NMR analysis of the obtained product confirmed the identity of the so-obtained solid as **bsmim**, but also revealed the presence of unreacted **AMS** as well as substantial amount of an unknown impurity. From the NMR signals, the compound was identified as 1-methyl-3-(sulfomethyl)imidazole (**msmim**), arising from the thermally induced decomposition of **bsmim** (**Scheme 47**).



**Scheme 47.** Thermally induced formation of **msmim** from **bsmim**.

The presence of **msmim** and **AMS** in the product is problematic. Although the former can be removed *via* recrystallization, this is at the expense of greatly diminished yields (to ca. 20%) due to the tendency of aqueous **bsmim** solutions to form immiscible phases with the acetone or methanol used to precipitate it. Thus, the next series of experiments were aimed towards preventing the formation of **msmim** while ensuring full consumption of **AMS**. The first approach assayed was the addition of excess reactants (1.5 equivalents), but this resulted in the formation of a tar once again (**Table 12**, entry 3). In the first successful reaction (**Table 12**, entry 2), the very water-insoluble **AMS** fully disappeared within 20 minutes, which should indicate near full conversion to the water-soluble products. Therefore, the next experiment involved running the reaction for a shorter amount of time to allow full conversion of **AMS** while minimizing the residency time of **bsmim** in the mixture. This attempt was more successful, obtaining **bsmim** in 47% yield and 86% purity, although leftover starting material and **msmim** were still present in the isolated solid (**Table 12**, entry 4). Increasing the temperature to 120 °C resulted in lower yields and increased amount of byproduct, most likely due to faster decomposition kinetics, while maintaining the same proportion of **AMS** (**Table 12**, entries 5 and 6).

Judging by the tentative mechanism of the decomposition reaction, a free anionic sulfonate provides the easiest pathway to the release of sulfur trioxide (**Scheme 47**). Thus, sulfuric acid was added to the reaction to shift the equilibrium towards the protonated sulfonic acid. This way, pure **bsmim** was obtained in 30% yield (**Table 12**, entry 7) under the standard conditions, which had previously resulted in decomposition (**Table 12**, entry 1). The solubility of **AMS** was also observed to be much higher in this acidic medium, so additional water was added for the next attempt, which finally afforded pure **bsmim** in 49% yield (**Table 12**, entry 8). Sustainability metrics were calculated for the final synthetic conditions, as compiled in **Table 13**.

**Table 13.** Sustainability metrics for the synthesis of **bsmim**.

| 5 mmol    | 5 mmol | 10 mmol |                         |       |       |          |          | <b>bsmim</b> (49%) |
|-----------|--------|---------|-------------------------|-------|-------|----------|----------|--------------------|
| Yield (%) | AE (%) | SF      | RME <sub>And.</sub> (%) | MRP   | VMR   | E-factor | EcoScale |                    |
| 49        | 82.6   | 1       | 5.1                     | 0.127 | 0.623 | 18.5     | 64       |                    |

In general terms, the process has acceptable scores, especially considering the difficulties encountered throughout the optimization studies. The high theoretical efficiency of the Arduengo imidazolium synthesis reflects on the excellent AE and SF values, which partially compensate for the moderate yield and low RME and MRP values. These, along with the E-factor, mainly arise from the addition of acetone to precipitate **bsmim** from the reaction mixture and could be significantly improved by removing water via lyophilization instead of forcing precipitation of the product. Still, the E-factor remains comfortably within the lower limits of fine chemical production (5 to 50) and, even with a hefty 25-point penalty due to the yield obtained, the EcoScale score remains in the higher range of “acceptable” methodologies (50 to 75 points), showing the potential of the synthetic process and encouraging further optimization studies to fine-tune the process.

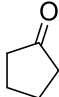
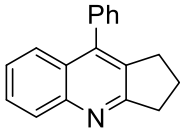
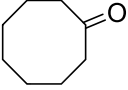
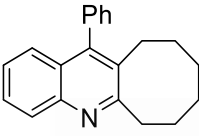
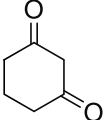
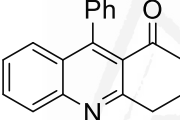
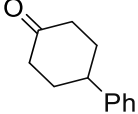
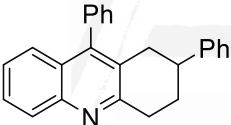
To assess the catalytic activity of the newly prepared **bsmim** against the first-generation IOS **bcmimCl**, the Friedländer synthesis of quinolines and the allylation of heterocycles developed in the first part of this chapter were selected as benchmark reactions. For the former, 2-aminobenzophenone was combined with a range of ketones in the presence of **bsmim**, obtaining the results detailed in **Table 14**. The conditions of the reaction were the same as those described in literature for the **bcmimCl**-catalyzed process, and the yields of the products were compared with those reported when appropriate.

**Table 14.** Scope of the Friedländer synthesis of quinolines catalyzed by **bsmim** or **bcmimCl**.

| Entry | Ketone | Product | N° | Yield with <b>bsmim</b> (%) | Yield with <b>bcmimCl</b> (%) <sup>148</sup> |
|-------|--------|---------|----|-----------------------------|--|
| 1     |        |         | 70 | 99                          | 94   |
| 2     |        |         | 71 | 98                          | 96   |
| 3     |        |         | 72 | 93                          | -  |
| 4     |        |         | 73 | 94                          | 90   |

Isolated yields of 0.5 mmol scale reactions after column chromatography.

**Table 14 (cont.).** Scope of the Friedländer synthesis of quinolines catalyzed by **bsmim** or **bcmimCl**.

| Entry | Ketone  | Product   | N° | Yield with <b>bsmim</b> (%) | Yield with <b>bcmimCl</b> (%) <sup>148</sup> |
|-------|---|---|----|-----------------------------|--|
| 5     |    |    | 74 | 93                          | 87   |
| 6     |    |    | 75 | 96                          | -  |
| 7     |   |   | 76 | 96                          | 81   |
| 8     |  |  | 77 | 97                          | -  |

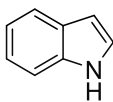
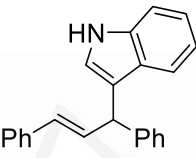
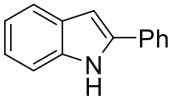
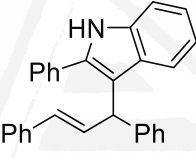
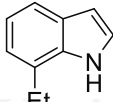
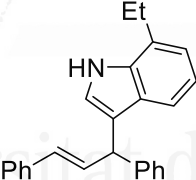
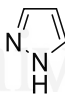
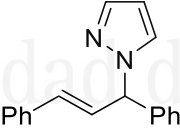
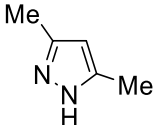
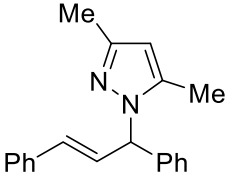
Isolated yields of 0.5 mmol scale reactions after column chromatography.

Using **bsmim** as catalyst resulted in products being obtained in excellent to quantitative yields across the board. The protocol tolerates a variety of substrates, including diketones, both linear and cyclic (**Table 14**, entries 1 and 7, respectively) as well as cyclic ketones, substituted or not, of several ring sizes (**Table 14**, entries 4, 5, 6 and 8). Enolizable esters are compatible with this methodology as well, with ethyl acetoacetate affording **71** in excellent yield (**Table 14**, entry 2). A slight reduction in yields is observed with electron-poor substrates, as evidenced by **72**, obtained from 6-chloro-2-aminobenzophenone (**Table 14**, entry 3).

Compared to **bcmimCl**, the sulfoimidazolium salt achieves up to 15% higher yields in this reaction (**Table 14**, entry 7), consistently outperforming the first-generation IOS. This is a particularly remarkable feat, considering that **bsmim**'s actual carbon analogue, **bcmim**, only manages 9% conversion for the synthesis of **70** under the same working conditions,<sup>148</sup> nicely highlighting the stark difference in baseline catalytic activity between the generations of imidazolium IOS.

Regarding the allylation of heterocycles, (*E*)-1,3-diphenylprop-2-en-1-ol was combined with representative substrates under the reaction conditions described for the **bcmimCl**-catalyzed process (Figures 33 and 36). The results obtained are compiled in Table 15.

**Table 15.** Scope of the allylation of heterocycles with **bsmim** and **bcmimCl**.

| $\text{Ph}-\text{CH}=\text{CH}-\text{CH}(\text{OH})-\text{Ph} + [\text{Het.}] \xrightarrow[\text{neat, } t \text{ (h), } 80 \text{ } ^\circ\text{C}]{\text{IOS (10 mol\%)}} \text{Ph}-\text{CH}=\text{CH}-\text{CH}(\text{Het})-\text{Ph}$ |   |   |    |  |  |
|--|---|---|----|--|--|
| Entry  | [Het.]  | Product   | N° | Yield with <b>bsmim</b> (%) <sup>†</sup> | Yield with <b>bcmimCl</b> (%) <sup>‡</sup> |
| 1  |    |    | 46 | 98                                       | 93   |
| 2  |   |   | 49 | 78                                       | 60   |
| 3  |  |  | 50 | 99                                       | 99   |
| 4  |  |  | 61 | 99                                       | 99   |
| 5  |  |  | 63 | 93                                       | 99   |

<sup>†</sup>GC-MS yields with durene as internal standard. <sup>‡</sup>Isolated yields of 0.5mmol scale reactions.

The results obtained indicate once more that **bsmim** is superior to **bcmimCl** in terms of catalytic activity, particularly evidenced by the preparation of **49**, in which the former obtains significantly higher yields (Table 15, entry 2). For the rest of compounds, yields are consistently in the





excellent to quantitative range (**Table 15**, entries 1, 3, 4, 5), within margin of error of those obtained with **bcmimCl**. It is worth noting that the use of **bcmim** in this transformation results in no reaction whatsoever, which once more highlights the improvements second-generation imidazolium IOS offer in terms of catalytic activity.



Universitat d'Alacant  
Universidad de Alicante

### C3.4. Conclusions

After the studies carried out in this chapter, the following conclusions were drawn:

-  The allylation of a variety of indoles with allylic alcohols promoted by **bcmimCl** in solventless conditions has been successfully attained, obtaining the corresponding 3-allyl indoles in good to quantitative yields. The protocol is scalable, and several products were obtained pure without the need for chromatographic purification. In addition, **bcmimCl** could be recovered and reused five times without loss of catalytic activity.
-  The allylation protocol has been extended to a broad range of nitrogen heterocycles, including pyrazoles, triazoles, tetrazoles, carbazoles, indazoles and benzotriazoles. As with indoles, good to quantitative yields have been obtained, with some examples not requiring additional purification after filtering off the catalyst.
-  Sustainability metrics have been calculated for the allylation of indoles with **bcmimCl** and compared with several representative synthetic processes reported in literature. Judging by the results obtained, the protocol described herein is significantly superior in terms of sustainability compared to the rest of methods studied.
-  An unprecedented methodology for the synthesis of **bsmim** has been developed. The catalytic activity of this second-generation IOS has been studied in the Friedländer quinoline synthesis and the allylation of heterocycles, with the results obtained indicating that **bsmim** has much higher catalytic performance than its carbon analogue and is generally superior to **bcmimCl**.

Universitat d'Alacant  
Universidad de Alicante





---

## **Chapter 4.**

**Novel zirconium Metal-Organic Frameworks  
derived from carboxy-imidazolium salts.**

---

Universitat d'Alacant  
Universidad de Alicante



## C4.1. Antecedents

### C4.1.1. Metal-Organic Frameworks. General considerations.

The term “Metal-Organic Frameworks” (MOF), coined by Omar M. Yaghi in 1995,<sup>309</sup> refers to a series of hybrid materials constituted by metallic centers bridged by organic molecules forming two- or three-dimensional coordination networks with permanent porosity.<sup>310</sup>

Metal nodes may be constituted by lone ions with simple connectivity or complex polynuclear inorganic clusters with multiple open positions for coordination.<sup>311</sup> These structures, named secondary building units (SBUs),<sup>312</sup> are the core elements of the MOF and their geometry generally dictates the final topology of the material.<sup>313</sup> More than 130 SBUs of different transition metals are known, with vacant coordination positions ranging from three to sixty-six.<sup>314</sup> Regarding organic linkers, they are molecules bearing at least two chelating groups (carboxylates are by far the most ubiquitous, although alcohols, amines, phosphates or nitriles are common as well) and having a certain degree of rigidity (Figure 39).<sup>310</sup>

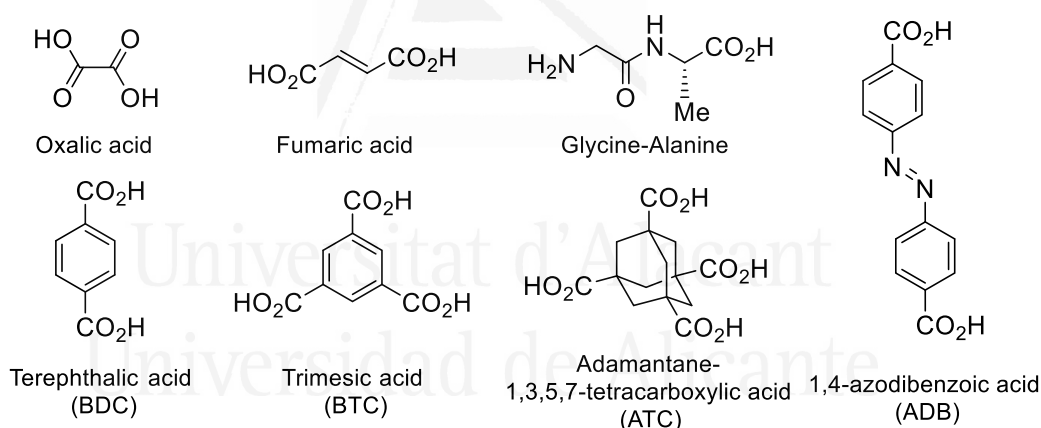


Figure 39. Representative examples of linkers for MOFs.

<sup>309</sup>Yaghi, O. M.; Li, H. *J. Am. Chem. Soc.* **1995**, *117*, 10401–10402.

<sup>310</sup>Furukawa, H.; Cordova, K. E.; O’Keeffe, M.; Yaghi, O. M. *Science* **2013**, *341*, 1230444.

<sup>311</sup>Wang, Q.; Astruc, D. *Chem. Rev.* **2020**, *120*, 1438–1511.

<sup>312</sup>Eddaoudi, M.; Moler, D. B.; Li, H.; Chen, B.; Reineke, T. M.; O’Keeffe, M.; Yaghi, O. M. *Acc. Chem. Res.* **2001**, *34*, 319–330.

<sup>313</sup>Kim, J.; Chen, B.; Reineke, T. M.; Li, H.; Eddaoudi, M.; Moler, D. B.; O’Keeffe, M.; Yaghi, O. M. *J. Am. Chem. Soc.* **2001**, *123*, 8239–8247.

<sup>314</sup>Tranchemontagne, D. J.; Mendoza-Cortés, J. L.; O’Keeffe, M.; Yaghi, O. M. *Chem. Soc. Rev.* **2009**, *38*, 1257–1283.

Rigidity is fundamental in the obtention of materials with permanent porosity, which is precisely what differentiates regular coordination polymers (CPs), known since the 1950s,<sup>315</sup> from MOFs.<sup>310</sup> CPs have semi-rigid structures arising from weak and flexible coordination bonds, which tend to collapse upon removal of solvent (leftover from their synthesis) trapped within their pores. This is known to happen with materials formed by  $\text{Cu}^{2+}$  cations linked by 4,4'-bipyridine struts, for instance.<sup>310,316</sup> MOFs, on the other hand, have their metal centers conformationally locked in place, often through the use of SBUs, which ensures the rigidity of the framework.<sup>316</sup> The most famous example is MOF-5, formed by  $\text{ZnO}_4(\text{CO}_2)_6$  SBUs and BTC linkers, which in 1999 was reported as the first metal-organic coordination network with permanent porosity.<sup>317</sup> A special kind of non-SBU-containing MOFs are zeolitic imidazolate frameworks (ZIF), formed by  $\text{Co}^{2+}$  or  $\text{Zn}^{2+}$  ions bonded by imidazolate linkers. These materials have very stable structures due to their short and completely rigid linkers, as well as the high bond strength between the components.<sup>314</sup>

Besides their mechanical stability, ZIFs are well-known for their very high tolerance to thermal and chemical stress. The Zn-based ZIF-8 is able to withstand immersion in refluxing concentrated sodium hydroxide solutions for up to a day, and is stable at temperatures exceeding 550 °C.<sup>310,318</sup> This is related to the bonding strength between the components, which has shown a good correlation with the Pearson hard-soft acid-base (HSAB) theory,<sup>319</sup> stating that hard Lewis bases (carboxylates are prime examples) are ideally combined with high-valent transition metals (e.g.,  $\text{Ti}^{4+}$ ,  $\text{Zr}^{4+}$ ,  $\text{Fe}^{3+}$ ), which are hard Lewis acids. This principle works the same for soft Lewis bases, such as nitriles and pyridines and low-valent transition metals, like  $\text{Cu}^{2+}$  or  $\text{Zn}^{2+}$ . Thus, ZIF-8, formed by the right combination of a soft ligand and metal, has very high chemical stability, whereas MOF-5, formed by a hard ligand and a soft metal, is structurally robust enough to withstand mechanical stress but slowly decomposes upon exposure to moisture.<sup>318</sup>

With the right choice of components, it is possible to obtain highly stable MOFs which, due to the intrinsic characteristics of their structures and bonding, offer a series of advantages over reference porous materials such as zeolites, silicas and activated carbons for certain applications.

As a direct consequence of their reticular structures, MOFs tend to have extremely high specific surface areas, much more so than their inorganic counterparts. While these have Brunauer-Emmett-Teller (BET) specific surface areas of around 1500  $\text{m}^2/\text{g}$ , the earliest MOFs already lingered around

---

<sup>315</sup>Kinoshita, Y.; Matsubara, I.; Higuchi, T.; Saito, Y. *Bull. Chem. Soc. Jpn.* **1959**, *32*, 1221–1226.

<sup>316</sup>Yaghi, O. M.; O'Keeffe, M.; Ockwig, N. W.; Chae, H. K.; Eddaoudi, M.; Kim, J. *Nature* **2003**, *423*, 705–714.

<sup>317</sup>Li, H.; Eddaoudi, M.; O'Keeffe, M.; Yaghi, O. M. *Nature* **1999**, *402*, 276–279.

<sup>318</sup>Yuan, S.; Feng, L.; Wang, K.; Pang, J.; Bosch, M.; Lollar, C.; Sun, Y.; Qin, J.; Yang, X.; Zhang, P.; Wang, Q.; Zou, L.; Zhang, Y.; Zhang, L.; Fang, Y.; Li, J.; Zhou, H.-C. *Adv. Mater.* **2018**, *30*, 1704303.

<sup>319</sup>Pearson, R. G. *J. Am. Chem. Soc.* **1963**, *85*, 3533–3539.

the 2000 m<sup>2</sup>/g mark.<sup>310,317</sup> By 2009, that benchmark value had more than doubled and in 2012, Hupp and coworkers achieved an impressive 7140 m<sup>2</sup>/g with the zirconium-based NU-110.<sup>320</sup>

With virtually endless combinations of metal nodes and linkers available, MOFs enjoy unparalleled modularity, allowing for the preparation of highly specialized materials to a level simply unattainable for their inorganic counterparts.<sup>310</sup> For instance, as the general topology of the MOF is dictated by the geometry of the metal node, it is possible to build a family of isorecticular MOFs from a single SBU structure by using differently sized rigid linkers, allowing total control over the pore size, density and specific surface area of the material while maintaining the same lattice shape.<sup>310,316</sup> The UiO-6x MOFs, consisting of octahedral Zr<sub>6</sub>O<sub>4</sub>(OH)<sub>4</sub> SBUs and BDC-based linkers, are prime examples of such approach (Figure 40).<sup>321,322</sup>

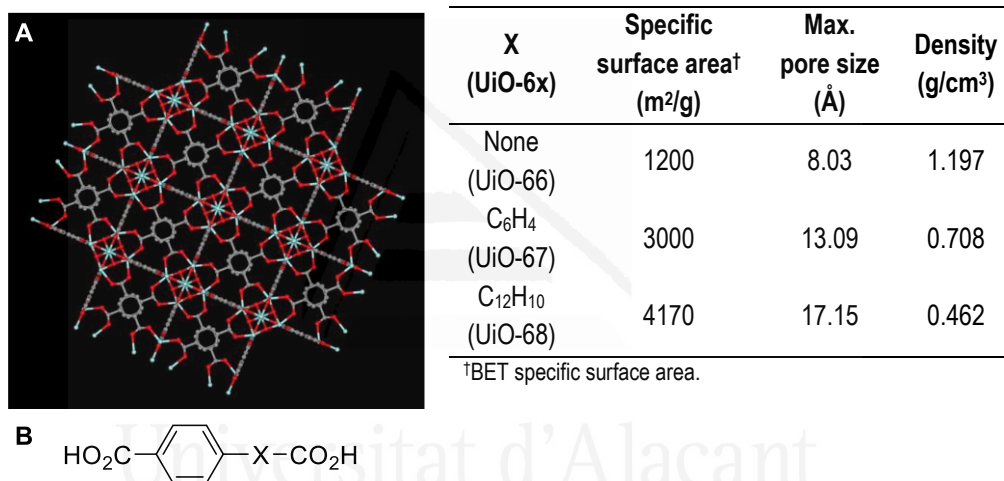


**Figure 40.** (A) Unit cell of UiO-66 obtained from data uploaded by Lamberti *et al.*<sup>323</sup> at the Cambridge Crystallographic Data Centre. (B) General structure of the UiO-6x linkers.

Even within the same MOF structure, it is possible to control parameters such as particle size, crystallinity and defect density (which to some extent affects pore size and surface area as well). This is achieved through the use of modulators, monodentate ligands bearing the same chelating group as the linker.<sup>324</sup>

<sup>320</sup>Farha, O. K.; Eryazici, I.; Jeong, N. C.; Hauser, B. G.; Wilmer, C. E.; Sarjeant, A. A.; Snurr, R. Q.; Nguyen, S. T.; Yazaydin, A. Ö.; Hupp, J. T. *J. Am. Chem. Soc.* **2012**, *134*, 15016–15021.

<sup>321</sup>Al-Jadir, T. M.; Siperstein, F. R. *Microporous Mesoporous Mater.* **2018**, *271*, 160–168.

<sup>322</sup>Winarta, J.; Shan, B.; McIntyre, S. M.; Ye, L.; Wang, C.; Liu, J.; Mu, B. *Cryst. Growth Des.* **2020**, *20*, 1347–1362.

<sup>323</sup>Valenzano, L.; Civalleri, B.; Chavan, S.; Bordiga, S.; Nilsen, M. H.; Jakobsen, S.; Lillerud, K. P.; Lamberti, C. *Chem. Mater.* **2011**, *23*, 1700–1718.

<sup>324</sup>Schaate, A.; Roy, P.; Godt, A.; Lippke, J.; Waltz, F.; Wiebcke, M.; Behrens, P. *Chem. Eur. J.* **2011**, *17*, 6643–6651.

The vast majority of MOFs are obtained *via* solvothermal processes, in which solutions of the components (commonly in polar solvents with high boiling points, such as DMF or water) are combined and subjected to vigorous heating for extended periods of time (80-120 °C for 24-72 hours is the norm).<sup>325,326</sup> Normally, the MOF immediately precipitates out of solution upon combination of the components as a somewhat amorphous powder due to fast nucleation, which rearranges under solvothermal conditions to a more crystalline material.<sup>318</sup> However, this process is slow, requires high temperatures and, although perfect networks are attainable given enough time, there is no control over the particle size or defect density (missing metallic nodes or linkers) of the material.<sup>324,325</sup>

Pioneered by the group of Behrens in 2011, the use of modulators allows to obtain highly crystalline materials by slowing down the rate at which the MOF structure is formed.<sup>324,327</sup> Upon synthesis, excess amount of these species is added to the reaction mixture, which causes the SBUs to be initially formed with the modulator rather than the linker.<sup>324</sup> The latter then replaces the modulator, with the kinetics of the process determined by the temperature and the modulator to linker ratio, which allows for fine control over the growth rate of the MOF.<sup>325,327</sup>

An interesting implication of the mechanism of action of modulators is that, as the initial MOF structure formed is highly defective i.e., many coordination positions at the SBUs are occupied by modulator molecules rather than linker, control over the defect density of the final material is attained by simply adjusting the reaction time.<sup>328</sup> Then, modulators attached to the clusters may be removed, providing highly porous MOFs with catalytically active free sites, or kept in place, obtaining node-functionalized materials (**Scheme 48**).<sup>329,330</sup> An excellent example of modulator is L-proline, which has been applied to great effect to the obtention of X-ray quality single-crystals of UiO-67<sup>331</sup> as well as the preparation of node-modified zirconium MOFs for heterogeneous asymmetric organocatalysis.<sup>330,332</sup>

---

<sup>325</sup>DeStefano, M. R.; Islamoglu, T.; Garibay, S. J.; Hupp, J. T.; Farha, O. K. *Chem. Mater.* **2017**, *29*, 1357–1361.

<sup>326</sup>Rechac, V. L.; Cirujano, F. G.; Corma, A.; Llabrés i Xamena, F. X. *Eur. J. Inorg. Chem.* **2016**, 4512–4516.

<sup>327</sup>Yun, W. C.; Yang, M. T.; Lin, K. Y. A. *J. Colloid Interface Sci.* **2019**, *543*, 52–63.

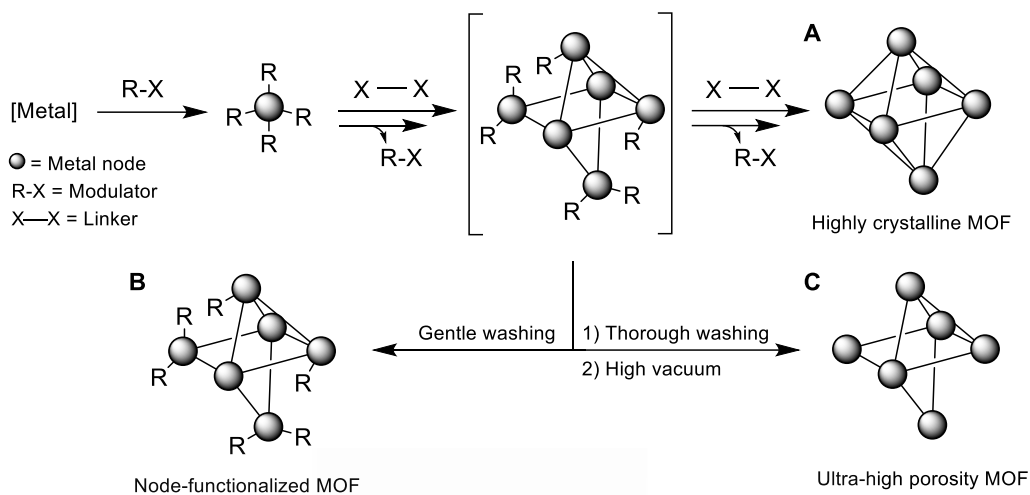
<sup>328</sup>Pakamoré, I.; Rousseau, J.; Rousseau, C.; Monflier, E.; Szilágyi, P. Á. *Green Chem.* **2018**, *20*, 5292–5298.

<sup>329</sup>Dhakshinamoorthy, A.; Santiago-Portillo, A.; Asiri, A. M.; Garcia, H. *ChemCatChem* **2019**, *11*, 899–923.

<sup>330</sup>Feng, X.; Jena, H. S.; Leus, K.; Wang, G.; Ouwehand, J.; Van Der Voort, P. *J. Catal.* **2018**, *365*, 36–42.

<sup>331</sup>Gutov, O. V.; Molina, S.; Escudero-Adán, E. C.; Shafir, A. *Chem. Eur. J.* **2016**, *22*, 13582–13587.

<sup>332</sup>Nguyen, K. D.; Kutzscher, C.; Drache, F.; Senkovska, I.; Kaskel, S. *Inorg. Chem.* **2018**, *57*, 1483–1489.



**Scheme 48.** Modulated synthesis for the obtention of (A) crystalline, (B) node-functionalized or (C) highly porous MOFs.

Beyond the ample variety of possible building blocks and controlled formation techniques, post-synthetic modification (PSM) methodologies offer additional control over the physical-chemical properties of MOFs and further extend their applicability.<sup>310</sup> These protocols are often divided in three distinct categories, namely post-synthetic exchange (PSE), post-synthetic functionalization (PSF) and post-synthetic insertion (PSI).<sup>318,333</sup>

As the name implies, PSE involves exchanging metals or linkers within the original framework for structurally equivalent replacements, resulting in hybrid or fully exchanged MOFs impossible to obtain through normal means.<sup>333,334</sup> This process is similar in principle to the use of modulators in synthesis, and is possible due to the relative lability of the non-covalent bonding between the components. It is commonly achieved by submerging the structure in a solution—usually on a protic solvent, such as methanol or water, capable of stabilizing the coordinatively unsaturated metal intermediates<sup>335</sup>—containing excess amount of the intended replacement components<sup>333</sup> (**Scheme 49**). Although heating is often applied to accelerate the process, it is not always required.<sup>336</sup>

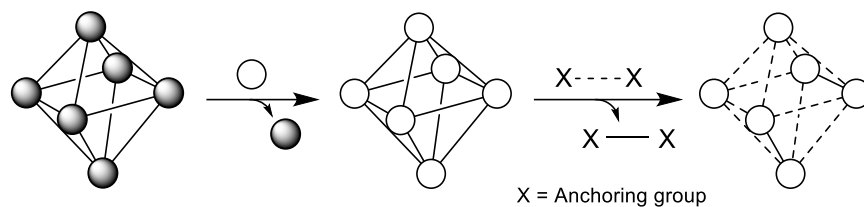
<sup>333</sup>Cui, P.; Wang, P.; Zhao, Y.; Sun, W.-Y. *Cryst. Growth Des.* **2019**, *19*, 1454–1470.

<sup>334</sup>Kim, M.; Cahill, J. F.; Fei, H.; Prather, K. A.; Cohen, S. M. *J. Am. Chem. Soc.* **2012**, *134*, 18082–18088.

<sup>335</sup>Marreiros, J.; Caratelli, C.; Hajek, J.; Krajnc, A.; Fleury, G.; Bueken, B.; De Vos, D. E.; Mali, G.; Roeyffers, M. B. J.; Van Speybroeck, V.; Ameloot, R. *Chem. Mater.* **2019**, *31*, 1359–1369.

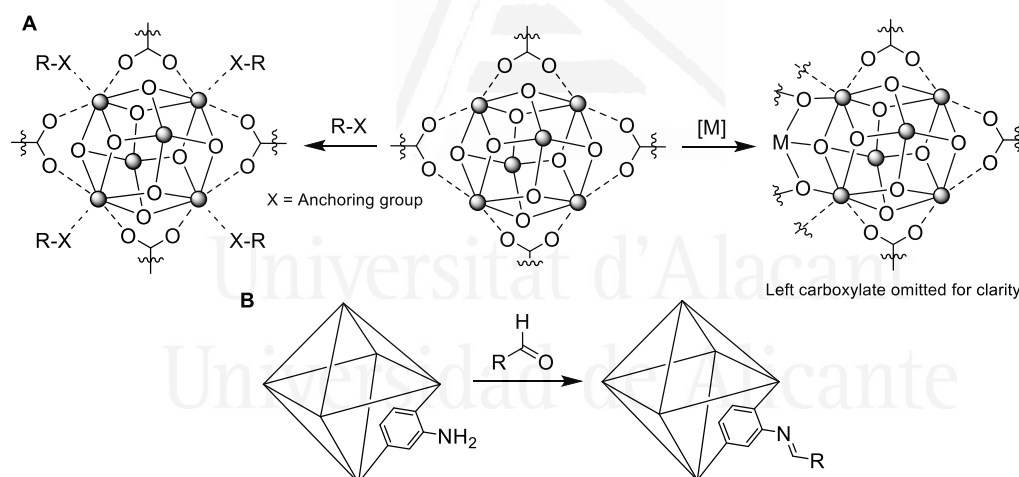
<sup>336</sup>Kalaj, M.; Prosser, K. E.; Cohen, S. M. *Dalton Trans.* **2020**, *49*, 8841–8845.





**Scheme 49.** Scheme of a generic two-step PSE process, replacing metal nodes (circles) and linkers (lines).

PSF, on the other hand, consists in the functionalization of the components of the MOF by means of heterogeneous-phase reactions.<sup>337</sup> Metal nodes are often modified by grafting organic species bearing monodentate chelating groups or using organometallic reagents to grow clusters of other metals on top of the existing SBU, which acts as a template.<sup>338–340</sup> Regarding the modification of the linkers, it often involves the transformation of a pre-functionalized unit—which may have been directly used to synthesize the base MOF or inserted *via* PSE—by a variety of means, depending on the target side-chain structure (**Scheme 50**).<sup>329,341</sup>



**Scheme 50.** (A) PSF of a generic carboxylate-oxo-cluster metal node and (B) example of PSF on an amino-functionalized linker.

<sup>337</sup>Zhang, Y.; Yang, X.; Zhou, H.-C. *Polyhedron* **2018**, *154*, 189–201.

<sup>338</sup>Sosa, J.; Bennett, T.; Nelms, K.; Liu, B.; Tovar, R.; Liu, Y. *Crystals* **2018**, *8*, 325.

<sup>339</sup>Yeon, J. S.; Lee, W. R.; Kim, N. W.; Jo, H.; Lee, H.; Song, J. H.; Lim, K. S.; Kang, D. W.; Seo, J. G.; Moon, D.; Wiers, B.; Hong, C. S. *J. Mater. Chem. A* **2015**, *3*, 19177–19185.

<sup>340</sup>Klet, R. C.; Wang, T. C.; Fernandez, L. E.; Truhlar, D. G.; Hupp, J. T.; Farha, O. K. *Chem. Mater.* **2016**, *28*, 1213–1219.

<sup>341</sup>Rasero-Almansa, A. M.; Corma, A.; Iglesias, M.; Sanchez, Felix. One-Pot. *ChemCatChem* **2013**, *5*, 3092–3100.

Regarding PSI, it involves the encapsulation of catalytically active species within the structure of the MOF.<sup>318,329</sup> The preparation of nanoparticles supported on MOFs is one of the most representative examples of PSI, achieved by insertion of the metallic precursor in the framework via PSF followed by *in-situ* reduction.<sup>318,329</sup> The PSI of organic compounds and metal complexes by diffusion of the substrate into the pores of the MOF is known,<sup>342</sup> although it is not very popular due to the high potential for leaching, with most research groups preferring the “bottle-around-a-ship” approach—adding the guest molecule to the growth media of the MOF— instead.<sup>343</sup>

With over 95,000 different structures compiled at the Cambridge Structure Database as of 2020,<sup>344</sup> MOFs are regarded by many as the greatest advance in the field of porous materials of the last 30 years. Their superior porosity and unparalleled modularity have allowed for the development of highly task-specific materials for application in selective gas adsorption and storage,<sup>310</sup> drug delivery,<sup>345</sup> as solid electrolytes, molecular sieves and templates for inorganic materials.<sup>338,346</sup>

Heterogeneous catalysis deserves a mention of its own, with MOF-based systems having been developed for almost every kind of organic transformation known (**Table 16**).<sup>337,347</sup> Besides the general advantages of supported catalysts (e.g., higher stability, easier recoverability), MOFs offer the possibility of controlling the pore openings of the framework, which can be exploited for the preparation of size-exclusive catalysts.<sup>343</sup>

Universitat d'Alacant  
Universidad de Alicante

---

<sup>342</sup>Vilhanova, B.; Ranocchiaro, M.; van Bokhoven, J. A. *ChemCatChem* **2016**, *8*, 308–312.

<sup>343</sup>Bogaerts, T.; Van Yperen-De Deyne, A.; Liu, Y. Y.; Lynen, F.; Van Speybroeck, V.; Van Der Voort, P. *Chem. Commun.* **2013**, *49*, 8021–8023.

<sup>344</sup>Daglar, H.; Keskin, S. *Coord. Chem. Rev.* **2020**, *422*, 213470.

<sup>345</sup>Wang, J.; Jin, J.; Li, F.; Li, B.; Liu, J.; Jin, J.; Wang, C.; Zeng, Y.; Wang, Y. *RSC Adv.* **2015**, *5*, 85606–85612.

<sup>346</sup>Hendon, C. H.; Rieth, A. J.; Korzyński, M. D.; Dincă, M. *ACS Cent. Sci.* **2017**, *3*, 554–563.

<sup>347</sup>Konnerth, H.; Matsagar, B. M.; Chen, S. S.; Precht, M. H. G.; Shieh, F.-K.; Wu, K. C.-W. *Coord. Chem. Rev.* **2020**, *416*, 213319.

**Table 16.** Representative examples of the use of MOFs in heterogeneous catalysis.

| Entry <sup>Ref.</sup> | MOF   | Transformation                  |
|-----------------------|---|---------------------------------|
| 1 <sup>326</sup>      | UiO-66  | Povarov synthesis of quinolines |
| 2 <sup>348</sup>      | MOF-5   | Friedel-Crafts reaction         |
| 3 <sup>349</sup>      | RSO <sub>3</sub> H@(Al)MIL-53-NH <sub>2</sub> | Mannich reaction                |
| 4 <sup>350</sup>      | Pd NPs@Co <sub>3</sub> (BDC) <sub>3</sub>     | Mizoroki-Heck cross-coupling    |
| 5 <sup>343</sup>      | Mn-salen@(Al)MIL-101                          | Enantioselective epoxidation    |
| 6 <sup>351</sup>      | L-Pro@(Al)MIL-101                             | Enantioselective aldol reaction |
| 7 <sup>352</sup>      | Rh(acac)(cod)@MOF-5                           | Hydroformylation of olefins     |

#### C4.1.2. Metal-Organic Frameworks based on 1,3-bis(carboxymethyl)imidazole

In 2005, Dyson and coworkers prepared the first **bcmim**-MOF by combination of the zwitterionic IOS (or its hydrobromide analogue) with strontium carbonate, obtaining a laminar material.<sup>353</sup> Due to its zwitterionic nature, **bcmim** derivatives behave in a completely different way to common dicarboxylic acids (e.g., BDC), offering multiple possible coordination modes with metals.<sup>354</sup> Coupled with their hydrogen-bond donor-acceptor capabilities and the flexibility provided by the methylene groups bridging the carboxylate moieties to the rigid heterocyclic ring,<sup>355</sup> these IOS are surprisingly effective for the formation of MOFs with low-valent alkaline and alkaline-earth metals (**bcmim** can form isolable CPs with even single-valent potassium and cadmium ions)<sup>356</sup> as well as with rare-earth elements, which due to their size, greatly benefit from the added mechanical flexibility and multiple coordination modes<sup>357</sup> (Table 17).

<sup>348</sup>Phan, N. T. S.; Le, K. K. A.; Phan, T. D. *Appl. Catal. A Gen.* **2010**, *382*, 246–253.

<sup>349</sup>Miao, Z.; Qi, C.; Wang, L.; Wensley, A. M.; Luan, Y. *Appl. Organomet. Chem.* **2017**, *31*, e3569.

<sup>350</sup>Ashouri, F.; Zare, M.; Bagherzadeh, M. *C. R. Chim.* **2017**, *20*, 107–115.

<sup>351</sup>Nießing, S.; Czekelius, C.; Janiak, C. *Catal. Commun.* **2017**, *95*, 12–15.

<sup>352</sup>Vu, T. V.; Kosslick, H.; Schulz, A.; Harloff, J.; Paetzold, E.; Lund, H.; Kragl, U.; Schneider, M.; Fulda, G. *Microporous Mesoporous Mater.* **2012**, *154*, 100–106.

<sup>353</sup>Fei, Z.; Geldbach, T. J.; Zhao, D.; Scopelliti, R.; Dyson, P. J. *Inorg. Chem.* **2005**, *44*, 5200–5202.

<sup>354</sup>Payne, M. K.; Laird, R. C.; Schnell, M. A.; Mackin, S. R.; Forbes, T. Z. *Cryst. Growth Des.* **2017**, *17*, 6498–6509.

<sup>355</sup>Chai, X.-C.; Sun, Y.-Q.; Lei, R.; Chen, Y.-P.; Zhang, S.; Cao, Y.-N.; Zhang, H.-H. *Cryst. Growth Des.* **2010**, *10*, 658–668.

<sup>356</sup>Fei, Z.; Geldbach, T. J.; Scopelliti, R.; Dyson, P. J. *Inorg. Chem.* **2006**, *45*, 6331–6337.

<sup>357</sup>You, L.-X.; Hao, J.-H.; Qi, D.; Xie, S.-Y.; Wang, S.-J.; Xiong, G.; Dragutan, I.; Dragutan, V.; Ding, F.; Sun, Y.-G. *Inorg. Chim. Acta* **2019**, *497*, 119075.

**Table 17.** MOFs reported in literature using **bcmim** derivatives as linkers.

| Entry <sup>Ref.</sup>            | Linker                  | Metal        |
|----------------------------------|-------------------------|--------------|
| <b>1</b> <sup>263,356</sup>      | <b>bcmimCl, bcmimBr</b> | Calcium      |
| <b>2</b> <sup>353,356</sup>      | <b>bcmim</b>            | Strontium    |
| <b>3</b> <sup>263,356</sup>      | <b>bcmimCl, bcmimBr</b> | Barium       |
| <b>4</b> <sup>358</sup>          | <b>bcmim</b>            | Manganese    |
| <b>5</b> <sup>359</sup>          | <b>bcmimCl</b>          | Cobalt       |
| <b>6</b> <sup>262,360</sup>      | <b>bcmim</b>            | Copper       |
| <b>7</b> <sup>359</sup>          | <b>bcmimCl</b>          | Zinc         |
| <b>8</b> <sup>361,362</sup>      | <b>bcmimCl, bcmimBr</b> | Lead         |
| <b>9</b> <sup>355</sup>          | <b>bcmim</b>            | Lanthanum    |
| <b>10</b> <sup>355</sup>         | <b>bcmim</b>            | Neodymium    |
| <b>11</b> <sup>357</sup>         | <b>bcmimCl</b>          | Praseodymium |
| <b>12</b> <sup>357,363</sup>     | <b>bcmimCl</b>          | Samarium     |
| <b>13</b> <sup>357,363,364</sup> | <b>bcmimCl</b>          | Europium     |
| <b>14</b> <sup>357,363</sup>     | <b>bcmimCl</b>          | Gadolinium   |
| <b>15</b> <sup>357,363</sup>     | <b>bcmimCl</b>          | Terbium      |
| <b>16</b> <sup>357,363</sup>     | <b>bcmimCl</b>          | Dysprosium   |
| <b>17</b> <sup>357</sup>         | <b>bcmimCl</b>          | Holmium      |
| <b>18</b> <sup>354,365</sup>     | <b>bcmim</b>            | Uranium      |

<sup>361</sup>Naga Babu, C.; Suresh, P.; Srinivas, K.; Sathyanarayana, A.; Sampath, N.; Prabusankar, G. *Dalton Trans.* **2016**, 45, 8164–8173.

<sup>362</sup>Wang, X.-W.; Han, L.; Cai, T.-J.; Zheng, Y.-Q.; Chen, J.-Z.; Deng, Q. *Cryst. Growth Des.* **2007**, 7, 1027–1030.

<sup>363</sup>You, L.-X.; Guo, Y.; Xie, S.-Y.; Wang, S.-J.; Xiong, G.; Dragutan, I.; Dragutan, V.; Ding, F.; Sun, Y.-G. *J. Solid State Chem.* **2019**, 278, 120900.

<sup>364</sup>Wang, Y.; Fu, X.; Zhang, T.; Xin, T.; Lu, C.; Yan, D. *J. Mol. Struct.* **2020**, 1200, 127081.

<sup>365</sup>Martin, N. P.; Falaise, C.; Volkringer, C.; Henry, N.; Farger, P.; Falk, C.; Delahaye, E.; Rabu, P.; Loiseau, T. *Inorg. Chem.* **2016**, 55, 8697–8705.






## C4.2. Objectives

Within **bcmim**-MOFs, the presence of transition metals is minor, with only a few structures reported in literature. Interestingly, although the dicarboxylate-bearing **bcmim** is theoretically a hard ligand, the examples described have been synthesized using soft metals,<sup>†</sup> namely manganese, copper, cobalt, zinc and lead, whereas the use of hard metals—the supposedly ideal choice—is completely unexplored.

Zirconium is by far the most ubiquitous transition metal in the field of MOFs, mostly present in the well-known UiO-6x family. These MOFs have high porosity, excellent physical-chemical properties, and very high stability, arising from the strong bonding between their octahedral  $Zr_6O_4(OH)_4$  SBUs and carboxylate linkers.<sup>322,329</sup>

Normally, UiO-6x MOFs are obtained by solvothermal processes by heating a mixture of the components in DMF for a certain amount of time.<sup>322</sup> Quite recently, a methodology for the room-temperature modulated synthesis of UiO-66-NH<sub>2</sub> in water was reported by Szilágyi and coworkers, which offers a significant improvement in terms of sustainability while affording a high-quality MOF structure.<sup>328</sup> Based on this, and the antecedents described above, the following objectives were set:

-  To develop a low-temperature, water-based methodology for the synthesis of zirconium MOFs using **bcmim** derivatives as linkers.
-  To study the materials obtained and determine prospective applications in catalysis or materials science.
-  To assess the environmental impact of the protocol designed using sustainability metrics.

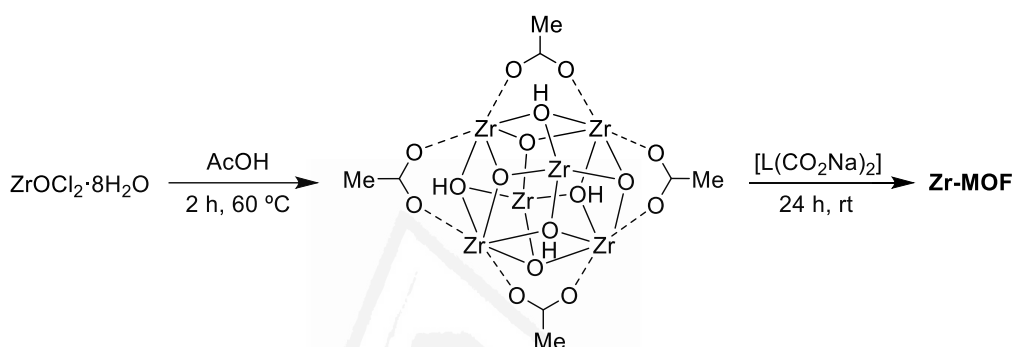
---

<sup>†</sup> According to the HSAB definition.



### C4.3. Results and discussion

The preparation of the zirconium-based **bcmim** MOFs (**bcmimZr**) was carried out following the two-step methodology described by Szilágyi and coworkers for the synthesis of UiO-66-NH<sub>2</sub>.<sup>328</sup> This process involves the pre-formation of the SBUs by treating the zirconium precursor with modulator for a certain amount of time, after which the disodium salt of the linker is added, causing the precipitation of the MOF, which is then aged in solution for 24 hours at room temperature (**Scheme 51**).



**Scheme 51.** Modulated synthesis of Zr-MOFs developed by Szilágyi.

Thus, a water solution of zirconium oxychloride octahydrate (zirconyl chloride) was treated with 22 equivalents of acetic acid at 60 °C for two hours under static conditions. After cooling down the mixture, an aqueous solution of the sodium salt of **bcmim** (**bcmimNa**, prepared by treating the zwitterion with equimolar amount of sodium hydroxide) was added to the flask, and the mixture was gently stirred for 24 hours at room temperature. At this point, the mixture remained clear, and no solid was present, so methanol was slowly added to the flask until the reaction medium became turbid, signaling the precipitation of the MOF. The mixture was then stirred for an additional 24 hours. Parallel to this, a second reaction without acetic acid was set up under the same conditions to evaluate the influence of the modulator in the **bcmimZr** structure.

Interestingly, whereas the modulated synthesis afforded a fine white powder, the reaction without modulator resulted in the formation of an opaque monolithic gel, which became a dark yellow glassy solid after removal of the solvent under vacuum. The formation of metal-organic gels (MOGs) has been reported for well-known MOF structures, such as MIL-53, ZIF-8, HKUST-1 or the UiO-6x family, and is associated to the rapid formation of a high concentration of nanoparticles, which colloiddally self-assemble in solution, mostly *via* Van der Waals forces.<sup>366,367</sup> It is worth noting that most reported

<sup>366</sup>Hou, J.; Sapnik, A. F.; Bennett, T. D. *Chem. Sci.* **2020**, *11*, 310–323.

<sup>367</sup>Wychowaniec, J. K.; Saini, H.; Scheibe, B.; Dubal, D. P.; Schneemann, A.; Jayaramulu, K. *Chem. Soc. Rev.* **2022**, *51*, 9068–9126.



examples of MOGs are obtained in polar organic solvents,<sup>366</sup> so the formation of MOG-hydrogels may offer a prospective advantage in terms of environmental impact.

To gain insight into the structural features of the dried **bcmimZr** samples, they were analyzed by powder X-ray diffraction (PXRD), obtaining the diffractograms of **Figure 41**.

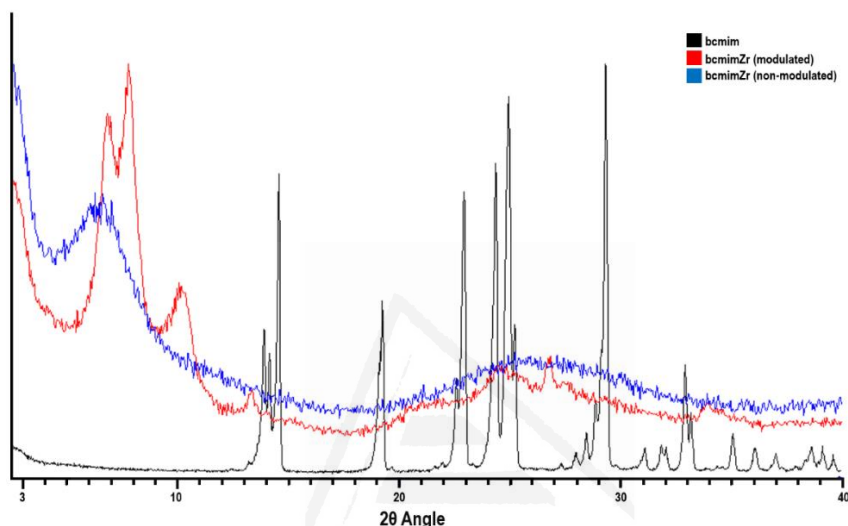


**Figure 41.** Powder X-ray diffractograms of **bcmim** (black), modulated (red) and non-modulated (blue) **bcmimZr**.

The PXRD patterns confirm both materials are indeed different from **bcmim**, as well as from each other. The **bcmimZr** powder obtained by modulated synthesis exhibits intense bands at 6.8° and 7.7°, along with secondary bands at 10.1° and 26.7°, in a pattern resembling that of UiO-66.<sup>323</sup> This strongly suggests **bcmimZr** may have a similar structure, which would be expected in accordance with the isoreticularity principle described earlier, as the SBU was formed under conditions designed for the preparation of UiO-66 and **bcmim** is roughly geometrically equivalent to BDC. The broad peaks obtained suggest microcrystallinity,<sup>368</sup> although they could also be attributed to heterogeneity in the crystal structures of the MOF arising from the flexibility of **bcmim**.

The PXRD diffractogram of the xerogel obtained from the unmodulated synthesis of **bcmimZr** exhibits a single, broad band at 6.6° and hints at the presence of another at around 25°. This pattern is very similar to that found in other MOF-xerogels<sup>369</sup> and is consistent with a nanocrystalline

<sup>368</sup>Londoño-Restrepo, S. M.; Jeronimo-Cruz, R.; Millán-Malo, B. M.; Rivera-Muñoz, E. M.; Rodríguez-García, M. E. *Sci. Rep.* **2019**, *9*, 5915.

<sup>369</sup>Bueken, B.; Van Velthoven, N.; Willhammar, T.; Stassin, T.; Stassen, I.; Keen, D. A.; Baron, G. V.; Denayer, J. F. M.; Ameloot, R.; Bals, S.; De Vos, D.; Bennett, T. D. *Chem. Sci.* **2017**, *8*, 3939–3948.

material<sup>368</sup>, which seems to confirm the formation of the hydrogel through nanoparticle aggregation. Using the Debye-Scherrer equation (**Equation S1**, see section **S5.2.**),<sup>370</sup> a mean particle size of 1 nm was estimated from the PXRD pattern.

Among other uses, MOGs have been studied as a novel approach for the formation of highly ordered monolithic MOFs with defined shape. The preparation of such structures is of great importance for the application of these materials beyond lab-scale, as the microcrystalline powder form most MOFs are obtained is not suitable for certain uses. Commonly, monolithic MOFs are obtained by compression or extrusion of the powder—which may cause the structure to deform under pressure and temperature— or by controlled growth on a surface—with the supporting structure becoming irreversibly embedded in the monolith—, so MOGs offer a clear advantage in this regard.<sup>366,367,369</sup> On broader terms, the development of novel hydrogels is of great interest, particularly in the field of chemical biology and biomedicine, where their water-based nature and non-persistence are key advantages.<sup>371</sup> Besides, they find application in quasi-solid-state electronics,<sup>372</sup> as well as sensors and actuators.<sup>371</sup> Thus, the attention was shifted towards the study of the **bcmimZr** hydrogels.

A series of experiments aimed at determining the influence of several parameters—namely source and concentration of zirconium, presence of counter-anion in the linker and reaction temperature—in the formation of the hydrogels were carried out. As per the results obtained before, no modulator was used in any of the experiments, which are detailed in **Table 18**.

**Table 18.** Studies on the formation of **bcmimZr** hydrogels.

| Entry | [Linker]       | [Zr]                                  | Zr % (w/w) | [Conditions]    | Result <sup>†</sup> |
|-------|----------------|---------------------------------------|------------|-----------------|---------------------|
| 1     | <b>bcmimNa</b> | ZrOCl <sub>2</sub> ·8H <sub>2</sub> O | 1.65       | rt, 24 hours    | <b>OG</b>           |
| 2     | <b>bcmim</b>   | ZrOCl <sub>2</sub> ·8H <sub>2</sub> O | 1.65       | 40 °C, 24 hours | <b>OG</b>           |
| 3     | <b>bcmimCl</b> | ZrOCl <sub>2</sub> ·8H <sub>2</sub> O | 1.15       | 40 °C, 24 hours | <b>TG</b>           |
| 4     | <b>bcmim</b>   | ZrCl <sub>4</sub>                     | 1.15       | 40 °C, 24 hours | <b>TG</b>           |

<sup>†</sup>OG = Opaque hydrogel; TG = Translucent hydrogel; SFG = Semifluid hydrogel; L = Liquid; N/D = Not formed.

<sup>370</sup>Scherrer, P. *Nachr. Ges. Wiss. Göttingen, Math. Phys. Kl.* **1918**, 2, 98–100.

<sup>371</sup>Zhang, Y. S.; Khademhosseini, A. *Science* **2017**, 356, eaaf3627.

<sup>372</sup>Leng, K.; Li, G.; Guo, J.; Zhang, X.; Wang, A.; Liu, X.; Luo, J. *Adv. Funct. Mater.* **2020**, 30, 2001317.

**Table 18 (cont.)**. Studies on the formation of **bcmimZr** hydrogels.

| $[\text{Zr}] + [\text{Linker}] \xrightarrow[\text{Water}]{[\text{Conditions}]} \text{bcmimZr}$ |                |                                       |            |                             |                     |
|--|----------------|---------------------------------------|------------|-----------------------------|---------------------|
| Entry  | [Linker]       | [Zr]                                  | Zr % (w/w) | [Conditions]                | Result <sup>†</sup> |
| 5  | <b>bcmimCl</b> | ZrCl <sub>4</sub>                     | 1.15       | 40 °C, 24 hours             | <b>TG</b>           |
| 6  | <b>bcmim</b>   | Zr(OH) <sub>4</sub>                   | 1.15       | 40 °C, 24 hours             | N/D                 |
| 7  | <b>bcmimCl</b> | Zr(OH) <sub>4</sub>                   | 1.15       | 40 °C, 24 hours             | N/D                 |
| 8  | <b>bcmimCl</b> | ZrOCl <sub>2</sub> ·8H <sub>2</sub> O | 0.75       | 40 °C, 24 hours             | <b>TG</b>           |
| 9  | <b>bcmimCl</b> | ZrOCl <sub>2</sub> ·8H <sub>2</sub> O | 0.25       | 40 °C, 24 hours             | <b>SFG</b>          |
| 10   | <b>bcmimCl</b> | ZrOCl <sub>2</sub> ·8H <sub>2</sub> O | 0.10       | 40 °C, 24 hours             | L                   |
| 11   | <b>bcmimCl</b> | ZrOCl <sub>2</sub> ·8H <sub>2</sub> O | 2.00       | 120 °C, 24 hours            | <b>OG</b>           |
| 12   | <b>bcmimCl</b> | ZrOCl <sub>2</sub> ·8H <sub>2</sub> O | 0.65       | 20 mL of MeOH, rt, 24 hours | <b>OG</b>           |

<sup>†</sup>OG = Opaque hydrogel; TG = Translucent hydrogel; SFG = Semifluid hydrogel; L = Liquid; N/D = Not formed.

Deprotonation of the linker does not seem necessary for gelation, as evidenced by the opaque hydrogel obtained using pristine **bcmim** (Table 18, entries 1 and 2). Similarly, the use of **bcmimCl** also resulted in hydrogel formation (Table 18, entry 3). Although it has been reported that zirconyl chloride is preferable for the preparation of MOF gels in non-aqueous solvents due to faster formation of the SBU,<sup>366</sup> zirconium chloride is perfectly compatible with the water methodology reported herein, affording the desired hydrogels with both **bcmim** and **bcmimCl** (Table 18, entries 4 and 5). The very low solubility in water of zirconium hydroxide prevented its use as a metal source, and no structure could be obtained even after addition of excess acetic acid and heating (Table 18, entries 6 and 7). Regarding the concentration of metal, the lower limit for the formation of **bcmimZr** MOGs was observed to be around 0.25% of zirconium (w/w) (Table 18, entries 8 to 10). Interestingly, reaction temperatures of up to 120 °C (Table 18, entry 11) and the inclusion of methanol as a co-solvent (Table 18, entry 12) were well tolerated, which suggests a highly robust system.

To gain further insight into the structure of the **bcmimZr** MOGs, the hydrogels of entries 3, 8 and 9 of Table 18 were air-dried at 50 °C over several days and the resulting xerogels were analyzed by PXRD, obtaining the results detailed in Figure 42.

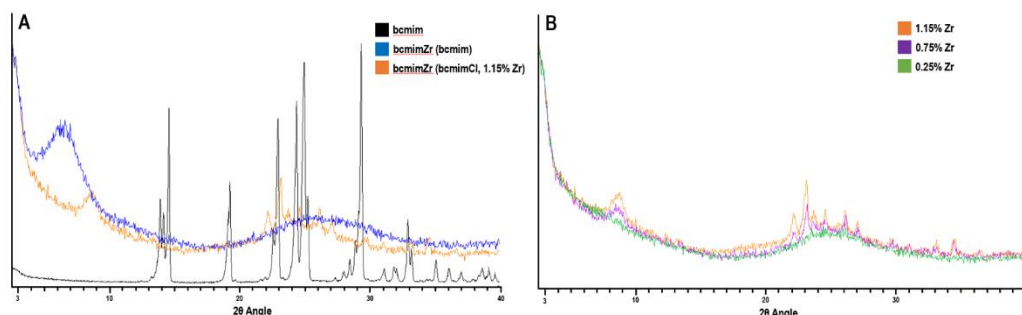


**Figure 42.** PXRD patterns of the xerogels derived from **bcmimCl** and zirconyl chloride (A) compared to **bcmim** and the xerogel derived from it and (B) compared to each other.

Interestingly, the diffraction pattern of the **bcmimCl**-based xerogels points at the formation of a different structure than that of **bcmim** or the **bcmimZr** gel (Figure 42, A), evidencing some degree of influence of the counter-anions of the linker in the morphology of the MOG. The PXRD patterns gradually lose features upon diminishing zirconium concentration, which may point to the formation of a non-crystalline polymer structure. Observation with optical microscopy of the xerogels obtained from the low-zirconium concentration samples shows regions with glass-like morphology, which suggests the presence of an amorphous phase in the material, although no definitive conclusions can be drawn at this resolution level (Figure 43).

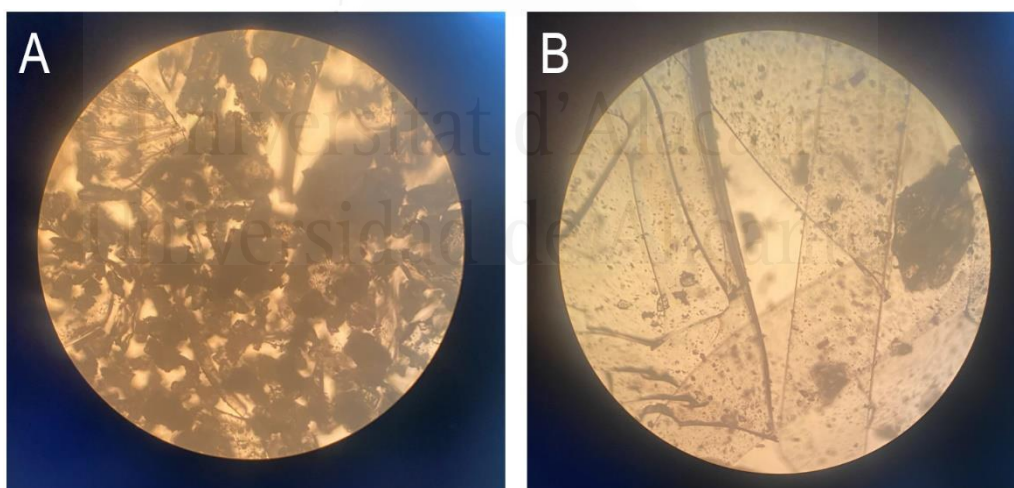


**Figure 43.** Optical microscopy image (x100 magnification) of glass-like (A) aggregated particles (B) and laminar regions of the 0.25% Zr xerogel.

In lieu of the results obtained and considering time and resource constraints, the system formed by **bcmim** and zirconium chloride (for which zirconium chloride is an intermediate on its hydrolysis,

thus being an essentially equivalent, but less expensive replacement) was selected for further experiments. First, hydrogels containing 1%, 0.75% and 0.5% of zirconium (by weight) were prepared and analyzed by DSC to determine the prospective sol-gel transition temperature and evaluate the influence of the concentration of zirconium in thermal behavior of the MOGs. However, upon analysis, no change in heat flow associated to the endothermic sol-gel transition could be observed for any of the samples. A small exothermic band at around 100 °C was observed for the 1 % and 0.5% MOGs (Table 19, entries 1 and 2), which could be attributed to a rearrangement of the gel phase to a more ordered state, in a manner not dissimilar to the behavior observed for the **mcmimCl**:urea LTTMs (see section SI.2.4 for the DSC traces of the MOGs).

**Table 19.** DSC studies of the **bcmimZr** hydrogels.

| Entry | Hydrogel                      | Onset of the event (°C) |
|-------|-------------------------------|-------------------------|
| 1     | <b>bcmimZr</b> 1% Zr (w/w)    | 102                     |
| 2     | <b>bcmimZr</b> 0.75% Zr (w/w) | 106                     |
| 3     | <b>bcmimZr</b> 0.5% Zr (w/w)  | -                       |

Thermal stability is often an issue with gels, due to increases in temperature disrupting the weak non-covalent interactions responsible for their structural integrity. Indeed, polyacrylamide hydrogels begin to degrade at temperatures around 80 °C, becoming completely liquid after 6 hours.<sup>373,374</sup> In the case of **bcmimZr** MOGs however, gel-state is maintained at temperatures up to 120 °C, as evidenced by the tests described in Table 18.

Next, the conductivity of the hydrogels was measured and compared with a state-of-the-art polyzwitterionic hydrogel based on zinc,<sup>372</sup> obtaining the results detailed in Table 20.

**Table 20.** Conductivity studies of the **bcmimZr** hydrogels.

| Entry | Hydrogel                      | Conductivity@20 °C (mS/cm <sup>-1</sup> ) |
|-------|-------------------------------|---|
| 1     | <b>bcmimZr</b> 1% Zr (w/w)    | 44  |
| 2     | <b>bcmimZr</b> 0.75% Zr (w/w) | 41  |
| 3     | <b>bcmimZr</b> 0.5% Zr (w/w)  | 38  |
| 4     | Zn-PSBMA <sup>†</sup>         | 32  |

<sup>†</sup>Poly[2-(methacryloyloxy)ethyl]dimethyl-(3-sulfopropyl).

<sup>373</sup>Kabiri, K.; Mirzadeh, H.; Zohuriaan-Mehr, M. J. *J. Appl. Polym. Sci.* **2008**, *110*, 3420–3430.

<sup>374</sup>Zareie, C.; Sefti, M. V.; Bahramian, A. R.; Salehi, M. B. *Iran. Polym. J.* **2018**, *27*, 577–587.

The **bcimZr** hydrogels exhibit remarkable electrical conductivities, well above the values reported for the Zn-PSBMA hydrogel at room temperature, which suggests the presence of highly mobile ionic species within the material, most likely chloride ions arising from the hydrolysis of zirconium chloride. Considering the high thermal resistance and robustness of the **bcimZr** hydrogels, they could be of interest as electrolytes in the fabrication of quasi-solid-state batteries.

To study the bonding of components within the **bcimZr** hydrogel matrix, a sample of the material containing 1% zirconium (w/w) was prepared in deuterium oxide and analyzed by proton nuclear magnetic resonance ( $^1\text{H}$  NMR) (Figure 44).

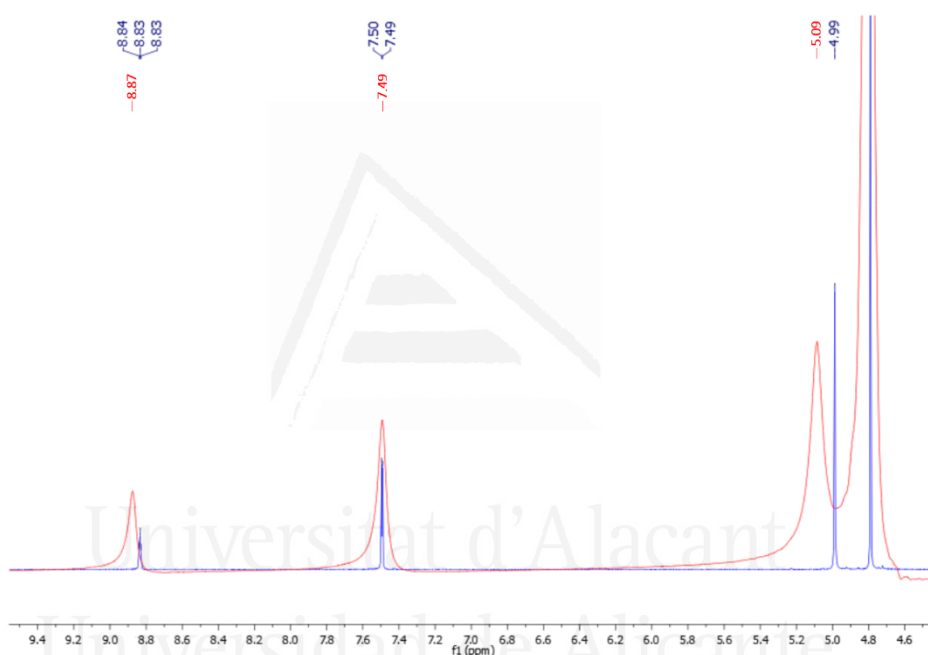


Figure 44.  $^1\text{H}$  NMR spectra of **bcimZr** (red) and **bcim** (blue) in  $\text{D}_2\text{O}$ .

Compared to the solution-state NMR spectrum of **bcim**, the most immediate difference is the shift downfield of the signal corresponding to the methylene units of the IOS (rightmost signal), consistent with the formation of the zirconium-carboxylate complex. A small deviation in chemical shift can also be observed for the proton at the C-2 position of the imidazole ring (leftmost signal), which may be attributed to weak hydrogen-bonding interactions with the chloride ions present in the hydrogel matrix. From the results obtained, it is apparent that the formation of the gel does not involve cross-linking hydrogen-bonding networks with the linker, but rather the aforementioned colloidal interactions between nanoparticles.

In lieu of time constraints for the elaboration of this manuscript, no further experiments were included in this chapter. The characterization of **bcmimZr** MOFs and MOGs by dynamic shear oscillation (DSO), cyclic voltammetry, electron microscopy (TEM and SEM), X-ray photoelectronic spectroscopy (XPS) and small-angle X-ray scattering (SAXS) is currently in progress, and future collaboration with other research groups is planned for advanced characterization techniques, namely electron crystallography (EC) and solid-state NMR (SSNMR).

In addition, a long-chain analogue of **bcmim**, 1,3-bis(carboxypropyl)imidazole (**bcpim**) has been prepared using a similar synthetic protocol (with  $\gamma$ -aminobutyric acid as precursor) and will be combined with zirconium salts to prepare elongated MOFs and MOGs derived from the **bcmimZr** structure, following the isorectularity principle.

From an environmental standpoint, comparing metal-organic materials using sustainability metrics is difficult. The synthesis of **bcmimZr** MOGs —and any other MOG for that matter— is extremely material-efficient, as every last component added to the reaction mixture ends up in the hydrogel, resulting on an E-factor of 0 and a VMR of 1, thus being a theoretically perfect process. The preparation of MOFs, on the other hand, is very inefficient, as large volumes of solvent (usually in the range of 250-350 grams per gram of precursor) and modulators (5 to 30 equivalents) are required to prepare a relatively small batch of product. Thus, in both cases, comparison between protocols by material efficiency metrics is pointless, with impact metrics painting a better picture, although they are only relevant in the case of MOFs —as gels with different solvents are not equivalent materials—. With this in mind, the EcoScale score for the synthesis of **bcmimZr** MOF was calculated and compared with the preparation of UiO-66 MOF by solvothermal synthesis in DMF (**Table 21**).

**Table 21.** EcoScale scores for the synthesis of **bcmimZr** and UiO-66 MOFs.

| Entry <sup>Ref.</sup> | MOF            | EcoScale        |
|-----------------------|----------------|-----------------|
| 1                     | <b>bcmimZr</b> | 62              |
| 2 <sup>324</sup>      | UiO-66         | 55 <sup>†</sup> |

<sup>†</sup>As yields are often not reported, the value was set as the same of entry 1 for a fair comparison.

The EcoScale score for the synthesis of **bcmimZr** is at the middle point of the “acceptable” range (50 to 75), due to its operational simplicity and the use of room-temperature water as reaction medium, although it gets heavily penalized due to the intensive use of materials (**Table 21**, entry 1). On the other hand, the solvothermal protocol is at the lower range of the “acceptable” scores, as it is even more resource-intensive —higher volumes of solvent due to lower overall solubility— and uses toxic DMF as reaction medium, with the associated safety penalty (**Table 21**, entry 2).

## C4.4. Conclusions

The following conclusions can be drawn from the studies described herein:

- ❖ A synthesis of zirconium-based MOFs with **bcmim** linkers has been developed, based on an environmentally friendly water-based methodology.
- ❖ A series of metal-organic hydrogels derived from **bcmim** and zirconium salts have been serendipitously obtained, and preliminary studies about their composition, structure and properties have been carried out. Although not reported in this manuscript due to time constraints, the complete characterization of the materials obtained is ongoing.
- ❖ The EcoScale score for the preparation of the **bcmimZr** MOF has been calculated and compared to a representative modulated solvothermal synthesis of the well-known zirconium MOF UiO-66 in DMF. The results obtained (62 against 55, respectively) highlight the decrease in environmental impact of the water-based protocol.







---

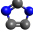
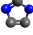

## **General conclusions**

---

Universitat d'Alacant  
Universidad de Alicante



The following conclusions are drawn from the work reported in this manuscript:

-  A series of very diverse heterogeneous catalytic systems and materials based on imidazole derivatives have been developed, emphasizing the versatility of the imidazolium scaffold.
-  These materials have been applied to a variety of organic transformations, designing protocols around the unique physical-chemical properties of each catalyst for maximum effectiveness and minimum environmental impact, with a heavy emphasis on solvent- and purification-free processes.
-  All protocols have been unbiasedly assessed in terms of sustainability using material efficiency and impact metrics and compared with representative methodologies. In all cases, the protocols designed for the imidazole-based catalysts reported herein have demonstrated comparable results with those reported in literature while having much lower environmental impact.



Universitat d'Alacant  
Universidad de Alicante





---

## **Experimental section**

---

Universitat d'Alacant  
Universidad de Alicante



## E.1. General remarks

### E.1.1. Materials and methods

All reagents and solvents are commercially available (Alfa Aesar, Apollo Scientific, Honeywell-Fluka, Fluorochem, Sigma-Aldrich (Merck), TCI) and were used without further purification. Flash silica for column chromatography was purchased from Silicycle (P60 230-400 mesh). P/UV254 silica gel with calcium sulfate supported on 20x20 cm glass plates was used for preparative thin layer chromatography.

Melting points were obtained using a Reichert ThermoVar heating-plate microscope (also used for optical microscopy with an S PI 10/0.25 160 mm objective and a K10x eyepiece, for a total 100x magnification) or a Gallenkamp MPD 350 BM 2.5 melting point apparatus and are expressed as uncorrected values.

NMR spectra were recorded at the Nuclear Magnetic Resonance Unit from the Research Technical Services of the University of Alicante (SSTTI-UA). <sup>1</sup>H NMR spectra were acquired at 300, 400 or 500 MHz, whereas proton-decoupled <sup>13</sup>C NMR experiments were obtained at 75, 100 or 125 MHz using Bruker AV300 Oxford, AV400 and Avance III HD NMR spectrometers. The solvents used were deuterated chloroform (CDCl<sub>3</sub>), with tetramethylsilane (TMS) as internal standard, deuterium oxide (D<sub>2</sub>O), deuterated acetone (COCD<sub>3</sub>) and deuterated methanol (CD<sub>3</sub>OD). Chemical shifts ( $\delta$ ) are provided in ppm and coupling constants ( $J$ ) are reported in hertz (Hz).

Low-resolution mass spectra of compounds were recorded on an Agilent 5973 Network mass spectrometer equipped with a 70 eV electronic impact (EI) ionization source and a quadrupolar mass detector operating in single ion monitoring (SIM) mode. Samples were introduced through an Agilent 6890N gas chromatography instrument equipped with a Technokroma TRB-5MS column (30 m x 0.25 mm x 0.25  $\mu$ m), using helium as mobile phase. For non-volatile samples, a SIS 73DIP-1 direct insertion probe (DIP) was used instead. Fragmentations are reported according to their mass to charge ratio ( $m/z$ ), along with their relative intensity in parenthesis.

Tandem mass spectra were recorded at the Mass Spectrometry Unit of the SSTTI-UA using an Agilent 1100 Series LC/MSD Trap SL apparatus equipped with an electrospray ionization source (ESI) operating in positive mode and an ion-trap mass analyzer. Samples were introduced through an Agilent 1100 Series HPLC instrument.

High-resolution mass spectra were recorded at the Mass Spectrometry Unit of the SSTTI-UA using an Agilent 7200 quadrupole-time of flight (QTOF) mass spectrometer equipped with an EI ionization source, with sample introduction *via* DIP or through an Agilent 7890B gas chromatography apparatus.



Differential Scanning Calorimetry experiments were performed at the Porous Solids and Thermal Analysis Unit from the SSTTI-UA with TA Instruments Q100 or Q250 differential scanning calorimeters using hermetically sealed aluminum crucibles under nitrogen atmosphere.

Powder X-ray diffractograms were recorded at the X-Ray Unit of the SSTTI-UA, using a Bruker D8-Avance instrument equipped with a Göebel mirror and a Kristalloflex K760-80F 3-kilowatt copper-anode (Cu K- $\alpha$  radiation,  $\lambda = 1.5406 \text{ \AA}$ ) X-ray source.

Conductivity measurements were recorded with a Mastech M92A digital multimeter using a two-probe setup with round copper electrodes held in position at exactly 1 cm from each other. Standard solutions of potassium chloride were used to calibrate the instrument.

### E.1.2. Sustainability metrics

Sustainability metrics (E-factor, AE, SF, MRP,  $RME_{\text{Andraos}}$  and the associated VMR) were calculated using the equations described in section **GI.3.2.** of this manuscript (**Equations 1 to 8**). The EcoScale scores were obtained using the online tool developed by the authors of the original manuscript, available at [ecoscale.cheminfo.org/calculator](https://ecoscale.cheminfo.org/calculator).<sup>†</sup>

For protocols reported in literature, calculations were performed considering the exact methods and quantities reported by the authors in their original work. For missing data regarding the use and recovery of materials, a series of standard values described in **Table E1** were applied.

**Table E1.** Standard values for the calculation of sustainability metrics on protocols with missing data.

| Parameter                                       | Value  |
|---|--|
| Solvent recovery (reaction, work-up)            | 80% of the initial mass if not requiring fractional distillation           |
| Water and saturated sodium chloride for work-up | Equal volume to the first fraction of organic solvent used                 |
| Work-up reported but not specified              | 3x10 mL/mmol of ethyl acetate and 10 mL/mmol of saturated sodium chloride. |
| Drying agents                                   | 1/5 <sup>th</sup> of the total mass of organic solvent                     |

---

<sup>†</sup> Webpage active as of February 13<sup>th</sup> 2023.

## E.2. Detailed experimental protocols

### E.2.1. Chapter 1

#### Synthesis of 1,3-bis(carboxymethyl)imidazole (bcmim)

Glyoxal (40% aq., 50 mmol, 5.7 mL), formaldehyde (37% aq., 50 mmol, 3.7 mL) and glycine (100 mmol, 7.5 g) were added to a round bottom flask and stirred at 95 °C for 2 h. After cooling the vessel to room temperature, a crystalline precipitate appeared, which was then vacuum filtered and washed with cold water (10 mL) and methanol (10 mL), then vacuum dried, affording 3.9 g of pure **bcmim** (87% yield) as a light brown solid.

#### Synthesis of 1,3-bis(carboxymethyl)imidazolium chloride (bcmimCl)

**Bcmim** (21 mmol, 3.9 g), hydrochloric acid (37% aq., 46 mmol, 4 mL) and water (4 mL) were added to a round bottom flask and refluxed for 30 minutes. After this time had elapsed, cooling the reaction down to room temperature caused the precipitation of a crystalline white solid, which was then filtered and washed with water (10 mL) and methanol (10 mL) and vacuum dried. 3.7 g of pure **bcmimCl** were obtained (81% yield).

#### Synthesis of 1-(methoxycarbonylmethyl)-3-methylimidazolium chloride (mcmimCl)

1-Methylimidazole (40 mmol, 3.2 mL) and methyl chloroacetate (40 mmol, 3.5 mL) were added to a reaction tube and sonicated for 1 hour, causing the precipitation of a dense white solid. The product was taken out onto a Petri dish and washed with a portion of diethyl ether (10 mL). After vacuum drying, 6.6 g of pure **mcmimCl** were obtained (87% yield).

#### Synthesis of 1-(carboxymethyl)-3-methylimidazolium chloride (cmimCl)

**McmimCl** (10 mmol, 1.9 g) was dissolved in hydrochloric acid (37% aq., 10 mmol, 0.8 mL) and refluxed for 1 hour. After cooling down the reaction, the resulting precipitate was vacuum filtered and washed with acetone (5 mL) and diethyl ether (5 mL). After drying under vacuum, 1.5 g of pure **cmimCl** were obtained.

#### General procedure for the oxidation of boron reagents with the mcmimCl:UHP LTTM

**McmimCl** (0.5 mmol, 95 mg) and UHP (1 mmol, 94 mg) were added to a glass tube and stirred at room temperature for 5 minutes, after which a suspension of organoborane in ethyl acetate (0.5 mmol in 0.5 mL of solvent) was added to the tube. The mixture was then stirred for an adequate amount of time, after which the top organic phase was removed and the LTTM was washed with 0.4 mL of ethyl acetate. The combined organic phases were filtered through silica and magnesium sulfate and evaporated under vacuum to afford the pure product.

#### Procedure for the preparative scale synthesis of 4-phenylphenol (**13**)

**McmimCl** (5 mmol, 950 mg) and UHP (10 mmol, 940 mg) were added to a glass round-bottom flask and stirred at room temperature for 5 minutes, after which a suspension of 4-phenylbenzeneboronic acid in ethyl acetate (5 mmol in 5 mL of solvent) was added. The mixture was then stirred for 30 minutes, after which the top organic phase was removed, and the LTTM was extracted with an additional 4 mL of solvent. The combined organic phases were filtered through silica and magnesium sulfate and evaporated under reduced pressure to afford 832 mg of pure **13** (99% yield).

#### Procedure for the cumulative synthesis of 4-phenylphenol (**13**)

**McmimCl** (0.5 mmol, 950 mg) and UHP (10 mmol, 940 mg) were added to a glass tube and stirred at room temperature for 5 minutes, after which a suspension of 4-phenylbenzeneboronic acid in ethyl acetate (0.5 mmol in 0.5 mL of solvent) was added. The mixture was then stirred for 30 minutes, after which the top organic phase was removed and fresh UHP (0.54 mmol, 50 mg) was added. After stirring for a minute to ensure full incorporation of the UHP into the LTTM, the cycle started over with the addition of more starting materials. Each iteration was treated as an individual reaction and subjected to the processing described in the general procedure.

### E.2.2. Chapter 2

#### Preparation of the IBIS

1-Butylimidazole (10 mmol, 1.3 mL) and methyl chloroacetate (10 mmol, 0.87 mL) were added to a round-bottom flask and stirred at 60°C for 48 hours. Then, iron(III) chloride (10 mmol, 1.62 g) was added to the mixture, which was then stirred at 50 °C for an additional 2 hours, affording 3.94 g of pure **IBIS** (99% yield).

#### General procedure for the synthesis of starting materials for products **27** and **28**

In a two-neck glass round-bottom flask, powdered magnesium (24 mmol, 683 mg) and iodine (catalytic, one crystal) were added. A capped reflux condenser was fitted to one of the necks of the vessel and the other was capped with a septum, after which the system was evacuated and filled with argon three times. Next, dry tetrahydrofuran (24 mL) and the corresponding brominated compound (24 mmol) were added through the septum and the mixture was sonicated for 15 minutes. The freshly formed Grignard reagent was then added dropwise to a dry tetrahydrofuran solution of anthranilonitrile (5 mmol, 590 mg in 10 ml of solvent) at 0 °C. After the addition was completed, the mixture was allowed to warm up to room temperature and stirred for 18 hours. Then, the reaction was quenched with 10 mL of ice-water and adjusted to pH 1 with 5 M hydrochloric acid, then stirred for an additional hour. Afterwards, the pH of the aqueous solution was readjusted to 8 using aqueous sodium bicarbonate

and it was extracted with ethyl acetate (3x15 mL). The combined organic phases were washed with brine (2x15 mL), dried over magnesium sulfate and evaporated under reduced pressure, affording the crude product, which was then purified by column chromatography using mixtures of hexane and ethyl acetate.

#### **General procedure for the synthesis of starting material for product 30**

4,5-Dimethoxy-2-nitrobenzaldehyde (1 mmol, 211 mg), ethanol (10 mL), iron powder (10 mmol, 560 mg), water (1 mL) and hydrochloric acid (37% aq., 50  $\mu$ L) were added to a round-bottom flask. The mixture was then refluxed for 90 minutes, after which the solvent was removed under vacuum and ethyl acetate (10 mL) was added. The organic phase was then washed with water (2x10 mL) and dried over magnesium sulfate and filtered through a column of silica. After removing the solvent, the purity of the crude product was determined by NMR and it was directly used for the preparation of **30**.

#### **General procedure for the synthesis of quinazolines**

A glass tube was charged with 2-aminocarbonyl compound (0.5 mmol), benzylamine (1.5 mmol) and **IBIS** (10 mol%, 20 mg). A 50 mL/min air flow was procured to the reaction by a glass nozzle connected to a peristaltic pump, and the mixture was stirred at 130 °C until completion (determined by GC-MS). Then, the crude products were purified by column chromatography using mixtures of hexane and ethyl acetate.

#### **Procedure for the gram scale synthesis of 2,4-diphenylquinazoline (22)**

In a round-bottom flask, 2-aminobenzophenone (5 mmol, 990 mg), benzylamine (15 mmol, 1.6 mL) and **IBIS** (10 mol%, 197 mg) were added. Using a glass nozzle, an air current at a flow rate of 50 mL/min was procured to the reaction, and the mixture was stirred at 130 °C for 24 hours. After completion, 971 mg of **22** were isolated by column chromatography (69% yield).

#### **General procedure for the synthesis of quinazolines from 2-nitrobenzaldehydes**

A glass tube was charged with 2-nitrobenzaldehyde (0.5 mmol), benzylamine (1.5 mmol) and **IBIS** (10 mol%, 20 mg). The tube was then capped and the mixture was stirred at 130 °C for 24 hours. The resulting crude products were purified by column chromatography using mixtures of hexane and ethyl acetate.

#### **Procedure for the preparation of imine 42**

In a glass tube, 2-nitrobenzaldehyde (2 mmol, 300 mg), benzylamine (2 mmol, 220  $\mu$ L), **bcmmCl** (10 mol%, 44 mg) and toluene (10 mL) were added. The mixture was stirred at room temperature for 24 hours. Then, it was filtered through celite and the solvent was removed under

vacuum, affording the crude product. After recrystallization from hot toluene, 380 mg of pure **42** were obtained as yellow crystals (72% yield).

### E.2.3. Chapter 3

#### Synthesis of 1,3-bis(carboxymethyl)imidazolium halides (**bcmimX**)

The general protocol for the preparation of **bcmimBr** is essentially equal to that of **bcmimCl**. Using hydrobromic acid, a 10 mmol scale reaction was performed, obtaining **bcmimBr** as light brown crystals (2.45 g, 92% yield). The synthesis of **bcmimI** also follows this protocol, although the product is washed with diethyl ether (2x10 mL) instead of water and methanol. This way, a 10 mmol scale reaction afforded **bcmimI** as deep purple crystals (2.46 g, 79% yield).

#### General procedure for the synthesis of starting materials for products 57 to 60

In a 50 mL round bottom flask, substituted chalcone (1 mmol) was dissolved in a tetrahydrofuran/methanol mixture (3 mL of each). Then, sodium borohydride (2 mmol, 76 mg) was added portionwise over 5 minutes, after which the reaction was stirred at room temperature for an additional 30 minutes. Then, the solvent was removed under reduced pressure and water (10 mL) was added. The aqueous suspension was extracted with ethyl acetate (3x10 mL), after which the combined organic phases were washed with water (10 mL) and brine (10 mL) and dried over magnesium sulfate. After removing the solvent under reduced pressure, the crude product was recrystallized in dichloromethane/hexane and directly used in the reaction.

#### General procedure for the allylation of heterocycles with IOS

In a glass tube, precisely weighed allyl alcohol (0.5 mmol), heterocycle (0.5 mmol) and **IOS** (10 mol%) were added. The mixture was then stirred at 80 °C until completion (monitored by GC-MS), after which the crude reaction mixture was diluted with ethyl acetate (1 mL) and filtered through a thin plug of silica to remove the catalyst. After evaporation of the solvent under reduced pressure, the corresponding allyl heterocycles were obtained, which were purified by column chromatography or preparative TLC when required.

#### Procedure for the gram scale synthesis of (*E*)-3-(1,3-diphenylallyl)-1*H*-indole (**46**)

(*E*)-1,3-Diphenyl-2-propen-1-ol (5 mmol, 1.05 g), indole (5 mmol, 590 mg) and **bcmimCl** (10 mol%, 110 mg) were added to a round bottom flask. The mixture was stirred at 80 °C for 2 hours, after which the reaction was diluted with 10 mL of ethyl acetate and filtered to remove the catalyst. Upon solvent removal under vacuum, 1.54 g of pure **46** were obtained (99% yield).

### Procedure for the recycling of **bcmimCl**

A glass tube was charged with (*E*)-1,3-diphenyl-2-propen-1-ol (0.25 mmol, 53 mg), indole (0.25 mmol, 29 mg) and **bcmimCl** (10 mol%, 5.5 mg), which were then stirred at 80°C for 2 hours. After completion, ethyl acetate was added (1 mL) and the organic phase was decanted off. After washing the catalyst with an additional portion of ethyl acetate (1 mL), fresh reagents were added and a new reaction cycle started. Five consecutive cycles were achieved without noticeable degradation of the catalyst.

### Procedure for the preparation of **bsmim**

Glyoxal (40% aq., 5 mmol, 0.57 mL), formaldehyde (37% aq., 5 mmol, 0.37 mL) and aminomethanesulfonic acid (10 mmol, 1.11 g) were added to a round-bottom flask along with water (2 mL) and sulfuric acid (catalytic, 100  $\mu$ L) and stirred at 95 °C for 20 minutes, after which it was quickly put in an ice-brine bath at -15 °C. Then, acetone (10 mL) was added and the mixture was vigorously stirred (1200 rpm), which caused the precipitation of a fluffy brown solid over the next 20 minutes. The solid was then filtered, affording 628 mg of pure **bsmim** (49% yield).

### General procedure for the Friedländer synthesis of quinolines promoted by **bsmim**

2-Aminobenzophenone (0.5 mmol, 99 mg), ketone (2.5 mmol) and **bsmim** (10 mol%, 13 mg) were added to a reaction tube. The reaction was then stirred at 80 °C for 16 hours, after which ethyl acetate was added (1 mL). After filtering the organic phase to remove the catalyst and removing the solvent under vacuum, the crude product was purified by column chromatography using mixtures of hexane and ethyl acetate.

## E.2.4. Chapter 4

### Modulated synthesis of the **bcmimZr** MOF

In a glass round-bottom flask, zirconium oxychloride octahydrate (5 mmol, 1.61 g) and acetic acid (110 mmol, 6.3 mL) were dissolved in 25 mL of water and heated to 60 °C under static conditions for 2 hours. Parallel to this, a solution of **bcmim** in water was prepared (5 mmol, 920 mg in 15 mL of water), to which sodium hydroxide (5 mmol, 0.20 g) were added, and the mixture was stirred at room temperature until clear. After cooling down the zirconium SBU solution, the **bcmimNa** solution was added on top, and the mixture was stirred at room temperature for 24 hours. As no precipitation took place during that time, methanol was slowly added to the solution until turbidity began to develop. The mixture was then stirred for an additional 24 hours, after which the MOF was isolated by centrifugation (8500 rpm) and then resuspended in 25 mL of water and stirred at room temperature for 2 hours, after which the solvent was once more decanted after centrifugation. The washing protocol was repeated twice with methanol (25 mL), and the so-obtained material was vacuum dried at room temperature for

24 hours, then in a conventional oven at 120 °C for an additional 24 hours. 1.1 g of a fine white powder were obtained (74% yield based on a  $C_{42}H_{46}N_{12}O_{32}Zr_6$  canonical structure).

**General protocol for the preparation of the bcmimZr MOGs**

In a round bottom flask, zirconium precursor (1 eq.) and **bcmimX** (1 eq.) were mixed with an adequate amount of water, then heated to the target temperature for 24 hours under static conditions.

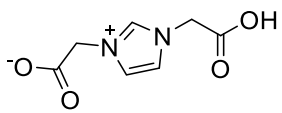
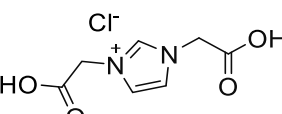
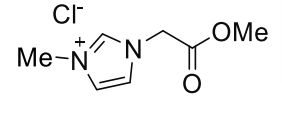
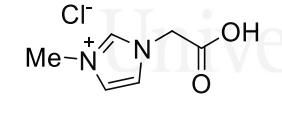
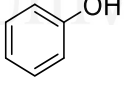
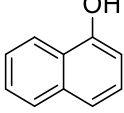
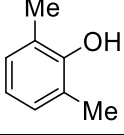


Universitat d'Alacant  
Universidad de Alicante

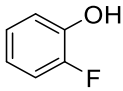
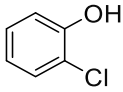
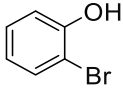
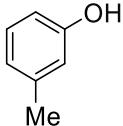
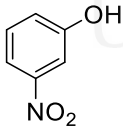
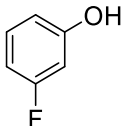
### E.3. Spectral data of all compounds

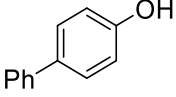
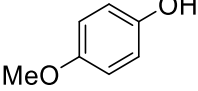
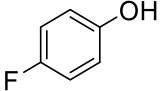
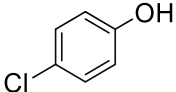
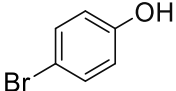
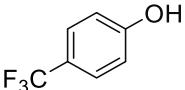
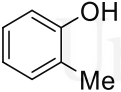
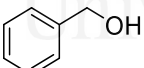
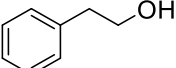
#### E.3.1. Chapter 1

All products described were obtained pure from the crude reaction mixture.

|   |   |
|---|---|
|    | <b>1,3-Bis(carboxymethyl)imidazole (bcmim):</b> Light brown solid, 87% yield; m.p. = 305 °C (decomp.) (lit. 290°C, decomp.) <sup>153</sup> ; <sup>1</sup> H NMR (300 MHz, D <sub>2</sub> O) $\delta_{\text{H}}$ = 8.83 (t, $J$ = 1.6 Hz, 1H, NCHN), 7.49 (d, $J$ = 1.6 Hz, 2H, NCHCHN), 4.99 (s, 4H, 2xCH <sub>2</sub> ); <sup>13</sup> C NMR (75 MHz, D <sub>2</sub> O) $\delta_{\text{C}}$ = 170.9, 137.7, 123.3, 50.9.   |
|    | <b>1,3-Bis(carboxymethyl)imidazolium chloride (bcmimCl):</b> White solid, 81% yield; m.p. = 223-226 °C (lit. 260 °C, decomp.) <sup>153</sup> ; <sup>1</sup> H NMR (300 MHz, D <sub>2</sub> O) $\delta_{\text{H}}$ = 8.92 (s, 1H, NCHN), 7.54 (d, $J$ = 1.6 Hz, 2H, NCHCHN), 5.13 (s, 4H, 2xCH <sub>2</sub> ); <sup>13</sup> C NMR (100 MHz, D <sub>2</sub> O) $\delta_{\text{C}}$ = 169.9, 138.2, 123.4, 50.1.  |
|  | <b>1-(Methoxycarbonylmethyl)-3-methylimidazolium chloride (mcmimCl):</b> White solid, 87% yield; m.p. = 201 °C (lit. 240 °C, decomp.) <sup>153</sup> ; <sup>1</sup> H NMR (300 MHz, CDCl <sub>3</sub> ) $\delta_{\text{H}}$ = 10.43 (s, 1H, NCHN), 7.72 (s, 1H, NCHCHN), 7.51 (s, 1H, NCHCHN), 5.60 (s, 2H, CH <sub>2</sub> ), 4.09 (s, 3H, NCH <sub>3</sub> ), 3.81 (s, 3H, OCH <sub>3</sub> ); <sup>13</sup> C NMR (100 MHz, CDCl <sub>3</sub> ) $\delta_{\text{C}}$ = 166.9, 138.8, 123.6, 53.4, 50.1, 36.8. |
|  | <b>1-(Carboxymethyl)-3-methylimidazolium chloride (cmimCl):</b> White solid, 85% yield; m.p. = 219-220 °C (lit. 204 °C) <sup>153</sup> ; <sup>1</sup> H NMR (300 MHz, D <sub>2</sub> O) $\delta_{\text{H}}$ = 8.75 (br s, 1H, NCHN), 7.44 (dd, $J$ = 3.6, 1.7 Hz, 2H, NCHCHN), 5.06 (s, 2H, CH <sub>2</sub> ), 3.88 (s, 3H, NCH <sub>3</sub> ); <sup>13</sup> C NMR (100 MHz, D <sub>2</sub> O) $\delta_{\text{C}}$ = 170.0, 137.2, 123.4, 49.9, 35.8.  |
|  | <b>Phenol (1):</b> Yellowish oil, 93% yield; <sup>1</sup> H NMR (400 MHz, CDCl <sub>3</sub> ) $\delta_{\text{H}}$ = 7.26-7.22 (m, 2H, CH <sub>Ar</sub> ), 6.95-6.90 (m, 1H, CH <sub>Ar</sub> ), 6.84-6.81 (m, 2H, CH <sub>Ar</sub> ); <sup>13</sup> C NMR (100 MHz, CDCl <sub>3</sub> ) $\delta_{\text{C}}$ = 155.6, 129.8, 120.9, 115.4.   |
|  | <b>1-Naphthol (2):</b> Colorless needles, 98% yield; <sup>1</sup> H NMR (400 MHz, CDCl <sub>3</sub> ) $\delta_{\text{H}}$ = 8.18-8.15 (m, 1H, CH <sub>Ar</sub> ), 7.81-7.77 (m, 1H, CH <sub>Ar</sub> ), 7.50-7.41 (m, 3H, CH <sub>Ar</sub> ), 7.34-7.21 (m, 1H, CH <sub>Ar</sub> ), 6.77 (dd, $J$ = 7.4, 0.9 Hz, 1H, CH <sub>Ar</sub> ); <sup>13</sup> C NMR (100 MHz, CDCl <sub>3</sub> ) $\delta_{\text{C}}$ = 151.5, 134.9, 127.8, 126.6, 125.9, 125.4, 124.5, 121.7, 120.8, 108.8.                          |
|  | <b>2,6-Dimethylphenol (3):</b> Yellow solid, 72% yield; <sup>1</sup> H NMR (400 MHz, CDCl <sub>3</sub> ) $\delta_{\text{H}}$ = 6.96-6.94 (m, 2H, CH <sub>Ar</sub> ), 6.77-6.73 (m, 1H, CH <sub>Ar</sub> ), 4.25 (br s, 1H, OH), 2.24 (s, 6H, 2xCH <sub>3</sub> ); <sup>13</sup> C NMR (100 MHz, MeOD-d <sub>4</sub> ) $\delta_{\text{C}}$ = 152.3, 128.7, 123.1, 120.3, 15.9.   |

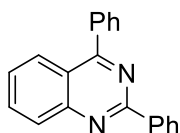


|   |   |
|---|---|
|    | <b>2-Methoxyphenol (4):</b> Yellow oil, 93% yield; $^1\text{H NMR}$ (400 MHz, $\text{CDCl}_3$ ) $\delta_{\text{H}}$ = 6.97-6.94 (m, 1H, $\text{CH}_{\text{Ar}}$ ), 6.91-6.86 (m, 3H, $\text{CH}_{\text{Ar}}$ ), 5.71 (br s, 1H, OH), 3.89 (s, 3H, $\text{CH}_3$ ); $^{13}\text{C NMR}$ (100 MHz, $\text{CDCl}_3$ ) $\delta_{\text{C}}$ = 146.7, 145.8, 121.6, 120.3, 114.7, 110.9, 55.9.  |
|    | <b>2-Hydroxyphenol (5):</b> Grey needles, 99% yield; $^1\text{H NMR}$ (400 MHz, $\text{MeOD-d}_4$ ) $\delta_{\text{H}}$ = 6.79-6.75 (m, 2H, $\text{CH}_{\text{Ar}}$ ), 6.68-6.64 (m, 2H, $\text{CH}_{\text{Ar}}$ ), 5.00 (br s, 2H, 2xOH); $^{13}\text{C NMR}$ (100 MHz, $\text{MeOD-d}_4$ ) $\delta_{\text{C}}$ = 146.12, 120.9, 116.4.  |
|    | <b>2-Fluorophenol (6):</b> Faint yellow oil, 93% yield; $^1\text{H NMR}$ (400 MHz, $\text{CDCl}_3$ ) $\delta_{\text{H}}$ = 7.09-7.04 (m, 1H, $\text{CH}_{\text{Ar}}$ ), 7.03-6.97 (m, 2H, $\text{CH}_{\text{Ar}}$ ), 6.87-6.82 (m, 1H, $\text{CH}_{\text{Ar}}$ ); $^{13}\text{C NMR}$ (100 MHz, $\text{CDCl}_3$ ) $\delta_{\text{C}}$ = 151.3 (d, $J$ = 237.0 Hz), 143.7 (d, $J$ = 14.1 Hz), 125.0 (d, $J$ = 3.7 Hz), 120.9 (d, $J$ = 6.5 Hz), 117.4 (d, $J$ = 1.4 Hz), 115.6 (d, $J$ = 18.0 Hz).                         |
|    | <b>2-Chlorophenol (7):</b> Faint yellow oil, 89% yield; $^1\text{H NMR}$ (400 MHz, $\text{CDCl}_3$ ) $\delta_{\text{H}}$ = 7.30 (dd, $J$ = 8.0, 1.5 Hz, 1H, $\text{CH}_{\text{Ar}}$ ), 7.17 (ddd, $J$ = 8.2, 7.4, 1.6 Hz, 1H, $\text{CH}_{\text{Ar}}$ ), 7.01 (dd, $J$ = 8.2, 1.5 Hz, 1H, $\text{CH}_{\text{Ar}}$ ), 6.86 (ddd, $J$ = 8.0, 7.4, 1.5 Hz, 1H, $\text{CH}_{\text{Ar}}$ ), 5.57 (br s, 1H, OH); $^{13}\text{C NMR}$ (100 MHz, $\text{CDCl}_3$ ) $\delta_{\text{C}}$ = 151.5, 129.1, 121.5, 116.4.             |
|  | <b>2-Bromophenol (8):</b> Faint yellow oil, 90% yield; $^1\text{H NMR}$ (300 MHz, $\text{CDCl}_3$ ) $\delta_{\text{H}}$ = 7.46 (dd, $J$ = 8.0, 1.5 Hz, 1H, $\text{CH}_{\text{Ar}}$ ), 7.22 (ddd, $J$ = 8.2, 7.3, 1.5 Hz, 1H, $\text{CH}_{\text{Ar}}$ ), 7.02 (dd, $J$ = 8.2, 1.5 Hz, 1H, $\text{CH}_{\text{Ar}}$ ), 6.80 (ddd, $J$ = 8.0, 7.4, 1.6 Hz, 1H, $\text{CH}_{\text{Ar}}$ ), 5.53 (br s, 1H, OH); $^{13}\text{C NMR}$ (75 MHz, $\text{CDCl}_3$ ) $\delta_{\text{C}}$ = 152.4, 132.2, 129.3, 121.9, 116.3, 110.4. |
|  | <b>3-Methylphenol (9):</b> Faint yellow oil, 94% yield; $^1\text{H NMR}$ (300 MHz, $\text{CDCl}_3$ ) $\delta_{\text{H}}$ = 7.12 (t, $J$ = 7.9 Hz, 1H, $\text{CH}_{\text{Ar}}$ ), 6.75 (br d, $J$ = 7.5 Hz, 1H, $\text{CH}_{\text{Ar}}$ ), 6.65-6.62 (m, 2H, $\text{CH}_{\text{Ar}}$ ), 4.41 (br s, 1H, OH), 2.30 (s, 3H, $\text{CH}_3$ ); $^{13}\text{C NMR}$ (75 MHz, $\text{CDCl}_3$ ) $\delta_{\text{C}}$ = 155.6, 139.9, 129.6, 121.7, 116.2, 112.4, 21.5.  |
|  | <b>3-Nitrophenol (10):</b> Yellow crystals, 99% yield; $^1\text{H NMR}$ (300 MHz, $\text{CDCl}_3$ ) $\delta_{\text{H}}$ = 7.81 (ddd, $J$ = 8.2, 2.1, 0.8 Hz, 1H, $\text{CH}_{\text{Ar}}$ ), 7.71 (t, $J$ = 2.3 Hz, 1H, $\text{CH}_{\text{Ar}}$ ), 7.41 (t, $J$ = 8.2 Hz, 1H, $\text{CH}_{\text{Ar}}$ ), 7.20 (ddd, $J$ = 8.2, 2.5, 0.9 Hz, 1H, $\text{CH}_{\text{Ar}}$ ); $^{13}\text{C NMR}$ (75 MHz, $\text{CDCl}_3$ ) $\delta_{\text{C}}$ = 156.5, 149.2, 130.4, 122.2, 115.9, 110.7.                                  |
|  | <b>3-Fluorophenol (11):</b> Faint yellow oil, 90% yield; $^1\text{H NMR}$ (300 MHz, $\text{CDCl}_3$ ) $\delta_{\text{H}}$ = 7.20-7.14 (m, 1H, $\text{CH}_{\text{Ar}}$ ), 6.68-6.55 (m, 3H, $\text{CH}_{\text{Ar}}$ ), 4.46 (br s, 1H, OH); $^{13}\text{C NMR}$ (75 MHz, $\text{CDCl}_3$ ) $\delta_{\text{C}}$ = 163.6 (d, $J$ = 245.4 Hz), 156.8 (d, $J$ = 11.3 Hz), 130.5 (d, $J$ = 10.0 Hz), 111.2 (d, $J$ = 2.8 Hz), 107.7 (d, $J$ = 21.3 Hz), 103.2 (d, $J$ = 24.6 Hz).   |
|  | <b>3-Methoxyphenol (12):</b> Orange oil, 87% yield; $^1\text{H NMR}$ (300 MHz, $\text{CDCl}_3$ ) $\delta_{\text{H}}$ = 7.11 (t, $J$ = 8.1 Hz, 1H, $\text{CH}_{\text{Ar}}$ ), 6.49-6.42 (m, 3H, $\text{CH}_{\text{Ar}}$ ), 5.07 (br s, 1H, OH), 3.75 (s, 3H, $\text{CH}_3$ ); $^{13}\text{C NMR}$ (75 MHz, $\text{CDCl}_3$ ) $\delta_{\text{C}}$ = 156.9, 130.3, 108.0, 106.6, 101.7, 55.4.  |

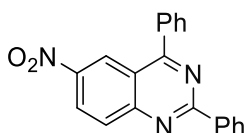
|   |  |
|---|--|
|    | <b>4-Phenylphenol (13):</b> Colorless needles, 99% yield; $^1\text{H NMR}$ (300 MHz, $\text{CDCl}_3$ ) $\delta_{\text{H}} = 7.54$ (br d, $J = 7.4$ Hz, 2H, $\text{CH}_{\text{Ar}}$ ), $7.48$ (br d, $J = 8.5$ Hz, 2H, $\text{CH}_{\text{Ar}}$ ), $7.41$ (br t, $J = 7.5$ Hz, 1H, $\text{CH}_{\text{Ar}}$ ), $6.90$ (br d, $J = 8.5$ Hz, 2H, $\text{CH}_{\text{Ar}}$ ); $^{13}\text{C NMR}$ (75 MHz, $\text{CDCl}_3$ ) $\delta_{\text{C}} = 155.2, 140.9, 134.2, 128.9, 128.5, 126.9, 115.8$ .                                |
|    | <b>4-Methoxyphenol (14):</b> Yellowish crystals, 88% yield; $^1\text{H NMR}$ (300 MHz, $\text{CDCl}_3$ ) $\delta_{\text{H}} = 6.80\text{--}6.75$ (m, 4H, $\text{CH}_{\text{Ar}}$ ), $4.85$ , (br s, 1H, OH), $3.76$ (s, 3H, $\text{CH}_3$ ); $^{13}\text{C NMR}$ (75 MHz, $\text{CDCl}_3$ ) $\delta_{\text{C}} = 153.7, 149.6, 116.2, 115.0, 55.9$ .   |
|    | <b>4-Fluorophenol (15):</b> Faint yellow oil, 99% yield; $^1\text{H NMR}$ (400 MHz, $\text{CDCl}_3$ ) $\delta_{\text{H}} = 6.94\text{--}6.90$ (m, 2H, $\text{CH}_{\text{Ar}}$ ), $6.78\text{--}6.75$ (m, 2H, $\text{CH}_{\text{Ar}}$ ); $^{13}\text{C NMR}$ (100 MHz, $\text{CDCl}_3$ ) $\delta_{\text{C}} = 157.4$ (d, $J = 237.9$ Hz), $151.2$ (d, $J = 1.8$ Hz), $116.4$ (d, $J = 8.0$ Hz), $116.1$ (d, $J = 23.3$ Hz).   |
|    | <b>4-Chlorophenol (16):</b> Yellow oil, 96% yield; $^1\text{H NMR}$ (400 MHz, $\text{CDCl}_3$ ) $\delta_{\text{H}} = 7.22\text{--}7.17$ (m, 2H, $\text{CH}_{\text{Ar}}$ ), $6.80\text{--}6.74$ (m, 2H, $\text{CH}_{\text{Ar}}$ ), $3.37$ (br s, 1H, OH); $^{13}\text{C NMR}$ (100 MHz, $\text{CDCl}_3$ ) $\delta_{\text{C}} = 154.3, 129.7, 125.8, 116.8$ .  |
|   | <b>4-Bromophenol (17):</b> Yellow oil, 94% yield; $^1\text{H NMR}$ (400 MHz, $\text{CDCl}_3$ ) $\delta_{\text{H}} = 7.35\text{--}7.30$ (m, 2H, $\text{CH}_{\text{Ar}}$ ), $6.75\text{--}6.70$ (m, 2H, $\text{CH}_{\text{Ar}}$ ), $4.45$ (br s, 1H, OH); $^{13}\text{C NMR}$ (100 MHz, $\text{CDCl}_3$ ) $\delta_{\text{C}} = 154.6, 132.5, 117.2, 112.9$ .   |
|  | <b>4-(Trifluoromethyl)phenol (18):</b> Faint yellow oil, 99% yield; $^1\text{H NMR}$ (400 MHz, $\text{CDCl}_3$ ) $\delta_{\text{H}} = 7.50$ (d, $J = 8.4$ Hz, 2H, $\text{CH}_{\text{Ar}}$ ), $6.90$ (d, $J = 8.4$ Hz, 2H, $\text{CH}_{\text{Ar}}$ ); $^{13}\text{C NMR}$ (100 MHz, $\text{CDCl}_3$ ) $\delta_{\text{C}} = 158.3, 127.3$ (q, $J = 3.8$ Hz), $124.5$ (q, $J = 271.1$ Hz), $123.4$ (q, $J = 32.6$ Hz), $115.6$ .  |
|  | <b>2-Methylphenol (19):</b> Yellow oil, 80% yield; $^1\text{H NMR}$ (400 MHz, $\text{CDCl}_3$ ) $\delta_{\text{H}} = 7.12$ (d, $J = 7.4$ Hz, 1H, $\text{CH}_{\text{Ar}}$ ), $7.09$ (td, $J = 7.5, 1.1$ Hz, 1H, $\text{CH}_{\text{Ar}}$ ), $6.86$ (td, $J = 7.4, 1.0$ Hz, 1H, $\text{CH}_{\text{Ar}}$ ), $6.76$ (dd, $J = 8.0, 0.6$ Hz, 1H, $\text{CH}_{\text{Ar}}$ ), $2.24$ (s, 3H, $\text{CH}_3$ ). $^{13}\text{C NMR}$ (100 MHz, $\text{CDCl}_3$ ) $\delta_{\text{C}} = 153.9, 131.2, 127.2, 123.9, 120.8, 115.0, 15.8$ . |
|  | <b>Benzyl alcohol (20):</b> Colorless oil, 95% yield; $^1\text{H NMR}$ (400 MHz, $\text{CDCl}_3$ ) $\delta_{\text{H}} = 7.38\text{--}7.25$ (m, 5H, $\text{CH}_{\text{Ar}}$ ), $4.64$ (s, 2H, $\text{CH}_2$ ), $2.39$ (br s, 1H, OH); $^{13}\text{C NMR}$ (100 MHz, $\text{CDCl}_3$ ) $\delta_{\text{C}} = 140.9, 128.6, 127.7, 127.1, 65.3$ .  |
|  | <b>2-Phenylethanol (21):</b> Colorless oil, 99% yield; $^1\text{H NMR}$ (400 MHz, $\text{CDCl}_3$ ) $\delta_{\text{H}} = 7.32\text{--}7.28$ (m, 2H, $\text{CH}_{\text{Ar}}$ ), $7.23\text{--}7.20$ (m, 2H, $\text{CH}_{\text{Ar}}$ ), $3.82$ (t, $J = 6.6$ Hz, 2H, O- $\text{CH}_2$ ), $2.84$ (t, $J = 6.6$ Hz, 2H, Ar- $\text{CH}_2$ ), $1.92$ (br s, 1H, OH); $^{13}\text{C NMR}$ (100 MHz, $\text{CDCl}_3$ ) $\delta_{\text{C}} = 138.6, 129.1, 128.6, 126.5, 63.7, 39.2$ .   |

## E.3.2. Chapter 2

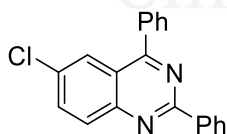
In lieu of the low yields obtained, products **41** to **45** were not characterized.



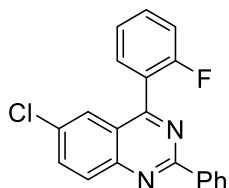
**2,4-Diphenylquinazoline (22):** Off-white solid; purification by column chromatography (hexane/ethyl acetate 9:1), 84% yield; m.p. 120-121 °C (lit. 117-119 °C)<sup>204</sup>; <sup>1</sup>H NMR (400 MHz, CDCl<sub>3</sub>): δ<sub>H</sub> = 8.71-8.68 (m, 2H, CH<sub>Ar</sub>), 8.17-8.09 (m, 2H, CH<sub>Ar</sub>), 7.89-7.83 (m, 3H, CH<sub>Ar</sub>), 7.60-7.48 (m, 7H, CH<sub>Ar</sub>); <sup>13</sup>C NMR (100 MHz, CDCl<sub>3</sub>): δ<sub>C</sub> = 168.5, 160.3, 152.0, 138.3, 137.8, 133.7, 130.7, 130.3, 130.1, 129.2, 128.8, 128.7, 127.1, 121.8; MS (EI, 70 eV) *m/z* (%): 283 (M+1, 13), 282 (M, 68), 281 (100), 205 (7), 178 (11), 151 (6), 77 (9).



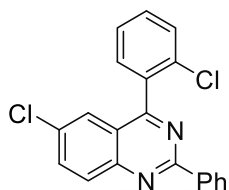
**6-Nitro-2,4-diphenylquinazoline (23):** Off white solid; purification by column chromatography (hexane/ethyl acetate 98:2 to 9:1), 61% yield; m.p. 214-216 °C (lit. 214-217 °C)<sup>212</sup>; <sup>1</sup>H NMR (400 MHz, CDCl<sub>3</sub>): δ<sub>H</sub> = 9.07 (d, *J* = 2.4 Hz, 1H, CH<sub>Ar</sub>), 8.76-8.73 (m, 2H, CH<sub>Ar</sub>), 8.65 (dd, *J* = 9.1, 2.1 Hz, 1H, CH<sub>Ar</sub>), 8.29 (d, *J* = 9.2 Hz, 1H, CH<sub>Ar</sub>), 7.93-7.91 (m, 2H, CH<sub>Ar</sub>), 7.69-7.67 (m, 3H, CH<sub>Ar</sub>), 7.58-7.56 (m, 3H, CH<sub>Ar</sub>); <sup>13</sup>C NMR (100 MHz, CDCl<sub>3</sub>): δ<sub>C</sub> = 170.7, 162.9, 154.5, 145.6, 137.1, 136.4, 131.9, 131.2, 131.1, 130.4, 129.4, 129.2, 128.9, 127.2, 124.4, 120.6; MS (EI, 70 eV): *m/z* (%): 328 (M+1, 11), 327 (M, 52), 326 (6), 311 (7), 310 (27), 297 (15), 296 (14), 282 (7), 281 (49), 280 (100), 279 (7), 207 (17), 204 (6), 203 (6), 178 (13), 177 (14), 151 (11), 150 (6), 140 (7), 77 (9) 75 (18).



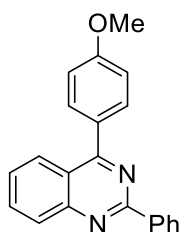
**6-Chloro-2,4-diphenylquinazoline (24):** Pure white solid; purification by column chromatography (hexane/ethyl acetate 99:1), 72% yield; m.p. 197-199 °C (lit. 193-195 °C)<sup>204</sup>; <sup>1</sup>H NMR (400 MHz, CDCl<sub>3</sub>): δ<sub>H</sub> = 8.69-8.66 (m, 2H, CH<sub>Ar</sub>), 8.13-8.11 (d, *J* = 9.0 Hz, 1H, CH<sub>Ar</sub>), 8.09-8.08 (d, *J* = 2.2 Hz, 1H, CH<sub>Ar</sub>), 7.87-7.85 (m, 2H, CH<sub>Ar</sub>), 7.82-7.79 (dd, *J* = 9.0, 2.2 Hz, 1H, CH<sub>Ar</sub>), 7.63-7.60 (m, 3H, CH<sub>Ar</sub>), 7.55-7.48 (m, 3H, CH<sub>Ar</sub>); <sup>13</sup>C NMR (100 MHz, CDCl<sub>3</sub>): δ<sub>C</sub> = 167.8, 160.5, 150.5, 137.8, 137.2, 134.7, 132.8, 130.9, 130.9, 130.4, 130.2, 128.8, 128.7, 125.9, 122.3; MS (EI, 70 eV) *m/z* (%): 319 (M+3, 6), 318 (M+2, 31), 317 (M+1, 50), 316 (M, 91), 315 (100), 282 (21), 281 (93), 239 (8), 203 (5), 178 (13), 177 (17), 158 (6), 151 (13), 140 (13), 110 (8), 77 (17), 75 (11), 51 (6).



**6-Chloro-4-(2-fluorophenyl)-2-phenylquinazoline (25):** Off white solid; purification by column chromatography (hexane/ethyl acetate 99:1), 65% yield; m.p. 185-186 °C (lit. 180-181 °C)<sup>213</sup>; <sup>1</sup>H NMR (300 MHz, CDCl<sub>3</sub>): δ<sub>H</sub> = 8.66-8.64 (m, 2H, CH<sub>Ar</sub>), 8.13 (d, *J* = 9.0 Hz, 1H, CH<sub>Ar</sub>), 7.82 (dd, *J* = 9.0, 2.3 Hz, 1H, CH<sub>Ar</sub>), 7.78-7.77 (m, 1H, CH<sub>Ar</sub>), 7.69 (td, *J* = 7.3, 1.8 Hz, 1H, CH<sub>Ar</sub>), 7.59 (dddd, *J* = 8.3, 7.2, 5.2, 1.8 Hz, 1H, CH<sub>Ar</sub>), 7.54-7.50 (m, 3H, CH<sub>Ar</sub>), 7.40 (td, *J* = 7.5, 1.1 Hz, 1H, CH<sub>Ar</sub>), 7.31 (ddd, *J* = 9.5, 8.4, 0.9 Hz, 1H, CH<sub>Ar</sub>); <sup>13</sup>C NMR (75 MHz, CDCl<sub>3</sub>): δ<sub>C</sub> = 164.2, 160.74, 160.0 (d, *J* = 250.4 Hz), 149.8, 137.5, 135.1, 133.1, 132.2 (d, *J* = 8.2 Hz), 131.9, 131.9, 131.1, 130.6, 128.9, 128.8, 125.8, 125.8, 125.1 (d, *J* = 21.4 Hz), 124.9 (d, *J* = 9.9 Hz), 123.1, 116.4 (d, *J* = 21.5 Hz); MS (EI, 70 eV) *m/z* (%): 337 (M+3, 7), 336 (M+2, 35), 335 (M+1, 49), 334 (M, 100), 333 (89), 300 (22), 299 (82), 281 (9), 239 (12), 213 (10), 208 (6), 207 (24), 195 (9), 178 (18), 177 (11), 151 (13), 149 (8), 139 (8), 110 (11), 77 (19), 76 (9), 75 (22).

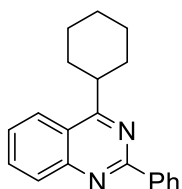


**6-Chloro-4-(2-chlorophenyl)-2-phenylquinazoline (26):** Yellowish solid; purification by column chromatography (hexane/ethyl acetate 98:2), 29% yield; m.p. 177-178 °C (lit. 172-173 °C)<sup>375</sup>; <sup>1</sup>H NMR (400 MHz, CDCl<sub>3</sub>): δ<sub>H</sub> = 8.65-8.63 (m, 2H, CH<sub>Ar</sub>), 8.12 (d, *J* = 9.0 Hz, 1H, CH<sub>Ar</sub>), 7.81 (dd, *J* = 8.9, 2.1 Hz, 1H, CH<sub>Ar</sub>), 7.61-7.60 (m, 2H, CH<sub>Ar</sub>), 7.54-7.48 (m, 6H, CH<sub>Ar</sub>); <sup>13</sup>C NMR (100 MHz, CDCl<sub>3</sub>): δ<sub>C</sub> = 166.6, 160.8, 149.9, 137.7, 136.0, 135.1, 133.0, 132.9, 131.2, 131.0, 131.0, 130.8, 130.3, 128.9, 128.8, 127.2, 125.7, 122.9; MS (EI, 70 eV) *m/z* (%): 354 (M+3, 11), 353 (M+2, 19), 352 (M+1, 64), 351 (M, 57), 350 (100), 349 (51), 317 (33), 316 (22), 315 (89), 239 (16), 213 (15), 178 (22), 177 (24), 176 (10), 175 (9), 151 (12), 110 (13), 77 (20), 75 (21).

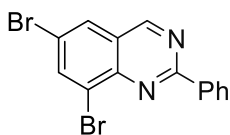


**4-(4-Methoxyphenyl)-2-phenylquinazoline (27):** Off white solid; purification by column chromatography (hexane/ethyl acetate 9:1), 73% yield; m.p. 127-129 °C (lit. 131-133 °C)<sup>221</sup>; <sup>1</sup>H NMR (400 MHz, CDCl<sub>3</sub>): δ<sub>H</sub> = 8.72-8.69 (m, 2H, CH<sub>Ar</sub>), 8.20-8.14 (m, 2H, CH<sub>Ar</sub>), 7.91-7.86 (m, 3H, CH<sub>Ar</sub>), 7.56-7.49 (m, 4H, CH<sub>Ar</sub>), 7.13-7.08 (m, 2H, CH<sub>Ar</sub>), 3.91 (s, 3H, OCH<sub>3</sub>); <sup>13</sup>C NMR (100 MHz, CDCl<sub>3</sub>): δ<sub>C</sub> = 168.0, 161.5, 160.1, 151.8, 138.1, 133.6, 132.0, 130.7, 130.2, 128.9, 128.9, 128.6, 127.2, 127.1, 121.7, 114.2, 55.6; MS (EI, 70 eV): *m/z* (%): 313 (M+1, 19), 312 (M, 88), 311 (100), 297 (8), 282 (11), 281 (51), 268 (18), 207 (14), 205 (14), 178 (14), 166 (5), 156 (7), 140, 103, 102 (8), 77 (17), 76 (16).

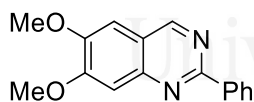
<sup>375</sup>Sarma, R.; Prajapati, D. *Green Chem.* **2011**, *13*, 718–722.



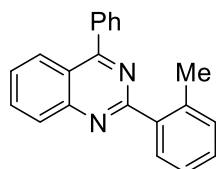
**4-Cyclohexyl-2-phenylquinazoline (28):** Yellow solid; purification by column chromatography (hexane/ethyl acetate 98:2), 60% yield; m.p: 98-99 °C (lit. 105-107 °C)<sup>215</sup>; <sup>1</sup>H NMR (400 MHz, CDCl<sub>3</sub>): δ<sub>H</sub> = 8.70-8.68 (m, 2H, CH<sub>Ar</sub>), 8.16-8.14 (m, 2H, CH<sub>Ar</sub>), 7.84 (ddd, *J* = 8.4, 6.9, 1.3 Hz, 1H, CH<sub>Ar</sub>), 7.58-7.49 (m, 4H, CH<sub>Ar</sub>), 3.58 (tt, *J* = 10.9, 3.5 Hz, 1 H, CH), 2.04-1.83 (m, 7H, CH<sub>2</sub>), 1.60-1.36 (m, 3H, CH<sub>2</sub>); <sup>13</sup>C NMR (100 MHz, CDCl<sub>3</sub>): δ<sub>C</sub> = 175.3, 160.0, 150.6, 138.4, 133.4, 130.6, 129.4, 128.9, 128.6, 126.8, 124.3, 121.8, 41.7, 32.2, 26.7, 26.3; MS (EI, 70 eV): *m/z* (%): 289 (M+1, 9), 288 (M, 42), 287 (51), 259 (15), 247 (9), 245 (14), 244 (6), 234 (21), 233 (100), 221 (6), 220 (36), 205 (7), 129 (7), 104 (5), 103 (8), 102 (5), 77 (8), 76 (5).



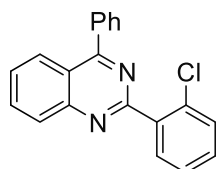
**6,8-Dibromo-2-phenylquinazoline (29):** Yellow solid; purification by column chromatography (hexane/ethyl acetate 9:1), 50% yield; m.p: 150-152 °C (lit. 151-153 °C)<sup>221</sup>; <sup>1</sup>H NMR (300 MHz, CDCl<sub>3</sub>): 9.34 (s, 1H, CH<sub>Ar</sub>), 8.70-8.67 (m, 2H, CH<sub>Ar</sub>), 8.29-8.28 (d, *J* = 2.0 Hz, 1H, CH<sub>Ar</sub>), 8.04-8.03 (d, *J* = 2.0 Hz, 1H, CH<sub>Ar</sub>), 7.55-7.52 (m, 3H, CH<sub>Ar</sub>); δ<sub>H</sub> = <sup>13</sup>C NMR (100 MHz, CDCl<sub>3</sub>): δ<sub>C</sub> = 161.9, 159.9, 147.2, 140.2, 137.2, 131.5, 129.0, 128.9, 128.9, 125.6, 125.2, 120.3; MS (EI, 70 eV): *m/z* (%): 367 (M+3, 7), 366 (M+2, 51), 365 (M+1, 19), 364 (M, 100), 363 (17), 362 (54), 339 (10), 337 (23), 335 (12), 258 (8), 256 (7), 207 (7), 182 (8), 177 (30), 155 (14), 153 (14), 142 (5), 141 (5), 104 (6), 103 (9), 102 (9), 101 (7), 100 (14), 77 (12), 76 (10), 75 (11), 74 (19).



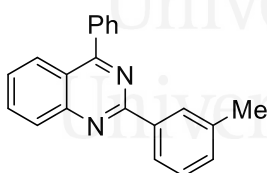
**6,7-Dimethoxy-2-phenylquinazoline (30):** White solid; purification by column chromatography, 85% yield; m.p. 174-176 °C (lit. 174-176 °C)<sup>209</sup>; <sup>1</sup>H NMR (400 MHz, CDCl<sub>3</sub>): δ<sub>H</sub> = 9.23 (d, *J* = 0.5 Hz, 1H, CH<sub>Ar</sub>), 8.55-8.52 (m, 2H, CH<sub>Ar</sub>), 7.54-7.47 (m, 3H, CH<sub>Ar</sub>), 7.38 (s, 1H, CH<sub>Ar</sub>), 7.11 (s, 1H, CH<sub>Ar</sub>), 4.08 (s, 3H, CH<sub>3</sub>), 4.04 (s, 3H, CH<sub>3</sub>); <sup>13</sup>C NMR (100 MHz, CDCl<sub>3</sub>): δ<sub>C</sub> = 160.1, 157.2, 156.4, 150.5, 148.8, 138.5, 130.3, 128.7, 128.3, 119.6, 107.0, 104.1, 56.6, 56.4.; MS (EI, 70 eV) *m/z* (%): 267 (M+1, 19), 266 (M, 100), 251 (16), 224 (5), 223 (12), 221 (7), 207 (8), 196 (9), 136 (6), 133 (10), 120 (14), 104 (8), 103 (6), 93 (6), 77 (6), 76 (5).



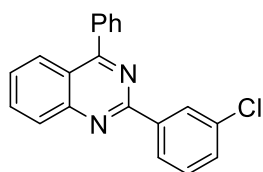
**2-(2-Methylphenyl)-4-phenylquinazoline (31):** Yellow solid; purification by column chromatography (hexane/ethyl acetate 95:5), 87% yield; m.p: 73-75 °C (lit. 74-75 °C)<sup>221</sup>; <sup>1</sup>H NMR (400 MHz, CDCl<sub>3</sub>):  $\delta_{\text{H}}$  = 8.18-8.15 (m, 2H, CH<sub>Ar</sub>), 7.99-7.97 (m, 1H, CH<sub>Ar</sub>), 7.93-7.89 (ddd,  $J$  = 8.3, 6.9, 1.4 Hz, 1H, CH<sub>Ar</sub>), 7.87-7.85 (m, 2H, CH<sub>Ar</sub>), 7.61-7.56 (m, 4H, CH<sub>Ar</sub>), 7.38-7.31 (m, 3H, CH<sub>Ar</sub>), 2.67 (s, 3H, CH<sub>3</sub>); <sup>13</sup>C NMR (100 MHz, CDCl<sub>3</sub>):  $\delta_{\text{C}}$  = 168.5, 163.3, 151.3, 138.4, 137.6, 137.5, 133.9, 131.4, 130.9, 130.3, 130.2, 129.6, 128.9, 128.7, 127.6, 127.2, 126.2, 121.1, 21.4; MS (EI, 70 eV)  $m/z$  (%): 297 (M+1, 13), 296 (M, 81), 295 (100), 294 (7), 293 (6), 219 (6), 218 (10), 147 (14).



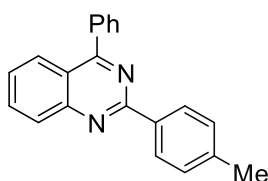
**2-(2-Chlorophenyl)-4-phenylquinazoline (32):** Yellow solid; purification by column chromatography (hexane/ethyl acetate 9:1), 81% yield; m.p: 90-92 °C (lit. 93-94 °C)<sup>221</sup>; <sup>1</sup>H NMR (400 MHz, CDCl<sub>3</sub>):  $\delta_{\text{H}}$  = 8.26-8.24 (d,  $J$  = 8.4 Hz, 1H, CH<sub>Ar</sub>), 8.22-8.19 (dd,  $J$  = 8.4 Hz, 0.7 Hz, 1H, CH<sub>Ar</sub>), 7.97-7.87 (m, 4H, CH<sub>Ar</sub>), 7.67-7.63 (m, 1H, CH<sub>Ar</sub>), 7.61-7.53 (m, 4H, CH<sub>Ar</sub>), 7.44-7.37 (m, 2H, CH<sub>Ar</sub>); <sup>13</sup>C NMR (100 MHz, CDCl<sub>3</sub>):  $\delta_{\text{C}}$  = 168.6, 161.2, 151.3, 138.2, 137.2, 134.1, 133.2, 131.9, 130.7, 130.5, 130.4, 130.3, 128.9, 128.8, 128.0, 127.2, 127.0, 121.5; MS (EI, 70 eV)  $m/z$  (%): 318 (M+2, 25), 317 (M+1, 48), 316 (M, 70), 315 (100), 281 (5), 239 (7), 203 (6), 179 (5), 178 (9), 177 (8), 151 (8), 102 (8), 76 (9).



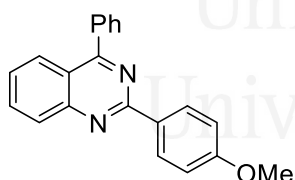
**2-(3-Methylphenyl)-4-phenylquinazoline (33):** Off white solid; purification by column chromatography (hexane/ethyl acetate 95:5), 84% yield; m.p: 94-96 °C (lit. 88-90 °C)<sup>215</sup>; <sup>1</sup>H NMR (400 MHz, CDCl<sub>3</sub>):  $\delta_{\text{H}}$  = 8.53-8.50 (m, 2H, CH<sub>Ar</sub>), 8.24 (bd,  $J$  = 8.4 Hz, 1H, CH<sub>Ar</sub>), 8.10 (dd,  $J$  = 8.4 Hz, 1H, CH<sub>Ar</sub>), 7.89-7.85 (m, 3H, CH<sub>Ar</sub>), 7.60-7.56 (m, 3H, CH<sub>Ar</sub>), 7.52 (ddd,  $J$  = 8.3 Hz, 6.8, 1.2 Hz, 1H, CH<sub>Ar</sub>), 7.42 (t,  $J$  = 7.5 Hz, 1H, CH<sub>Ar</sub>), 7.31 (bd,  $J$  = 7.6 Hz, 1H, CH<sub>Ar</sub>), 2.48 (s, 3H, CH<sub>3</sub>); <sup>13</sup>C NMR (100 MHz, CDCl<sub>3</sub>):  $\delta_{\text{C}}$  = 168.8, 160.3, 151.5, 138.3, 137.7, 133.9, 131.7, 130.4, 130.3, 129.4, 128.8, 128.7, 128.6, 127.2, 127.2, 126.2, 121.7, 21.7; MS (EI, 70 eV)  $m/z$  (%): 297 (M+1, 13), 296 (M, 67), 295 (100), 148 (5), 147 (7).



**2-(3-Chlorophenyl)-4-phenylquinazoline (34):** Off white solid; purification by column chromatography (hexane/ethyl acetate 95:5), 88% yield; m.p: 120-123 °C (lit. 116-118 °C)<sup>376</sup>; <sup>1</sup>H NMR (400 MHz, CDCl<sub>3</sub>): δ<sub>H</sub> = 8.70-8.69 (m, 1H, CH<sub>Ar</sub>), 8.60-8.58 (m, 1H, CH<sub>Ar</sub>), 8.17-8.11 (m, 2H, CH<sub>Ar</sub>), 7.91-7.86 (m, 3H, CH<sub>Ar</sub>), 7.61-7.59 (m, 3H, CH<sub>Ar</sub>), 7.56 (ddd, *J* = 8.2, 7.0, 1.2 Hz, CH<sub>Ar</sub>), 7.47-7.42 (m, 2H, CH<sub>Ar</sub>); <sup>13</sup>C NMR (100 MHz, CDCl<sub>3</sub>): δ<sub>C</sub> = 168.7, 158.9, 151.8, 140.0, 137.5, 134.8, 133.9, 130.6, 130.3, 130.2, 129.9, 129.2, 128.8, 128.7, 127.6, 127.2, 126.9, 121.9; MS (EI, 70 eV) *m/z* (%): 318 (M+2, 23), 317 (M+1, 45), 316 (M, 67), 315 (100), 203 (6), 178 (8), 177 (8), 151 (8), 140 (6), 102 (7), 76 (9).

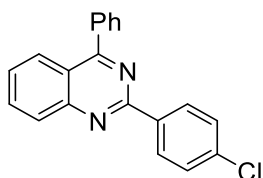


**2-(4-Methylphenyl)-4-phenylquinazoline (35):** Off white solid; purification by column chromatography (hexane/ethyl acetate 95:5), 60% yield; m.p: 165-166 °C (lit. 163-165 °C)<sup>215</sup>; <sup>1</sup>H NMR (300 MHz, CDCl<sub>3</sub>): δ<sub>H</sub> = 8.60-8.58 (m, 2H, CH<sub>Ar</sub>), 8.14 (d, *J* = 8.4 Hz, 1H, CH<sub>Ar</sub>), 8.09 (dd, *J* = 8.4, 0.8 Hz, 1H, CH<sub>Ar</sub>), 7.88-7.83 (m, 3H, CH<sub>Ar</sub>), 7.61-7.55 (m, 3H, CH<sub>Ar</sub>), 7.50 (ddd, *J* = 8.2, 6.9, 1.1 Hz, 1H, CH<sub>Ar</sub>), 7.33-7.31 (m, 2H, CH<sub>Ar</sub>), 2.43 (s, 1H, CH<sub>3</sub>); <sup>13</sup>C NMR (75 MHz, CDCl<sub>3</sub>): δ<sub>C</sub> = 168.4, 160.4, 151.9, 140.9, 137.8, 135.5, 133.6, 130.3, 130.0, 129.4, 129.1, 128.8, 128.6, 127.1, 126.9, 121.7, 21.7; MS (EI, 70 eV) *m/z* (%): 297 (M+1, 14), 296 (M, 71), 295 (100), 192 (5), 148 (7), 147 (7).

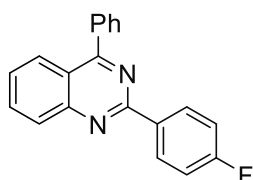


**2-(4-Methoxyphenyl)-4-phenylquinazoline (36):** Beige solid; purification by column chromatography (hexane/ethyl acetate 95:5), 93% yield; m.p: 161-162 °C (lit. 159-160 °C)<sup>221</sup>; <sup>1</sup>H NMR (400 MHz, CDCl<sub>3</sub>): δ<sub>H</sub> = 8.72-8.70 (def d, *J* = 8.8 Hz, 2H, CH<sub>Ar</sub>), 8.29-8.27 (d, *J* = 8.3 Hz, 1H, CH<sub>Ar</sub>), 8.12-8.09 (d, *J* = 8.3 Hz, 1H, CH<sub>Ar</sub>), 7.90-7.87 (m, 3H, CH<sub>Ar</sub>), 7.61-7.59 (m, 3H, CH<sub>Ar</sub>), 7.55-7.51 (def t, *J* = 7.6 Hz, 1H, CH<sub>Ar</sub>), 7.06-7.03 (def d, *J* = 8.9 Hz, 2H, CH<sub>Ar</sub>), 3.90 (s, 3H, OCH<sub>3</sub>); <sup>13</sup>C NMR (100 MHz, CDCl<sub>3</sub>): δ<sub>C</sub> = 168.9, 162.2, 159.6, 150.9, 137.5, 134.0, 130.7, 130.3, 130.2, 128.6, 128.1, 127.2, 126.9, 121.3, 113.9, 55.4; MS (EI, 70 eV) *m/z* (%): 313 (M+1, 20), 312 (M, 95), 311 (100), 268 (9), 191 (5), 192 (5), 179 (6), 156 (9), 133 (11), 77 (6), 73 (5).

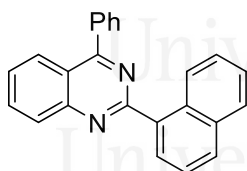
<sup>376</sup>Szczepankiewicz, W.; Wagner, P.; Danicki, M.; Suwiński, J. *Tetrahedron Lett.* **2003**, *44*, 2015–2017.



**2-(4-Chlorophenyl)-4-phenylquinazoline (37):** Off white solid; purification by column chromatography (hexane/ethyl acetate 9:1), 76% yield; m.p: 190-191 °C (lit. 191-193 °C)<sup>221</sup>; <sup>1</sup>H NMR (400 MHz, CDCl<sub>3</sub>): δ<sub>H</sub> = 8.69-8.66 (m, 2H, CH<sub>Ar</sub>), 8.23 (bd, *J* = 8.4 Hz, 1H, CH<sub>Ar</sub>), 8.13 (bd, *J* = 8.4, 0.7 Hz, 1H, CH<sub>Ar</sub>), 7.93-7.86 (m, 3H, CH<sub>Ar</sub>), 7.61-7.55 (m, 4H, CH<sub>Ar</sub>), 7.50-7.48 (m, 2H, CH<sub>Ar</sub>); <sup>13</sup>C NMR (100 MHz, CDCl<sub>3</sub>): δ<sub>C</sub> = 168.9, 159.2, 151.6, 137.5, 137.1, 136.4, 134.0, 130.3, 130.3, 130.3, 128.9, 128.7, 127.5, 127.2, 121.8.; MS (EI, 70 eV) *m/z*: 318 (M+2, 25), 317 (M+1, 45), 316 (M, 70), 315 (100), 203 (5), 179 (5), 178 (9), 177 (8), 158 (6), 151 (8), 140 (6), 102 (8), 77 (5), 76 (10), 75 (5).

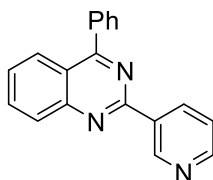


**2-(4-Fluorophenyl)-4-phenylquinazoline (38):** White solid; purification by column chromatography (hexane/ethyl acetate 98:2), 65% yield; m.p: 158-160 °C (lit. 154-156 °C)<sup>215</sup>; <sup>1</sup>H NMR (300 MHz, CDCl<sub>3</sub>): δ<sub>H</sub> = 8.73-8.66 (m, 2H, CH<sub>Ar</sub>), 8.13-8.08 (m, 2H, CH<sub>Ar</sub>), 7.86 (tdd, *J* = 6.0, 3.6, 1.4 Hz, 3H, CH<sub>Ar</sub>), 7.60-7.57 (m, 3H, CH<sub>Ar</sub>), 7.52 (ddd, *J* = 8.3, 6.9, 1.2 Hz, 1H, CH<sub>Ar</sub>), 7.21-7.16 (m, 2H, CH<sub>Ar</sub>); <sup>13</sup>C NMR (75 MHz, CDCl<sub>3</sub>): δ<sub>C</sub> = 168.5, 164.8 (d, *J* = 250.0 Hz), 159.4, 152.0, 137.7, 134.5 (d, *J* = 2.9 Hz), 133.8, 130.9 (d, *J* = 8.6 Hz), 130.3, 130.1, 129.2, 128.7, 127.2, 121.7, 115.6 (d, *J* = 21.6 Hz); MS (EI, 70 eV) *m/z*: 301 (M+1, 11), 300 (M, 71), 299 (100), 223 (6), 196 (6), 150 (7), 102 (6), 76 (10).



**2-(1-Naphthyl)-4-phenylquinazoline (39):** Faint yellow oil; purification by column chromatography (hexane/ethyl acetate 96:4), 82% yield; <sup>1</sup>H NMR (400 MHz, CDCl<sub>3</sub>): δ<sub>H</sub> = 8.82 (dd, *J* = 8.3, 0.7 Hz, 1H, CH<sub>Ar</sub>), 8.29-8.21 (m, 3H, CH<sub>Ar</sub>), 8.00-7.91 (m, 5H, CH<sub>Ar</sub>), 7.66-7.52 (m, 7H, CH<sub>Ar</sub>); <sup>13</sup>C NMR (100 MHz, CDCl<sub>3</sub>): δ<sub>C</sub> = 168.6, 162.9, 151.8, 137.6, 136.6, 134.4, 133.9, 131.5, 130.4, 130.3, 130.1, 129.8, 129.3, 128.7, 128.6, 127.6, 127.2, 126.9, 126.2, 125.9, 125.4, 121.4; MS (EI, 70 eV) *m/z* (%): 333 (M+1, 22), 332 (M, 97), 331 (100), 329 (11), 256 (8), 255 (41), 228 (9), 227 (6), 166 (11), 165 (22), 153 (15), 152 (7), 151 (6), 127 (11), 126 (9), 77 (6).





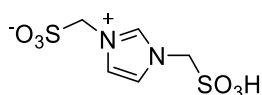
**4-Phenyl-2-(3-pyridyl)quinazoline (40):** White solid; purification by recrystallization (EtOH), 69% yield; m.p. 161-163 °C (lit. 158-160 °C)<sup>221</sup>; <sup>1</sup>H NMR (300 MHz, CDCl<sub>3</sub>): δ<sub>H</sub> = 9.79 (d, *J* = 1.5 Hz, 1H, CH<sub>Ar</sub>), 8.92-8.77 (m, 1H, CH<sub>Ar</sub>), 8.63 (dd, *J* = 4.8, 1.7 Hz, 1H, CH<sub>Ar</sub>), 8.05 (dddd, *J* = 8.4, 4.2, 1.3, 0.6 Hz, 2H, CH<sub>Ar</sub>), 7.85-7.72 (m, 3H, CH<sub>Ar</sub>), 7.55-7.43 (m, 4H, CH<sub>Ar</sub>), 7.35 (ddd, *J* = 8.0, 4.8, 0.8 Hz, 1H, CH<sub>Ar</sub>); <sup>13</sup>C NMR (100 MHz, CDCl<sub>3</sub>): δ<sub>C</sub> = 168.7, 158.3, 151.9, 150.9, 150.2, 137.4, 136.2, 133.9, 133.9, 130.3, 130.2, 129.3, 128.7, 127.7, 127.2, 123.5, 121.9; MS (EI, 70 eV) *m/z* (%): 284 (M+1, 15), 283 (M, 80), 282 (100), 255 (8), 179 (13), 141 (6), 102 (6), 77 (8), 76 (11).

---

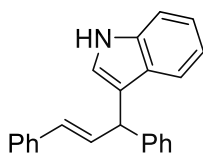


Universitat d'Alacant  
Universidad de Alicante

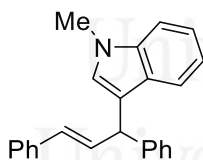
## E.3.3. Chapter 3



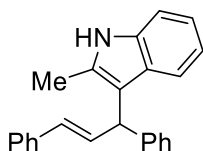
**1,3-Bis(sulfomethyl)imidazole (bsmim):** Light brown solid, 49% yield; m.p. = 291-294 °C;  $^1\text{H}$  NMR (400 MHz,  $\text{D}_2\text{O}$ )  $\delta_{\text{H}}$  = 9.26 (s, 1H, NCHN), 7.76 (d,  $J$  = 1.6 Hz, 2H, NCHCHN), 5.43 (s, 4H,  $\text{CH}_2$ );  $^{13}\text{C}$  NMR (100 MHz,  $\text{D}_2\text{O}$ )  $\delta_{\text{C}}$  = 138.3, 123.5, 62.6. MS (EI, 70 eV)  $m/z$  (%): 66 (5), 64 (100), 48 (40); MS/MS (ESI<sup>+</sup>) [256]: 261 (11), 242 (26), 238 (20), 193 (13), 176 (100), 163 (27).



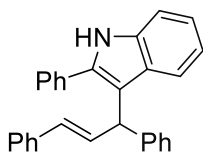
**(E)-3-(1,3-Diphenylallyl)-1H-indole (46):** Yellow oil, obtained pure, 99% yield;  $^1\text{H}$  NMR (400 MHz,  $\text{CDCl}_3$ ):  $\delta_{\text{H}}$  = 7.96 (br s, 1H, NH), 7.51 (d,  $J$  = 8.0 Hz, 1H,  $\text{CH}_{\text{Ar}}$ ), 7.45-7.22 (m, 12H,  $\text{CH}_{\text{Ar}}$ ), 7.10 (ddd,  $J$  = 8.0, 7.1, 1.0 Hz, 1H,  $\text{CH}_{\text{Ar}}$ ), 6.93 (d,  $J$  = 1.3 Hz, 1H,  $\text{CH}_{\text{Ar}}$ ), 6.80 (dd,  $J$  = 15.9, 7.4 Hz, 1H,  $\text{PhC}=\text{CH}$ ), 6.52 (br d,  $J$  = 15.9 Hz, 1H,  $\text{C}=\text{CHPh}$ ), 5.19 (br d,  $J$  = 7.4 Hz, 1H,  $\text{C}=\text{CCH}$ );  $^{13}\text{C}$  NMR (100 MHz,  $\text{CDCl}_3$ ):  $\delta_{\text{C}}$  = 143.5, 137.6, 136.8, 132.7, 130.7, 128.6, 128.6, 127.3, 126.9, 126.5, 126.5, 122.7, 122.2, 120.0, 119.6, 118.8, 111.2, 46.3; MS (EI, 70 eV)  $m/z$  (%): 310 ( $\text{M}^{+1}$ , 25), 309 ( $\text{M}^+$ , 100), 308 ( $\text{M}^{+1}$ , 39), 294 (10), 233 (7), 232 (36), 231 (7), 230 (20), 218 (15), 217 (17), 206 (28), 205 (8), 204 (22), 202 (8), 192 (14), 191 (16), 178 (9), 130 (19), 115 (17).



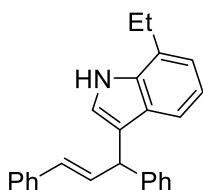
**(E)-3-(1,3-Diphenylallyl)-1-methyl-1H-indole (47):** Yellow oil, purified by preparative TLC (hexane/ethyl acetate 9:1), 78% yield;  $^1\text{H}$  NMR (300 MHz,  $\text{CDCl}_3$ ):  $\delta_{\text{H}}$  = 7.43-7.40 (m, 1H,  $\text{CH}_{\text{Ar}}$ ), 7.37-7.15 (m, 12H,  $\text{CH}_{\text{Ar}}$ ), 7.00 (ddd,  $J$  = 8.0, 6.9, 1.1 Hz, 1H,  $\text{CH}_{\text{Ar}}$ ), 6.72 (s, 1H, CHN), 6.71 (dd,  $J$  = 15.9, 7.4 Hz, 1H,  $\text{PhC}=\text{CH}$ ), 6.43 (br d,  $J$  = 15.9 Hz, 1H,  $\text{C}=\text{CHPh}$ ), 5.10 (br d,  $J$  = 7.4 Hz, 1H,  $\text{C}=\text{CCH}$ ), 3.69 (s, 3H,  $\text{CH}_3$ );  $^{13}\text{C}$  NMR (75 MHz,  $\text{CDCl}_3$ ):  $\delta_{\text{C}}$  = 143.7, 137.6, 137.5, 132.8, 130.5, 128.6, 128.5, 127.5, 127.3, 127.3, 126.5, 126.4, 121.7, 120.1, 119.0, 117.2, 109.3, 46.3, 32.8; MS (EI, 70 eV)  $m/z$  (%): 324 ( $\text{M}^{+1}$ , 25), 323 ( $\text{M}^+$ , 100), 322 ( $\text{M}^{+1}$ , 35), 247 (8), 246 (41), 244 (10), 232 (10), 231 (9), 230 (7), 220 (25), 219 (7), 218 (14), 217 (9), 204 (9), 202 (7), 192 (9), 191 (13), 144 (22), 131 (7), 115 (11).



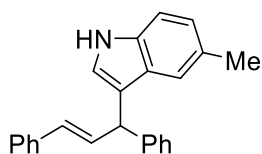
**(E)-3-(1,3-Diphenylallyl)-2-methyl-1H-indole (48):** Yellow oil, purified by preparative TLC (hexane/ethyl acetate 9:1), 81% yield;  $^1\text{H}$  NMR (300 MHz,  $\text{CDCl}_3$ ):  $\delta_{\text{H}} = 7.64$  (br s, 1H, NH), 7.33-7.17 (m, 12H,  $\text{CH}_{\text{Ar}}$ ), 7.06 (t,  $J = 7.3$  Hz, 1H,  $\text{CH}_{\text{Ar}}$ ), 6.96 (t,  $J = 7.3$  Hz, 1H,  $\text{CH}_{\text{Ar}}$ ), 6.82 (dd,  $J = 15.9$ , 7.1 Hz, 1H,  $\text{PhC}=\text{CH}$ ), 6.40 (br d,  $J = 15.9$  Hz, 1H,  $\text{C}=\text{CHPh}$ ), 5.11 (d,  $J = 7.1$  Hz, 1H,  $\text{C}=\text{CCH}$ ), 2.28 (s, 3H,  $\text{CH}_3$ );  $^{13}\text{C}$  NMR (75 MHz,  $\text{CDCl}_3$ ):  $\delta_{\text{C}} = 143.5, 137.6, 135.4, 132.3, 131.8, 130.6, 128.6, 128.4, 128.4, 128.0, 127.2, 126.4, 126.2, 120.9, 119.5, 119.3, 112.8, 110.4, 45.1, 12.4$ ; MS (EI, 70 eV)  $m/z$  (%): 324 ( $\text{M}^{+1}$ , 26), 323 ( $\text{M}^+$ , 100), 322 ( $\text{M}^{+1}$ , 16), 309 (17), 308 (66), 247 (7), 246 (32), 244 (11), 232 (15), 231 (12), 230 (21), 220 (15), 218 (29), 217 (20), 204 (9), 202 (9), 192 (11), 191 (22), 189 (7), 144 (29), 131 (9), 130 (10), 115 (12).



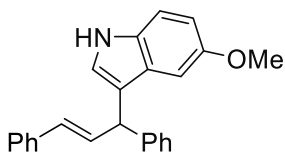
**(E)-3-(1,3-Diphenylallyl)-2-phenyl-1H-indole (49):** Faint orange oil, purified by preparative TLC (hexane/ethyl acetate 9:1), 60% yield;  $^1\text{H}$  NMR (300 MHz,  $\text{CDCl}_3$ ):  $\delta_{\text{H}} = 8.02$  (br s, 1H, NH), 7.52-7.48 (m, 2H,  $\text{CH}_{\text{Ar}}$ ), 7.44-7.12 (m, 16H,  $\text{CH}_{\text{Ar}}$ ), 6.98 (ddd,  $J = 8.0, 7.1, 1.0$  Hz, 1H,  $\text{CH}_{\text{Ar}}$ ), 6.88 (dd,  $J = 15.8, 7.3$  Hz, 1H,  $\text{PhC}=\text{CH}$ ), 6.39 (dd,  $J = 15.8, 1.0$  Hz, 1H,  $\text{C}=\text{CHPh}$ ), 5.27 (br d,  $J = 7.3$  Hz, 1H,  $\text{C}=\text{CCH}$ );  $^{13}\text{C}$  NMR (75 MHz,  $\text{CDCl}_3$ ):  $\delta_{\text{C}} = 143.6, 137.6, 136.3, 135.7, 133.0, 132.4, 131.2, 128.9, 128.7, 128.6, 128.4, 128.2, 128.0, 127.2, 126.4, 126.2, 122.2, 121.3, 119.8, 113.9, 111.1, 45.2$ ; MS (EI, 70 eV)  $m/z$  (%): 386 ( $\text{M}^{+1}$ , 30), 385 ( $\text{M}^+$ , 100), 384 ( $\text{M}^{+1}$ , 19), 309 (12), 308 (46), 307 (7), 306 (17), 304 (11), 295 (21), 294 (96), 293 (29), 292 (9), 291 (11), 282 (17), 281 (8), 280 (18), 278 (8), 230 (14), 218 (9), 217 (13), 207 (9), 206 (47), 205 (8), 204 (23), 203 (8), 202 (9), 194 (9), 193 (45), 192 (22), 191 (22), 189 (8), 178 (9), 176 (7), 165 (14), 153 (9), 152 (10), 146 (9), 115 (9), 91 (7).



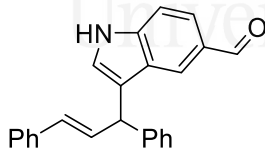
**(E)-3-(1,3-Diphenylallyl)-9-ethyl-1H-indole (50):** Reddish oil, obtained pure, 99% yield;  $^1\text{H}$  NMR (300 MHz,  $\text{CDCl}_3$ )  $\delta_{\text{H}} = 7.89$  (br s, 1H, NH), 7.36-7.15 (m, 11H,  $\text{CH}_{\text{Ar}}$ ), 7.02-6.97 (m, 2H, CHN,  $\text{CH}_{\text{Ar}}$ ), 6.84 (dd,  $J = 2.4, 0.9$  Hz, 1H,  $\text{CH}_{\text{Ar}}$ ), 6.72 (dd,  $J = 15.8, 7.4$  Hz, 1H,  $\text{PhC}=\text{CH}$ ), 6.43 (br d,  $J = 15.8$  Hz, 1H,  $\text{C}=\text{CHPh}$ ), 5.10 (br d,  $J = 7.4$  Hz, 1H,  $\text{C}=\text{CCH}$ ), 2.82 (q,  $J = 7.6$  Hz, 2H,  $\text{CH}_2$ ), 1.34 (t,  $J = 7.6$  Hz, 3H,  $\text{CH}_3$ );  $^{13}\text{C}$  NMR (75 MHz,  $\text{CDCl}_3$ ):  $\delta_{\text{C}} = 143.6, 137.6, 135.6, 132.7, 130.6, 128.6, 128.6, 128.5, 127.3, 126.7, 126.6, 126.4, 122.3, 120.7, 119.8, 119.2, 117.8, 46.4, 24.1, 13.9$ ; MS (EI, 70 eV)  $m/z$  (%): 338 ( $\text{M}^{+1}$ , 27), 337 ( $\text{M}^+$ , 100), 336 ( $\text{M}^{+1}$ , 34), 334 (9), 333 (28), 332 (9), 308 (20), 261 (7), 260 (33), 234 (23), 231 (9), 230 (24), 218 (9), 217 (14), 204 (10), 192 (17), 191 (20), 189 (7), 158 (15), 130 (12), 115 (11); HRMS (QTOF) calculated for  $\text{C}_{25}\text{H}_{23}\text{N}$  = 337.1830, observed = 337.1823.



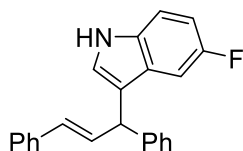
**(E)-3-(1,3-Diphenylallyl)-5-methyl-1H-indole (51):** Faint yellow oil, purified by column chromatography (hexane/ethyl acetate 9:1), 92% yield;  $^1\text{H NMR}$  (400 MHz,  $\text{CDCl}_3$ ):  $\delta_{\text{H}} = 7.68$  (br s, 1H, NH), 7.33-7.14 (m, 12H,  $\text{CH}_{\text{Ar}}$ ), 6.96 (dd,  $J = 8.3, 1.5$  Hz, 1H,  $\text{CH}_{\text{Ar}}$ ), 6.75 (s, 1H, CHN), 6.69 (dd,  $J = 15.8, 7.3$  Hz, 1H,  $\text{PhC}=\text{CH}$ ), 6.39 (dd,  $J = 15.8, 0.6$  Hz, 1H,  $\text{C}=\text{CHPh}$ ), 5.06 (br d,  $J = 7.3$  Hz, 1H,  $\text{C}=\text{CCH}$ ), 2.34 (s, 3H,  $\text{CH}_3$ );  $^{13}\text{C NMR}$  (100 MHz,  $\text{CDCl}_3$ ):  $\delta_{\text{C}} = 143.6, 137.7, 135.1, 132.8, 130.6, 128.7, 128.6, 128.5, 127.2, 127.2, 126.4, 123.8, 122.9, 119.5, 118.1, 110.9, 46.2, 21.7$ ; MS (EI, 70 eV)  $m/z$  (%): 324 ( $\text{M}^{+1}$ , 25), 323 ( $\text{M}^+$ , 100), 322 ( $\text{M}^{-1}$ , 39), 308 (15), 247 (8), 246 (39), 244 (11), 232 (9), 231 (12), 230 (10), 204 (12), 192 (12), 191 (16), 144 (17), 115 (15).



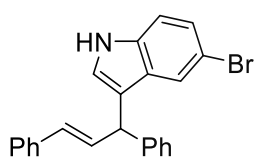
**(E)-3-(1,3-Diphenylallyl)-5-methoxy-1H-indole (52):** Brownish oil, purified by column chromatography (hexane/ethyl acetate 9:1), 83% yield;  $^1\text{H NMR}$  (300 MHz,  $\text{CDCl}_3$ ):  $\delta_{\text{H}} = 7.89$  (br s, 1H, NH), 7.35-7.21 (m, 11H,  $\text{CH}_{\text{Ar}}$ ), 6.86-6.81 (m, 3H, CHN,  $\text{CH}_{\text{Ar}}$ ), 6.71 (dd,  $J = 15.8, 7.3$  Hz, 1H,  $\text{PhC}=\text{CH}$ ), 6.44 (br d,  $J = 15.8$  Hz, 1H,  $\text{C}=\text{CHPh}$ ), 5.06 (br d,  $J = 7.3$  Hz, 1H,  $\text{C}=\text{CCH}$ ), 3.70 (s, 3H,  $\text{OCH}_3$ );  $^{13}\text{C NMR}$  (75 MHz,  $\text{CDCl}_3$ ):  $\delta_{\text{C}} = 153.9, 143.4, 137.6, 132.6, 131.9, 130.7, 128.6, 128.6, 127.3, 127.3, 126.5, 126.4, 123.6, 118.4, 112.3, 111.9, 101.9, 55.9, 46.3$ ; MS (EI, 70 eV)  $m/z$  (%): 340 ( $\text{M}^{+1}$ , 25), 339 ( $\text{M}^+$ , 100), 338 ( $\text{M}^{-1}$ , 34), 337 (7), 335 (8), 324 (10), 308 (10), 263 (8), 262 (35), 236 (22), 217 (9), 204 (10), 192 (14), 191 (18), 160 (14), 147 (7), 115 (7).



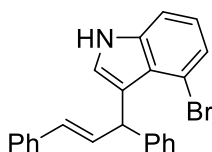
**(E)-3-(1,3-Diphenylallyl)-5-formyl-1H-indole (53):** Faint yellow oil, purified by column chromatography (hexane/ethyl acetate 8:2), 99% yield;  $^1\text{H NMR}$  (400 MHz,  $\text{CDCl}_3$ ):  $\delta_{\text{H}} = 9.92$  (s, 1H, CHO), 8.40 (br s, 1H, NH), 7.94 (m, 1H,  $\text{CH}_{\text{Ar}}$ ), 7.77 (dd,  $J = 8.5, 1.5$  Hz, 1H,  $\text{CH}_{\text{Ar}}$ ), 7.44 (d,  $J = 8.5$  Hz, 1H,  $\text{CH}_{\text{Ar}}$ ), 7.38-7.20 (m, 10H,  $\text{CH}_{\text{Ar}}$ ), 7.03 (dd,  $J = 2.3, 0.9$  Hz, 1H,  $\text{CH}_{\text{Ar}}$ ), 6.72 (dd,  $J = 15.8, 7.3$  Hz, 1H,  $\text{PhC}=\text{CH}$ ), 6.45 (br d,  $J = 15.8$  Hz, 1H,  $\text{C}=\text{CHPh}$ ), 5.18 (br d,  $J = 7.3$  Hz, 1H,  $\text{C}=\text{CCH}$ );  $^{13}\text{C NMR}$  (100 MHz,  $\text{CDCl}_3$ ):  $\delta_{\text{C}} = 192.6, 142.9, 140.3, 137.4, 132.0, 131.2, 129.6, 128.8, 128.7, 128.6, 127.5, 126.9, 126.9, 126.5, 125.6, 124.5, 122.5, 120.9, 111.9, 46.1$ ; MS (EI, 70 eV)  $m/z$  (%): 338 ( $\text{M}^{+1}$ , 32), 337 ( $\text{M}^+$ , 100), 336 ( $\text{M}^{-1}$ , 24), 308 (22), 260 (23), 234 (14), 218 (14), 217 (10), 209 (15), 208 (19), 204 (25), 193 (20), 192 (35), 191 (31), 115 (21); HRMS (QTOF) calculated for  $\text{C}_{24}\text{H}_{19}\text{NO} = 337.1467$ , observed = 337.1455.



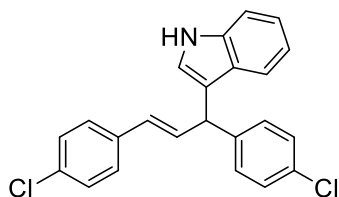
**(E)-3-(1,3-Diphenylallyl)-5-fluoro-1H-indole (54):** Faint yellow oil, obtained pure, 99% yield;  $^1\text{H NMR}$  (300 MHz,  $\text{CDCl}_3$ ):  $\delta_{\text{H}} = 7.93$  (br s, 1H, NH), 7.37-7.17 (m, 12H,  $\text{CH}_{\text{Ar}}$ ), 7.03 (dd,  $J = 9.8, 2.5$  Hz, 1H,  $\text{CH}_{\text{Ar}}$ ), 6.93-6.86 (m, 2H,  $\text{CH}_{\text{Ar}}$ ), 6.68 (dd,  $J = 15.8, 7.3$  Hz, 1H,  $\text{PhC}=\text{CH}$ ), 6.41 (br d,  $J = 15.8$  Hz, 1H,  $\text{C}=\text{CHPh}$ ), 5.17 (br d,  $J = 7.3$  Hz, 1H,  $\text{C}=\text{CCH}$ );  $^{13}\text{C NMR}$  (75 MHz,  $\text{CDCl}_3$ ):  $\delta_{\text{C}} = 157.7$  (d,  $J = 234.4$  Hz), 143.1, 137.43, 133.23, 132.19, 130.84, 128.64, 128.53, 127.39, 127.2 (d,  $J = 10.0$  Hz), 126.7, 126.4, 124.5, 118.9 (d,  $J = 4.7$  Hz), 111.8 (d,  $J = 9.7$  Hz), 110.6 (d,  $J = 26.5$  Hz), 104.9 (d,  $J = 23.5$  Hz), 46.25; MS (EI, 70 eV)  $m/z$  (%): 328 ( $\text{M}^{+1}$ , 25), 327 ( $\text{M}^+$ , 100), 326 ( $\text{M}^{+1}$ , 39), 312 (10), 250 (31), 249 (8), 248 (21), 236 (16), 235 (16), 224 (26), 223 (7), 222 (19), 192 (16), 191 (15), 148 (18), 115 (13).



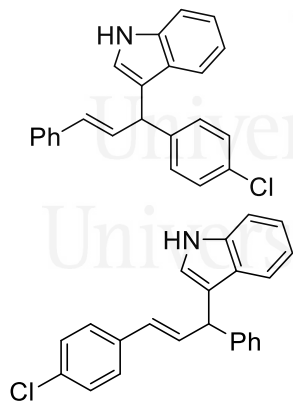
**(E)-5-Bromo-3-(1,3-diphenylallyl)-1H-indole (55):** Faint yellow oil, purified by column chromatography (hexane/ethyl acetate 9:1), 96% yield;  $^1\text{H NMR}$  (300 MHz,  $\text{CDCl}_3$ ):  $\delta_{\text{H}} = 7.87$  (br s, 1H, NH), 7.52 (d,  $J = 1.8$  Hz, 1H,  $\text{CH}_{\text{Ar}}$ ), 7.36-7.13 (m, 11H,  $\text{CH}_{\text{Ar}}$ ), 7.10 (br d,  $J = 8.6$  Hz, 1H,  $\text{CH}_{\text{Ar}}$ ), 6.80-6.78 (m, 1H,  $\text{CH}_{\text{Ar}}$ ), 6.64 (dd,  $J = 15.8, 7.3$  Hz, 1H,  $\text{PhC}=\text{CH}$ ), 6.37 (br d,  $J = 15.8$  Hz, 1H,  $\text{C}=\text{CHPh}$ ), 5.01 (br d,  $J = 7.3$  Hz, 1H,  $\text{C}=\text{CCH}$ );  $^{13}\text{C NMR}$  (75 MHz,  $\text{CDCl}_3$ ):  $\delta_{\text{C}} = 143.0, 137.4, 135.3, 132.2, 130.9, 128.6, 128.5, 127.4, 126.7, 126.4, 125.1, 123.9, 122.3, 118.4, 112.8, 112.7, 45.9$ ; MS (EI, 70 eV)  $m/z$  (%): 390 ( $\text{M}^{+3}$ , 24), 389 ( $\text{M}^{+2}$ , 97), 388 ( $\text{M}^{+1}$ , 51), 387 ( $\text{M}^+$ , 100), 386 ( $\text{M}^{+1}$ , 29), 312 (20), 311 (7), 310 (25), 308 (19), 307 (14), 306 (16), 293 (9), 286 (20), 284 (23), 231 (19), 230 (42), 229 (8), 228 (10), 217 (26), 216 (7), 210 (12), 208 (12), 205 (7), 204 (27), 203 (13), 202 (14), 192 (26), 191 (25), 189 (10), 176 (10), 154 (7), 115 (19).



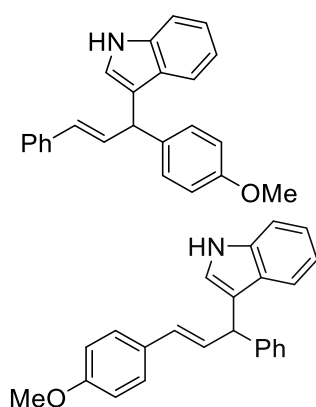
**(E)-4-Bromo-3-(1,3-diphenylallyl)-1H-indole (56):** Faint yellow oil, purified by column chromatography (hexane), 99% yield;  $^1\text{H NMR}$  (400 MHz,  $\text{CDCl}_3$ ):  $\delta_{\text{H}} = 8.04$  (br s, 1H, NH), 7.34-7.15 (m, 12H,  $\text{CH}_{\text{Ar}}$ ), 6.98 (d,  $J = 7.9$  Hz, 1H,  $\text{CH}_{\text{Ar}}$ ), 6.89 (d,  $J = 2.1$  Hz, 1H,  $\text{CH}_{\text{Ar}}$ ), 6.71 (dd,  $J = 15.9, 6.6$  Hz, 1H,  $\text{PhC}=\text{CH}$ ), 6.22 (dd,  $J = 15.9, 1.3$  Hz, 1H,  $\text{C}=\text{CHPh}$ ), 5.89 (br d,  $J = 6.5$  Hz, 1H,  $\text{C}=\text{CCH}$ );  $^{13}\text{C NMR}$  (100 MHz,  $\text{CDCl}_3$ ):  $\delta_{\text{C}} = 144.0, 137.9, 137.8, 133.9, 130.9, 129.1, 128.6, 128.4, 127.2, 126.4, 126.3, 125.0, 124.6, 123.1, 119.4, 114.6, 110.6, 44.9$ ; MS (EI, 70 eV)  $m/z$  (%): 390 ( $\text{M}^{+3}$ , 25), 389 ( $\text{M}^{+2}$ , 100), 388 ( $\text{M}^{+1}$ , 44), 387 ( $\text{M}^+$ , 99), 386 ( $\text{M}^{+1}$ , 19), 312 (20), 311 (7), 310 (26), 309 (10), 308 (32), 307 (9), 306 (14), 304 (7), 298 (7), 296 (8), 286 (17), 284 (23), 231 (15), 230 (30), 229 (7), 228 (11), 217 (31), 210 (17), 208 (18), 205 (8), 204 (32), 203 (13), 202 (17), 201 (7), 192 (26), 191 (27), 189 (10), 177 (8), 176 (14), 165 (7), 115 (20).



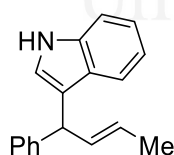
**(E)-3-(1,3-Bis(4-chlorophenyl)allyl)-1H-indole (57):** Yellow oil, obtained pure, 95% yield;  $^1\text{H NMR}$  (400 MHz,  $\text{CDCl}_3$ ):  $\delta_{\text{H}} = 7.98$  (br s, 1H, NH), 7.37-7.31 (m, 2H,  $\text{CH}_{\text{Ar}}$ ), 7.26-7.14 (m, 8H,  $\text{CH}_{\text{Ar}}$ ), 7.02 (ddd,  $J = 8.0, 7.1, 1.0$  Hz, 1H,  $\text{CH}_{\text{Ar}}$ ), 6.84 (s, 1H, CHN), 6.62 (dd,  $J = 15.8, 7.3$  Hz, 1H,  $\text{PhC}=\text{CH}$ ), 6.33 (dd,  $J = 15.9, 1.2$  Hz, 1H,  $\text{C}=\text{CHPh}$ ), 5.05 (br d,  $J = 7.2$  Hz, 1H,  $\text{C}=\text{CCH}$ );  $^{13}\text{C NMR}$  (100 MHz,  $\text{CDCl}_3$ ):  $\delta_{\text{C}} = 141.7, 136.8, 135.8, 132.9, 132.7, 132.3, 129.9, 129.8, 128.8, 128.7, 127.6, 126.6, 122.7, 122.4, 119.8, 119.7, 117.9, 111.4, 45.6$ ; MS (EI, 70 eV)  $m/z$  (%): 381 ( $\text{M}^{+4}$ , 12), 380 ( $\text{M}^{+3}$ , 19), 379 ( $\text{M}^{+2}$ , 66), 378 ( $\text{M}^{+1}$ , 46), 377 ( $\text{M}^+$ , 100), 376 ( $\text{M}^{-1}$ , 37), 375 (9), 342 (17), 340 (7), 268 (13), 267 (8), 266 (40), 264 (12), 242 (11), 241 (8), 240 (35), 238 (8), 231 (7), 230 (18), 228 (7), 227 (7), 225 (15), 217 (15), 204 (23), 203 (9), 202 (10), 189 (10), 176 (9), 512 (9), 151 (8), 149 (7), 130 (24).



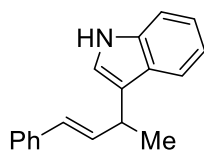
**(E)-3-(1-(4-Chlorophenyl)-3-phenylallyl)-1H-indole (58, top) and (E)-3-(3-(4-chlorophenyl)-1-phenylallyl)-1H-indole (58', bottom):** Yellow oil, obtained pure as an inseparable mixture of isomers, 99% yield;  $^1\text{H NMR}$  (400 MHz,  $\text{CDCl}_3$ ):  $\delta_{\text{H}} = 8.01$  (br s, 2H, NH, **13** and **13'**), 7.48-7.20 (m, 24H,  $\text{CH}_{\text{Ar}}$ , **13** and **13'**), 7.10-7.06 (m, 2H,  $\text{CH}_{\text{Ar}}$ , **13** and **13'**), 6.94-6.91 (m, 2H,  $\text{CH}_{\text{Ar}}$ , **13** and **13'**), 6.78-6.70 (m, 2H,  $\text{PhC}=\text{CH}$ , **13** and **13'**), 6.48-6.41 (m, 2H,  $\text{C}=\text{CHPh}$ , **13** and **13'**), 5.17-5.13 (m, 2H,  $\text{C}=\text{CCH}$ , **13** and **13'**);  $^{13}\text{C NMR}$  (100 MHz,  $\text{CDCl}_3$ ):  $\delta_{\text{C}} = 143.2, 141.9, 137.3, 136.7, 136.7, 136.0, 133.3, 132.7, 132.1, 131.9, 130.9, 129.9, 129.9, 129.4, 128.7, 128.6, 128.5, 128.5, 127.6, 127.4, 126.8, 126.6, 126.6, 126.4, 125.9, 122.7, 122.3, 122.2, 119.9, 119.8, 119.6, 119.5, 118.5, 118.2, 111.3, 111.2, 46.2, 45.6$ ; MS (EI, 70 eV)  $m/z$  (%): 346 ( $\text{M}^{+3}$ , 8), 345 ( $\text{M}^{+2}$ , 36), 344 ( $\text{M}^{+1}$ , 36), 343 ( $\text{M}^+$ , 100), 342 ( $\text{M}^{-1}$ , 39), 339 (7), 308 (9), 266 (18), 240 (15), 232 (20), 231 (7), 230 (20), 228 (7), 226 (7), 225 (7), 218 (10), 217 (15), 206 (18), 205 (7), 204 (21), 203 (7), 202 (9), 191 (14), 189 (9), 176 (8), 130 (21), 115 (11) (Isomer 1), 346 ( $\text{M}^{+3}$ , 8), 345 ( $\text{M}^{+2}$ , 35), 344 ( $\text{M}^{+1}$ , 37), 343 ( $\text{M}^+$ , 100), 342 ( $\text{M}^{-1}$ , 40), 339 (11), 266 (19), 240 (13), 232 (19), 231 (8), 230 (21), 228 (7), 226 (8), 225 (7), 218 (11), 217 (15), 206 (16), 205 (8), 204 (24), 202 (9), 191 (13), 189 (9), 176 (7), 130 (19), 115 (7) (Isomer 2).



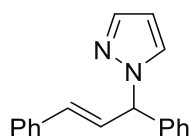
**(E)-3-(1-(4-Methoxyphenyl)-3-phenylallyl)-1H-indole (59, top) and (E)-3-(3-(4-methoxyphenyl)-1-phenylallyl)-1H-indole (59', bottom):** Yellow oil, obtained pure as an inseparable mixture of isomers (52/48 by NMR), 99% yield;  $^1\text{H}$  NMR (300 MHz,  $\text{CDCl}_3$ ):  $\delta_{\text{H}}$  = 7.92 (br s, 2H, NH, **14** and **14'**), 7.42 (d,  $J$  = 7.9 Hz, 2H,  $\text{CH}_{\text{Ar}}$ , **14** and **14'**), 7.36-7.12 (m, 18H,  $\text{CH}_{\text{Ar}}$ , **14** and **14'**), 7.40-6.98 (m, 2H,  $\text{CH}_{\text{Ar}}$ , **14** and **14'**), 6.85-6.79 (m, 6H,  $\text{CH}_{\text{Ar}}$ , **14** and **14'**), 6.70 (dd,  $J$  = 15.8, 7.3 Hz, 1H,  $\text{PhC}=\text{CH}$ , **14**), 6.57 (dd,  $J$  = 15.8, 7.3 Hz, 1H,  $\text{PhC}=\text{CH}$ , **14'**), 6.43-6.34 (m, 2H,  $\text{C}=\text{CHPh}$ , **14** and **14'**), 5.09-5.04 (m, 2H,  $\text{C}=\text{CCH}$ , **14** and **14'**), 3.76 (m, 6H,  $\text{OCH}_3$ , **14** and **14'**);  $^{13}\text{C}$  NMR (75 MHz,  $\text{CDCl}_3$ ):  $\delta_{\text{C}}$  = 158.9, 158.2, 143.7, 137.6, 136.8, 135.6, 132.9, 130.5, 130.4, 130.4, 130.0, 129.5, 128.6, 128.5, 127.5, 127.2, 126.9, 126.9, 126.4, 122.7, 122.7, 122.2, 120.0, 119.5, 119.0, 118.9, 55.4, 55.4, 46.3, 45.5; MS (EI, 70 eV)  $m/z$  (%): 340 ( $\text{M}^{+1}$ , 25), 339 ( $\text{M}^+$ , 100), 338 ( $\text{M}^{-1}$ , 41), 335 (16), 324 (7), 308 (10), 262 (12), 236 (17), 232 (12), 230 (14), 223 (11), 222 (54), 221 (10), 218 (10), 217 (9), 207 (29), 206 (10), 204 (9), 192 (8), 191 (11), 179 (14), 178 (29), 176 (7), 165 (8), 152 (9), 130 (13), 117 (22), 115 (8), 90 (8), 89 (9) (Isomer 1), 340 ( $\text{M}^{+1}$ , 25), 339 ( $\text{M}^+$ , 100), 338 ( $\text{M}^{-1}$ , 37), 336 (8), 335 (27), 324 (7), 308 (7), 291 (9), 262 (13), 236 (16), 232 (12), 230 (14), 223 (8), 222 (42), 221 (9), 218 (11), 217 (11), 207 (24), 206 (11), 204 (16), 191 (7), 179 (12), 178 (27), 176 (8), 152 (8), 145 (7), 130 (11), 117 (18), 90 (8), 89 (7) (Isomer 2); HRMS (QTOF) calculated for  $\text{C}_{24}\text{H}_{21}\text{NO}$  = 339.1623, observed = 337.1618.



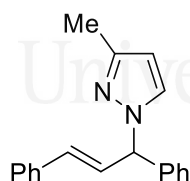
**(E)-3-(1-Phenylbut-2-en-1-yl)-1H-indole (60):** Colorless oil, purified by preparative TLC (hexane), 26% yield;  $^1\text{H}$  NMR (400 MHz,  $\text{CDCl}_3$ ):  $\delta_{\text{H}}$  = 7.93 (br s, 1H, NH), 7.40-7.30 (m, 4H,  $\text{CH}_{\text{Ar}}$ ), 7.26-7.10 (m, 4H,  $\text{CH}_{\text{Ar}}$ ), 7.01 (ddd,  $J$  = 8.0, 7.1, 1.0 Hz, 1H,  $\text{CH}_{\text{Ar}}$ ), 6.86 (br d,  $J$  = 1.4 Hz, 1H,  $\text{CH}_{\text{Ar}}$ ), 5.96 (ddq,  $J$  = 15.1, 7.5, 1.6 Hz, 1H,  $\text{CH}=\text{CMe}$ ), 5.52 (dq,  $J$  = 15.1, 6.5, 1.2 Hz, 1H,  $\text{C}=\text{CHMe}$ ), 4.89 (br d,  $J$  = 7.5 Hz, 1H,  $\text{PhCH}$ ), 1.72 (ddd,  $J$  = 6.5, 1.6, 1.0 Hz, 3H,  $\text{CH}_3$ );  $^{13}\text{C}$  NMR (100 MHz,  $\text{CDCl}_3$ ):  $\delta_{\text{C}}$  = 144.3, 136.8, 133.6, 128.4, 128.4, 126.9, 126.2, 126.1, 122.4, 122.1, 120.0, 119.6, 119.4, 111.2, 46.2, 18.1; MS (EI, 70 eV)  $m/z$  (%): 248 ( $\text{M}^{+1}$ , 19), 247 ( $\text{M}^+$ , 100), 246 ( $\text{M}^{-1}$ , 39), 232 (35), 230 (13), 218 (9), 217 (10), 206 (24), 204 (17), 178 (9), 170 (21), 154 (10), 130 (17), 129 (8), 128 (8), 117 (8), 115 (21).



**(E)-3-(4-Phenylbut-3-en-2-yl)-1H-indole (60')**: Yellowish oil, purified by preparative TLC (hexane), 39% yield;  $^1\text{H NMR}$  (400 MHz,  $\text{CDCl}_3$ ):  $\delta_{\text{H}} = 7.93$  (br s, 1H, NH), 7.67 (br d,  $J = 8.0$  Hz, 1H,  $\text{CH}_{\text{Ar}}$ ), 7.36-7.32 (m, 3H,  $\text{CH}_{\text{Ar}}$ ), 7.29-7.24 (m, 2H,  $\text{CH}_{\text{Ar}}$ ), 7.20-7.15 (m, 2H,  $\text{CH}_{\text{Ar}}$ ), 7.08 (ddd,  $J = 8.0, 7.1, 1.0$  Hz, 1H,  $\text{CH}_{\text{Ar}}$ ), 7.01 (br d,  $J = 1.7$  Hz, 1H,  $\text{CH}_{\text{Ar}}$ ), 6.53-6.43 (m, 2H, HC=CH), 3.97-3.90 (m, 1H, HMe), 1.56 (d,  $J = 7.0$  Hz, 3H,  $\text{CH}_3$ );  $^{13}\text{C NMR}$  (100 MHz,  $\text{CDCl}_3$ ):  $\delta_{\text{C}} = 137.9, 136.7, 135.6, 128.6, 128.3, 127.0, 126.3, 122.1, 120.6, 120.5, 119.8, 119.4, 111.3, 34.4, 20.9$ ; MS (EI, 70 eV)  $m/z$  (%): 248 ( $\text{M}^{+1}$ , 19), 247 ( $\text{M}^+$ , 100), 246 ( $\text{M}^{-1}$ , 14), 233 (17), 232 (94), 231 (8), 230 (19), 217 (10), 202 (8), 170 (10), 154 (11), 144 (8), 130 (17), 115 (37).

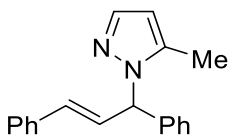


**(E)-1-(1,3-Diphenylallyl)-1H-pyrazole (61)**: Colorless oil, obtained pure, 99% yield;  $^1\text{H NMR}$  (300 MHz,  $\text{CDCl}_3$ ):  $\delta_{\text{H}} = 7.60$  (d,  $J = 1.4$  Hz, 1H,  $\text{CH}_{\text{Ar}}$ ), 7.45 (d,  $J = 2.2$  Hz, 1H,  $\text{CH}_{\text{Ar}}$ ), 7.39-7.20 (m, 10H,  $\text{CH}_{\text{Ar}}$ ), 6.71 (dd,  $J = 16.0, 6.9$  Hz, 1H, PhC=CH), 6.43 (br d,  $J = 16.0$  Hz, 1H, C=CHPh), 6.30-6.28 (m, 1H,  $\text{CH}_{\text{Ar}}$ ), 6.18 (br d,  $J = 6.9$  Hz, 1H, C=CCH);  $^{13}\text{C NMR}$  (75 MHz,  $\text{CDCl}_3$ ):  $\delta_{\text{C}} = 139.6, 139.4, 136.1, 133.8, 128.9, 128.7, 128.2, 127.4, 127.3, 126.8, 105.7, 67.6$ ; MS (EI, 70 eV)  $m/z$  (%): 261 ( $\text{M}^{+1}$ , 15), 260 ( $\text{M}^+$ , 78), 259 ( $\text{M}^{-1}$ , 24), 232 (7), 193 (28), 192 (43), 191 (55), 190 (11), 189 (23), 184 (8), 183 (55), 179 (7), 178 (33), 169 (31), 165 (21), 157 (18), 156 (36), 144 (21), 143 (8), 117 (9), 115 (100), 91 (27), 89 (7), 77 (8).

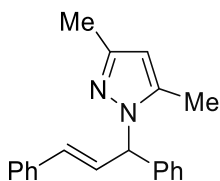


**(E)-1-(1,3-Diphenylallyl)-3-methyl-1H-pyrazole (62)**: Yellowish solid, purified by preparative TLC (hexane/ethyl acetate 9:1), 54% yield; m.p. 77-79 °C;  $^1\text{H NMR}$  (400 MHz,  $\text{CDCl}_3$ ):  $\delta_{\text{H}} = 7.40$ -7.20 (m, 11H,  $\text{CH}_{\text{Ar}}$ ), 6.68 (dd,  $J = 15.9, 6.9$  Hz, 1H, PhC=CH), 6.42 (br d,  $J = 15.9$  Hz, 1H, C=CHPh), 6.13 (br d,  $J = 6.9$  Hz, 1H, C=CCH), 6.07 (d,  $J = 2.2$  Hz, 1H,  $\text{CH}_{\text{Ar}}$ ), 2.31 (s, 3H,  $\text{CH}_3$ );  $^{13}\text{C NMR}$  (100 MHz,  $\text{CDCl}_3$ ):  $\delta_{\text{C}} = 148.9, 139.7, 136.3, 133.8, 129.3, 128.9, 128.7, 128.2, 128.1, 127.6, 127.5, 126.8, 105.4, 67.4, 13.8$ ; MS (EI, 70 eV)  $m/z$  (%): 275 ( $\text{M}^{+1}$ , 13), 274 ( $\text{M}^+$ , 62), 273 ( $\text{M}^{-1}$ , 19), 198 (10), 197 (68), 194 (7), 193 (38), 192 (21), 191 (32), 190 (8), 189 (17), 183 (15), 179 (7), 178 (33), 171 (14), 170 (34), 165 (16), 158 (10), 156 (8), 116 (11), 115 (100), 91 (26).

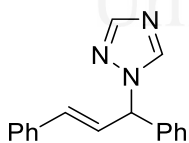




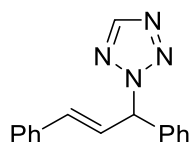
**(E)-1-(1,3-Diphenylallyl)-5-methyl-1H-pyrazole (62')**: White solid, purified by preparative TLC (hexane/ethyl acetate 9:1), 22% yield; m.p. 87-89 °C; <sup>1</sup>H NMR (400 MHz, CDCl<sub>3</sub>): δ<sub>H</sub> = 7.51 (br d, *J* = 1.6 Hz, 1H, CH<sub>Ar</sub>), 7.42-7.40 (m, 2H, CH<sub>Ar</sub>), 7.35-7.23 (m, 6H, CH<sub>Ar</sub>), 7.18-7.16 (m, 2H, CH<sub>Ar</sub>), 6.88 (dd, *J* = 15.9, 7.3 Hz, 1H, PhC=CH), 6.46 (br d, *J* = 15.9 Hz, 1H, C=CHPh), 6.08 (dd, *J* = 1.6, 0.9 Hz, 1H, CH<sub>Ar</sub>), 6.03 (br d, *J* = 6.9 Hz, 1H, C=CCH), 2.25 (s, 3H, CH<sub>3</sub>); <sup>13</sup>C NMR (100 MHz, CDCl<sub>3</sub>): δ<sub>C</sub> = 139.9, 138.7, 138.4, 136.4, 132.9, 128.8, 128.6, 128.1, 127.9, 127.2, 126.9, 105.9, 64.6, 11.5; MS (EI, 70 eV) *m/z* (%): 275 (M<sup>+</sup>+1, 14), 274 (M<sup>+</sup>, 66), 273 (M<sup>+</sup>-1, 21), 198 (12), 197 (79), 193 (33), 192 (20), 191 (32), 190 (8), 189 (17), 183 (24), 179 (7), 178 (32), 171 (13), 170 (28), 165 (16), 158 (12), 156 (11), 116 (11), 115 (100), 94 (7), 91 (26).



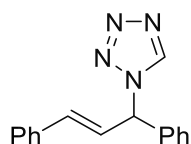
**(E)-1-(1,3-Diphenylallyl)-3,5-dimethyl-1H-pyrazole (63)**: White solid, obtained pure, 99% yield; m.p. 108-110 °C; <sup>1</sup>H NMR (400 MHz, CDCl<sub>3</sub>): δ<sub>H</sub> = 7.43-7.41 (m, 2H, CH<sub>Ar</sub>), 7.33-7.23 (m, 6H, CH<sub>Ar</sub>), 7.16-7.14 (m, 2H, CH<sub>Ar</sub>), 6.88 (dd, *J* = 15.9, 7.5 Hz, 1H, PhC=CH), 6.51 (br d, *J* = 15.9 Hz, 1H, C=CHPh), 5.98 (br d, *J* = 7.5 Hz, 1H, C=CCH), 5.87 (s, 1H, MeCCH), 2.27 (s, 3H, CH<sub>3</sub>), 2.17 (s, 3H, CH<sub>3</sub>); <sup>13</sup>C NMR (100 MHz, CDCl<sub>3</sub>): δ<sub>C</sub> = 147.8, 140.2, 139.2, 136.5, 133.1, 128.8, 128.6, 128.0, 127.9, 127.7, 126.9, 126.9, 105.9, 64.5, 13.8, 11.5; MS (EI, 70 eV) *m/z* (%): 289 (M<sup>+</sup>+1, 10), 288 (M<sup>+</sup>, 50), 287 (M<sup>+</sup>-1, 18), 273 (8), 212 (16), 211 (100), 194 (7), 193 (38), 192 (14), 185 (9), 184 (9), 178 (30), 170 (12), 165 (3), 116 (10), 115 (91), 108 (8), 91 (25).



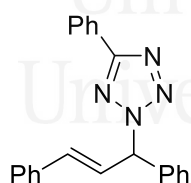
**(E)-1-(1,3-Diphenylallyl)-1H-1,2,4-triazole (64)**: Colorless oil, obtained pure, 99% yield; <sup>1</sup>H NMR (300 MHz, CDCl<sub>3</sub>): δ<sub>H</sub> = 8.17 (s, 1H, CH<sub>Ar</sub>), 8.02 (s, 1H, CH<sub>Ar</sub>), 7.41-7.25 (m, 10H, CH<sub>Ar</sub>), 6.67 (dd, *J* = 15.8, 7.0 Hz, 1H, PhC=CH), 6.50 (br d, *J* = 15.8 Hz, 1H, C=CHPh), 6.19 (br d, *J* = 7.5 Hz, 1H, C=CCH); <sup>13</sup>C NMR (75 MHz, CDCl<sub>3</sub>): δ<sub>C</sub> = 151.9, 142.7, 137.7, 135.5, 134.8, 129.2, 128.8, 128.7, 128.6, 127.5, 126.9, 125.6, 66.2; MS (EI, 70 eV) *m/z* (%): 261 (M<sup>+</sup>, 33), 234 (9), 233 (26), 206 (18), 193 (30), 192 (97), 191 (85), 190 (13), 189 (23), 179 (7), 178 (31), 165 (24), 157 (17), 146 (11), 145 (100), 144 (14), 130 (9), 117 (16), 116 (10), 115 (77), 91 (23), 89 (10), 77 (14).



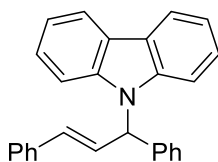
**(E)-2-(1,3-Diphenylallyl)-2H-tetrazole (65):** Yellowish oil, purified by preparative TLC (hexane/ethyl acetate 9:1), 41% yield;  $^1\text{H NMR}$  (300 MHz,  $\text{CDCl}_3$ ):  $\delta_{\text{H}} = 8.56$  (s, 1H, NCHN), 7.44-7.28 (m, 10H,  $\text{CH}_{\text{Ar}}$ ), 6.87 (dd,  $J = 15.7, 7.8$  Hz, 1H,  $\text{PhC}=\text{CH}$ ), 6.74 (br d,  $J = 7.8$  Hz, 1H,  $\text{C}=\text{CCH}$ ), 6.63 (br d,  $J = 15.7$  Hz, 1H,  $\text{C}=\text{CHPh}$ );  $^{13}\text{C NMR}$  (75 MHz,  $\text{CDCl}_3$ ):  $\delta_{\text{C}} = 153.1, 137.0, 135.5, 135.3, 129.2, 129.1, 128.9, 128.8, 127.5, 127.0, 124.7, 69.9$ ; MS (EI, 70 eV)  $m/z$  (%): 262 ( $\text{M}^+$ , 27), 233 (9), 207 (12), 206 (66), 205 (9), 203 (12), 202 (11), 194 (15), 193 (67), 192 (23), 191 (36), 190 (12), 189 (18), 180 (23), 179 (19), 178 (43), 165 (23), 152 (7), 130 (8), 129 (11), 128 (22), 127 (7), 116 (13), 115 (100), 104 (38), 103 (11), 102 (9), 91 (44), 89 (15), 78 (7), 77 (16), 65 (7), 51 (8).



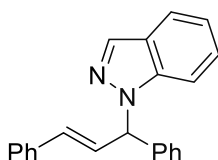
**(E)-1-(1,3-Diphenylallyl)-1H-tetrazole (65')**: Yellowish oil, purified by preparative TLC (hexane/ethyl acetate 9:1), 36% yield;  $^1\text{H NMR}$  (300 MHz,  $\text{CDCl}_3$ ):  $\delta_{\text{H}} = 8.59$  (s, 1H, NCHN), 7.45-7.29 (m, 10H,  $\text{CH}_{\text{Ar}}$ ), 6.69 (dd,  $J = 15.2, 7.2$  Hz, 1H,  $\text{PhC}=\text{CH}$ ), 6.56-6.49 (m, 2H,  $\text{C}=\text{CHPh}$ ,  $\text{C}=\text{CCH}$ );  $^{13}\text{C NMR}$  (75 MHz,  $\text{CDCl}_3$ ):  $\delta_{\text{C}} = 142.1, 136.4, 135.8, 135.1, 129.6, 129.6, 129.1, 128.9, 127.6, 127.0, 124.2, 65.5$ ; MS (EI, 70 eV)  $m/z$  (%): 262 ( $\text{M}^+$ , 23), 233 (14), 206 (29), 194 (16), 193 (73), 192 (26), 191 (26), 190 (7), 189 (14), 180 (27), 179 (18), 178 (40), 165 (21), 130 (13), 116 (13), 115 (100), 104 (44), 103 (16), 102 (8), 91 (31), 89 (11), 78 (7), 77 (16), 51 (7).



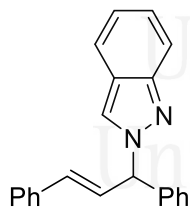
**(E)-2-(1,3-Diphenylallyl)-5-phenyl-2H-tetrazole (66):** Colorless oil, obtained pure, 99% yield;  $^1\text{H NMR}$  (300 MHz,  $\text{COCD}_6$ ):  $\delta_{\text{H}} = 8.17$ -8.14 (m, 2H,  $\text{CH}_{\text{Ar}}$ ), 7.58-7.27 (m, 13H,  $\text{CH}_{\text{Ar}}$ ), 7.12 (dd,  $J = 15.7, 8.0$  Hz, 1H,  $\text{PhC}=\text{CH}$ ), 6.99 (br d,  $J = 8.0$  Hz, 1H,  $\text{C}=\text{CCH}$ ), 6.88 (br d,  $J = 15.7$  Hz, 1H,  $\text{C}=\text{CHPh}$ );  $^{13}\text{C NMR}$  (75 MHz,  $\text{COCD}_6$ ):  $\delta_{\text{C}} = 165.7, 138.6, 136.7, 135.6, 131.2, 130.1, 129.8, 129.8, 129.5, 129.3, 128.4, 128.3, 127.7, 127.4, 126.1, 70.4$ ; MS (EI, 70 eV)  $m/z$  (%): 283 (20), 282 (87), 281 (17), 267 (14), 266 (7), 265 (14), 252 (9), 205 (30), 204 (35), 203 (40), 202 (35), 192 (17), 191 (100), 190 (10), 189 (19), 179 (7), 178 (16), 165 (17), 152 (7), 126 (7), 91 (8).



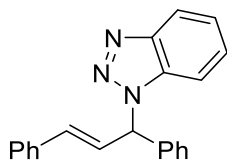
**(E)-9-(1,3-Diphenylallyl)-9H-carbazole (67):** Yellowish oil, purified by preparative TLC (hexane), 62% yield;  $^1\text{H NMR}$  (400 MHz,  $\text{CDCl}_3$ ):  $\delta_{\text{H}} = 8.23\text{-}8.21$  (m, 2H,  $\text{CH}_{\text{Ar}}$ ),  $7.46\text{-}7.29$  (m, 16H,  $\text{CH}_{\text{Ar}}$ ),  $7.02$  (dd,  $J = 15.8$ ,  $7.0$  Hz, 1H,  $\text{PhC}=\text{CH}$ ),  $6.70\text{-}6.66$  (m, 2H,  $\text{C}=\text{CHPh}$ ,  $\text{C}=\text{CCH}$ );  $^{13}\text{C NMR}$  (100 MHz,  $\text{CDCl}_3$ ):  $\delta_{\text{C}} = 140.2$ ,  $139.1$ ,  $136.2$ ,  $134.2$ ,  $128.9$ ,  $128.7$ ,  $128.2$ ,  $127.9$ ,  $127.3$ ,  $126.8$ ,  $125.9$ ,  $125.7$ ,  $123.6$ ,  $120.4$ ,  $119.3$ ,  $110.5$ ,  $59.9$ ; MS (EI, 70 eV)  $m/z$  (%): 359 ( $\text{M}^+$ , 10), 194 (17), 193 (100), 192 (42), 191 (29), 189 (14), 178 (15), 168 (8), 167 (57), 166 (18), 165 (13), 140 (8), 139 (10), 115 (44), 91 (9).



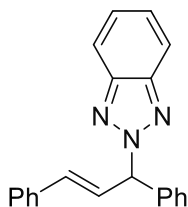
**(E)-1-(1,3-Diphenylallyl)-1H-indazole (68):** Yellowish solid, purified by column chromatography (hexane/ethyl acetate 96:4), 60% yield; m.p.  $100\text{-}102$  °C;  $^1\text{H NMR}$  (400 MHz,  $\text{CDCl}_3$ ):  $\delta_{\text{H}} = 8.01$  (s, 1H,  $\text{NNCH}$ ),  $7.76$  (dd,  $J = 8.8$ ,  $0.8$  Hz, 1H,  $\text{CH}_{\text{Ar}}$ ),  $7.65$  (br d,  $J = 8.4$  Hz, 1H,  $\text{CH}_{\text{Ar}}$ ),  $7.49\text{-}7.19$  (m, 11H,  $\text{CH}_{\text{Ar}}$ ),  $7.09$  (ddd,  $J = 8.4$ ,  $6.7$ ,  $0.8$  Hz, 1H,  $\text{CH}_{\text{Ar}}$ ),  $6.83$  (dd,  $J = 16.2$ ,  $6.7$  Hz, 1H,  $\text{PhC}=\text{CH}$ ),  $6.55\text{-}6.51$  (m, 2H,  $\text{C}=\text{CHPh}$ ,  $\text{C}=\text{CCH}$ );  $^{13}\text{C NMR}$  (100 MHz,  $\text{CDCl}_3$ ):  $\delta_{\text{C}} = 148.4$ ,  $138.7$ ,  $135.9$ ,  $134.8$ ,  $129.1$ ,  $128.8$ ,  $128.6$ ,  $128.5$ ,  $127.6$ ,  $126.9$ ,  $126.6$ ,  $126.5$ ,  $122.6$ ,  $122.1$ ,  $121.7$ ,  $120.5$ ,  $117.6$ ,  $69.2$ ; MS (EI, 70 eV)  $m/z$  (%): 310 ( $\text{M}^+$ , 21), 194 (18), 193 (100), 192 (7), 191 (7), 189 (7), 178 (23), 165 (8), 116 (8), 115 (73), 91 (19).



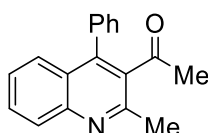
**(E)-2-(1,3-Diphenylallyl)-2H-indazole (68'):** Yellowish solid, purified by column chromatography (hexane/ethyl acetate 96:4), 38% yield; m.p.  $135\text{-}137$  °C;  $^1\text{H NMR}$  (400 MHz,  $\text{CDCl}_3$ ):  $\delta_{\text{H}} = 8.10$  (d,  $J = 0.7$  Hz, 1H,  $\text{NNCH}$ ),  $7.75$  (dt,  $J = 8.1$ ,  $1.0$  Hz, 1H,  $\text{CH}_{\text{Ar}}$ ),  $7.42\text{-}7.21$  (m, 12H,  $\text{CH}_{\text{Ar}}$ ),  $7.14$  (ddd,  $J = 7.8$ ,  $6.7$ ,  $1.0$  Hz, 1H,  $\text{CH}_{\text{Ar}}$ ),  $6.96$  (dd,  $J = 16.0$ ,  $7.2$  Hz, 1H,  $\text{PhC}=\text{CH}$ ),  $6.55$  (br d,  $J = 16.0$  Hz, 1H,  $\text{C}=\text{CHPh}$ ),  $6.48$  (br d,  $J = 7.2$  Hz, 1H,  $\text{C}=\text{CCH}$ );  $^{13}\text{C NMR}$  (100 MHz,  $\text{CDCl}_3$ ):  $\delta_{\text{C}} = 139.6$ ,  $139.4$ ,  $136.3$ ,  $133.7$ ,  $133.5$ ,  $128.8$ ,  $128.7$ ,  $128.2$ ,  $128.1$ ,  $127.4$ ,  $127.3$ ,  $126.9$ ,  $126.5$ ,  $124.6$ ,  $121.4$ ,  $120.9$ ,  $109.9$ ,  $65.2$ ; MS (EI, 70 eV)  $m/z$  (%): 311 ( $\text{M}^+ + 1$ , 7), 310 ( $\text{M}^+$ , 28), 194 (18), 193 (100), 191 (10), 189 (7), 178 (24), 165 (8), 116 (8), 115 (74), 91 (18).



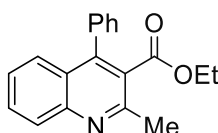
**(E)-1-(1,3-Diphenylallyl)-1H-benzo[d][1,2,3]triazole (69):** Yellowish solid, purified by preparative TLC (hexane/ethyl acetate 9:1), 85% yield; m.p. 132-134 °C (lit. 129 °C)<sup>283</sup>; <sup>1</sup>H NMR (300 MHz, CDCl<sub>3</sub>): δ<sub>H</sub> = 8.11-8.07 (m, 1H, CH<sub>Ar</sub>), 7.41-7.24 (m, 13H, CH<sub>Ar</sub>), 6.99 (dd, *J* = 15.7, 7.2 Hz, 1H, PhC=CH), 6.77 (br d, *J* = 7.2 Hz, 1H, C=CCH), 6.60 (br d, *J* = 15.7 Hz, 1H, C=CHPh); <sup>13</sup>C NMR (75 MHz, CDCl<sub>3</sub>): δ<sub>C</sub> = 146.3, 137.8, 135.7, 134.6, 132.5, 129.1, 128.7, 128.6, 128.5, 127.5, 127.3, 126.9, 125.5, 124.2, 120.1, 110.5, 65.6; MS (EI, 70 eV) *m/z* (%): 311 (M<sup>+</sup>, 20), 283 (11), 282 (43), 206 (20), 204 (9), 194 (20), 193 (100), 191 (16), 191 (15), 189 (10), 180 (9), 179 (10), 178 (27), 165 (13), 152 (8), 116 (8), 115 (60), 91 (21).



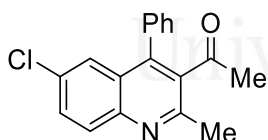
**(E)-2-(1,3-Diphenylallyl)-2H-benzo[d][1,2,3]triazole (69')**: Yellow solid, purified by preparative TLC (Hx:AcOEt 9:1), 10% yield; <sup>1</sup>H NMR (300 MHz, CDCl<sub>3</sub>): δ<sub>H</sub> = 7.90 (dd, *J* = 6.6, 3.0 Hz, 1H, CH<sub>Ar</sub>), 7.47-7.28 (m, 14H, CH<sub>Ar</sub>), 7.05 (dd, *J* = 15.9, 7.9 Hz, 1H, PhC=CH), 6.79-6.59 (m, 2H, C=CHPh, C=CCH); MS (EI, 70 eV) *m/z* (%): 311 (M<sup>+</sup>, 18), 282 (16), 194 (19), 193 (100), 192 (7), 191 (10), 189 (7), 178 (22), 165 (8), 116 (8), 115 (69), 91 (18).



**3-Acetyl-2-methyl-4-phenylquinoline (70):** Yellow solid, purification by column chromatography (hexane/ethyl acetate 7:3), 99% yield; m.p. 120-122 °C (lit. 117-119 °C)<sup>148</sup>; <sup>1</sup>H NMR (300 MHz, CDCl<sub>3</sub>): δ<sub>H</sub> = 8.13 (d, *J* = 8.4 Hz, 1H, CH<sub>Ar</sub>), 7.74 (ddd, *J* = 8.4, 6.9, 1.4 Hz, 1H, CH<sub>Ar</sub>), 7.65-7.62 (m, 1H, CH<sub>Ar</sub>), 7.53-7.46 (m, 4H, CH<sub>Ar</sub>), 7.38-7.35 (m, 2H, CH<sub>Ar</sub>), 2.73 (s, 3H, NCCH<sub>3</sub>), 2.00 (s, 3H, COCH<sub>3</sub>); <sup>13</sup>C NMR (100 MHz, CDCl<sub>3</sub>): δ<sub>C</sub> = 205.5, 153.7, 147.1, 144.7, 135.2, 134.9, 130.6, 130.1, 129.2, 128.9, 128.6, 126.9, 126.4, 125.2, 32.1, 23.7; MS (EI, 70 eV) *m/z* (%): 261 (M<sup>+</sup>, 49), 247 (19), 246 (100), 219 (7), 218 (38), 217 (31), 176 (22), 151 (8).

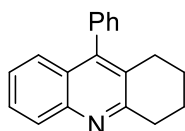


**3-(Ethoxycarbonyl)-2-methyl-4-phenylquinoline (71):** Yellow solid, purification by column chromatography (hexane/ethyl acetate 9:1), 98% yield; m.p. 99-100 °C (lit. 98-100 °C)<sup>377</sup>; <sup>1</sup>H NMR (400 MHz, CDCl<sub>3</sub>): δ<sub>H</sub> = 8.06 (d, *J* = 8.1 Hz, 1H, CH<sub>Ar</sub>), 7.68 (ddd, *J* = 8.4, 6.8, 1.4 Hz, 1H, CH<sub>Ar</sub>), 7.56 (dd, *J* = 8.4, 0.9 Hz, 1H, CH<sub>Ar</sub>), 7.47-7.43 (m, 3H, CH<sub>Ar</sub>), 7.41-7.33 (m, 3H, CH<sub>Ar</sub>), (q, *J* = 7.1 Hz, 2H, CH<sub>2</sub>), 2.78 (s, 3H, NCCH<sub>3</sub>), 0.92 (t, *J* = 7.1 Hz, 3H, COCCH<sub>3</sub>); <sup>13</sup>C NMR (100 MHz, CDCl<sub>3</sub>): δ<sub>C</sub> = 168.5, 154.6, 147.7, 146.4, 135.8, 130.3, 129.4, 128.9, 128.5, 128.3, 127.5, 126.5, 126.5, 125.2, 61.4, 23.8, 13.7; MS (EI, 70 eV) *m/z* (%): 292 (M<sup>+</sup>+1, 20), 291 (M<sup>+</sup>, 96), 263 (8), 262 (8), 247 (20), 246 (100), 245 (34), 219 (10), 218 (44), 217 (41), 216 (14), 177 (8), 176 (23), 151 (8).

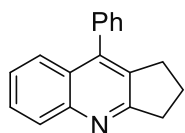


**3-Acetyl-6-chloro-2-methyl-4-phenylquinoline (72):** Yellow solid, purification by column chromatography (hexane/ethyl acetate 85:15), 93% yield; m.p. 160-161 °C (lit. 149-152 °C)<sup>377</sup>; <sup>1</sup>H NMR (400 MHz, CDCl<sub>3</sub>): δ<sub>H</sub> = 8.06 (d, *J* = 8.9 Hz, 1H, CH<sub>Ar</sub>), 7.66 (dd, *J* = 8.9, 2.3 Hz, 1H, CH<sub>Ar</sub>), 7.58 (d, *J* = 2.3 Hz, 1H, CH<sub>Ar</sub>), 7.55-7.52 (m, 3H, CH<sub>Ar</sub>), 7.35-7.32 (m, 2H, *J* = 8.9, 2.3 Hz, 1H, CH<sub>Ar</sub>), 2.69 (s, 3H, NCCH<sub>3</sub>), 1.99 (s, 3H, COCH<sub>3</sub>); <sup>13</sup>C NMR (100 MHz, CDCl<sub>3</sub>): δ<sub>C</sub> = 204.9, 154.1, 145.3, 143.9, 135.7, 134.4, 132.9, 131.5, 130.0, 129.5, 129.1, 126.1, 125.1, 31.9, 23.6; MS (EI, 70 eV) *m/z* (%): 297 (M<sup>+</sup>+2, 16), 296 (M<sup>+</sup>+1, 10), 295 (M<sup>+</sup>, 46), 282 (33), 281 (19), 280 (100), 254 (7), 252 (22), 218 (8), 217 (32), 216 (13), 189 (8), 176 (23).

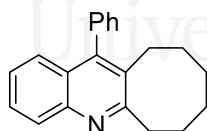
<sup>377</sup>Tanwar, B.; Kumar, A.; Yogeewari, P.; Sriram, D.; Chakraborti, A. K. *Bioorg. Med. Chem. Lett.* **2016**, *26*, 5960–5966.



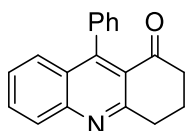
**9-Phenyl-1,2,3,4-tetrahydroacridine (73):** Yellow solid, purification by column chromatography (hexane/ethyl acetate 8:2), 94% yield; m.p. 151-153 °C (lit. 152-155 °C)<sup>148</sup>; <sup>1</sup>H NMR (300 MHz, CDCl<sub>3</sub>): δ<sub>H</sub> = 8.13 (d, *J* = 8.5 Hz, 1H, CH<sub>Ar</sub>), 7.66-7.60 (m, 1H, CH<sub>Ar</sub>), 7.56-7.45 (m, 3H, CH<sub>Ar</sub>), 7.35-7.33 (m, 2H, CH<sub>Ar</sub>), 7.25-7.22 (m, 2H, CH<sub>Ar</sub>), 3.27 (t, *J* = 6.6 Hz, 2H, NCCH<sub>2</sub>), 2.62 (t, *J* = 6.4 Hz, 2H, PhCCCH<sub>2</sub>), 2.02-1.93 (m, 2H, NCCCH<sub>2</sub>), 1.84-1.76 (m, 2H, PhCCCCH<sub>2</sub>); <sup>13</sup>C NMR (75 MHz, CDCl<sub>3</sub>): δ<sub>C</sub> = 158.9, 147.7, 145.4, 136.9, 129.1, 129.0, 128.8, 128.7, 128.1, 127.7, 126.9, 126.0, 125.9, 33.8, 28.1, 23.0, 22.8; MS (EI, 70 eV) *m/z* (%): 260 (M<sup>+</sup>+1, 19), 259 (M<sup>+</sup>, 100), 258 (M<sup>+</sup>-1, 66), 244 (8), 230 (14), 182 (8).



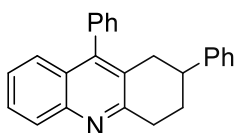
**9-Phenyl-2,3-dihydro-1H-cyclopenta[b]quinoline (74):** Faint yellow solid, purification by column chromatography (hexane/ethyl acetate 98:2), 93% yield, m.p. 138-141 °C (lit. 138-139 °C)<sup>148</sup>; <sup>1</sup>H NMR (400 MHz, CDCl<sub>3</sub>): δ<sub>H</sub> = 8.02-8.00 (m, 1H, CH<sub>Ar</sub>), 7.57-7.53 (m, 2H, CH<sub>Ar</sub>), 7.47-7.37 (m, 3H, CH<sub>Ar</sub>), 7.32-7.28 (m, 3H, CH<sub>Ar</sub>), 3.17 (t, *J* = 7.7 Hz, 2H, NCCH<sub>2</sub>), 2.83 (t, *J* = 7.4 Hz, 2H, PhCCCH<sub>2</sub>), 2.13-2.07 (m, 2H, NCCCH<sub>2</sub>); <sup>13</sup>C NMR (100 MHz, CDCl<sub>3</sub>): δ<sub>C</sub> = 167.5, 147.9, 142.9, 136.9, 133.8, 129.4, 128.9, 128.6, 128.4, 128.1, 126.4, 125.8, 125.7, 35.3, 30.5, 23.7; MS (EI, 70 eV) *m/z* (%): 246 (M<sup>+</sup>+1, 18), 245 (M<sup>+</sup>, 100), 244 (M<sup>+</sup>-1, 80), 243 (12), 242 (12), 241 (7), 217 (9), 168 (15), 167 (10), 108 (7).



**12-Phenyl-6,7,8,9,10,11-hexahydrocycloocta[b]quinoline (75):** Faint yellow solid, purification by column chromatography (hexane/ethyl acetate 95:5), 96% yield; m.p. 209-211 °C (lit. 214-215 °C)<sup>377</sup>; <sup>1</sup>H NMR (300 MHz, CDCl<sub>3</sub>): δ<sub>H</sub> = 8.01-7.98 (m, 1H, CH<sub>Ar</sub>), 7.54-7.48 (m, 1H, CH<sub>Ar</sub>), 7.46-7.36 (m, 3H, CH<sub>Ar</sub>), 7.27-7.11 (m, 4H, CH<sub>Ar</sub>), 3.17-3.13 (m, 2H, NCCH<sub>2</sub>), 2.69-2.65 (m, 2H, PhCCCH<sub>2</sub>), 1.88-1.84 (m, 2H, CH<sub>2</sub>), 1.42-1.27 (m, 6H, 3xCH<sub>2</sub>); <sup>13</sup>C NMR (75 MHz, CDCl<sub>3</sub>): δ<sub>C</sub> = 163.5, 146.7, 146.3, 137.7, 131.9, 129.4, 128.5, 128.4, 127.7, 127.3, 126.2, 125.5, 36.3, 31.3, 31.3, 28.2, 26.8, 25.9; MS (EI, 70 eV) *m/z* (%): 288 (M<sup>+</sup>+1, 20), 287 (M<sup>+</sup>, 93), 286 (M<sup>+</sup>-1, 100), 272 (9), 260 (8), 259 (17), 258 (40), 256 (9), 245 (8), 244 (25), 243 (9), 242 (9), 232 (19), 231 (14), 230 (16), 217 (14), 216 (7), 202 (8), 189 (10).



**9-Phenyl-3,4-dihydroacridin-1(2H)-one (76):** Yellow solid, purification by column chromatography (hexane/ethyl acetate 8:2), 96% yield; m.p. 163-165 °C (lit. 161-162 °C)<sup>148</sup>; <sup>1</sup>H NMR (400 MHz, CDCl<sub>3</sub>): δ<sub>H</sub> = 8.18 (d, *J* = 8.4 Hz, 1H, CH<sub>Ar</sub>), 7.80 (ddd, *J* = 8.4, 6.6, 1.6 Hz, 1H, CH<sub>Ar</sub>), 7.53-7.41 (m, 5H, CH<sub>Ar</sub>), 7.19-7.17 (m, 2H, CH<sub>Ar</sub>), 3.45 (t, *J* = 6.3 Hz, 2H, NCCH<sub>2</sub>), 2.72 (t, *J* = 6.1 Hz, 2H, COCH<sub>2</sub>), 2.28-2.25 (m, 2H, COCCH<sub>2</sub>); <sup>13</sup>C NMR (100 MHz, CDCl<sub>3</sub>): δ<sub>C</sub> = 197.6, 162.1, 152.5, 147.7, 137.4, 132.4, 128.4, 128.3, 128.1, 127.9, 127.7, 126.9, 124.0, 40.7, 34.1, 21.4; MS (EI, 70 eV) *m/z* (%): 274 (M<sup>+</sup>+1, 19), 273 (M<sup>+</sup>, 100), 272 (M<sup>+</sup>-1, 94), 246 (7), 245 (47), 244 (97), 217 (32), 216 (31), 214 (8), 190 (9), 189 (16), 176 (7).



**2,9-Diphenyl-1,2,3,4-tetrahydroacridine (77):** Yellow solid, purification by column chromatography (hexane/ethyl acetate 9:1), 97% yield; <sup>1</sup>H NMR (400 MHz, CDCl<sub>3</sub>): δ<sub>H</sub> = 7.98-7.96 (m, 1H, CH<sub>Ar</sub>), 7.57-7.52 (m, 1H, CH<sub>Ar</sub>), 7.41-7.35 (m, 3H, CH<sub>Ar</sub>), 7.25-7.10 (m, 9H, CH<sub>Ar</sub>), 3.37-3.22 (m, 2H, CH<sub>Alk</sub>), 2.95 (tdd, *J* = 11.4, 4.7, 3.0 Hz, 1H, CH<sub>Alk</sub>), 2.83 (ddd, *J* = 17.1, 4.9, 2.0 Hz, 1H, CH<sub>Alk</sub>), 2.68 (dd, *J* = 17.1, 4.9 Hz, 1H, CH<sub>Alk</sub>), 2.25-2.19 (m, 1H, CH<sub>Alk</sub>), 2.13-2.02 (m, 1H, CH<sub>Alk</sub>); <sup>13</sup>C NMR (100 MHz, CDCl<sub>3</sub>): δ<sub>C</sub> = 158.4, 146.9, 146.6, 145.9, 136.9, 129.2, 129.0, 128.9, 128.8, 128.7, 128.7, 128.5, 127.9, 127.8, 127.0, 126.8, 126.5, 126.0, 125.7, 40.9, 36.2, 34.4, 30.3; MS (EI, 70 eV) *m/z* (%): 336 (M<sup>+</sup>+1, 14), 335 (M<sup>+</sup>, 65), 334 (M<sup>+</sup>-1, 100), 231 (8), 230 (19), 91 (8).

---

## **Abbreviations, units and symbols**

---

Universitat d'Alacant  
Universidad de Alicante





|                     |   |
|---------------------|---|
| @                   | Supported on/at   |
| €                   | Euro  |
| $\Sigma$            | Sum   |
| $\approx$           | Approximately   |
| $^{13}\text{C}$ NMR | Carbon-13 Nuclear Magnetic Resonance Spectroscopy                                 |
| $^1\text{H}$ NMR    | Proton Nuclear Magnetic Resonance Spectroscopy                                    |
| 2-MeTHF             | 2-Methyltetrahydrofuran   |
| Å                   | Amstrong (unit of length)   |
| acac                | Acetylacetonate   |
| Ad                  | Adamantyl   |
| ADB                 | 1,4-Azodibenzoic acid   |
| AE                  | Atom Economy  |
| AF                  | Air flow  |
| Alk                 | Alkyl   |
| AMS                 | Aminomethanesulfonic acid   |
| aq.                 | Aqueous   |
| Ar                  | Aryl  |
| ATC                 | Adamantane-1,3,5,7-tetracarboxylic acid   |
| ATCC                | American Type Culture Collection, a distributor of reference cell culture samples |
| atm.                | Atmosphere (unit of pressure)   |
| bar                 | Unit of pressure  |
| BASF                | Badische Anilin- und Sodafabrik, German chemical manufacturing company            |
| BASIL               | Biphasic Acid Scavenging utilizing Ionic Liquids                                  |
| <b>bcmim</b>        | 1,3-Bis(carboxymethyl)imidazole   |
| <b>bcmimBr</b>      | 1,3-Bis(carboxymethyl)imidazolium bromide   |
| <b>bcmimCl</b>      | 1,3-Bis(carboxymethyl)imidazolium chloride  |
| <b>bcmimI</b>       | 1,3-Bis(carboxymethyl)imidazolium iodide  |
| <b>bcmimNa</b>      | Sodium salt of 1,3-bis(carboxymethyl)imidazole                                    |
| BDC                 | Terephthalic acid   |
| BET                 | Brunauer-Emmett-Teller theory (related to specific surface area calculation)      |
| Bmim                | 1-Butyl-3-methylimidazolium cation  |
| <b>bcpim</b>        | 1,3-Bis(carboxypropyl)imidazole   |

|                |  |
|----------------|--|
| br             | Broad  |
| <b>bsmim</b>   | 1,3-Bis(sulfomethyl)imidazole                                  |
| BTC            | Trimesic acid  |
| ca.            | Approximately (from the Latin word <i>circa</i> )              |
| Cat.           | Catalyst/catalytic   |
| <b>cmimCl</b>  | 1-(Carboxymethyl)-3-methylimidazolium chloride                 |
| cod            | Cyclooctadiene   |
| Conv.          | Conversion   |
| Cont.          | Continuation   |
| CP             | Coordination Polymer   |
| CT             | Charge-transfer  |
| Cy             | Cyclohexyl   |
| D              | Debye (electric dipole moment unit)/Deuterium                  |
| d              | Doublet  |
| DDQ            | 2,3-Dichloro-5,6-dicyano-1,4-benzoquinone                      |
| DES            | Deep Eutectic Solvent  |
| DIP            | Direct Insertion Probe   |
| DMF            | <i>N,N</i> -Dimethylformamide                                  |
| DSC            | Differential Scanning Calorimetry                              |
| DSO            | Dynamic Shear Oscillation                                      |
| E              | E-factor/Standard potential                                    |
| e <sup>-</sup> | Electron   |
| e.g.           | For example (from the Latin expression <i>exempli gratia</i> ) |
| EC             | Electron crystallography                                       |
| EDG            | Electron-donating group  |
| EI             | Electronic Impact (Ionization)                                 |
| emim           | 1-Ethyl-3-methylimidazolium cation                             |
| EMY            | Effective Mass Yield   |
| EQ             | Environmental Quotient   |
| eq.            | Equivalent   |
| ESI            | Electrospray Ionization  |
| Et             | Ethyl  |

|             |   |
|-------------|---|
| eV          | Electron-volt (unit of energy)                                  |
| EWG         | Electron-withdrawing group                                      |
| Exo         | Exothermic  |
| g           | Gram  |
| GC-MS       | Gas Chromatography coupled to Mass Spectrometry                 |
| GO          | Graphene oxide  |
| h           | Hour  |
| HBA         | Hydrogen Bond Acceptor  |
| HBD         | Hydrogen Bond Donor   |
| Het.        | Heterocycle   |
| HFIP        | 1,1,1,3,3,3-Hexafluoroisopropanol                               |
| HKUST       | Hong Kong University of Science and Technology (family of MOFs) |
| HOMO        | Highest Occupied Molecular Orbital                              |
| HPLC        | High-Performance Liquid Chromatography                          |
| HSAB        | Pearson Hard-Soft Acid-Base theory                              |
| $h\nu$      | Irradiation with light  |
| Hz          | Hertz (unit of frequency)                                       |
| i.e.        | That is (from the Latin expression <i>id est</i> )              |
| <b>IBIS</b> | Iron-Based Imidazolium Salt                                     |
| IBX         | Iodoxybenzoate  |
| ICE         | Internal Combustion Engine                                      |
| IL          | Ionic Liquid  |
| IOS         | Ionic Organic Solid   |
| <i>i</i> Pr | Isopropyl   |
| ISO         | International Organization for Standardization                  |
| J           | Joule (unit of energy)  |
| <i>J</i>    | Coupling constant   |
| <i>k</i>    | Constant  |
| K           | Kelvin (unit of temperature)                                    |
| L           | Liter   |
| L           | Liquid  |
| LCA         | Life-Cycle Assessment   |

|                |  |
|----------------|--|
| L-Pro          | L-Proline  |
| lit.           | (Reported) in literature                               |
| LTTM           | Low Transition Temperature Mixture                     |
| LUMO           | Lowest Unoccupied Molecular Orbital                    |
| m              | Meter  |
| m              | Multiplet  |
| m.p.           | Melting point  |
| <i>m/z</i>     | Mass to charge ratio                                   |
| <b>mcmimCl</b> | 1-(Methoxycarbonylmethyl)-3-methylimidazolium chloride |
| Me             | Methyl   |
| Mes            | Mesityl  |
| MIL            | Lavoisier Materials Institute (family of MOFs)         |
| min            | Minute   |
| mmol           | Millimole  |
| MOF            | Metal-Organic Framework                                |
| MOG            | Metal-Organic Gel                                      |
| mol%           | Percentage in mol (in regard to the limiting reagent)  |
| MRP            | Materials Recovery Parameter                           |
| MS             | Mass Spectrometry                                      |
| <b>msmim</b>   | 1-Methyl-3-(sulfomethyl)imidazole                      |
| MS/MS          | Tandem Mass Spectrometry                               |
| MTBE           | Methyl <i>tert</i> -butyl ether                        |
| MW             | Molecular Weight                                       |
| N/D            | Not determined   |
| NADES          | Natural Deep Eutectic Solvent                          |
| NBS            | <i>N</i> -bromosuccinimide                             |
| NHC            | <i>N</i> -Heterocyclic Carbene                         |
| NLO            | Non-linear Optics                                      |
| NMR            | Nuclear Magnetic Resonance                             |
| N°             | Number   |
| NP             | Nanoparticle   |
| Nu             | Nucleophile  |

|            |   |
|------------|---|
| NU         | Northwestern University (family of MOFs)                                |
| <i>o</i> - | Ortho (position)  |
| °          | Degree  |
| OAc        | Acetate   |
| °C         | Degree Celsius  |
| OG         | Opaque gel  |
| OIPC       | Organic Ionic Plastic Crystal   |
| OTf        | Trifluoromethanesulfonate   |
| OX         | Oxidizer  |
| P          | Pressure  |
| <i>p</i> - | Para (position)   |
| $P_c$      | Critical pressure   |
| PEPPSI     | Pyridine-Enhanced Precatalyst Preparation, Stabilization and Initiation |
| PFC        | Perfluorinated Compound   |
| Ph         | Phenyl  |
| pH         | Inverse of the concentration of hydronium ions (H) in solution          |
| $pK_a$     | Inverse of the dissociation constant of an acid ( $K_a$ )               |
| PMI        | Process Mass Intensity  |
| PSBMA      | Poly[2-(methacryloyloxy)ethyl]dimethyl-(3-sulfopropyl)                  |
| PSE        | Post-synthetic Exchange   |
| PSF        | Post-synthetic Functionalization  |
| PSI        | Post-synthetic Insertion  |
| PSM        | Post-synthetic Modification   |
| PXRD       | Powder X-ray Diffraction  |
| Q          | Environmental Unfriendliness Quotient                                   |
| q          | Quartet/quintet   |
| QTOF       | Quadrupole-Time of Flight   |
| RME        | Reaction Mass Efficiency  |
| rpm        | Revolutions per minute (unit of frequency)                              |
| rt         | Room temperature  |
| RTIL       | Room-Temperature Ionic Liquid   |
| S          | Stoichiometric coefficient/Siemens (unit of conductivity)               |

|                |   |
|----------------|---|
| s              | Singlet   |
| salen          | Salicylaldehyde-ethylenediamine                           |
| SAXS           | Small-angle X-ray Scattering                              |
| SBU            | Secondary Building Unit                                   |
| SCE            | Saturated Calomel Electrode                               |
| SCF            | Supercritical Fluid                                       |
| SEM            | Scanning Electron Microscopy                              |
| SF             | Stoichiometric Factor                                     |
| SFG            | Semi-fluid gel  |
| SIM            | Single-ion Monitoring                                     |
| SLE            | Solid-liquid Equilibria                                   |
| S <sub>N</sub> | Nucleophilic substitution                                 |
| Solv.          | Solvent   |
| SSNMR          | Solid-state NMR   |
| SSTTI-UA       | Research Technical Services of the University of Alicante |
| Subst.         | Substrate   |
| T              | Temperature   |
| t              | Time/triplet  |
| taut.          | Tautomerization   |
| TBHP           | <i>tert</i> -Butyl hydroperoxide                          |
| <i>t</i> -Bu   | <i>tert</i> -Butyl  |
| T <sub>c</sub> | Critical temperature                                      |
| TCNQ           | Tetracyanoquinodimethane                                  |
| TEL            | Tetraethyllead  |
| TEM            | Transmission Electron Microscopy                          |
| TEMPOL         | 4-Hydroxy-2,2,6,6-tetramethylpiperidin-1-oxyl             |
| T <sub>g</sub> | Glass transition temperature                              |
| TG             | Translucent gel   |
| TMEDA          | Tetramethylethylenediamine                                |
| TMS            | Trimethylsilyl/tetramethylsilane                          |
| TMTSF          | Tetramethyltetraselenafulvalene                           |
| TosMIC         | Tosylmethyl isocyanide                                    |

|           |  |
|-----------|--|
| Ts        | Tosyl  |
| TSA       | Toluenesulfonic acid   |
| TSF       | Tetraselenafulvalene   |
| TTF       | Tetrathiafulvalene   |
| UHP       | Urea-hydrogen peroxide adduct  |
| UiO       | University of Oslo (family of MOFs, from the Norwegian <i>Universitet i Oslo</i> ) |
| V         | Volt (unit of electric potential)  |
| VMR       | Vector Magnitude Ratio   |
| VOC       | Volatile Organic Compound  |
| W         | Watt (unit of power)   |
| w/w       | (Percentage) by weight   |
| XPS       | X-ray Photoelectronic Spectroscopy   |
| Y         | Reaction yield   |
| ZIF       | Zeolitic Imidazolate Framework   |
| $\Delta$  | Heat   |
| $\delta$  | Chemical shift   |
| $\lambda$ | Wavelength   |
| $\theta$  | Bragg angle (PXRD unit)  |
| $\chi$    | Mole fraction  |





---

## **Acknowledgements**

---

Universitat d'Alacant  
Universidad de Alicante



Ah yes, finally, this is the part where I get to say whatever I want without needing to battle it out with my (frankly inadequate) reference manager. All in all, this doctoral period has been quite nice, and I have met quite a lot of people along the way whom I need to thank for making it so. I'm terrible at this sort of thing, so there's that.

First and foremost, my dear boss, Isidro. Always patient, with something nice to say in tough moments, good advice to provide and an excellent scientific and personal role model to look up to. We had damn good fun lashing out at dodgy papers or incoherent analysis results, as well as very enlightening conversations about our beloved imidazoles. You have treated me as an equal while providing guidance, allowing me to become the (somewhat lacking but hey, that was a factory defect) passionate scientist that I am today, and for that I will always be grateful.

Speaking about patience, we have our next entry, my dear predecessors María and Patricia. You both have endured quite a bit of the consequences of my ill-fated contraptions while always providing a helping hand. From proofreading my early scientific ramblings to teaching me how not to burn the lab (non-intentionally at least) while answering pretty much every sort of random question I had (and I tend to produce a fair amount of those, mind you), so a big part of this is down to you too.

I suppose I should be including now meu irmão not-actually-from-Brazil and Mrs. Always Hungry. I had good fun with both. If by fun you mean looking at a damn HPLC trace at 8:00 pm on a Friday to see an *excellent* enantiomeric excess of 9%, that is. Still, my man Alex stood there looking at the screen while very fluidly cursing in a variety of languages (multiculturalism is a perk of the job) with me. On another note, I do not even need to know the date in which I defend this manuscript you're reading (I know why you're here, but believe it or not, this book has some actual science in it), because I'll have a life-saving voice reminding me. Overall, you two have been great pals with whom to share my time at the university, and I will miss you a bit.

*Her Who Droppeth.* My dear Sarah. A great conversationalist, even greater (and FREE) native English teacher. You and I have had great fun (tell you what, English is a *rich* language for childish jokes) and even talked some science, although the usual conclusion about our scientific discussions has typically been "hit it with a hammer".<sup>378</sup> Of course, we need to mention the one and only *Theresa of They Who Droppeth*, with whom I've shared a fair amount of laughs/rants/rants, mostly regarding clogged microsyringes and general lab annoyances. Tell you what, work is going to be quite boring without you two.

The Necroporra Team, Pawel, Diego (founding member of the Bruker Bois as well) and Jos(z)é. Ramblings, polish lessons (mostly swearing, in case you're wondering), a worrying amount of deeply

---

<sup>378</sup>Clarkson, J. C. *Top Gear*, 2013, 19, 154.

## *Acknowledgements*

---

dank memes and memories that will last a lifetime. I take this opportunity to pay my respects to Larry, Alatrizzte and Fernando Zzéptimo.

As to not make this infinitely long (I spent an entire thesis lecturing you about sustainability, so consuming an entire 50-meter tree to print this thing would be a bit hypocritical) I will rapid fire everyone now, beginning with those who preceded me, Xavi, Diego R., Natalia, Bea, Iris, Edu and Ana.

Now, people currently in the labs, Juan Fran (master rice maker, party machine and all in all great guy), Loris (our dear resident Milanese, great fan of De Pizzzo), as well as James, Ester, Raquel, María, Fran, Lesly and Tatiana. The next generation of ISO (not to be mistaken with IOS, I'm sorry but although these people are very nice, they do not have catalytic properties), José, Paula and Lara. And last, but not least, those who were only here for a short time, namely Dani, Azahara, Manel, José and Jara. I take a moment now to thank Débora, Irene and Damián for the great times we had working together on the Liberate project.

Multiculturalism is a perk of the job, as I mentioned before. Indeed, during this time I have met great people from many different countries. Elisa and Natasha from Manchester, Matteo and Debora from Italy, my dear Ediz and Zafer from Frankfurt, Tom from Edinburgh, and Felipe from Brazil.

Jag glöm inte mina svenska vänner! My time in Göteborg gave me quite a lot (for starters, a crippling fear of shared living spaces), but the thing I value the most are the good friends I made there. *Doktor* August and Martin (our trusty Slavic chef), with whom I shared the 9065 Man Cave and, ahem, *language courses*. Sara, who provided a lot of laughs and a much-needed anchoring point to my homeland, as well as Ishan, a man of many talents with a penchant for very dark humor, photography and flamenco. Of course, the rest of the 9<sup>th</sup> floor too, namely Flavia, Jelka, Agnes, Savannah and Skjosé María Štefan. At the 8<sup>th</sup>, Carlos and Clara, as well as the rest of Sundén's group, Ganesh S., Ganesh G. and Simon. And nothing of this would have been possible without Prof. Henrik Sundén, who gave me the opportunity of joining his team, access to all resources (including their AUTOMATIC columns) and made me feel right at home from the start. Tack så mycket!

Now, a special one for the people who had to endure me in the lab. Belén, Yanira, Pablo and Anna. You have all been a joy to work with, and well, a "thank you" is in order for your patience with my ramblings. You are all truly special people to me.

'Course, speaking about patience, I cannot go without mentioning my parents and little sis, as well as my other half, Mónica, who has been enduring me full-time for over 8 years now, supporting yours truly throughout my latter academic years and providing me with copious amounts of cat content and Formula 1 memes. ¿A quién no le va a gustaahr?

I probably forgot someone, so yeah, thanks everyone.

Ah yes, Bianca too. I like your car.



Universitat d'Alacant  
Universidad de Alicante